JUSTUS-LIEBIG-
UNIVERSITÄT
GIESSEN

How humans choose where to grasp objects

Dissertation

zur Erlangung des Doktorgrades der
Naturwissenschaften (Dr. rer. nat) der

Justus-Liebig-Universität Gießen

Fachbereich 06, Psychologie und Sportwissenschaften
Otto-Behaghel-Straße 10F, 35394 Gießen

vorgelegt am 22. November 2022 von

Lina Katharina Klein

Datum der Disputation: 05. Juni 2023

GutachterInnen:

Prof. Dr. Roland W. Fleming (Justus Liebig University Giessen, Giessen, Germany & Center for Mind, Brain and Behavior (CMBB), Philipps-Universität Marburg and Justus Liebig University Giessen, Marburg, Germany)

Prof. Dr. Katja Dörschner-Boyaci (Justus Liebig University Giessen, Giessen, Germany & Center for Mind, Brain and Behavior (CMBB), Philipps-Universität Marburg and Justus Liebig University Giessen, Marburg, Germany)

Mitglieder der Prüfungskommission:

Prof. Dr. Jody C. Culham (University of Western Ontario, London, ON, Canada)

Prof. Dr. Katja Fiehler (Justus Liebig University Giessen, Giessen, Germany & Center for Mind, Brain and Behavior (CMBB), Philipps-Universität Marburg and Justus Liebig University Giessen, Marburg, Germany)

Prof. Dr. Thomas Schenk (Ludwig-Maximilians-Universität München, Munich, Germany)

Acknowledgements

*Hi, Roland! *waves**

Words cannot express my gratitude to my professor, Roland W. Fleming, who welcomed me into his wonderful team and provided invaluable guidance, feedback, and a kind and encouraging work environment. Thank you for supporting my journey through the various projects and for always being there with pristinely worded scientific, career, and personal advice. I am extremely grateful for your mentorship and for all "Flemingos" (as all former and current Fleming lab members will henceforth be known) for the fun and supportive atmosphere in Giessen, as well as at every conference and retreat location around the world. I felt right at home with our shared "love language" being sarcasm as well as taking hours to give feedback on every detail on a conference presentation. Then, I would like to thank one very special Flemingo, Guido Maiello, genius and best friend, for joyfully and patiently sharing his insights, generous support, and his silliness with me. I could not have asked for a more lovely group of colleagues and friends and I feel extremely lucky to have made such wonderful connections during the past six years. Oh, the fun we've had!

I also could not have undertaken this journey without Jody C. Culham, who generously provided knowledge and expertise. Visiting Jody at Western University proved to be an exciting learning opportunity. There, I picked up tips on designing, performing, and analyzing fMRI experiments, and learned that anything involving the 7T-scanner makes for a frightening Halloween pumpkin design. I am grateful to have been welcomed and supported by Jody's great team members, who generously shared their professional and social networks and invited me to participate in their endeavors.

I wish to express my deepest appreciation to the many friends and colleagues, who are and were a part of Karl R. Gegenfurtner's group. Thank you for the inspiring input and lively discussions, whether those occurred during joint trips to the Mensa or the squash place. It certainly felt like an enormous privilege to have such an abundance of brilliant minds, eager to share their wisdom, merely a knock on the door away. Sure, I might have gotten sidetracked here and there on my path to solving grasping, but the journey was never boring and I am grateful for all the times I got to pick their brains!

I feel very fortunate to have had a somewhat unusual PhD experience: my experiments generally worked well on the first try, I frequently got to talk about science on an international stage, and I was encouraged to collaborate with many colleagues, using different methods and various setups, without having to worry about job security. Thank you, Roland, for including me in the IRTG and enabling me to continue my research for as long as I have. Having such freedom to follow my interests, I built strong connections with my colleagues and became a part of a very inspiring, inclusive environment.

Last, but certainly not least, a huge thank you to my parents, Irene Klein and Hermann Klein, and my sister, Karen Klein, and my brother, Florian Klein, as well as my husband, Kim Klein, who somehow managed to be nothing but supportive. I wish to thank you for your constant positivity, encouragement, and unconditional love. There are no words to convey how much I love you and what you mean to me. Thank you for believing in me!

Abstract

Look around. Nearly everything we see, we can act upon with our hands. We utilize our hands as all-purpose tools to feel and touch the world, to climb, point, create art (e.g., by playing musical instruments, drawing, or sculpting), communicate, and to pick up objects. Throughout these actions the hand shapes differently. When reaching out to grasp something, the human hand unfolds into a shape that is appropriate for grasping and manipulating the object securely. Humans can grasp an object in a variety of ways by varying their digit placements on it. Even when we consider a precision grip, where only thumb and index finger are in contact with, e.g., a coffee cup, there might already be several thousand combinations of finger and thumb locations on the cup's surface available to choose from. Computationally, this choice is far from trivial. However, selecting the proper grasp locations is necessary to ensure successful interaction with the object. Despite that computational challenge, humans are able to determine secure, comfortable grasp locations that minimize slippage and torsion by considering an object's shape, material characteristics, and the desired action outcome. The aim of this thesis was to understand how humans achieve this complex task.

Study 1 investigated which factors determined where humans grasped 3D objects and how these were prioritized according to their relative importance. We used motion tracking to record and analyze participants' grasping behavior with blocky wooden and brass objects and merged those findings with a computational model in order to predict where novel 3D-printed plastic objects would be grasped. We found that the limits force closure imposed on a grasp, the participants' natural grip axis (NGA), and grasp aperture were the three key factors that participants considered to determine ideal grasp locations. The amount of torque a grasp would produce, and to what extend the participant's hand would occlude the object, were factors that we found to carry less relevance for grasp choice. Whether torque, specifically, would be considered, depended on the overall weight of the object. Predicting human grasps, even for the novel objects, worked remarkably well and our research had thus far demonstrated that human grasps followed our ideal grasp rules. Moving on, we were interested in how grasp rules might interact.

Study 2 inspected whether grasp locations would be chosen so that the grasp would be aligned to the NGA, or so that the grasp would fall on the higher friction contact areas and result in a more secure grasp pose. Our goal was to understand how the interactions between these two factors influenced grasp preference. NGA alignments were manipulated by rotating a cubic target object, whereas grasp stability was manipulated by altering the object's surface characteristics. We discovered that participants favored the higher friction surfaces and sacrificed alignments with their NGA in order to create stable grasp configurations. Having researched the various factors that influenced grasp locations, their relative importance and, to some extent, their interactions, we aimed to understand how the brain computes and combines these constraints to produce appropriate motor outputs.

Study 3 used functional magnetic resonance imaging (fMRI) to examine, how grasp-relevant information is represented across sensorimotor brain areas. Participants planned and carried out pre-selected grasps to multi-material 3D objects, designed to disentangle how the brain coded the NGA, object mass, and grasp aperture. We found that the orientation of the grasp was predominantly encoded during grasp planning in dorsal regions. The size of the grasp was, encoded during both planning and execution phases in various groupings of dorsal and ventral regions. Predominantly

during execution, we found encoding of object mass throughout dorsal, ventral, and motor areas. Taken together, these sets of experiments provide insights into how humans use a combination of factors to make decisions about where to place their grasps.

Table of contents

Chapter 1

INTRODUCTION

1.1 The complexity of human grasping

In our every-day life we interact with a multitude of different objects and materials. Without consciously thinking about it, we can see an object and form appropriate grasps to interact with it. Our hands have a very delicate and complex structure, with their muscles and joints offering a great range of movement and precision. While typing away at my laptop, I can lift up my coffee cup to take a sip of coffee. I visually perceive the cup's location, move my hand to the cup and effortlessly wrap my fingers around its handle to transport the cup to my lips. Certainly, I had previously left it in a position now known to me and in an orientation that made it easy to lift it up by its handle. However, even unknown objects in unknown orientations can be grasped and manipulated by us with ease. Yet, the underlying computational problem of how to successfully grasp a novel object is far more complex than we may feel it is.

In order to successfully interact with the world and the objects around us, we must select a grasp strategy that satisfies both task and object requirements. That means the goal of our grasping action (e.g. quenching one's thirst by guiding a cup of tea to one's mouth and subsequently tilting it) must be combined appropriately with the object's requirements (grasping the cup by its handle, to avoid the hot surface as well as keeping it level to avoid spillage). Choosing and performing the appropriate grasp for a given object is a computationally complex problem, due to an essentially infinite number of possible grasp locations and grasp movements. Even if we consider a simplified version of a grasping task with only two contact points, using only thumb and index finger, the question remains:

How do we select a grasp strategy that satisfies task and object requirements?

To address and expand on the challenges described above that we face in investigating grasping, this thesis is structured to first examine the specific properties of objects, then move on to describe the human hand as well as the specifics of grasping movements. Lastly, the Introduction will finish with an outlook onto the individual studies included into this dissertation (Chapters 2-4).

1.2 The object

1.2.1 Perception of object properties

Already before a grasp commences, we can visually acquire information about the object to be grasped. We can detect the object's location, which can be coded in allocentric or egocentric

coordinates. An egocentric reference frame represents the absolute position of the object with respect to the viewer, and an allocentric reference frame encodes the position of the object with respect to other objects in the environment (Colby, 1998). Humans can recognize and categorize objects quickly and accurately (Masquelier & Thorpe, 2010; Rousselet et al., 2002; Thorpe et al., 2001; Wiebel et al., 2013), even quicker than they can do so with materials (Sharan, 2009; Sharan et al., 2014). How we perceive material properties, such as texture, color, or transparency, has been the focus of scientific experiments for over two centuries already (Julesz, 1981; Metelli, 1970; von Helmholtz, 1867; Young, 1802). Upon perceiving material, studies suggest we can recognize it belongs to a specific class, estimate its specific properties, or figure out how to manipulate the things around us (for a review, see Fleming, 2017).

Figure 1.1: Office desk with four folders, a steaming cup of coffee, a glass filled with soda and ice cubes, a plate of raspberries, a light bulb, two computer screens with a keyboard and mouse, a plush bunny, a potted cactus, a stapler, a desk lamp, and a pair of scissors (left to right).

Being able to predict an object's material properties allows us to foresee suitable ways for interacting with that object. It is necessary to modify grasps, to account for an object's material properties, such as mass, friction, and fragility. Not only can we estimate stable grasp locations, we can further predict the object's response to our touch if we can work out what the object is made of. Lightweight, fragile objects, such as a raspberry in Figure 1.1, will need a gentler touch than the sturdy, much heavier glass filled to the rim. Yet, to visually estimate an object's fragility, or its stiffness, is a challenge, because stiffness is not optically defined. We can, however, make assumptions based on prior knowledge associated with material classes or look for deformation cues (Paulun et al., 2017). Not only are we using visual cues related to shape deformation, motion, and optical appearance to decide which posture we choose to grasp an object. That choice might also depend on the object's relationship to the environment, as well as our spatial relationship to the object to be grasped. Jeannerod (1981) differentiates between extrinsic and intrinsic object properties, which are discussed in detail below.

1.2.2 Extrinsic object properties

Extrinsic properties are spatial object properties in an egocentric body space, such as its location or distance (Sivak & Mackenzie, 1992), orientation with respect to the body (Chan et al., 1990; Jeannerod

& Decety, 1990), and, when the object is moving, its velocity and direction (Paulignan et al., 1991). These properties may include support constraints, such as the desk supporting the stapler's underside (Figure 1.1), and additional obstacle constraints (e.g., the soda glass one has to reach around when trying to grasp the coffee cup in Figure 1.1 or Figure 1.2 (top)), as well. Even though orientation was initially categorized as extrinsic (Jeannerod, 1981), it is sometimes considered to be intrinsic (Jeannerod et al., 1995).

1.2.3 Intrinsic object properties

Intrinsic object properties are physical properties of objects that are fundamental to their design. These include structural properties (shape, size, distribution of mass and overall weight), surface properties (texture, hardness, and temperature), and functional properties (part motion, specific function). Participants can extract many intrinsic object properties relevant to the grasping task using the visual or the haptic system (Klatzky, 1990; Klatzky et al., 1987).

During the planning phase of a grasping movement, humans can visually perceive object shape (Jeannerod, 1984; Klatzky & Lederman, 1988), volume (Klatzky & Lederman, 1988), surface spatial density (Klatzky et al., 1987) can infer the location of the center of mass, the CoM (Mason, 1986), and, while performance is better in extreme lighting directions, they can even perceive surface roughness (Bergmann Tiest & Kappers, 2007; Ho et al., 2006; Lawrence et al., 2007; Pont & Koenderink, 2008). In several experiments, participants were asked to report object size by matching the distance between two opposable surfaces of a target object by separating their thumb and index finger. When participants could see the object, but not see their own hands, mean grip size correlated positively with object size (Jeannerod & Decety, 1990). Even without visual cues, participants successfully reported object size through an aperture between thumb and index finger, after holding the object in their other hand and feeling its size (Chan et al., 1990).

Some intrinsic properties may even be inferred through auditory cues (Owens et al., 2016). Using isolated simple sound events, listeners were able to determine object properties, such as size and shape (Carello, 1998; Grassi, 2005; Grassi et al., 2013; Houben et al., 2004; Kunkler-Peck & Turvey, 2000; Lakatos et al., 1997), or material (Kunkler-Peck & Turvey, 2000). Once in contact with the object, humans can use the haptic sense to extract information about the object, such as roughness (Bergmann Tiest & Kappers, 2007; Lawrence et al., 2007). Specifically, through exploratory hand motions, we can perceive surface roughness, temperature, and weight (Klatzky et al., 1987), whereas weight can also be inferred from holding and jiggling the object (Brodie & Ross, 1985; Raj et al., 1985). Length, weight, moment of inertia, and center of mass can be perceived through wielding (Hoisington, 1920; Solomon et al., 1989).

Grasp posture is affected in multiple ways by intrinsic object properties, as object size and shape can impose limits onto potential contact locations for the fingers and hand. The same holds true for weight distribution and shape. Object surfaces in contact with other objects (such as the stapler's underside resting flat on the desk in Figure 1.1) will not be available as initial contact locations for the grasp. The object's weight and its hardness interact to constrain how many fingers can be used in a grasp and how strong the grip can be (Iberall & Mackenzie, 1994). The hardness of an object also influences the force required to impart motion to the object (Iberall & Mackenzie, 1994). The application of forces underlies frictional constraints, which are affected by object texture (Iberall & Mackenzie, 1994).

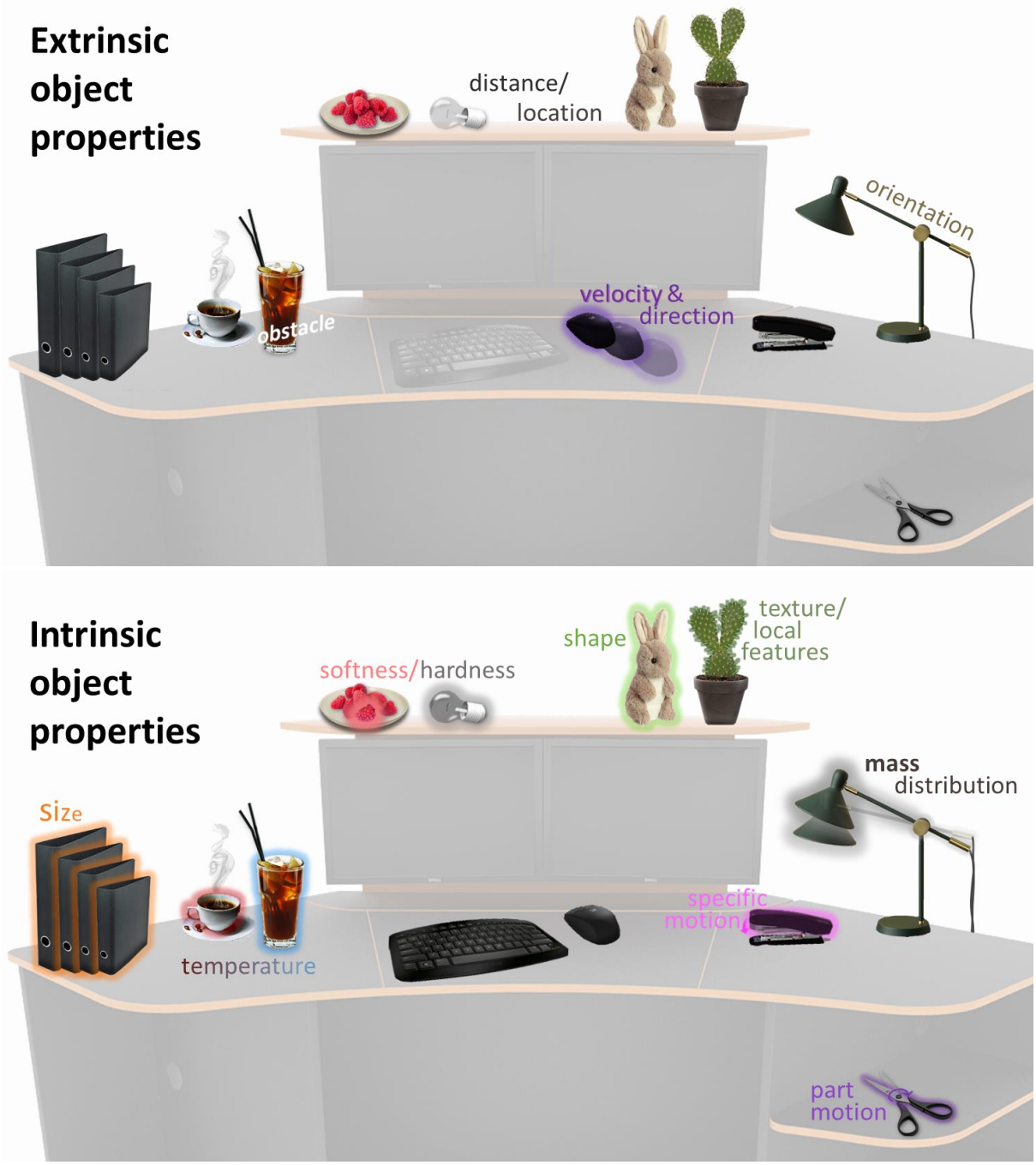

Figure 1.2: Office desk with items highlighted to visualize extrinsic (top) and intrinsic (bottom) object properties. Top: Examples of extrinsic object properties. The glass of soda presents an obstacle, when reaching for the cup of coffee. All items are positioned at a certain location and with a specific distance to the observer. When moving the mouse around on the desk, it has a certain velocity and moves in a specific direction. The desk lamp's top part is set up in a specific orientation. Bottom: Examples of intrinsic object properties. Four folders differ in their size. A steaming cup of coffee is hot. The glass filled with soda and ice cubes is cold. A raspberry is soft and delicate, whereas the light bulb is hard. The plush bunny and the potted cactus show a similar global shape (the bunny's ears and head are shaped similarly to the cactus), but the cactus has a different texture and local features. The stapler is used with a specific downwards motion, the pair of scissors with a rotational part motion. The desk lamp might tilt, depending on its mass distribution.

1.3 The human hand as an end effector

The human hand is highly versatile with over 25 degrees of freedom (i.e. independent states of a system or the number of values free to vary independently (Pitarch et al., 2005; Touvet et al., 2012).

It is composed of a collection of bones, muscles, tendons, ligaments, fascia, and vascular structures wrapped in a thin layer of skin. First, we reach out and our hand opens up into a suitable shape to grasp and manipulate the object according to the task we envisioned. Yet, we do not consciously plan explicit movements for individual fingers or joints, nor do we need to see the entire object from all possible perspectives in order to form the grasp. When our fingers move towards and touch an object, thousands of sensors in the skin, muscles, and joints can send information about the current state to our brain. We use our hands every day to touch and feel, to pick up and manipulate objects, to explore the world around us. Using small movements of as little as one digit, we can scroll through the internet on our smart phones, buy musical instruments, and even learn to play them.

Taking into account what the human hand is capable of, we aim to adopt a stable grasp pose while being able to produce the movements needed for the given task. What exactly determines a stable grasp, depends on the object's properties, as well as the forces applied by our hand. When we speak of a stable grasp, it is considered to keep the grasped object secure in the grasp, even when the object turns out to be more slippery than anticipated, or it unexpectedly collides during transport with another object. That means, if any error in object position brought on by a disturbance goes away soon after the disturbance goes away, the grasp is stable (Bruyninckx et al., 1998; Howard & Kumar, 1996; Lin et al., 1997). Specifically, the skin of our hand and fingers offers properties critical for secure grasping: no (or minimal) hair growth enables high friction. Our skin provides sensibility, force generation, compliance, adhesion through the specific characteristics of our epidermis, dermis, and the papillary ridges, the visible ridges on the skin of our palms and fingers. These characteristics are found almost exclusively in the friction surfaces of primates and marsupials (Montagna & Parakkal, 1974). These ridges help increasing grip and facilitating weight bearing through the increased surface area and specific pattern. Thus, our hands seem to be equipped to form a secure grasp. Below, it will be discussed, how the entire grasp movement can be divided into its individual components.

1.3.1 The stages of a grasp

When we want to investigate how grasping is controlled, we should first describe and understand the individual stages of the grasping movement and explore the parameters that influence it. Marc Jeannerod's influential study (1981) declared the grasp as a combination of transporting the hand and adjusting the grip. Jeannerod connected hand posture to the graspable object's size and shape (intrinsic properties) and movements of wrist and arm segments to be governed by extrinsic object properties, such as location.

1.3.1.1 Approach/ reach

Once we have made the decision to grasp an object, e.g., the stapler from Figure 1.1 and Figure 1.2, our hand can start moving towards that object following a curved trajectory. The exact path can be influenced by many factors, such as the distance between us and the target object (Jakobson & Goodale, 1991) or the orientation of the object (Desmurget & Prablanc, 1997; Fan et al., 2006; Gentilucci et al., 1996; Mamassian, 1997). Obstacles located close to the trajectory or the object can also affect the approach trajectory, as the presence of obstacles may limit the range of possible postures, thus influencing the choice of grasping points. Grasp locations, however, only seemed to be affected by the presence of obstacles, if they were placed too close to the otherwise preferred grasp locations and therefore constrained the movement (Garzorz et al., 2018; Rosenbaum et al., 2001; Voudouris et al., 2012b).

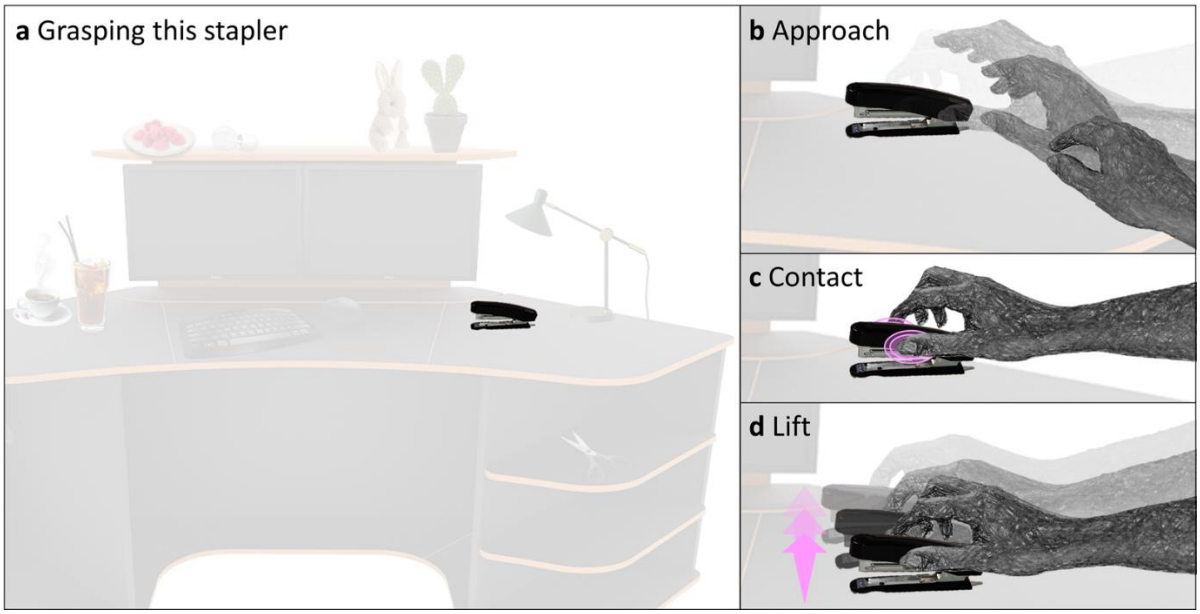

Figure 1.3: The stages of the grasp. (a) Graspable object: stapler on this office desk. (b) Hand approaching the stapler to grasp it. (c) Thumb and index finger making contact with the stapler, initiating the Contact phase of the grasp. (d) The stapler is lifted off the desk in the Lift phase.

The reach component of the grasp is divided into a shorter acceleration phase at the beginning and a longer deceleration phase towards the end of the movement (e.g., Jeannerod, 1984; Mon-Williams & Tresilian, 2001; Smeets & Brenner, 1999). When the precision requirements of grasping and aiming tasks are varied (pointing vs. grasping; grasping a tennis ball vs. a light bulb; placing vs. throwing; (Marteniuk et al., 1987)) the deceleration phase at the end of the movement is lengthened disproportionally to the rest of the movement. The duration of the reach movement depends on the distance between the hand's start location and target object (Jakobson & Goodale, 1991), but also the perceived slipperiness of the object's surface (Fikes et al., 1994) or perceived fragility of the object (Savelsbergh et al., 1996) and was shown to increase with object distance (Kudoh et al., 1997) and decrease with object size (Marteniuk et al., 1990).

As our hand moves towards the object, our fingers are already preshaped in anticipation of the object's shape (Jeannerod, 1981). For the most commonly studied grasp, the precision grip, the maximum distance between index finger and thumb during the approach is called maximum grip aperture (MGA) (Jeannerod, 1984, 1986; Smeets & Brenner, 1999), which occurs when the hand is decelerating towards the object (Castiello, 2005; Jeannerod, 1984; Mon-Williams & Tresilian, 2001; Smeets & Brenner, 1999). The MGA's size and timing can be affected by the object's shape (Cuijpers et al., 2004; Verheij et al., 2014), size (larger MGA for larger objects; e.g., Jeannerod, 1981; Marteniuk et al., 1990, size and distance (Jakobson & Goodale, 1991)), weight (higher weight increases the MGA; (Eastough & Edwards, 2006); higher weight increases movement duration; (Fleming et al., 2002)), or other factors. Depending on how the target object is oriented and which surfaces are available as potential contact locations, that will constrain the orientation of the reach. As object shape, material, and orientation continue to be factors influencing different stages of the grasp, they will be investigated in our studies as well.

1.3.1.2 Contact

Upon contact with the object, the approach ends and the touch phase begins. Our fingers are pressed against the object on contact, stabilizing the object. Where our digits make contact with the objects has presumably already been determined before the approach began (Voudouris et al., 2010) even though adjustments may occur during movement execution (Chen & Saunders, 2015). Initial grasp selection may be influenced by several object properties, such as its shape (Cuijpers et al., 2004; Goodale et al., 1994; Kleinholdermann et al., 2013; Lederman & Wing, 2003), size (Paulignan et al., 1997), surface friction (Fikes et al., 1994), mass, mass distribution, and center of mass (Crajé et al., 2011; Eastough & Edwards, 2006; Endo et al., 2011; Goodale et al., 1994; Kleinholdermann et al., 2007; Lederman & Wing, 2003; Lukos et al., 2007; Paulun et al., 2016), and position (Desmurget & Prablanc, 1997; Paulignan et al., 1997; Schot et al., 2010), as well as factors determined by the way our hand is positioned within our body structure and the way our digits can move, i.e., grasp orientation (Cuijpers et al., 2004; Lederman & Wing, 2003; Paulun et al., 2016; Roby-Brami et al., 2000; Schot et al., 2010; Voudouris et al., 2010) and the size of the grasp (Cesari & Newell, 1999). Starting out from a relaxed posture, where your right hand and arm rest on a table surface in front of you, it might be possible to grasp an espresso cup, located slightly to your left side with ease. However, if you had to grasp a big, two-liter water bottle, located on a higher shelf to the right of your hand, you might want to readjust your entire body position before coming in contact with the object. The fact that our hands are asymmetrical and the way our hands can move does constrain factors such as grasp orientation or the size of the grasp.

1.3.1.3 Lift

We start applying forces at our fingertips as soon as we touch the object's surface. Grip force is exerted perpendicular to the surface normal whereas load force counteracts gravity tangentially to the object's surface (Edin et al., 1992; Forssberg et al., 1991; Johansson, 1991; Johansson & Westling, 1984b, 1988; Kinoshita et al., 1997; Macefield et al., 1996; Westling & Johansson, 1984). The grip force humans use when lifting and manipulating objects follows an optimization process: it is large enough to prevent the object from slipping, but not so large as to cause the object or hand to be damaged or the muscles to become fatigued. As load forces increase or decrease, grip force (normal to the grasp surface) is automatically adjusted along with them (Johansson & Westling, 1984b; Westling & Johansson, 1984). Before the object is lifted up and right at the beginning of the movement, both forces increase simultaneously (Johansson & Westling, 1984b; Westling & Johansson, 1984). For a heavier object, this handling or loading phase (time between touching and lifting the object) is longer, because overcoming gravity requires more force than with a lighter object (Johansson & Westling, 1984b). When asked to pick up objects of varying weights, both grip and load force were affected (Johansson & Westling, 1984b; Westling & Johansson, 1984, 1987). Varying the surface texture on the other hand, seemed to influence only grip force, not load force (Johansson & Westling, 1984a, 1990), suggesting that participants had to grip a more slippery object more forcefully to achieve the same load force.

It has also been shown that participants grasp objects with more force than necessary to keep the object from slipping (Westling & Johansson, 1984), with this additional force, or safety margin, being fairly constant (Goodwin et al., 1998; Jenmalm et al., 1998).

1.3.1.4 Objective of the Grasp

A grasp is dexterous if the hand can manipulate the object in a manner that is appropriate for the task at hand. What follows the lift depends on which task we wish to accomplish and which goal is imposed on the grasp (Napier, 1956). After an object is lifted up from a table, it can be held and released back onto the table, or can be transported to be released elsewhere. If planning a specific action (e.g., rotating an object a certain amount), we may select grasps that consider the end-state comfort of the movement (Rosenbaum et al., 1990). That is the tendency to choose an initially potentially uncomfortable grasp pose to allow a more comfortable end pose, once the grasping task is completed. As an example, you can think of grasping a light bulb. You might pick it up differently, depending on what you aim to do with it – depending on the task. If you want to pick it up to place it into a box, you might grasp its metal part. However, if you want to screw it into your lamp, you will pick it up at the glass part and turn your hand to an initially potentially strained joint angle, in order to allow guiding its grooves in a rotating fashion into your lamp. That way, by the time you let go of the light bulb, you end the contact phase in a more comfortable position compared to how you initially started the rotation movement. Similarly, we can think of joint actions, where we anticipate our partner's goal (Sacheli et al., 2012, 2013, 2015) and even their end-state comfort (Dötsch et al., 2021; Dötsch & Schubö, 2015). When I am asked to hand a screwdriver to a friend, I will pick it up by the pointy end to place the handle into my partner's hand. That way, they can use the screwdriver right away.

1.3.2 Important factors for stable grasps (precision grips)

To create, maintain, and release a stable grasp involves considering a variety of forces and torques, as there are many complex interactions between the skin and the object surfaces. Furthermore, it is important that a stable grasp is maintained during further manipulations. The hand should be able to generate torques and forces that will restore stability even after small external perturbations. Where stable grasps can be achieved on an object depends on a variety of factors, which I will introduce for the precision grip in this section. Working similar to tweezers, in a precision grip (or pinch grip), the thumb is located opposite the fingertip and can thereby manipulate even delicate objects (Napier, 1956). The precision grip allows the hand to grasp even small objects with a controlled grip.

1.3.2.1 Force closure

We start applying grip force as soon as we touch the object's surface. To avoid the object slipping out of the grasp under the grip force, potential grasp locations should be in force closure, a criterion borrowed from the robotics literature (Nguyen, 1988). In earlier studies Jameson and Leifer (1987) and Ji (1987) suggested algorithms for finding "double normals" (i.e., faces with opposed, collinear normals) on the object surface and Iberall, Bingham, and Arbib (1986) called this requirement the *opposition space*. A grasp that fulfills the requirements of force closure (like the grey grasp in Figure 1.4a) is considered stable and can resist an arbitrary wrench applied to the object. Force closure is a physical necessity for a successful grasp. The surface normals of a two-digit force closure grasp are required to be approximately aligned (see purple arrows in Figure 1.4a). That means, in order to hold the object steadily, the index and thumb surface normals should align with those of the object's surface at the contact points. Where the surface normals are too far from alignment, the object will slip out of the grasp (purple grasp in Figure 1.4a).

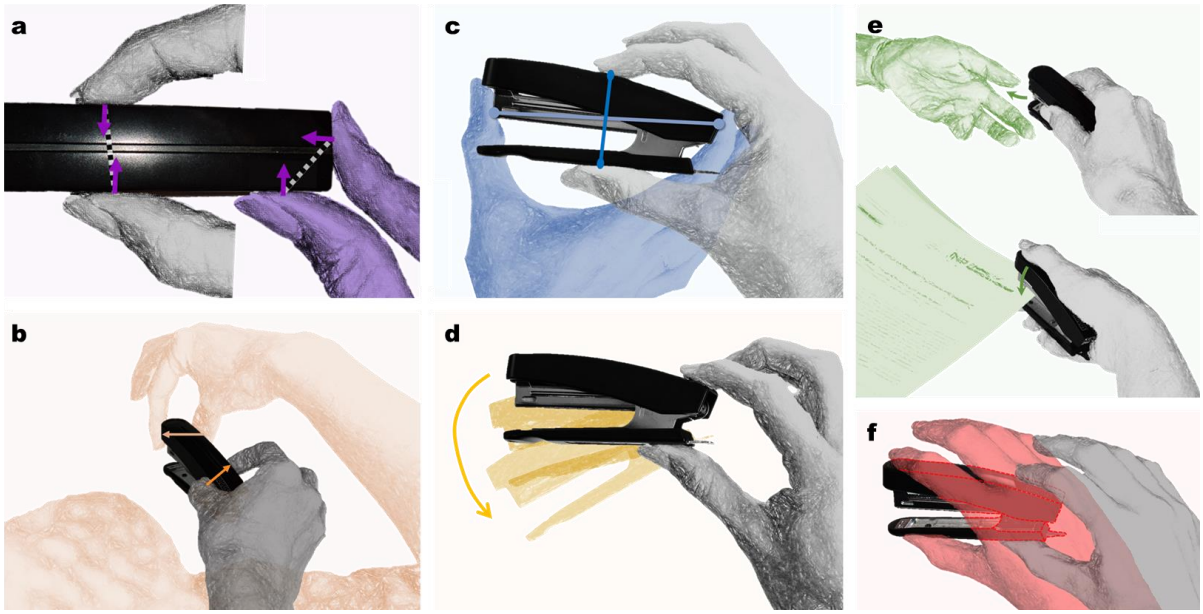

Figure 1.4: Important factors at play when grasping a stapler. a) Force closure. b) Grasp axis. c) Grasp aperture. d) Torque. e) Different tasks of either handing the stapler off to another person (top) or using it to staple together some pages. f) Visibility/ object occlusion.

1.3.2.2 Friction

How far from alignment is tolerable, depends on the friction coefficient. The object and the hand surfaces together determine the coefficient of friction. Westling and Johansson (1984b) examined how to grasp objects that have different textures and weights with precision grips. Sandpaper, for example, has a higher frictional component to the interactive forces than suede or silk, which have a lower frictional component. Not only can different objects be made of various materials and therefore have different friction coefficients, also the skin of our fingers can change. Naylor (1955) found that the coefficient of friction varied with changes in the skin's surface caused by environmental conditions, as he had participants sweat by sitting under blankets. A stable grasp is always required to have its grasp axis (the dotted lines connecting the two contact points in Figure 1.4a) fall within the cones of friction (Iberall et al., 1986; Kerr & Roth, 1986) of both digits. This is an important physical constraint for a successful grasp, because this way the object will stay securely between thumb and index finger, even once it is grasped and lifted.

1.3.2.3 Torque

Another factor that can be used to evaluate grip quality is torque (Goodale et al., 1994). A preferred grasp location will minimize the distance between grasping axis and the object's center of mass (CoM) (Lederman & Wing, 2003). A grasp, where the connection between index finger and thumb contact point on the object (i.e. the grasping axis) leads through the object's CoM, will yield low torque and it will be easier to lift the object straight up compared to a high torque grasp. A grasp far from the object's CoM will instead cause the object to rotate under the force of gravity (see Figure 1.4d), likely making subsequent object manipulation unstable. Yet, grasps with similar torques my still require different grip forces to keep the object from rotating between your fingertips. In some cases it is possible to partially compensate for torque by vertically offsetting the position of the fingers. In other

cases, applying larger grip forces will satisfy the requirement for rotational friction (Hartmann, 2022; Maiello, 2022).

1.3.2.4 Natural grasp axis and comfortable grasp poses

Our arm and hand have a specific number of degrees of freedom and a limited range of motion. Consequently, there are natural movements and configurations of our hand in space that will feel comfortable and stable for grasping. It has been argued that we usually use hand postures that keep our joint stabilized and where forces can be applied optimally while avoiding strain on ligaments and muscles (Chao et al., 1976). This becomes apparent, when we perform grasps, or in this case, imagine to perform them: Imagine moving your hand to grasp the stapler in Figure 1.1. There certainly are some movements and hand poses that can feel much more comfortable and natural (grey hand pose in Figure 1.4b) than others (orange hand pose in Figure 1.4b). This becomes drastically clear if you were to try and rotate your hand to switch your thumb and index finger positions on a grasp. Hence, the factor of comfort is an important aspect of grasping that determines how we move and orient our wrist for a grasp (Kleinholdermann et al., 2013; Lederman & Wing, 2003). When asked to pick up cylinders with a precision grips, participants clearly had a preference for a certain grip angle (Cuijpers et al., 2004; Lederman & Wing, 2003) which depended on object location (Schot et al., 2010). We can measure the vector between thumb and index finger (orange arrows in Figure 1.4b) in this preferred configuration and call this the NGA. Small deviations from the natural grasp axis (NGA) will still be comfortable and possible, whereas large deviations will be uncomfortable and difficult.

1.3.2.5 Comfortable grasp aperture

Cesari and Newell (1999) have shown that for small lightweight objects, humans use precision grasps, but with increasing object size and weight, they switch to multi-digit grasps. A comfortable grasp aperture depends on a human's individual hand size and their specific grip size, as well as the object's material properties. A grasp pose with our optimal grip size (i.e. distance between thumb and index finger tip) can best apply forces at the fingertips. The small aperture grey grasp in Figure 1.4c allows for a stable grasp. Large deviations from this aperture will make it difficult or even impossible to apply the necessary forces for a successful grasp (see blue grasp in Figure 1.4c).

1.3.2.6 Visibility

Object visibility can be affected by how we choose to position our hand (Bozzacchi et al., 2018; Huang et al., 2012; Maiello et al., 2019; Paulun et al., 2014; Volcic & Domini, 2014). In Figure 1.4f, the red grasp occludes the majority of the grasped object, whereas the grey grasp leaves almost the entire stapler visible during the grasp. Visual feedback is found to be particularly important during later stages of the reach movement (Bozzacchi et al., 2018; Churchill et al., 2000; Fukui & Inui, 2013a, 2013b; Gentilucci et al., 1994; Rand et al., 2007), but it was also found that during handling, grasp locations that allow for more visibility of the object are preferred over occluding grasp points (Maiello & Paulun, 2019).

1.3.2.7 Task

Even though, the touch technically only consists of the two components making contact (object and hand), the task or goal of movement, however, is another key factor influencing where and how we execute the movement to perform the grasp (Napier, 1956). The timing of the movement onset is not merely limited by the muscles' electromechanical delay times, but task complexity as well. Henry and Rogers (1960) found that reaction times increased with task complexity. It has also been shown that

we may even choose an initially more uncomfortable grasp pose, in order to achieve a comfortable pose at the end of the grasp movement, where we might release the grasp. This concept is known as end-state comfort (Rosenbaum et al., 1990).

These factors have been extensively studied and continue to amaze researchers interested in grasping. It has not yet been solved, how the human brain computes how these factors affect stable grasping, how they interact, and what their relative importance is. This thesis will investigate the importance and the interaction of multiple factors, as well as how our brain computes successful grasp locations.

1.4 Beyond precision grips

Objects can be grasped and moved in different ways: using power grips or precision grips. With ease, we can configure our hands in many distinct ways. This depends on the size, shape, weight, and ease of handling of the object. Precision grips are used for small, delicate objects, whereas power grips are better suited for large, heavy objects. But how do we go from a visual representation of an object in front of us with a specific task in mind (e.g. seeing the stapler on my desk and wanting to staple my latest publication) to configuring our hand in a pose, appropriate to perform the required action (stapling a couple pages together at the top corner (see Figure 1.4e))? Even if we think of the goal of the action as "stapling", most grasping actions' key goals include not dropping the object and therefore establishing and maintaining a stable grasp.

Even over the course of a single task with a single object, the hand adopts different grips to adjust to changing force/torque conditions. The role of task forces and torques on grip choice is most apparent when the hand shifts between grips during a task. Imagine, e.g., unscrewing a jar lid. In this case, additional friction and torque are desired, as they are required to open the jar. For extra torque, the palm of the hand is pressed against the lid in the beginning. With the lid loosening, dexterity becomes more important than torque, causing the hand to adopt a light grip where only the fingertips touch the jar lid. Napier first noticed this task dependence (Napier, 1956) and suggested categorizing grasps based on their function rather than their appearance. He divided grasps into precision grips and power grips.

1.4.1 Power grips

Power grips are characterized by large areas of contact between the grasped object and the fingers and palm, and almost no ability for the fingers to impart motion. Power grips are used to hold objects in the palm of the hand and use long flexor tendons to pull the fingers and thumb in order to tightly grasp them. Where considerations of stability and security predominate (as in holding a hammer or getting a jar lid unstuck) a power grasp is chosen. A heavier object and a smoother surface require more strength to move and hold. Where considerations of sensitivity and dexterity predominate instead, a precision grasp is chosen. In precision grasps, the object is held with the tips of the fingers and thumb.

1.4.2 Grasp Taxonomies

There are several examples of grasp taxonomies in the literature (Abbasi et al., 2016; Feix et al., 2016; Stival et al., 2019). In one study, concerned with grasp classification, canonical hand poses are primarily based on observations. The recent study (Feix et al., 2016) has converged on a set of 33 different grasp types, by comparing publications from the field of robotics, biomechanics,

occupational therapy, and developmental medicine. They divide grasps into power, intermediate, and precision grips using two to five digits. How these, however, compare to our everyday grasp poses used in unconstrained life remains unclear. A data driven approach is needed to check, how grasps cluster. Ideally, an approach capable of replicating soft tissue deformations while grasping. These occur at the fingertips of the human hand during contact, as a human grasp does not only produce one individual contact point per finger/thumb. In fact, humans can use haptic feedback, also derived through these deformations and tactile mapping to recognize objects and infer their characteristics.

A more recent study (Sundaram et al., 2019) presents a tactile glove, for which a cognitive neural network (CNN) can accurately classify eight different pantomimed grasps. The same glove is used to grasp 26 objects, which can be recognized by how their surface connects to our hand. This compares our hand's surface to a haptic grip retina. In the future modelling will open the door into predicting grips, even taking into account soft tissue deformations that occur at our fingertips or wherever else the skin deforms upon contact with the grasped object or itself. As a result, we will be able to move from the selection of contact points to studying contact areas on an object.

1.5 Two-streams hypothesis

The human brain controls fine and complex movements, such as grasping. The right hand is controlled by the left hemisphere of the brain and vice versa. In the early 1990s David Milner and Mel Goodale proposed the two-streams hypothesis (TSH) that argued for a dorsal visual processing stream associated with vision-for-action and an anatomically and functionally independent ventral processing stream that deals with object perception and recognition. This model has been extremely successful in driving forward our understanding of the visual brain and has inspired a considerable amount of research investigating visually guided behavior.

After performing multiple macaque monkey lesion studies, Unglerleider and Mishkin were the first to postulate that the dorsal processing stream, the ‘where-pathway’, spreads from V1 dorsally to the parietal lobe and processes location, distance, relative position, position in egocentric space, and motion (Mishkin & Ungerleider, 1982). The ventral processing stream, the ‘what-pathway’, allows perceiving and recognizing shape, orientation, size, objects, faces, and text.

Milner’s and Goodale’s TSH suggested the different perceptual processing streams should be outlined in terms of what the visual information is used for, instead of what type of input is received. The TSH postulates a clear anatomical and functional separation between the two steams, with no or minimal cross-talk between the two pathways. The ventral pathway (the ‘what-pathway’) is concerned with visual recognition, memory, and emotional content and may lead to a conscious percept. No introspection is possible along the dorsal route (the ‘how-pathway’), which processes visual information for action and feeds into the motor cortex and frontal lobe. In both cases the TSH assumes a linear, hierarchical relationship between the posterior and anterior processing stages of each pathway.

When the availability of research methods grew, the original TSH has been challenged a number of times (e.g., de Haan & Cowey, 2011; Jackson & Shaw, 2000; Jeannerod & Jacob, 2005; Mishkin & Ungerleider, 1982; Rizzolatti & Matelli, 2003; Rossetti et al., 2003; Schenk & McIntosh, 2010; Singh-Curry & Husain, 2009). Functional brain imaging became available and made whole-brain, connectivity, and functional brain network analyses possible. Together with the use of computer-intensive modelling some objections to core ideas of the TSH were raised. Specifically, the clear

anatomical and functional independence of the two streams, based on a double dissociation of visual form agnosia and optic ataxia, could no longer be sustained.

On the journey of understanding visual perception for action, which is what this thesis is concerned with, functional brain imaging provides an exciting tool to investigate how brain networks encode object material and object weight for grasping. Given that visual perception of object shape and material distribution are putatively a ventral-stream function; whereas, grasping is putatively a dorsal-stream function, we investigated the role of brain regions in both streams during grasping of multi-material objects. Compared to the original TSH, the brain's functional anatomy is argued to have (1) increased complexity in the processing of object representations and visually guided actions, to have (2) more visual processing streams than originally hypothesized, as well as (3) a set of highly interactive brain networks that can combine flexibly and dynamically according to the tasks at hand. In Chapter 4, we provide insights into which regions from both visual streams are recruited, when materials and their distribution are relevant for grasping.

1.6 Overview: Motivation and core questions

Precision grip grasping seems like a trivial task, but there are many combinations of two contact points between object and digit, which yield uncomfortable and impossible grasps. Consequently, the task of finding and executing successful and suitable grasps is far from trivial. In our research, we aim to answer the questions:

How does our brain compute which grasp configuration will be successful?

Which factors play the largest role in grasp selection
and how do multiple factors interact?

STUDY I

Predicting precision grip grasp locations on three-dimensional objects

Our first study aimed at solving which grasp configurations were employed to pick up objects and to reveal what individual aspects of those grasps made them favorable. We recorded and analyzed grasping behavior and then combined the results with a computational model to predict where novel objects would be grasped to answer the question:

What factors determine optimal grasp locations
and optimal human grasp poses?

In our experiments, human participants grasped different 3D objects with a precision grip. We tracked their movements with markers on their thumb and index finger, connected to an Optotrak motion capture system, to measure the contact points between object surface and thumb and index finger. The objects varied in shape, material configuration, and orientation and were made up of wooden and brass cubes. For our final experiment, we 3D printed smooth plastic objects.

We found that human grasps were highly regular and constrained. For any given object, grasp clusters occupied only a very small portion of the entire graspable space available to the thumb and index finger. Our research showed that the grasps on our objects clustered following only a few constraints. These *optimal grasp constraints* included criteria based on:

Force closure

The surface normals of a two-digit grasp in force closure needed to be approximately aligned for a stable grasp. This is a physical necessity.

Minimum torque

A high torque grasp (where the connection between digit contact points was far from the object's center of mass) would produce an unstable grasp where the object tended to rotate under gravity. Our experiments confirmed that object mass and mass distribution modulated grasp point selection in such a way that participants aimed to reduce torque.

Natural grasp axis (NGA)

When grasping spheres, cylinders, or simple shapes, humans exhibited a preferred grasp orientation, in which the vector between thumb and index finger is called the *Natural grasp axis, or NGA* (Cuijpers et al., 2004; Lederman & Wing, 2003; Paulun et al., 2016; Roby-Brami et al., 2000; Schot et al., 2010; Voudouris et al., 2010).

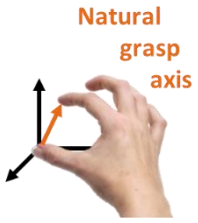

Optimal grasp aperture (OGA)

Due to their limited movement range, our fingers have an optimal grip size (i.e. distance between thumb and index finger tip) in which we can best apply forces at the fingertips. Large deviations from this *Optimal grasp aperture (OGA)* would make it challenging or even unmanageable to apply the necessary forces to form a successful grasp.

Optimal visibility

Related behavioral work (Maiello et al., 2019) suggested that participants aimed to keep object occlusion to a minimum as they grasped it. In our study, we observed that participants favored grasps that enabled good visibility of the object over grasps where their hand would occlude large portions of the object.

For each constraint and each arbitrary 3D object, we could compute how far away every possible grasp was from optimally satisfying each of the five constraints. We computed for every combination of index finger and thumb contact points on the object, how far that combination was away from fulfilling e.g., force closure. We used this procedure to reveal optimal grasp configurations for each factor. We then combined the results for all five factors to create a global *penalty map*, which showed at its minima the overall optimal grasp locations. Projecting the human grasps from our experiments onto our maps, revealed that they neatly aligned with the maps' minima.

Conversely, to investigate where predicted, optimal grasp locations were located on the objects, we projected optimal grasp locations, i.e., minima from our maps, onto our objects. We found that those were very similar to the human data. Furthermore, the model even worked beyond the blocky, wooden and brass objects for which the model was initially designed: in a final experiment, we 3D printed novel, curvy objects out of a lightweight plastic. Even these were grasped by participants at locations very similar to those predicted by our model.

Thus far, our work showed that human grasps align with our optimal grasp constraints. Yet, there were various questions that still needed to be addressed. We were interested in where and how humans computed these constraints and how they interacted.

STUDY II

Friction in preferred over grasp configuration in precision grip grasping

An object's material properties affect how humans can appropriately interact with it. In our first study, we had incorporated the material related properties of object mass and mass distribution through the factor *torque* into our model. Previous studies suggest that *surface friction* is another important factor affecting the selection of grasp locations, because low friction surfaces required greater grasp force to stabilize the grasp. In this study, we therefore evaluated the importance of surface friction in grasp selection by posing the question

How do multiple grasp relevant factors interact:
is grasp stability or grasp configuration considered more important?

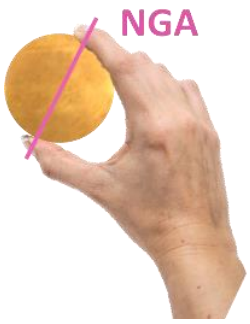

In this study we pitched surface friction against a constraint that had a strong influence on grasping in our previous study: the natural grasp axis (NGA). First, we measured each individual participant's preferred grasp posture, their NGA, using a brass cylinder. Then we used three cuboids of identical weight made of brass with manipulated surfaces. One object was a brass cuboid, the other was the same brass cuboid, except that two opposing sides were covered with a thin strip of wood, providing slightly higher friction than the brass surfaces. Two of the third cuboid's sides were covered with sandpaper while the other sides were smeared with Vaseline to make them slippery.

In one experimental condition the objects' corners were aligned to the individual NGA. That means that the NGA effectively splits the object in half along its diagonal. If the NGA were the only factor influencing where participants grasped, by design, participants should not have had a preferred pair of sides in this experimental condition. Consequently, their grasps should have fallen on either side 50% of the time. If, however, surface friction played a role in choosing where to grasp, their grasps should have fallen on a favored pair of sides. We found that the latter hypothesis held true, as participants favored the higher friction surfaces.

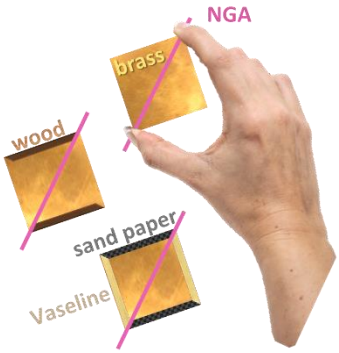

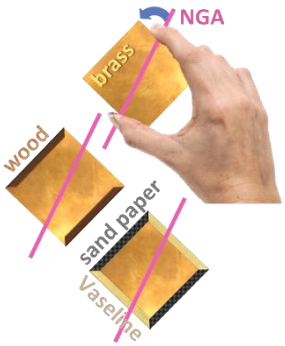

The second set of conditions investigated further, how this strong influence of surface friction compared to the previously identified strong influence of the NGA. We rotated the object corners away from the NGA, practically aligning one pair of sides with the NGA. While the brass object was grasped almost exclusively at the NGA-aligned pair of sides, the sand paper-Vaseline object was grasped away from the NGA, when the Vaseline-covered sides were aligned with it. We found that surface friction played a key role in grasp selection, strong enough to even overrule grasp locations potentially dictated by the NGA. Participants adopted even highly unusual grasp poses in order to grasp higher friction surfaces.

STUDY III

Distinct neural components of visually guided grasping during planning and execution

We conducted an fMRI study to identify the brain networks for planning and executing visually guided grasping. We focused on a subset of factors that previous research confirmed to be relevant to grasp selection: Grasp axis, aperture, and object weight. Specifically, we selected specific grasps on L-shaped, multi-material objects that disentangled the relative contributions of these factors, by using a computational approach, which predicted human grasp locations. Which brain networks were responsible for computing certain grasping constraints was still unknown. Previous studies suggested that selection of the grasp axis and aperture were putatively a dorsal stream function, while visually estimating material properties relevant for estimating torque was putatively a ventral stream task. Furthermore, the timing of these computations remained unclear. That lead to the questions:

Which distinct grasping constraints are
represented in distinct cortical areas and which brain networks?
Which attributes of grasping are coded before and which after initiation of the grasp?

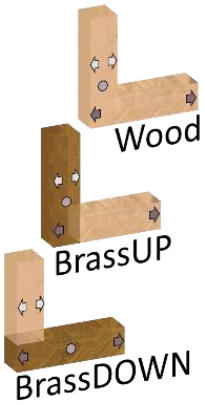

We asked participants to grasp three real L-shaped objects, one made of wood and the others made of wood and brass. Specific grasps were cued on the objects, preselected in order to differentiate our three components of grasping. I.e., in terms of the necessary hand orientation, a chosen grasp would be close to ideal, but its aperture might be suboptimal. In each trial, participants first visually planned and then executed the cued grasp. As these grasps were being planned and executed, we examined blood-oxygen-level-dependent (BOLD) activity using fMRI.

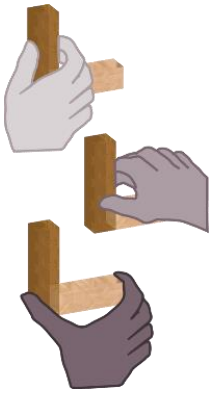

The conditions were selected, specifically so that they would create three uncorrelated representational dissimilarity matrices (RDMs) for each model of interest. We correlated neural activation patterns in regions of interest (ROIs) along both, dorsal and ventral streams, with our model RDMs during planning and execution phases.

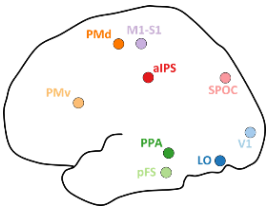

We found that grasp axis was strongly encoded through visual and motor regions along the dorsal pathway during the planning phase. Grasp aperture was encoded in ventral and pre-motor areas during both planning and execution of the grasp. Object mass was more robustly encoded during grasp execution in dorsal and ventral stream and motor areas. In general, sensorimotor processing switched from grasp planning in the dorsal stream over to the ventral stream during grasp execution. Overall, dorsal and pre-motor areas encoded the components tied to our hand movements during grasp planning, whereas ventral areas involved in encoding grasp-relevant object properties were recruited in the execution phase. Presumably, this was when forces, related to object mass, needed to be applied and adjusted.

Taken together, the research presented in this thesis shows that humans used visually perceived, action-relevant physical object properties to plan how to grasp an object. Our behavioral experiments demonstrate how intrinsic and extrinsic object properties were combined with constraints imposed by the anatomy of the human hand to determine grasp locations. Specifically, our approach uncovered interactions between different constraints, which allowed us to accurately predict grasp locations for novel objects. Our neuroimaging investigations instead uncovered, for different the stages of a grasp, the distinct networks of brain areas involved in computing the different constraints.

Chapter 2

STUDY I
Predicting precision grip grasp locations on three-dimensional objects

A similar version of this manuscript has been published as:

Klein, L. K., Maiello, G., Paulun, V. C., & Fleming, R. W. (2020). Predicting precision grip grasp locations on three-dimensional objects. PLOS Computational Biology, 16(8), e1008081. https://doi.org/10.1371/journal.pcbi.1008081

We rarely experience difficulty picking up objects, yet of all potential contact points on the surface, only a small proportion yield effective grasps. Here, we present extensive behavioral data alongside a normative model that correctly predicts human precision grasping of unfamiliar 3D objects. We tracked participants' forefinger and thumb as they picked up objects of 10 wood and brass cubes configured to tease apart effects of shape, weight, orientation, and mass distribution. Grasps were highly systematic and consistent across repetitions and participants. We employed these data to construct a model which combines five cost functions related to force closure, torque, natural grasp axis, grasp aperture, and visibility. Even without free parameters, the model predicts individual grasps almost as well as different individuals predict one another's, but fitting weights reveals the relative importance of the different constraints. The model also accurately predicts human grasps on novel 3D-printed objects with more naturalistic geometries and is robust to perturbations in its key parameters. Together, the findings provide a unified account of how we successfully grasp objects of different 3D shape, orientation, mass, and mass distribution.

2.1 Introduction

In everyday life, we effortlessly grasp and pick up objects without much thought. However, this ease belies the computational complexity of human grasping. Even state of the art robotic AIs fail to grip objects nearly 20% of the time (Levine et al., 2018). To pick something up, our brains must work out which surface locations will lead to stable, comfortable grasps, so we can perform desired actions (Figure 2.1a). Most potential grasps would actually be unsuccessful, e.g., requiring thumb and forefinger to cross, or failing to exert useful forces (Figure 2.1b). Even many possible grasps would be unstable, e.g., too far from the object's center, so it rotates when lifted (Figure 2.1c). Somehow, the brain must infer which, of all potential grasps, would actually succeed. Despite this, we rarely drop objects or find ourselves unable to complete actions because we are holding them inappropriately. How does the brain select stable, comfortable grasps onto arbitrary 3D objects, particularly objects we have never seen before?

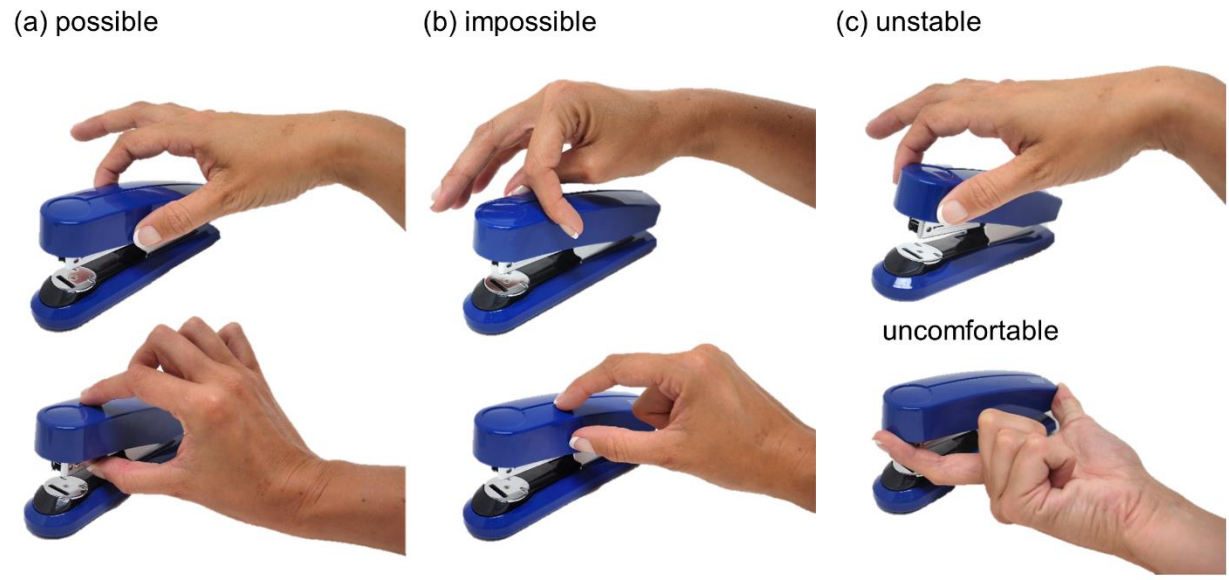

Figure 2.1. The computational complexity of human grasp selection. (a) Possible (b) Impossible (c) Possible but uncomfortable or unstable grasps.

Despite the extensive literature describing human grasping patterns, movement kinematics, and grip force adjustments (Bozzacchi et al., 2016; Christopoulos & Schrater, 2009; Eloka & Franz, 2011; Goodwin et al., 1998; Jenmalm & Johansson, 1997; Johansson & Westling, 1984b; Karok & Newport, 2010; Rosenbaum, Meulenbroek, Vaughan, & Elsinger, 1999; Rosenbaum, Meulenbroek, Vaughan, & Jansen, 1999; Smeets & Brenner, 1999; Smeets & Brenner, 2001; Volcic & Domini, 2014, 2016), little is understood about the computational basis of initial grasp selection. Few authors have attempted to study and model how humans select grasps (e.g. Gilster et al., 2012; Kleinholdermann et al., 2013), and even then, only for 2D shapes. This is because, even for two-digit precision grip, many factors influence grasping. Object shape must be considered, since the surface normals at contact locations must be approximately aligned (a concept known as force closure (Nguyen, 1988)), otherwise the object will slip through our fingertips (Figure 2.1b, bottom). Object mass and mass distribution must be evaluated, since for grips with high torques (i.e. far from the center of mass, CoM (Eastough & Edwards, 2006; Goodale et al., 1994; Lederman & Wing, 2003; Lukos et al., 2007; Paulun et al., 2016))

the object will tend to rotate under gravity and potentially slip out of our grasp (Figure 2.1c, top). The orientation (Lederman & Wing, 2003; Paulun et al., 2016; Roby-Brami et al., 2000; Schot et al., 2010; Voudouris et al., 2010) and size (Cesari & Newell, 1999) of grasps on an object must be considered, since the arm and hand can move and apply forces only in specific ways. Grasps that do not conform to the natural configuration of our hand in 3D space might be impossible (Figure 2.1b, top), or uncomfortable (Figure 2.1c, bottom). The hand's positioning may also determine an object's visibility (Bozzacchi et al., 2018; Huang et al., 2012; Maiello et al., 2019; Paulun et al., 2014; Volcic & Domini, 2014).

Most previous research did not assess the relative importance of these factors, nor how they interact. Here we sought to unify these varied and fragmented findings into a single normative framework. We therefore constructed a rich dataset in which we could tease apart how an object's 3D shape, mass, mass distribution, and orientation influence grasp selection. We devised a set of objects made of wood and brass cubes in various configurations (Figure 2.2), and asked participants to pick them up with a precision grip, move them a short distance and place them at a target location, while we tracked their thumb and forefinger. We measured initial contact locations (i.e. not readjusted contact regions during movement execution). By varying the shapes and orientation of the objects in Experiment 1, we (i) determined how consistent at selecting grasp locations participants are with themselves and other people, and (ii) measured the interactions between allocentric 3D shape and egocentric perspective on those shapes. If actors take the properties of their own effectors into account (e.g., hand orientation, grasp size), we should expect the same shape to be grasped at different locations depending on its orientation relative to the observer (Lederman & Wing, 2003). In Experiment 2, we varied the mass and mass distribution of the objects (Figure 2.2c) to test the relative role of 3D shape and mass properties. If participants take torques into account, identical shapes with different mass distributions should yield systematically different grasps (Eastough & Edwards, 2006; Goodale et al., 1994; Lukos et al., 2007; Paulun et al., 2016).

Next, we employed this rich dataset to develop a computational model to predict human grasp patterns. We reasoned that grasps are selected to minimize costs associated with instability and discomfort. Accordingly, we implemented a model that combines five factors computed from the object's shape, mass distribution, and orientation: (i) force closure (Nguyen, 1988), (ii) torque (Eastough & Edwards, 2006; Goodale et al., 1994; Lederman & Wing, 2003; Lukos et al., 2007; Paulun et al., 2016) (iii) natural grasp axis (Lederman & Wing, 2003; Roby-Brami et al., 2000; Schot et al., 2010; Voudouris et al., 2010), (iv) natural grasp aperture for precision grip (Cesari & Newell, 1999) and (v) visibility (Huang et al., 2012; Paulun et al., 2014). The model takes as input a near-veridical 3D mesh representation of on object to be grasped, performs free-body computations on the mesh, and outputs minimum-cost, optimal grasp locations on the object. We found that the optimal grasps predicted by the model matched human grasp patterns on the wooden and brass polycube objects from Experiments 1 and 2 strikingly well. We then employed the model to generate predictions regarding where humans should grasp novel shapes with curved surfaces. In a final Experiment 3, we had participants grasp these novel 3D-printed, curved, plastic objects. Human grasps well aligned with the model predictions. Finally, we employed these data to show that model predictions are robust to perturbations in the model input and key parameters.

2.2 Results

2.2.1 Experiment 1: 3D shape and orientation

2.2.1.1 Human grasps are tightly clustered and represent a highly constrained sample from the space of potential grasps

Twelve participants grasped four objects made of beech wood presented at two orientations (Figure 2.2a,b; see Methods). Figure 2.3a shows how grasp patterns tend to be highly clustered. In each condition, different grasps have similar sizes (finger-to-thumb distance) and orientations, and also cover the same portions of the objects. Fitting multivariate Gaussian mixture models to the responses reveals that grasps cluster around only 1, 2, or 3 modes. Figure 2.3b shows three distinct modes for object U at orientation 2 in a unitless 2D representation of grasp space. Human grasps cover only a minute portion of the space of potential grasps. Note that we define the space of potential grasps as the set of all combinations of thumb and index finger positioning attemptable on the accessible surfaces of an object (i.e., those not in contact with the table). Figure 2.3c also shows how, for one representative condition, different grasps from the same subjects are more clustered than grasps from different subjects, since individuals predominantly selected only one (70%) or two (27%) modes, and only rarely (3%) grasped objects in three separate locations.

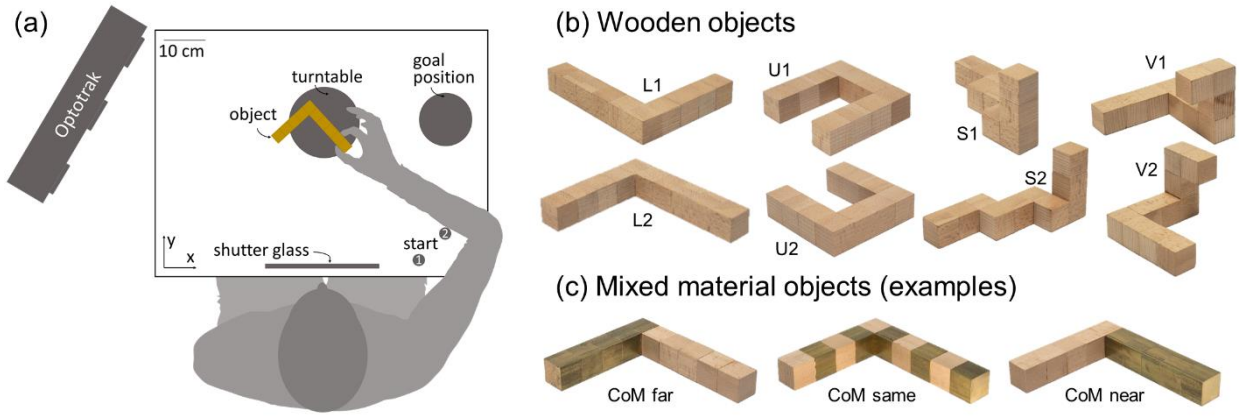

Figure 2.2. Setup and stimuli for Experiments 1 and 2. (a) Experimental setup. Seated participants performed grasping movements with their right hand. Following an auditory signal (coinciding with the shutter window turning transparent) they moved from one of the starting positions to the object and grasped it with a precision grip. They transported and released the object at the goal position and returned to the start position. (b) In Experiment 1 we employed four objects made of wooden cubes. Each object had a unique shape (that here we name L, U, S, V) and was presented at one of two different orientations with respect to the participant. (c) In Experiment 2 the objects had the same shapes as in Experiment 1, but now were made of wood and brass cubes. The brass and wood cubes were organized either in an alternate pattern (middle), so that the CoM of the object would remain approximately the same as for the wooden object, or grouped so that the CoM would be shifted either closer to (right) or away from (left) the participant's hand starting location.

To further quantify how clustered these grasping patterns are we designed a simple metric of similarity between grasps (see Methods). Figure 2.3d shows how both between- and within-subject grasp similarity are significantly higher than the similarity between random grasps only constrained by accessible object geometry ($t(7)=9.96$, $p=2.2*10^{-5}$ and $t(7)=26.15$, $p=3.1*10^{-8}$ respectively).

Additionally, within-subject grasp similarity is significantly higher than between subjects (t(7)=3.89, p=0.0060). Nevertheless, the high similarity between grasps from different participants demonstrates that different individuals tend to grasp objects in similar ways. The even higher level of within-subject grasp similarity further demonstrates that grasp patterns from individual participants are idiosyncratic, which may reflect differences in the strategies employed by individual participants, or may be related to physiological differences in hand size, strength, or skin slipperiness. We observe no obvious learning effects across trial repetitions: between-subject grasp similarity does not change from first to last repetition across objects and orientations (t(7)=0.62, p=0.56).

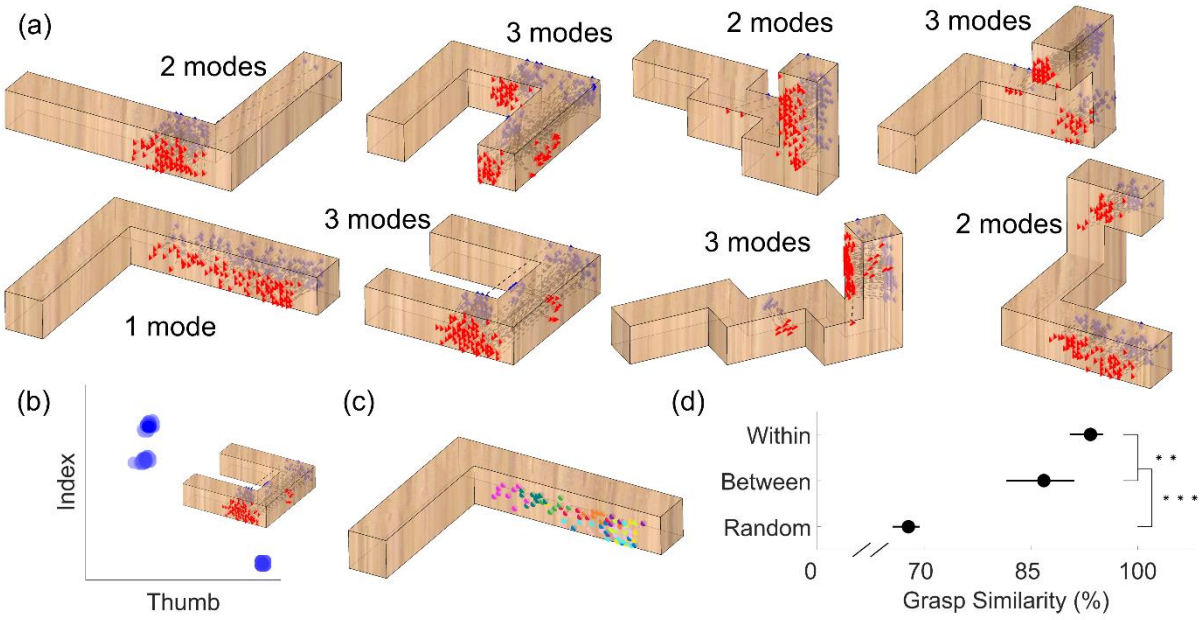

*Figure 2.3. Human grasps are clustered. (a) Human grasps from Experiment 1. Grasps are represented as thumb (red triangles) and index finger (blue diamonds) contact positions, connected by dotted black lines. (b) Human grasps (blue blobs) for object U, orientation 2, when projected in a unitless 2D representation of the space of potential grasps, cluster around three distinct modes. (c) Distribution of thumb contact points on object L, orientation 2. Different colors represent grasps from different participants. (d) The level (%) of grasp similarity expected for grasps randomly distributed on the object surface (i.e. random combinations of thumb and index finger positioning attemptable on an object) and the observed level of between- and within-participant grasp similarity, averaged across objects and orientations. Error bars are 95% bootstrapped confidence intervals of the mean. ** p<0.01, *** p<0.001*

2.2.1.2 Findings reproduce several known effects in grasp selection

Previous research suggests haptic space is encoded in both egocentric and allocentric coordinates (Volcic & Kappers, 2008), and that grasps are at least partly encoded in egocentric coordinates to account for the biomechanical constraints of our arm and hand (Lederman & Wing, 2003). Our findings reproduce and extend these observations. If humans selected grasps in allocentric coordinates tied to an object's 3D shape, then grasps onto the same object in different orientations should be located on the same portions of the object but in different 3D world coordinates. Conversely, if actors take their own effectors into account, they should grasp objects at different locations depending on the object's orientation. For each object we computed grasp similarity across the two orientations in both

egocentric (tied to the observer) and allocentric coordinates (tied to the object). Figure 2.4a shows that, as the extent of the object rotation increases, grasp encoding shifts from allocentric to egocentric coordinates. Across small rotations (object S, 55 degree rotation), grasps are more similar if encoded in allocentric coordinates ($t(11)=13.90$, $p=2.5*10^{-8}$), whereas for large rotations (object L, 180 degrees) grasps are more similar if encoded in egocentric coordinates ($t(11)=4.59$, $p= 7.8*10^{-4}$). Therefore, both 3D shape as well as movement constraints influence grasps.

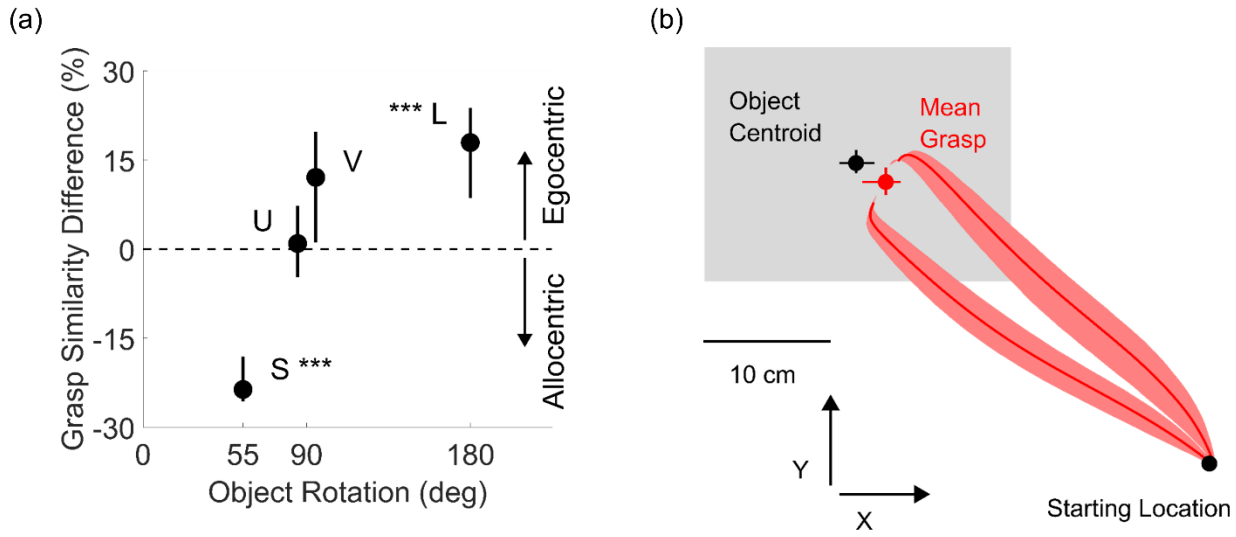

*Figure 2.4. Spatial encoding and bias. (a) Difference in grasp similarity across orientations when grasps were encoded in object-centered (allocentric) vs human-centered (egocentric) coordinates, as a function of magnitude of rotation across the two orientation conditions. (b) Average grasp trajectories viewed in the x-y plane (red curves) from start location towards the objects (always contained within the gray shaded region). The average human grasp (red dot) across conditions is biased toward shorter reaching movements compared to the object centroids (black dot). In both panels data are means, error bars/regions represent 95% bootstrapped confidence intervals. *** p<0.001*

Figure 2.4b shows that participants also selected grasps that were on average 26 mm closer to the starting location than the object centroid ($t(11)=9.74$, $p=9.6*10^{-7}$), reproducing known spatial biases in human grasp selection (Desanghere & Marotta, 2015; Glowania et al., 2017; Kleinholdermann et al., 2013; Maiello et al., 2019; Paulun et al., 2014).

Consistent with Kleinholdermann et al. (2013) but contrary to previous claims (Eastough & Edwards, 2006; Goodale et al., 1994; Lederman & Wing, 2003; Lukos et al., 2007; Paulun et al., 2016), our findings suggest humans care little about torque when grasping lightweight objects (of ~100 g). If actors sought to minimize torque, the selected grasps should be as close as possible to the CoM. Conversely, if participants were to disregard torque, then grasps should be at least as distant from the CoM as grasps randomly selected on the surface of the object. Figure 2.5a plots the difference between the CoM distance of participant grasps and the average CoM distance of random grasps, which we name 'CoM attraction compared to random grasps'. In Experiment 1, grasps were on average 9 mm farther from the CoM than the average distance to the object's CoM of grasps uniformly sampled onto the surface of the objects ($t(11)=4.53$, $p=8.6*10^{-4}$). This negative value means that

participants grasped the objects towards their extremities, farther from the CoM than even random chance.

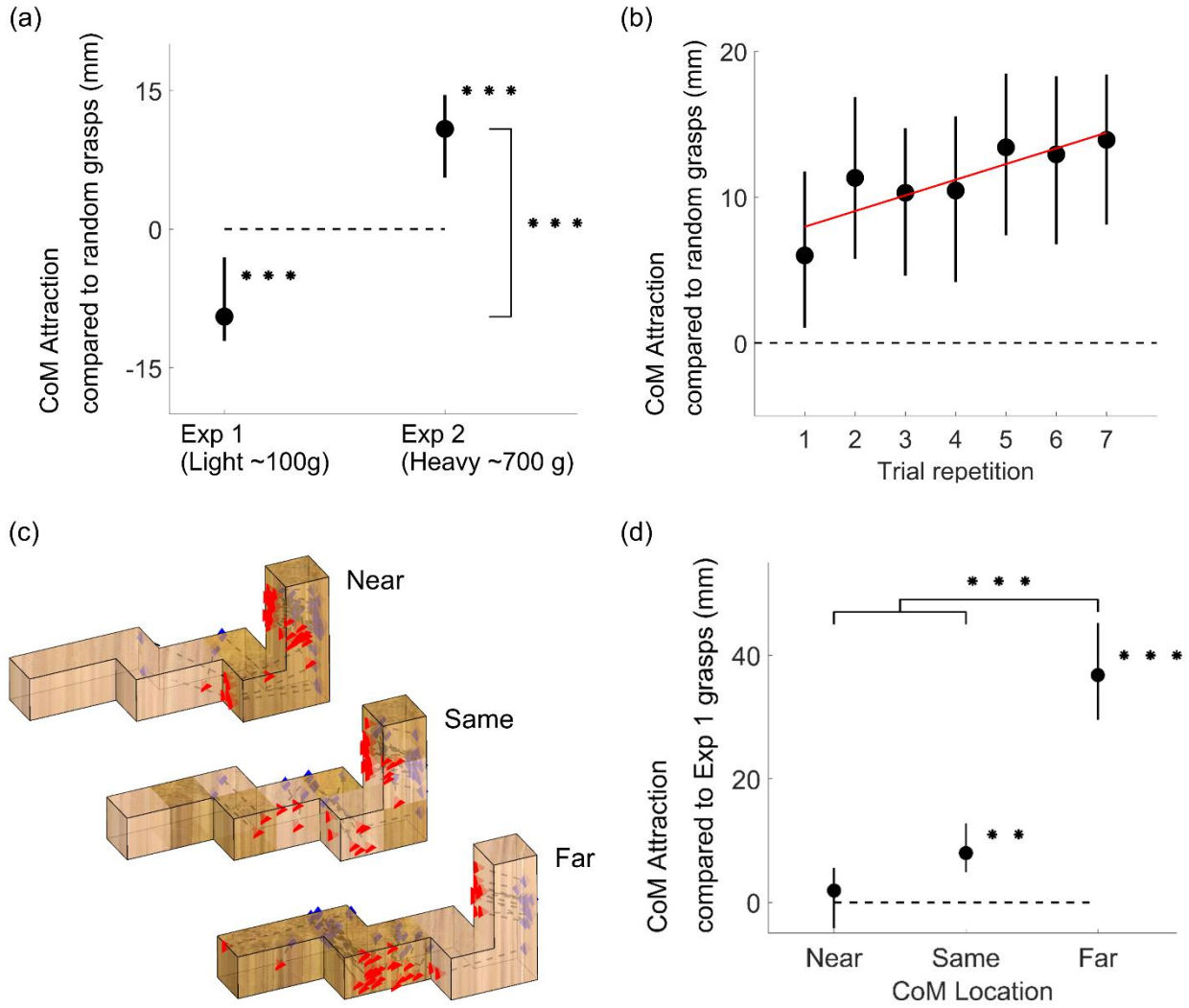

*Figure 2.5. Mass and Mass Distribution. (a) Attraction towards the object CoM for grasps executed onto light (Experiment 1) and heavy (Experiment 2) objects compared to the average CoM distance of grasps uniformly distributed on the object surfaces (zero reference). (b) Attraction towards the object CoM in Experiment 2 as a function of trial repetition. Red line is the best-fitting regression line through the data (c) Human grasps from Experiment 2 onto object S presented at orientation 2. (d) Attraction towards the object CoM compared to Experiment 1 grasps (zero reference), for Experiment 2 grasps onto heavy objects whose CoM is closer, the same distance as, or farther than the light wooden objects from Experiment 1. In panels a, b, and d, data are means, error bars represent 95% bootstrapped confidence intervals. ** p<0.01, *** p<0.001*

2.2.2 Experiment 2: Mass and Mass Distribution

2.2.2.1 Humans grasp objects close to their center of mass when high grip torques are possible and instructions demand the object does not rotate

Due to the low density of beech wood, even the grasps farthest from the CoM in Experiment 1 would produce relatively low torques. Therefore, in Experiment 2 we tested whether participants grasp

objects closer to the CoM when higher torques are possible. We did this by using objects of greater mass and asymmetric mass distributions. Specifically, for each of the shapes in Experiment 1, we made three new objects, each made of five brass and five wooden cubes: two 'bipartite' objects, with brass clustered on one or the other half of the object, and one 'alternating' object, with brass and wood alternating along the object's length. These objects had the same 3D shapes as in Experiment 1, but were nearly tenfold heavier (Figure 2.2c, see Methods).

Figure 2.5a shows how human grasps are indeed significantly attracted towards the CoM of heavy objects, presumably to counteract the larger torques associated with higher mass. In Experiment 2, grasps were on average 11 mm closer to the object CoM than grasps sampled uniformly from the objects' surfaces ($t(13)=4.89$, $p= 2.9*10^{-4}$), and on average 20 mm closer than the grasps from Experiment 1 ($t(24)=6.60$, $p= 8.0*10^{-7}$). Figure 2.5b shows how this behavior was evident already from the very first trial performed by participants, but also that grasps clustered more toward the object CoM in later trials, presumably as participants refined their estimates of CoM location (correlation between CoM attraction and trial repetition: $r = 0.86$, $p = 0.13$). Importantly, participants shifted their grasps towards the CoM—not the geometrical centroid—of the objects (observe how the grasp patterns shift in Figure 2.5c). Figure 2.5d shows that when the object CoM was shifted towards the hand's starting location, participants did not significantly adjust their grasping strategy compared to Experiment 1 ($t(13)=0.81$, $p=0.43$). Conversely, when the object CoM was in the same position as in Experiment 1, grasps shifted on average by 8 mm towards the CoM ($t(13)=3.92$, $p=0.0017$). When the CoM was shifted away from the hand's starting position, grasps were on average 37 mm closer to the CoM compared to Experiment 1 ($t(13)=8.49$, $p=1.2*10^{-6}$), a significantly greater shift than both the near and same CoM conditions ($t(13)=8.66$, $p=9.2*10^{-7}$ and $t(13)=7.58$, $p=4.0*10^{-6}$). These differential shifts indicate that participants explicitly estimated each object's CoM from visual material cues.

Even with the heavier objects, participants still systematically selected grasps that were closer to the starting location than the object centroid ($t(13)=4.03$, $p=0.0014$). However, now participants exhibited only a 9 mm bias, which was significantly smaller than the 26 mm bias observed for the light wooden objects in Experiment 1 ($t(24)=4.67$, $p= 9.6*10^{-5}$).

Together these findings suggest that participants combine multiple constraints to select grasp locations, taking into consideration the shape, weight, orientation, and mass distribution of objects, as well as properties of their own body to decide where to grasp objects. We next sought to develop a unifying model that could predict these diverse effects based on a few simple underlying principles.

2.2.2.2 Normative model of human grasp selection.

Based on the insights gained from our empirical findings, we developed a model to predict human grasp locations. The model takes as input 3D descriptions of the objects' shape, mass distribution, orientation, and position relative to the participant, and computes as output a *grasp cost function*, describing the costs associated with every possible combination of finger and thumb position on accessible surface locations (i.e., those not in contact with table). We reasoned that humans would tend to grasp objects at or close to the minima of this cost function, as these would yield the most stable, comfortable grasps. Low cost grasps can then be projected back onto the object to compare against human grasps. It is important to note that this is not intended as a process model describing internal visual or motor representations (i.e., we do not suggest that the human brain explicitly

evaluates grasp cost for all possible surface locations). Rather, it is a normative model for predicting which grasps are optimal under a set of pre-defined constraints. It provides a single, unifying framework based on a subset of the factors that are known to influence human grasp selection (Kleinholdermann et al., 2013).

For each object, we create a triangulated mesh model in a 3D coordinate frame, from which we can sample (Figure 2.6a-b). For precision grip, we assume one contact point each for thumb and index finger. Thus, all possible precision grip grasps can be ordered on a 2D plane, with all possible thumb contact points along the x-axis, and on the y-axis, all possible index contacts in the same ordering as for the thumb.

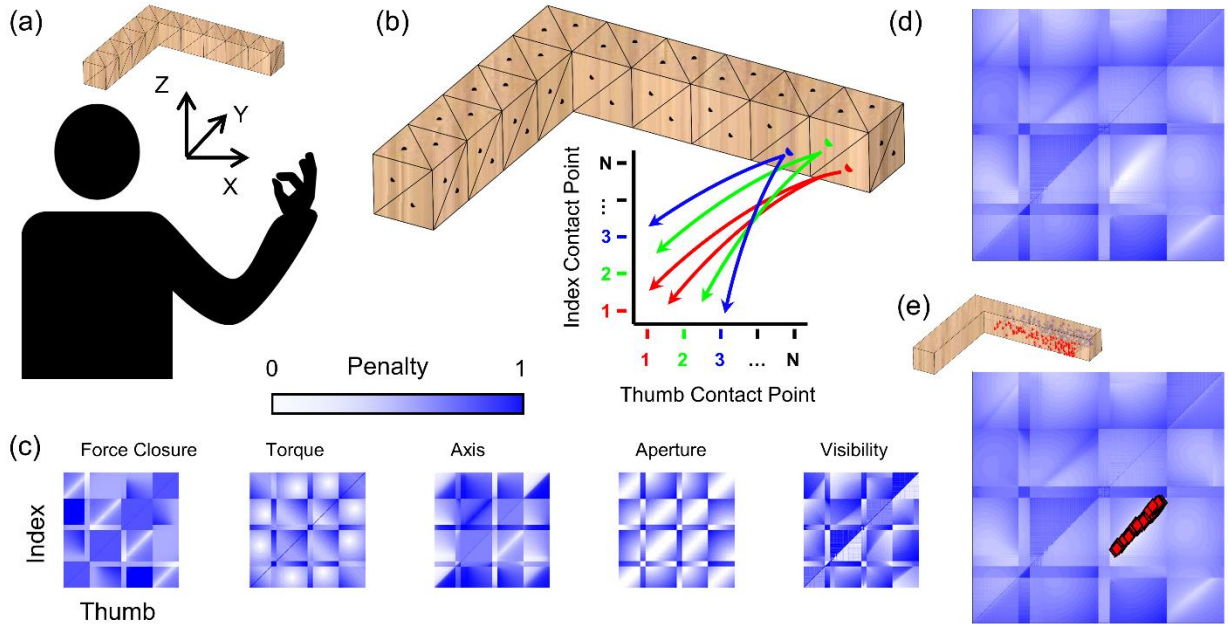

Figure 2.6. A framework that unifies distinct aspects of grasp selection. (a) Mesh model of object in same 3D reference frame as participant poised to execute grasp. (b) Discrete sampling of the reachable surface defines a 2D space containing all potential combinations of index and thumb contact points on the object. (c) Color-coded maps showing penalty values for each potential grasp for each penalty function. (d) Overall penalty function computed as the linear combination of maps in (c). (e) Human grasps projected into 2D penalty-function space neatly align with minimum of combined penalty map.

To estimate the cost associated with each grasp, we take the combination of five *penalty functions*, determined by the object's physical properties (surface shape, orientation, mass, mass distribution) as well as constraints of the human actuator (i.e. the human arm/hand). Specifically, we consider optimality criteria based on: (i) optimum force closure (Nguyen, 1988), (ii) minimum torque (Eastough & Edwards, 2006; Goodale et al., 1994; Lederman & Wing, 2003; Lukos et al., 2007; Paulun et al., 2016), (iii) alignment with the natural grasp axis (Lederman & Wing, 2003; Roby-Brami et al., 2000; Schot et al., 2010; Voudouris et al., 2010), (iv) optimal grasp aperture (Cesari & Newell, 1999), and (v) optimal visibility (Huang et al., 2012; Maiello et al., 2019; Paulun et al., 2014) (see Methods for mathematical definitions). Figure 2.6c shows maps for each penalty function: white indicates low penalty, dark blue high penalty. To compare and combine penalty, values are normalized to [0,1].

Force closure

Force closure is fulfilled when the two contact-point surface normals, along which gripping forces are applied, are directed towards each other (Nguyen, 1988). Thus, we penalize lateral offsets between the grasp point normals (Figure 2.7).

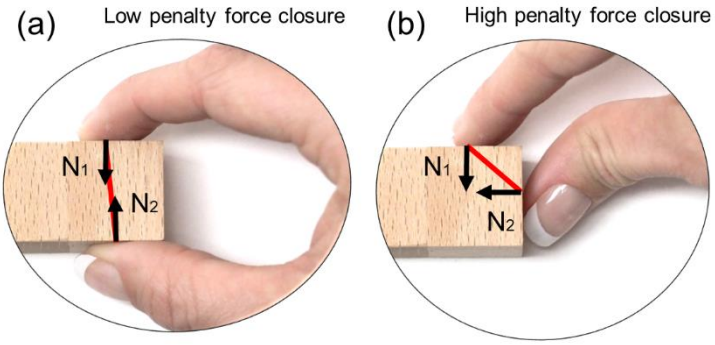

Figure 2.7. Force Closure. Examples of grasps with (a) low penalty and (b) high penalty force closure.

Minimum torque

Grasping an object far from its CoM results in high torque, which causes the object to rotate when picked up (Eastough & Edwards, 2006; Goodale et al., 1994; Lederman & Wing, 2003; Lukos et al., 2007; Paulun et al., 2016). Large gripping forces would be required to prevent the object from rotating. We therefore penalize torque magnitude (Figure 2.8).

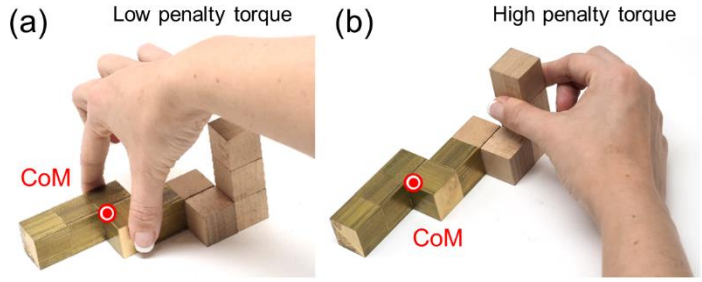

Figure 2.8. Torque. Examples of grasps with (a) low penalty and (b) high penalty torque.

Natural grasp axis

When executing precision grip grasps, humans exhibit a preferred hand posture known as the *natural grasp axis* (Lederman & Wing, 2003; Roby-Brami et al., 2000; Schot et al., 2010; Voudouris et al., 2010). Grasps that are rotated away from this axis result in uncomfortable or restrictive hand/arm configurations (Figure 2.9). We therefore penalize angular misalignment between each candidate grasp and the natural grasp axis (taken from Schot et al., 2010). Unlike force closure and torque, this penalty map is asymmetric about the diagonal: swapping index and thumb positioning produces the same force closure and torque penalties, but changes the penalty for the natural grasp axis by 180 degrees.

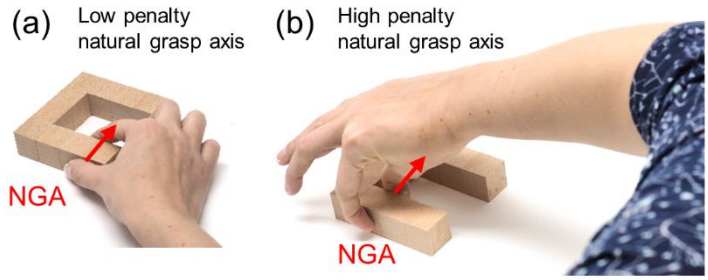

Figure 2.9. Natural grasp axis. Examples of grasps with (a) low penalty and (b) high penalty grasp axis.

Optimal grasp aperture

For two-digit precision grips humans prefer the distance between finger and thumb at contact ('grasp aperture') to be below 2.5 cm (Cesari & Newell, 1999). We therefore penalize grasp apertures above 2.5 cm (Figure 2.10).

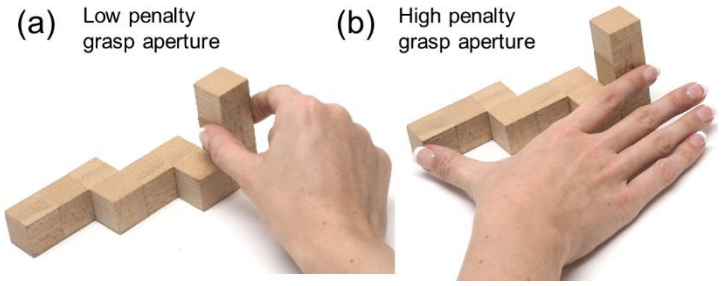

Figure 2.10. Optimal grasp aperture. Examples of grasps with (a) low penalty and (b) high penalty aperture.

Optimal visibility

Our behavioral data, and previous studies, suggest humans exhibit spatial biases when grasping. It has been proposed that these may arise from an attempt to minimize energy expenditures through shorter reach movements (Huang et al., 2012). However, Paulun et al. (2014) have shown that these biases may in fact arise from participants attempting to optimize object visibility. While our current dataset was not designed to untangle these competing hypotheses, re-analyzing published data (Maiello et al., 2019; Paulun et al., 2016) confirms that object visibility—not reach length—is most likely responsible for the biases. We therefore penalized grasps that hindered object visibility (Figure 2.11). We also designed a penalty function for reach length and verified that, since reach length and object visibility are correlated in our dataset, employing one or the other penalty function yields very similar results.

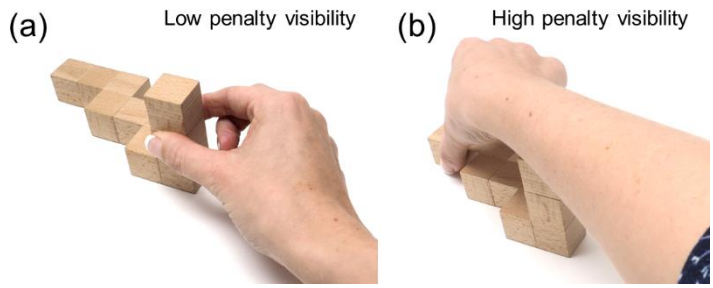

Figure 2.11. Optimal visibility. Examples of grasps with (a) low penalty and (b) high penalty visibility.

We assume that participants select grasps with low overall costs across all penalty functions. Thus, to create the overall grasp penalty function, we take the sum of the individual penalty maps. The minima of this full penalty map represent grasps that best satisfy all criteria simultaneously. The map in Figure 2.6d exhibits a clear minimum: the white region in its lower right quadrant.

To assess the agreement between human and optimal grasps, we may visualize human grasps in the 2D representation of the grasp manifold. The red markers in Figure 2.6e are the human grasps from object L at orientation 2, projected in 2D and overlain onto the full penalty map. Human grasps neatly align with the minima of the penalty map, suggesting that human grasps are nearly optimal in terms of the cost criteria we use.

Model Fitting

The simple, equal combination of constraints considered thus far already agrees with human grasping behavior quite well. However, it is unlikely that actors treat all optimality criteria as equally important. Different persons likely weight the constraints differently (e.g., due to strength or hand size). Therefore, we developed a method for fitting full penalty maps to participants' responses. We assigned variable weights to each optimality criterion, and fit these weights to the grasping data from each participant, to obtain a set of full penalty maps whose minima best align with each participant's grasps (see Methods).

Model grasps are nearly indistinguishable from measured human grasps

To compare human and optimal grasps directly, we can sample predicted optimal grasps from around the minimum of the full penalty map (see Methods) and project back onto the objects. Figure 2.12a shows human grasps (left) and unfitted model predictions (right) on a few representative objects (see Figure 2.S1 for complete set). Human and predicted grasps have similar size and orientation, and also cover similar portions of the objects.

Figure 2.12b depicts grasp similarity at the population level, i.e., across participants and between human and unfitted model grasps. Grasp similarity between participants was computed (for each object and condition), as the similarity between the medoid grasp of each participant and the medoid grasp across all others. Grasp similarity between human and model grasps was computed as the similarity between the medoid unfitted model grasp and the medoid grasp across all participants.

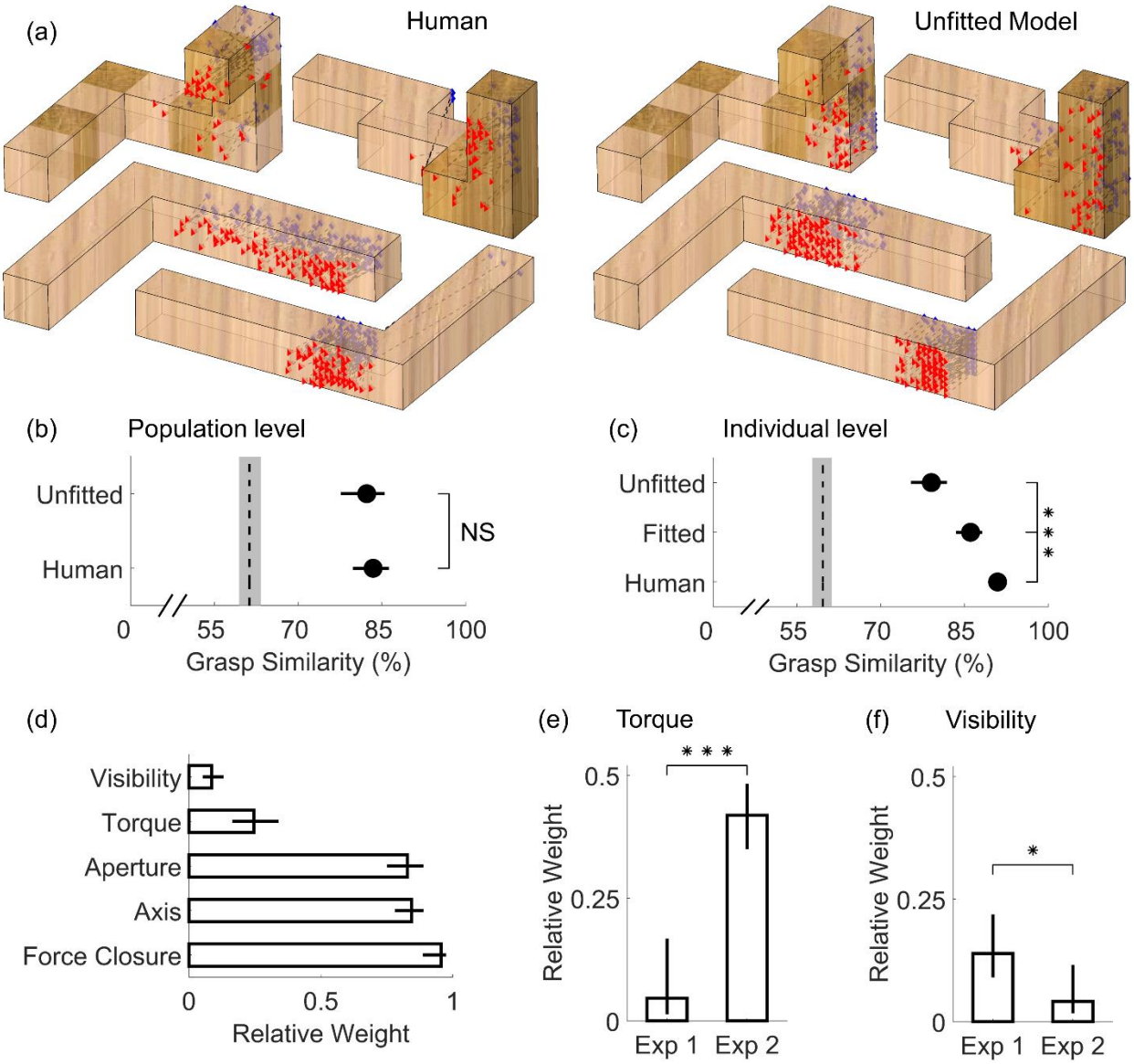

*Figure 2.12. Model Results. (a) Grasping patterns reconstructed through the normative framework (right) closely resemble human grasps onto real objects varying in shape, orientation, and material (left). Simulated grasp patterns are generated with no knowledge of our human data (i.e. model not fit to human grasps). (b) Population level grasp similarity, i.e. similarity of human and unfitted model grasps to medoid human grasp across all participants. (c) Individual level grasp similarity, i.e. similarity of human, unfitted, and fitted model grasps to the medoid grasp of each participant. In panels (b, c), dashed line is estimated chance level of grasp similarity due to object geometry, bounded by 95% bootstrapped confidence intervals. (d) Pattern of fitted weights across Experiments 1 and 2. (e) Relative weight of the minimum torque constraint in Experiments 1 and 2. (f) Relative weight of the visibility constraint in Experiments 1 and 2. Data are means; error bars, 95% bootstrapped confidence intervals. ***p<0.001*

Unfitted model grasps were significantly more similar to human grasps than chance ($t(31)=9.34$, $p=1.6*10^{-10}$), and effectively indistinguishable from human-level grasps similarity ($t(31)=0.53$, $p=0.60$). Note that this does not mean our current approach perfectly describes human grasping patterns; it suggests instead that our framework is able to predict the medoid human grasping patterns nearly as well as the grasps of a random human on average approximate the medoid human grasp.

Fitting the model can account for individual grasp patterns

In both Experiments, participants repeatedly grasped the same objects in randomized order. Figure 2.12c depicts how similar human and model grasps are to the medoid grasp of each individual participant in each experimental condition. Individual subjects are highly consistent when grasping the same object on separate trials. Grasps predicted through our framework with no knowledge of the empirical data were significantly less similar to the medoid grasps of individual humans ($t(31)=9.28$, $p=1.9*10^{-10}$). This is unsurprising, since the unfitted model predicts the average pattern across observers, but there is no mechanism for it to capture idiosyncrasies of individual humans. Fitting the model to the human data (see Methods) significantly improved grasp similarity ($t(31)=4.26$, $p=1.8*10^{-4}$). Note however that model grasp patterns fit to a single participant are still distinguishable from random real grasps by the same individual ($t(31)=4.91$, $p=2.8*10^{-5}$).

Force closure, hand posture, and grasp size explain most of human grasp point selection

The pattern of fitted weights across both experiments (Figure 2.12d) reveals the relative importance of the different constraints. Specifically, we find that force closure is the most important constraint on human grasping, which makes sense because force closure is a physical requirement for a stable grasp. Next in importance are natural grasp axis and optimal grasp aperture, both constraints given by the posture and size of our actuator (our hand). In comparison, participants appear to care only marginally about minimizing torque, and almost negligibly about object visibility.

Analyzing the patterns of fitted weights confirms our empirical findings

The model also replicates our main empirical findings in a single step. Figure 2.12e shows that the relative importance of torque was much greater for the heavy objects tested in Experiment 2 compared to the light objects from Experiment 1 ($t(24)=7.93$, $p=3.7*10^{-8}$). Conversely, Figure 2.12f shows that the relative importance of object visibility instead decreased significantly from Experiment 1 to Experiment 2 ($t(24)=2.62$, $p=0.015$). Additionally, by simulating grasps from the fitted model, we are able to recreate the qualitative patterns of all behavioral results presented in Figures 3,4 and 5 (see Figure 2.S2).

2.2.3 Experiment 3: Model Validation

To further validate the model, we tested whether the model makes sensible predictions on novel objects and whether the model is robust to perturbations.

2.2.3.1 Model Predictions on Novel Objects

The model was designed from the insights derived from Experiments 1 and 2 with polycube objects made of brass and wood. To test whether the model generalizes beyond this type of object, we selected four mesh models of objects with smooth, curved surfaces from an in-house database (two familiar, two unfamiliar objects). We input these meshes to the model and generated grasp predictions (Figure 2.13a). The model was instantiated using the weights derived from Experiment 1. Next, we 3D printed these objects out of light plastic (~80g, comparable to Experiment 1 objects), and asked 14 human participants to grasp these novel objects. Figure 2.13b shows how human grasps agree with model predictions. Human and model grasps once again have similar size and orientation, and also cover similar portions of the objects. Figure 2.13c confirms this observation: predicted model grasps are as similar to medoid human grasps as grasps from a random human participant ($t(13)=1.21$, $p=0.25$).

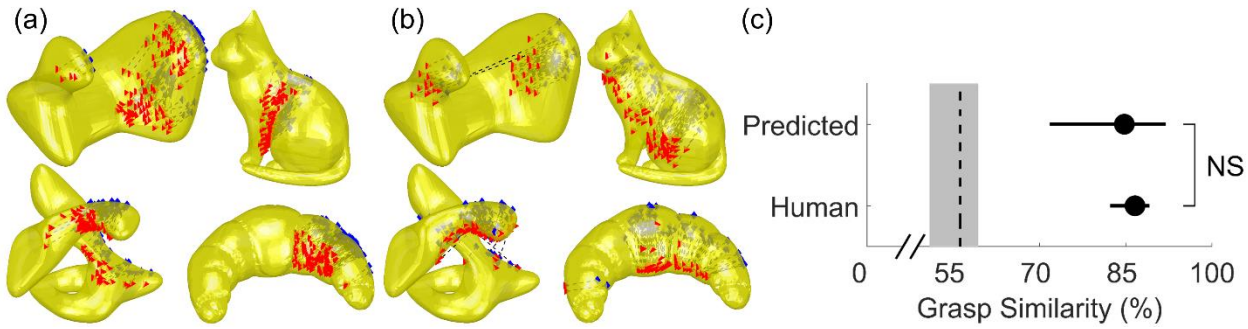

Figure 2.13. Model predictions for novel objects align with human grasps. (a) Grasping patterns predicted through the normative framework for novel objects with smooth and curved surface geometry. (b) Human grasps onto 3D printed versions of the objects align with model predictions. (c) Similarity of human and predicted model grasps to medoid human grasp across objects and participants. Dashed line is estimated chance level of grasp similarity, bounded by 95% bootstrapped confidence intervals.

2.2.3.2 Model Perturbation Analysis

The model designed thus far receives as input a near-veridical representation of the objects to grasp. However, it is unlikely that humans have access to such a veridical object representation. We therefore implemented some perturbations to the inputs and key parameters of the model and observed how robust the model is to these perturbations. Specifically, we tested how model performance in predicting human grasping patterns from Experiment 3 varies as a functions of these perturbations.

The model input thus far consisted of densely sampled 3D mesh models. It's unlikely that humans also have such a dense, accurate 3D representation of an object's surface. Figure 2.14a therefore shows model performance (in terms of similarity with human grasping patterns) with different levels of surface mesh subsampling. Model performance is robust to relatively high levels of subsampling, and decreases only once sampled surface locations are on average more than 4 mm distant from one another (below 5% mesh subsampling).

Since the backside of objects is occluded from view, it is unlikely that participants have an accurate estimate of the required grip aperture across the whole object. Additionally, since we constrained participants to two-digit precision grips, grasps above the threshold defined by Cesari and Newell (1999) might be acceptable, as long as these are within a maximum comfortable grasp span. Figure 2.14b shows that indeed model performance is robust to increases in aperture threshold up to 100 mm.

Similarly, humans might also exhibit some tolerance for grasps oriented away from the natural grasp axis. Given that the ease of a rotation of the arm and hand is likely asymmetric along different directions, these tolerances likely also vary depending on rotation direction. Figure 2.14c shows how model performance does indeed decrease for perturbations of the natural grip axis along the transverse plane, and this decrease is more steep for clockwise (negative) rotations, as already suggested by Kleinholdermann and colleagues (2013). Model performance is instead more robust to perturbations along the sagittal plane (Figure 2.14d), and particularly for (positive) counterclockwise rotations in which the thumb tilts below the index finger.

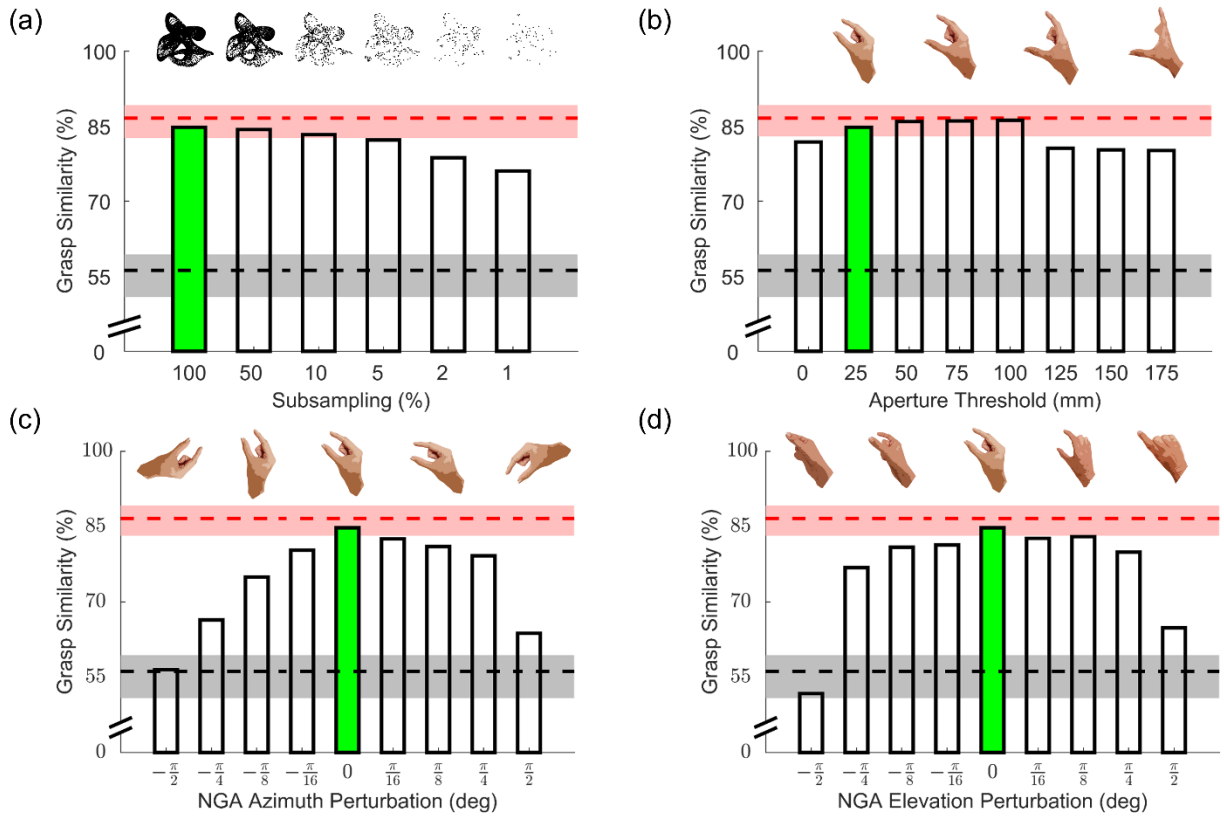

Figure 2.14. Perturbation Results. All panels show model performance (in terms of grasp similarity to human data from Experiment 3) as a function of different perturbations. Grasp similarity for the original model implementation is shown in green. Red and black dashed lines are respectively human and chance levels of grasp similarity, bounded by 95% bootstrapped confidence intervals. (a) Model grasp similarity with input meshes subsampled by varying degrees. (b) Model grasp similarity for model implementations employing increasing aperture thresholds. (c, d) Model grasp similarity for models implemented with deviated natural grasp axis along the transverse (c) and sagittal (s) planes.

2.3 Discussion

We investigated how an object's 3D shape, orientation, mass, and mass distribution jointly influence how humans select grasps. Our empirical analyses showed that grasping patterns are highly systematic, both within and across participants, suggesting that a common set of rules governs human grasp selection of complex, novel 3D objects. Our findings reproduce, unify, and generalize many effects observed previously: (i) both 3D shape and orientation determine which portion of the object people grasp (Chen & Saunders, 2015; Cuijpers et al., 2004, 2006; Eloka & Franz, 2011; Goodale et al., 1994; Kleinholdermann et al., 2013; Lederman & Wing, 2003; Schettino et al., 2003).; (ii) humans exhibit spatial biases even with complex 3D objects varying in shape and mass (Desanghere & Marotta, 2015; Glowania et al., 2017; Kleinholdermann et al., 2013; Maiello et al., 2019; Paulun et al., 2014); (iii) object weight modulates how much humans take torque into account when selecting where to grasp objects (Eastough & Edwards, 2006; Goodale et al., 1994; Lederman & Wing, 2003; Lukos et al., 2007; Paulun et al., 2016). We then combined this diverse set of observations into a unified theoretical framework that predicts human grasping patterns strikingly well, even with no free parameters. By fitting this normative model to human behavioral data, we showed that force closure, hand posture, and grasp size are the primary determinants of human grasp selection, whereas torque and visibility

modulate grasping behavior to a much lesser extent. We further demonstrated that the model is able to generate sensible predictions for novel objects and is robust to perturbations.

2.3.1 3D Shape

Behavioral research on the influence of shape on grasping is surprisingly scarce, primarily employs 2D or simple geometric 3D stimuli of uniform materials, and rarely investigates grasp selection (Chen & Saunders, 2015; Cuijpers et al., 2004, 2006; Eloka & Franz, 2011; Goodale et al., 1994; Lederman & Wing, 2003; Schettino et al., 2003). For example, by using 3D stimuli that only varied in shape by a few centimeters, Schettino et al. (2003) concluded that object shape influences hand configuration only during later phases of a reaching movement during which subjects use visual feedback to optimize their grasp. Here, we show that distinct 3D shapes are grasped in systematically distinct object locations, and our behavioral and model analyses can predict these locations directly from the object 3D shape.

2.3.2 Orientation

When grasping spheres or simple geometrical shapes, humans exhibit a preferred grasp orientation (the NGA) (Lederman & Wing, 2003; Roby-Brami et al., 2000; Schot et al., 2010; Voudouris et al., 2010), and most previous work on how object orientation influences grasping has primarily focused on hand kinematics (Cuijpers et al., 2006; Goodale et al., 1994; Mamassian, 1997; Paulun et al., 2016). Conversely, with more complex 3D shapes we show that the same portion of an object is selected within a range of orientations relative to the observer, whereas for more extreme rotations the grasp selection strategy shifts significantly. Therefore, object shape and orientation together determine which portion of an object will be grasped, and thus the final hand configuration.

2.3.3 Spatial Biases

The spatial biases we observe are consistent with participants attempting to increase object visibility (Maiello et al., 2019; Paulun et al., 2014), and our data also replicate the finding that these biases are reduced when object weight increases (Paulun et al., 2014, 2016).

2.3.4 Material/Weight/Torque

Goodale et al. (1994) were among the first to show that participants tend to grasp objects through their CoM, presumably to minimize torque. Lederman and Wing (2003) found similar results, yet in both studies low-torque grasps also correlated with grasps that satisfied force closure and aligned with the natural grasp axis. Kleinholdermann et al. (2013) found torque to be nearly irrelevant in grasp selection, yet Paulun et al. (2016) observed that grasp distance to CoM was modulated by object weight and material. More recent work by Paulun et al. has further shown that participants are fairly accurate at visually judging the location of the CoM even for bipartite objects made of two different materials (Paulun et al., 2019). Our findings resolve these conflicting findings. By using stimuli that decorrelate different aspects of grasp planning, we find that shape and hand configuration are considerably more important than torque for light weight objects, and that the importance of minimizing torque scales with mass. Additionally, shifting an object's mass distribution significantly attracted grasp locations towards the object's shifted CoM, demonstrating that participants could reliably combine global object shape and material composition to successfully infer the object's CoM.

2.3.5 Modelling Grasp Selection

Previous models of grasping have mainly focused on hand kinematics and trajectory synthesis (Christopoulos & Schrater, 2009; Rosenbaum, Meulenbroek, Vaughan, & Elsinger, 1999; Rosenbaum, Meulenbroek, Vaughan, & Jansen, 1999; Smeets & Brenner, 1999; Smeets & Brenner, 2001) whereas we attempt to predict which object locations will be selected during grasping. Our modelling approach takes inspiration from Kleinholdermann et al., (2013), which to the best of our knowledge is the only previous model of human two-digit contact point selection, but only for 2D shape silhouettes. In addition to dealing with 3D objects varying in mass, mass distribution, orientation, and position, our modeling addresses several limitations of previous approaches. The fitting procedure quantifies the relative importance of different constraints, and can be applied to any set of novel objects to test how experimental manipulations affect this relative weighting. Additionally, while model fitting significantly improved the similarity between model and individual participant grasps, the agreement was not perfect. This suggests that grasp planning may involve additional, undiscovered constraints, which our approach would be sensitive enough to detect. The modular nature of the model specifically allows additional constraints to be included, excluded or given variable importance. For example, we know that end-state comfort of the hand plays a role in grip selection (Rosenbaum et al., 1990; Short & Cauraugh, 1999), yet the tradeoff between initial and final comfort is unclear (Lee Hughes et al., 2012). By varying the participants' task to include object rotations, and by including a penalty function penalizing final hand rotations away from the natural grasp axis, it would be possible to assess the relative importance of initial, final (or indeed intermediate) hand configurations on grasp planning. Relatedly, the effect of obstacles (and self-obstacles, such as the vertically protruding portions of some of the objects employed in this study) could also be assessed. The presence of obstacles could affect grasp selection by requiring reach-to-grasp trajectories that avoid an obstacle, although previous research has shown that forcing different hand paths does not affect selected grasp locations (Voudouris et al., 2010). Alternatively, the presence of obstacles might alter the configuration of the arm and hand during a grasp (Voudouris et al., 2012), which could be incorporated into the model by modifying the grip comfort penalties.

Previous literature has also shown that object surface properties such as curvature (Goodwin et al., 1998), tilt (Jenmalm & Johansson, 1997), and friction (Burstedt et al., 1999; Cadoret & Smith, 1996) modulate the fingertip forces employed during grasping. While the current study was not designed to examine how these factors influence grasp selection, the current model is already able to predict grasp patterns for objects with curved surfaces, even if not perfectly. Model performance with these objects could likely be improved by including into our framework penalty functions that take into account local surface structure and friction. Incorporating friction into the model could even improve model performance for our composite objects from Experiment 2, as wood and brass may have different friction coefficients. Since surface friction plays a decisive role in determining force closure, friction coefficients could even be directly integrated into the force closure computations. Friction is also a particularly interesting test case for our assumption of a weighted linear combination of costs, as it may interact with other factors. When friction is low, it could cause the cost of torque to be upregulated, to avoid slipping (Paulun et al., 2016). This would require the addition of parameters describing interactions between factors. Alternatively, friction and torque might be unified into a single penalty function capturing the magnitude of grip force required to avoid slippage. However, incorporating friction into the model would be non-trivial, since the coefficient of friction between

skin and different materials depends on several factors, including temperature, hydration, and age (Veijgen et al., 2013).

The model should also be extended to multi-digit grasping, by adding to each penalty function three dimensions for each additional finger considered (the x,y,z coordinates of the contact point). This approach is consistent with (and complementary to) the approach by Smeets and Brenner (Smeets & Brenner, 1999; J. Smeets & Brenner, 2001), who posit that grasping is a combination of multiple pointing movements. Given that human participants adjust the number of digits they employ to grasp an object depending on grip size and object weight (Cesari & Newell, 1999), multiple size/weight thresholds could be employed to determine the preferred multi-digit grip. Future models should also generalize from contact points to contact patches of nonzero area, as real human grasp locations are not only points but larger areas of contact between digit and object. To facilitate such developments, we provide all data and code (doi: 10.5281/zenodo.3891663).

2.3.6 Neuroscience of Grasping

While our model is not intended as a model of brain processes, there are several parallels with known neural circuitry underlying visual grasp selection (for reviews see Castiello, 2005; Castiello & Begliomini, 2008; Janssen & Scherberger, 2015). Of particular relevance is the circuit formed between the Ventral Premotor Cortex (Area F5), Dorsal Premotor Cortex (Area F2), and the Anterior Intraparietal Sulcus (AIP). Area F5 exhibits 3D-shape-selectivity during grasping tasks and is thought to encode grip configuration given object shape (Murata et al., 1997; Raos et al., 2006; Theys et al., 2012), whereas area F2 encodes the grip-wrist orientation required to grasp objects under visual guidance (Raos et al., 2004). Both regions exhibit strong connections with AIP, which has been shown to represent the shape, size, and orientation of 3D objects, as well as the shape of the handgrip, grip size, and hand-orientation (Murata et al., 2000). Additionally, visual material properties, including object weight, are thought to be encoded in the ventral visual cortex (Cant & Goodale, 2011; Gallivan et al., 2014; Goda et al., 2014, 2016; Hiramatsu et al., 2011), and it has been suggested that AIP might play a unique role in linking components of the ventral visual stream involved in object recognition to hand motor system (Borra et al., 2008). Therefore, the neural circuit formed between F5, F2, and particularly AIP is a strong candidate for combining the multifaceted components of visually guided grasping identified in this work (Davare et al., 2010; Jeannerod et al., 1995; Sakata et al., 1995; Srivastava et al., 2009; Theys et al., 2015). combining targeted investigations of brain activity with the behavioral and modelling framework presented here holds the potential to develop a unified theory of visually guided grasp selection.

2.4 Materials and Methods

2.4.1 Participants

Twelve naïve participants (5 males and 7 females between the ages of 20 and 31, mean age: 25.2 years) participated in Experiment 1. A different set of fourteen naïve participants (9 males and 5 females between the ages of 21 and 30, mean age: 24.4 years) participated in Experiment 2. An additional, different set of fourteen naïve participants (5 males and 9 females between the ages of 19 and 58, mean age: 25.1 years) participated in Experiment 3. Participants were students at the Justus Liebig University Giessen, Germany and received monetary compensation for participating. All participants reported having normal or corrected to normal vision and being right handed. All

procedures were approved by the local ethics board and adhered to the declaration of Helsinki. All participants provided written informed consent prior to participating.

2.4.2 Apparatus

Experiments 1 and 2 were programmed in Matlab version R2007a using the Optotrak Toolbox by V. H. Franz (Franz, 2004). Participants were seated at a table with their head positioned in a chinrest (Figure 2.2a), in front of an electronically controlled pane of liquid crystal shutter glass (Milgram, 1987), through which only part of the table was visible and which became transparent only for the duration of a trial. Objects were placed at a target location, 34 cm from the chinrest in the participant's sagittal plane. Small plastic knobs placed on participants' right side specified the hand starting positions. A plate (28.5 cm to the right of the target location and with a 13 cm diameter at 26 cm from start position 1 in the participant's sagittal plane) specified the movement goal location. We tracked participants' fingertip movements with sub-millimeter accuracy and resolution using an Optotrak 3020 infrared tracking system. The Optotrak cameras were located to the left of the participants. To record index finger and thumb movement, sets of three infrared markers (forming a rigid body) were attached to the base of the participants' nails. The fingertip and tip of the thumb were calibrated in relation to the marker position, as participants grasped a wooden bar with a precision grip, placing their fingertips at two known locations on the bar.

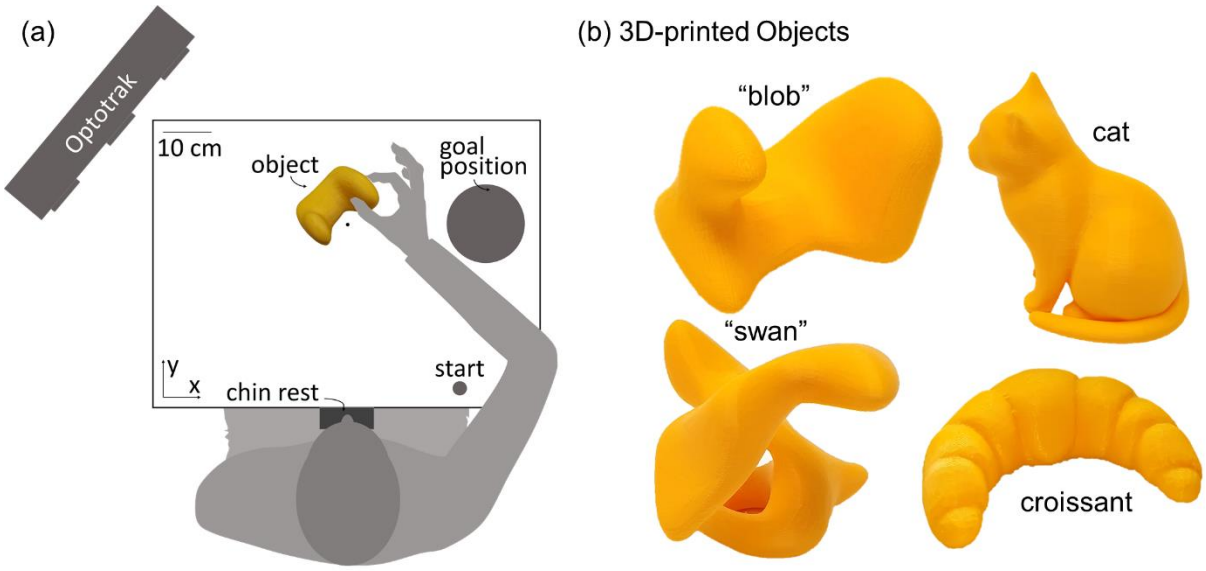

Figure 2.15. Setup and stimuli for Experiment 3. (a) Experimental setup. Seated participants performed grasping movements with their right hand. Following an auditory signal, they opened their eyes, and moved from the starting position to the object and grasped it with a precision grip. They transported and released the object at the goal position and returned to the start position. (b) We employed four 3D-printed objects. Two objects had an abstract shape (that here we name 'swan' and 'blob'), the other two objects were printed versions of a croissant and a cat. They were presented to the participant in the orientations displayed in here.

Experiment 3 was programmed in Matlab version R2019b using the Motom Toolbox (Derzsi & Volcic, 2018). Participants were seated at a table with their head positioned in a chinrest and had their eyes open only for the duration of the movement execution (Figure 2.15a). Objects were placed at a target location, 36 cm from the chinrest in the participant's sagittal plane. A piece of tape placed 30 cm to the right of the chinrest specified the hand starting position. A plate (30 cm to the right of the target

location and with an 18 cm diameter at 30 cm from the start position in the participant's sagittal plane) specified the movement goal location. We tracked participants' fingertip movements using an Optotrak Certus infrared tracking system. The Optotrak cameras were located to the left of the participants. To record index finger and thumb movement, sets of three infrared markers (forming a rigid body) were attached to the base of the participants' nails. The fingertip and tip of the thumb were calibrated in relation to the marker position, as participants touched another marker using a precision grip, placing their finger- and thumb tip at the center of the marker one after the other.

2.4.3 Stimuli

2.4.3.1 Experiment 1: Light objects made of wood.

Four differently shaped objects (defined as objects L, U, S and V; Figure 2.2b) each composed of 10 wooden (beech) cubes (2.5^3 cm^3), served as stimuli. Objects were fairly light with a mass of 97 g. Two of the objects featured cubes stacked on top of each other, whereas the other two objects were composed exclusively of cubes lying flat on the ground. The objects were presented to the participants at one of two orientations. Across orientations, object L was rotated by 180 degrees, objects U and V were rotated by 90 degrees, and object S was rotated by 55 degrees. Figure 2.2b shows the objects positioned as if viewed by a participant.

2.4.3.2 Experiment 2: Heavy composite objects made of wood and brass.

For each of the 4 shapes from Experiment 1, we created 3 new objects (12 in total) to serve as stimuli for Experiment 2 (Figure 2.2c). Individual cubes were made of either wood or brass. The objects were composed of 5 cubes of each material, which made them fairly heavy with a mass of 716g. By reordering the sequence of wood and brass cubes, we shifted the location of each shape's CoM. For each shape we made one object in which brass and wooden cubes alternated with one another, and two bipartite objects, where the 5 brass cubes were connected to one another to make up one side of the object with the wooden cubes making up the other side. This configuration was also inverted, (i.e., wooden and brass cubes switched locations). The 'alternating' objects had approximately the same CoM as their wooden counterparts (mean ± sd distance: 5.1±2.5 mm). Conversely, the CoM of bipartite objects was noticeably shifted to one side of the object compared to their wooden counterparts (mean ± sd distance: 33.3±4.4 mm). The CoM locations for all stimuli are shown in Supplementary Figure 2.S3. All objects were presented at the same two orientations as Experiment 1.

2.4.3.3 Experiment 3: Curved 3D-printed object.

Four novel, differently shaped objects were 3D-printed. They were made from a yellow plastic with a stabilizing mesh inside. Two objects were abstract, curved shapes objects (defined as 'swan' (64g) and 'blob' (121g), the other two objects were known shapes: a cat (72g) and a croissant (74g). All objects were presented to participants in one orientation, as displayed in Figure 2.15b.

2.4.3.4 Object meshes.

For Experiments 1 and 2 triangulated mesh replicas of all objects were created in Matlab; each cube face consisted of 128 triangles. For Experiment 3 we selected non-uniform mesh model objects from an in-house database, each mesh consisting of between 4500 and 9000 triangles. To calibrate mesh orientation and position, we measured, using the Optotrak, four non planar points on each object at each orientation. We aligned the model to the same coordinate frame employed by the Optotrak using Procrustes analysis.

2.4.4 Procedure

2.4.4.1 Experiments 1 and 2

Prior to each trial, participants placed thumb and index finger at a pre-specified starting location. In Experiment 1, two start locations were used (start 1 at 28 cm to the right of the chinrest in the participant's coronal plane and 9.5 cm forward in the sagittal plane; start 2 9 cm further to the right and 3 cm further forward, 23 cm from the center of the goal plate). Given that we observed no effect of starting position in our data, in Experiment 2 only the first starting location was employed. When the subject was at the correct start position, the experimenter placed one of the stimulus objects at the target location behind the opaque shutter screen. Each object could be presented at one of two orientations with respect to the participant. The experimenter could very precisely position each object at the correct location and orientation by aligning two small groves under each object with two small pins on the table surface.

Once both stimulus and participant were positioned correctly, a tone indicated the beginning of a trial, at which point the shutter window turned translucent. Participants were then required to pick up the object using only forefinger and thumb and place it at the goal location. Participants had 3 seconds to complete the task before the shutter window turned opaque. In Experiment 1, no instructions were given regarding how the objects had to be transported, yet we observed that participants never allowed the objects to rotate. Therefore, to match the movement task across experiments, in Experiment 2 participants were instructed to keep the objects as level as possible.

Experiment 1 had sixteen conditions: two starting locations, four wooden objects of different shapes, each object presented at two orientations. Each participant repeated each condition five times (eighty trials per participant).

Experiment 2 had thirty-six conditions: twelve distinct objects (four shapes in three material configurations) presented at two orientations. Half of the participants handled only shapes L and V, the other half handled shapes U and S. Each participant repeated each condition seven times (eighty-four trials per participant). In both experiments trial order was randomized.

Following each trial, the experimenter visually inspected the movement traces to determine whether the trial was successful or not. Unsuccessful grasps were marked as error trials, added to the randomization queue, and repeated.

2.4.4.2 Experiment 3

Prior to each trial, participants placed thumb and index finger at the starting location, closed their eyes, and the experimenter placed one of the stimulus objects at the target location. The experimenter could precisely position each object by aligning it with its outline, drawn on millimeter paper. Once both stimulus and participant were positioned correctly, a tone indicated the beginning of a trial, at which point the participants opened their eyes. Participants were then required to pick up the object using only forefinger and thumb and place it at the goal location. Participants had 3 seconds to complete the task. Each participant picked up each object seven times (28 trials per participant). Trial order was randomized. Following each trial, the experimenter visually inspected the movement traces to determine whether the trial was successful or not. Unsuccessful grasps were marked as error trials, and repeated immediately.

2.4.4.3 Error trials

A total of 397 error trials (13.8% of trials from Experiment 1, 13.9% from Experiment 2, and 6.9% from Experiment 3) were not analyzed. Trials were deemed unsuccessful when participants did not conclude the movement within the allotted time (10.1% of error trials in Experiment 1, 41.4% of error trials in Experiment 2, and 0% in Experiment 3), and/or when tracking was lost (94.2% of error trials in Experiment 1, 88.7% of error trials in Experiment 2, and 100% of error trials in Experiment 3), or when participants placed the objects too hastily on the goal location, which resulted in the objects toppling over off the goal plate where they were supposed to rest (this occurred only twice throughout the study). Note that there was some overlap between causes of error. The trajectories of lost-tracking error trials, where the data are available, fall within the clusters of trajectories of corresponding non-error trials in 92.2% and 99.0% of cases across Experiments 1 and 2 respectively. In Experiment 3 the experimenter manually recorded grasp locations for error trials, and these locations are all represented in the final dataset. It is therefore unlikely that excluded error trials differed strongly from the data included in our analyses.

2.4.5 Training

At the beginning of the experiments, each participant completed six practice trials in Experiments 1 and 2 (using a Styrofoam cylinder in Experiment 1, and by lifting random objects from the shapes not used in that participant's run in Experiment 2) and five practice trials in Experiment 3 (using the wooden L-object from Experiment 1). This was done to give participants a sense for how fast their movement should be in order to complete the entire movement within three seconds. Prior to Experiment 2, participants were familiarized with the relative weight of brass and wood using two rectangular cuboids of dimensions 12.5x2.5x2.5 cm, one of wood (50 g) and one of brass (670 g). Practice trial data were not used in analyses. Prior to Experiment 3, participants were familiarized with the weight of all four test objects by having each object placed on the flat, extended palm of their right hand.

2.4.6 Analyses

All analyses were performed in Matlab version R2018a. Differences between group means were assessed via paired or unpaired t-tests, or through Pearson correlation, as appropriate. Values of $p<0.05$ were considered statistically significant.

2.4.6.1 Contact points

Contact points of both fingers with the object were determined as the fingertip coordinates at the time of first contact, projected onto the surface of the triangulated mesh models of the object. The time of contact with the object was determined using the methods developed by Schot et al. (2010) and previously described in Paulun et al. (2016).

2.4.6.2 Grasp similarity

We described each individual grasp $\vec{G}$ as a 6D vector of the x-, y-, z-coordinates of the thumb and index finger contact points:

$$\vec{G} = [x_T, y_T, z_T, x_I, y_I, z_I]$$

To compute the similarity S between two grasps $\overrightarrow{G_1}$ and $\overrightarrow{G_2}$, we first computed the Euclidian distance between the two 6D grasp vectors. We then divided this distance by the largest possible distance between two points on the specific object D_{max}, determined from the mesh models of the objects. Finally, similarity was defined as 1 minus the normalized grasp distance, times 100:

$$S = 100 * \left(1 - \frac{\| \overrightarrow{G_1} - \overrightarrow{G_2}, \|}{D_{max}}\right)$$

In this formulation, two identical grasps, which occupy the same point in a 6D space, will be 100% similar, whereas the two farthest possible grasps onto a specific object will be 0% similar. Within-subject grasp similarity was the similarity between grasps from the same participant to the participant's own medoid[1] grasp. Between-subject grasp similarity was the similarity between the medoid grasp of each participant and the medoid grasp across all other participants.

2.4.7 Normative model

The model takes as input 3D meshes of the stimuli and outputs a cost function describing the costs associated with every possible combination of finger and thumb position on the accessible surface locations of our objects (i.e., those not in contact with the table plane). First, we define the center of each triangle in the mesh as a potential contact point. Then, given all possible combinations of thumb and index finger contact points $\overrightarrow{CP_T} = [x_T, y_T, z_T]$; $\overrightarrow{CP_I} = [x_I, y_I, z_I]$, the surface normal at both contact points $\overrightarrow{n_T} = [x_T^n, y_T^n, z_T^n]$; $\overrightarrow{n_I} = [x_I^n, y_I^n, z_I^n]$, and the CoM of the object $\overrightarrow{CoM} = [x_{CoM}, y_{CoM}, z_{CoM}]$, the five penalty functions we combined into a normative model of grasp selection were defined as follows:

2.4.7.1 Force closure

For two-digit grasping, a grasp fulfills force closure when the grasp axis connecting thumb and index contact points lies within the friction cones resulting from the friction coefficient between object and digits (Nguyen, 1988). A grasp that does not fulfill force closure will not be able to lift and freely manipulate the object, no matter the amount of force applied at the fingertips. A grasp perfectly fulfills force closure when the grasp axis is perfectly aligned with the vectors along which gripping forces are applied, which are the opposite of the contact-point surface normals. Therefore, we defined the force closure penalty function as the sum of the angular deviances (computed using the atan2 function) of the grasp axis from both force vectors $\overrightarrow{F_T} = -\overrightarrow{n_T}$; $\overrightarrow{F_I} = -\overrightarrow{n_I}$:

$$P_{FC}(\overrightarrow{CP_T}, \overrightarrow{CP_I}) = atan2(\|\overrightarrow{F_T} \times (\overrightarrow{CP_I} - \overrightarrow{CP_T})\|, \overrightarrow{F_T} \cdot (\overrightarrow{CP_I} - \overrightarrow{CP_T}))$$
$$+ atan2(\|\overrightarrow{F_I} \times (\overrightarrow{CP_T} - \overrightarrow{CP_I})\|, \overrightarrow{F_I} \cdot (\overrightarrow{CP_T} - \overrightarrow{CP_I}))$$

2.4.7.2 Torque

If a force is applied at some position away from the CoM, the object will tend to rotate due to torque, given by the cross product of force vector and lever arm (the vector connecting CoM to the point of force application). Under the assumption that is possible to apply forces at the thumb and index contact points that counteract the force of gravity $\overrightarrow{F_g}$, we can compute the total torque of a grip as

[1] The medoid (a concept similar to the mean) is the element of a set that minimizes its distance to all other elements. We employ the medoid over the mean because it better represents the grasp data: while the medoid grasp belongs to the set of executed grasps, the mean grasp can result in a grasp that falls inside or outside of the grasped object.

the sum of torques exerted by each contact point. Therefore, we defined the torque penalty function as the magnitude of the total torque exerted by a grip:

$$\boldsymbol{P_T}\left(\overrightarrow{\boldsymbol{CP_T}}, \overrightarrow{\boldsymbol{CP_I}}\right) = \left\|\left(\overrightarrow{\boldsymbol{CoM}} - \overrightarrow{\boldsymbol{CP_T}}\right) \times \overrightarrow{-\boldsymbol{F_g}} + \left(\overrightarrow{\boldsymbol{CoM}} - \overrightarrow{\boldsymbol{CP_I}}\right) \times \overrightarrow{-\boldsymbol{F_g}}\right\|$$

2.4.7.3 Natural grasp axis

Schot, Brenner, and Smeets (2010) have carefully mapped out how human participants grasp spheres placed at different positions throughout the peripersonal space, and provide a regression model that determines the naturally preferred posture of the arm when grasping a sphere. We input the configuration of our current experimental setup into the regression model developed by these authors, and found the natural grasp axis for our participants to be $\overrightarrow{\boldsymbol{NGA}} = [\boldsymbol{0.49\ 0.87\ 0}]$. We therefore defined the natural grasp axis penalty function as the angular deviance from this established natural grasp axis:

$$\boldsymbol{P_{NGA}}\left(\overrightarrow{\boldsymbol{CP_T}}, \overrightarrow{\boldsymbol{CP_I}}\right) = \boldsymbol{atan2}\left(\left\|\overrightarrow{\boldsymbol{NGA}} \times \left(\overrightarrow{\boldsymbol{CP_I}} - \overrightarrow{\boldsymbol{CP_T}}\right)\right\|, \overrightarrow{\boldsymbol{NGA}} \cdot \left(\overrightarrow{\boldsymbol{CP_I}} - \overrightarrow{\boldsymbol{CP_T}}\right)\right)$$

2.4.7.4 Optimal grasp aperture for precision grip

Cesari and Newell (1999) have shown that, when free to employ any multi-digit grasp, human participants selected precision grip grasps only for cubes smaller than 2.5 cm in length. As cube size increases, humans progressively increase the number of digits employed in a grasp. Therefore, since our participants were instructed only to employ precision grip grasps, we defined the optimal grasp aperture penalty function as 0 for grasp sizes smaller than 2.5 cm, and as a linearly increasing penalty for grasp sizes larger than 2.5 cm:

$$\boldsymbol{P_{OGA}}\left(\overrightarrow{\boldsymbol{CP_T}}, \overrightarrow{\boldsymbol{CP_I}}\right) = \begin{cases} 0, & if\ \left\|\overrightarrow{\boldsymbol{CP_I}} - \overrightarrow{\boldsymbol{CP_T}}\right\| < 25mm \\ \left\|\overrightarrow{\boldsymbol{CP_I}} - \overrightarrow{\boldsymbol{CP_T}}\right\| - 25, & if\ \left\|\overrightarrow{\boldsymbol{CP_I}} - \overrightarrow{\boldsymbol{CP_T}}\right\| > 25\ mm \end{cases}$$

In pilot work, we observed that a penalty map linearly increasing from 0 cm worked equally as well as one linearly increasing from 2.5 cm. In Experiment 3 we further observed that increasing this threshold up to 10 cm did not hinder model performance. However, constructing this penalty function with the 2.5 cm threshold motivated by previous literature will allow us, in future work, to construct penalty functions with multiple thresholds for multi-digit grasping, as those observed by Cesari and Newell (1999).

2.4.7.5 Object Visibility

Under the assumption that humans are attempting to minimize the portion of the objects hidden from view by their hand, we defined the optimal visibility penalty function as the proportion of object still visible during each possible grasp. We first defined the line on the XZ plane that passes through the thumb and index finger contact points. We made the simplifying assumption that, given all possible surface points on the object $\boldsymbol{SP_{TOT}}$, the surface points $\boldsymbol{SP_{OCC}}\left(\overrightarrow{\boldsymbol{CP_T}}, \overrightarrow{\boldsymbol{CP_I}}\right)$ that fall to the side of the line where the hand is located will be occluded. Therefore, the object visibility penalty function was defined as:

$$\boldsymbol{P_{OGA}}\left(\overrightarrow{\boldsymbol{CP_T}}, \overrightarrow{\boldsymbol{CP_I}}\right) = \frac{Length\left(\boldsymbol{SP_{OCC}}\left(\overrightarrow{\boldsymbol{CP_T}}, \overrightarrow{\boldsymbol{CP_I}}\right)\right)}{Length(\boldsymbol{SP_{TOT}})}$$

2.4.7.6 Overall grasp penalty function

To obtain the overall grasp penalty function, each grasp penalty function was first normalized to the [0 1] range (i.e., across all possible grasps for each given object, independently of the other objects). Then, we took the sum of the individual penalty functions:

$$\boldsymbol{P_O}\left(\overrightarrow{\boldsymbol{CP_T}}, \overrightarrow{\boldsymbol{CP_I}}\right) = \boldsymbol{P_{FC}}\left(\overrightarrow{\boldsymbol{CP_T}}, \overrightarrow{\boldsymbol{CP_I}}\right) + \boldsymbol{P_T}\left(\overrightarrow{\boldsymbol{CP_T}}, \overrightarrow{\boldsymbol{CP_I}}\right) + \boldsymbol{P_{NGA}}\left(\overrightarrow{\boldsymbol{CP_T}}, \overrightarrow{\boldsymbol{CP_I}}\right) + \boldsymbol{P_{OGA}}\left(\overrightarrow{\boldsymbol{CP_T}}, \overrightarrow{\boldsymbol{CP_I}}\right) + \boldsymbol{P_{RT}}\left(\overrightarrow{\boldsymbol{CP_T}}, \overrightarrow{\boldsymbol{CP_I}}\right)$$

For display purposes this final function was normalized to the [0 1] range. The minima of this overall grasp penalty function represent the set of grasps that best satisfy the largest number of constraints at the same time.

2.4.7.7 Model fitting

In both Experiments 1 and 2, human participants executed repeated grasps to the same objects at each orientation. To fit the overall grasp penalty function to these human data, for each participant in each condition we first defined a human grasp penalty function $\boldsymbol{P_H}\left(\overrightarrow{\boldsymbol{CP_T}}, \overrightarrow{\boldsymbol{CP_I}}\right)$ in which all grasps selected by a participant onto an object were set to have 0 penalty, and all grasps that had not been selected were set to have a penalty of 1. Then, we fit the function:

$$\boldsymbol{P_{O,fit}}\left(\overrightarrow{\boldsymbol{CP_T}}, \overrightarrow{\boldsymbol{CP_I}}\right) = \sqrt{\sum_i w_i * \boldsymbol{P_i}\left(\overrightarrow{\boldsymbol{CP_T}}, \overrightarrow{\boldsymbol{CP_I}}\right)^2}$$

to the human grasp penalty function. More specifically, we employed a nonlinear least-squares solver to search for the set of weights $w_i = [w_{FC}; w_T; w_{NGA}; w_{OGA}; w_{RT}]$ that minimized the function:

$$\boldsymbol{F(w_i)} = \sqrt{\boldsymbol{R}\left(\overrightarrow{\boldsymbol{CP_T}}, \overrightarrow{\boldsymbol{CP_I}}\right)} * \left[\sqrt{\sum_i w_i * \boldsymbol{P_i}\left(\overrightarrow{\boldsymbol{CP_T}}, \overrightarrow{\boldsymbol{CP_I}}\right)^2} - \boldsymbol{P_H}\left(\overrightarrow{\boldsymbol{CP_T}}, \overrightarrow{\boldsymbol{CP_I}}\right)\right]$$

i.e. we searched for the set of weights for which $\boldsymbol{P_{O,fit}}$ best approximated the human grasp penalty function $\boldsymbol{P_H}$. The solver employed the trust-region-reflective algorithm; we set the lower and upper bounds of the weights to be 0 and 1, and 0.2 as the starting value for all weights. The number of non-selected grasps with $\boldsymbol{P_H}\left(\overrightarrow{\boldsymbol{CP_T}}, \overrightarrow{\boldsymbol{CP_I}}\right) = 1$ vastly outnumbered the few selected grasps for which $\boldsymbol{P_H}\left(\overrightarrow{\boldsymbol{CP_T}}, \overrightarrow{\boldsymbol{CP_I}}\right) = 0$. To avoid overfitting the model to the regions of the grasp space where $\boldsymbol{P_H}\left(\overrightarrow{\boldsymbol{CP_T}}, \overrightarrow{\boldsymbol{CP_I}}\right) = 1$, we designed $\boldsymbol{R}\left(\overrightarrow{\boldsymbol{CP_T}}, \overrightarrow{\boldsymbol{CP_I}}\right)$ as a regularization function which served to give equal importance to high and low penalty grasps in the human grasp penalty function. Thus, for grasps where $\boldsymbol{P_H}\left(\overrightarrow{\boldsymbol{CP_T}}, \overrightarrow{\boldsymbol{CP_I}}\right) = 0$, $\boldsymbol{R}\left(\overrightarrow{\boldsymbol{CP_T}}, \overrightarrow{\boldsymbol{CP_I}}\right)$ was equal to the number of times the participant had selected that specific grasp. For grasps where $\boldsymbol{P_H}\left(\overrightarrow{\boldsymbol{CP_T}}, \overrightarrow{\boldsymbol{CP_I}}\right) = 1$ instead, $\boldsymbol{R}\left(\overrightarrow{\boldsymbol{CP_T}}, \overrightarrow{\boldsymbol{CP_I}}\right) = \frac{N_{G,selected}}{N_{G,non-selected}}$; where $N_{G,selected}$ was the total number of grasps performed by the participant onto the object, and $N_{G,non-selected}$ was the total number of non-selected grasps within the grasp manifold. This way for both selected and non-selected grasp regions, the sum of $\boldsymbol{R}\left(\overrightarrow{\boldsymbol{CP_T}}, \overrightarrow{\boldsymbol{CP_I}}\right)$ was $N_{G,selected}$, and both regions of grasp space were accounted for equally during the fitting.

2.4.7.8 Predicting Grasps

The minima of both the equally weighted (non-fitted) and the fitted overall grasp penalty functions represent the set of grasps predicted to be optimal under the weighted linear combination of the five penalty functions included in our normative model. To visualize these predicted optimal grasps, we sampled them from the minima of the penalty functions. First, we removed all grasps with penalty values greater than the lower 0.1th percentile. This percentile value was selected to approximately match the proportion of grasp space actually covered by human grasps. The remaining grasps were therefore all optimal or near-optimal. From this subset, we then randomly selected (with replacement) a number of grasps equal to the number of grasps executed by the human participants. The probability with which any one grasp was selected was set to be 1 minus the grasp penalty, thus grasps with zero penalty had the highest probability of being selected. These sampled grasps can then be projected back onto the objects for visualization purposes (Figure 2.12a, 2.13a), or they can be directly compared to human grasps using the grasp similarity metric described above (Figures 12b,c, 13c).

Chapter 3

STUDY II
Friction is preferred over grasp configuration in precision grip grasping

A similar version of this manuscript has been published as:

Klein, L. K., Maiello, G., Fleming, R. W., & Voudouris, D. (2021). Friction is preferred over grasp configuration in precision grip grasping. Journal of Neurophysiology, 125(4), 1330–1338. https://doi.org/10.1152/jn.00021.2021

How humans visually select where to grasp an object depends on many factors, including grasp stability and the final grasp configuration. We examined how endpoints are selected when these two factors are brought into conflict: Do people favor stable grasps or do they prefer their natural grasp configurations? Participants reached to grasp one of three cuboids that was oriented so that its two corners were either aligned with each individual's natural grasp axis (NGA) or rotated 22.5° away from that NGA. All objects were made of brass (mass: 420 g) but the surfaces of their sides were manipulated to alter friction: 1) all-brass, 2) two opposing sides covered with wood, while the other two remained of brass, or 3) two opposing sides covered with sandpaper, and the two remaining brass sides smeared with vaseline. Grasps were evaluated as either clockwise (thumb to the left of finger in frontal plane) or counterclockwise of the NGA. Grasp endpoints depended on both object orientation and surface material. For the all-brass object, grasps were bimodally distributed for the NGA-aligned object but predominantly clockwise for the NGA-unaligned object. These data reflected the participants' natural grasp configuration independently of surface material. When grasping objects with different surface materials, endpoint selection changed: Participants sacrificed their usual grasp configuration to choose the more stable object sides. A model in which surface material shifts participants' preferred grip angle proportionally to the perceived friction of the surfaces accounts for our results. Our findings demonstrate that a stable grasp is more important than a biomechanically comfortable grasp configuration.

3.1 Introduction

When grasping, humans must select appropriate contact points with the object out of a plethora of possible options. This choice is nontrivial and depends on several characteristics of the object, such as its position in relation to the actor (Brière & Proteau, 2011; Paulignan et al., 1997), orientation (Paulun et al., 2016; Voudouris, Smeets, et al., 2013), size (Hesse & Franz, 2009; Kamp et al., 2009), center of mass (J. Lukos et al., 2007; Voudouris et al., 2019), surface material (Fikes et al., 1994; Wing & Lederman, 2009), and visibility (Maiello et al., 2019; Paulun et al., 2016). We have recently shown computationally that grasp endpoint selection is determined by an intersection of constraints derived from these factors (Klein et al., 2020; Maiello et al., 2021). Two critical underlying factors for endpoint selection are the prioritization of a stable grasp and the adoption of the natural grasp configuration.

Stable grasps are ensured by applying forces within the cone of friction, so humans bring their digits orthogonally to the object's surface (Kleinholdermann et al., 2007). When grasping low-friction objects, humans reduce endpoint variability (Paulun et al., 2016) and tailor each digit's grip forces to the local surface properties (Burstedt et al., 1999), suggesting more careful endpoint selection when anticipating unstable grasps. Unsurprisingly, when grasping elongated objects of combined smooth and rough surfaces, humans choose endpoints on the rough surfaces, presumably to foster grasp stability. Interestingly, though, endpoints are chosen on smooth surfaces if doing so minimizes the torques associated with subsequent object manipulation (Glowania et al., 2017; Wing & Lederman, 2009), suggesting that, although grasp stability is important, other energetic factors are also considered when choosing endpoints.

Grasp control attempts to optimize energy expenditures (Glowania et al., 2017) and minimize travel and spatial error costs (Rosenbaum et al., 2001). A key aspect for selecting the grasp configuration is that extreme joint angles should be avoided (Rosenbaum et al., 2001) because such configurations increase spatial errors (Rossetti et al., 1994). To this end, humans keep their final grasp configurations approximately invariant (Grea et al., 2000; Rosenbaum & Jorgensen, 1992; Voudouris, Radhakrishnan, et al., 2013), even when obstacles hinder these configurations (Voudouris et al., 2012b). When grasping cuboid objects that can be grasped with only two configurations, one of which requires the digits to be placed on object positions that are occluded, humans still prioritize their natural grasp configuration by tolerating invisible endpoints (b). These examples further highlight the importance of grasp configuration in the selection of endpoints.

Considering the critical role that both grasp stability and final grasp configuration have in grasp endpoint selection, an emerging question relates to the trade-off between these two factors. If grasp stability is prioritized, humans should choose endpoints that provide stable grasps, even when this requires unusual grasp configurations. Alternatively, if final grasp configuration is prioritized, humans should keep their natural grasp posture invariant, even if this would lead to unstable endpoints. To examine this, we asked participants to reach, grasp, and lift cuboid objects of different surface materials. By using cuboids, participants could choose endpoints on only one of the two pairs of opposing surfaces, requiring grasp configurations orthogonal to each other. By manipulating the friction properties of each pair of surfaces, we disentangled the contributions of grasp stability and grasp configuration by examining whether humans prioritize their usual grasp configuration, even if this would sacrifice grasp stability, or whether they prioritize grasp stability by adopting awkward final grasp postures.

3.2 Materials and Methods

3.2.1 Participants

Twenty-one naïve self-reported right-handed participants (mean age: 24.4 years, 16 females) with normal or corrected-to-normal vision participated in our study. This sample size was selected though a-priori power analysis, based on a pilot experiment (N=7), to guarantee that we could detect the smallest effect of interest at the 95% confidence level with 80% power. All procedures were approved by the local ethics board and adhered to the declaration of Helsinki (2013). All participants provided written informed consent prior to the experiment and received monetary compensation for their efforts.

3.2.2 Apparatus

A schematic depiction of the setup is shown in Figure 3.1a. Participants sat at a table with their right hand at a start position aligned to their shoulder, 9 cm from the table's edge. Objects were placed in front of the participants at a target position aligned with their midline, 16 cm from the table's edge. Movements of the participants' right thumb and index fingers were recorded at 100 Hz with an Optotrak Certus (Northern Digital Inc., Waterloo, ON, Canada) that tracked the position of small infrared markers attached to the respective fingernails (with sub-millimeter accuracy and resolution). A monitor was placed on the table in front of the experimenter, who sat next to the participants. The monitor displayed to the experimenter which condition to set up on each trial. The experiment was programmed in Matlab R2019b using the Motom Toolbox (Derzsi & Volcic, 2018).

The target objects and the experimental conditions are shown in Figure 3.1b. In the main experiment, the object was one of three possible cuboids (5 cm x 5 cm x 2 cm) that was oriented either with its corners aligned to the participant's individual NGA or rotated 22.5° counterclockwise. All objects were made of brass (mass: 420 g) but the surface material of the sides was manipulated, so that the sides were either all-brass (*baseline object*), or two of the opposing sides were covered with wood and the other two remained with brass (*wooden object*), or two of the opposing sides were covered with sandpaper and the other two brass sides were made slippery using Vaseline ("*brasseline"* object). Each of the wooden and *brasseline* objects could be placed in two configurations, such that their higher- and lower-friction sides were alternated clockwise and counterclockwise.

3.2.3 Procedure

Before each trial, participants placed their thumb and index finger at the start position and the experimenter placed the object at the target position at the appropriate orientation and configuration. The experimenter could very precisely position each object at the correct angle by aligning the edges with the corresponding outlines on a protractor template on the table. An auditory cue prompted participants to reach and grasp the object using only their thumb and index finger, and then lift it ~10 cm high while keeping it level. Participants had to place the object back down at roughly the same position before returning to the start position in anticipation of the next trial. Participants were to execute the task in 3 seconds and could see the object at all times during the experiment. No other instructions were given.

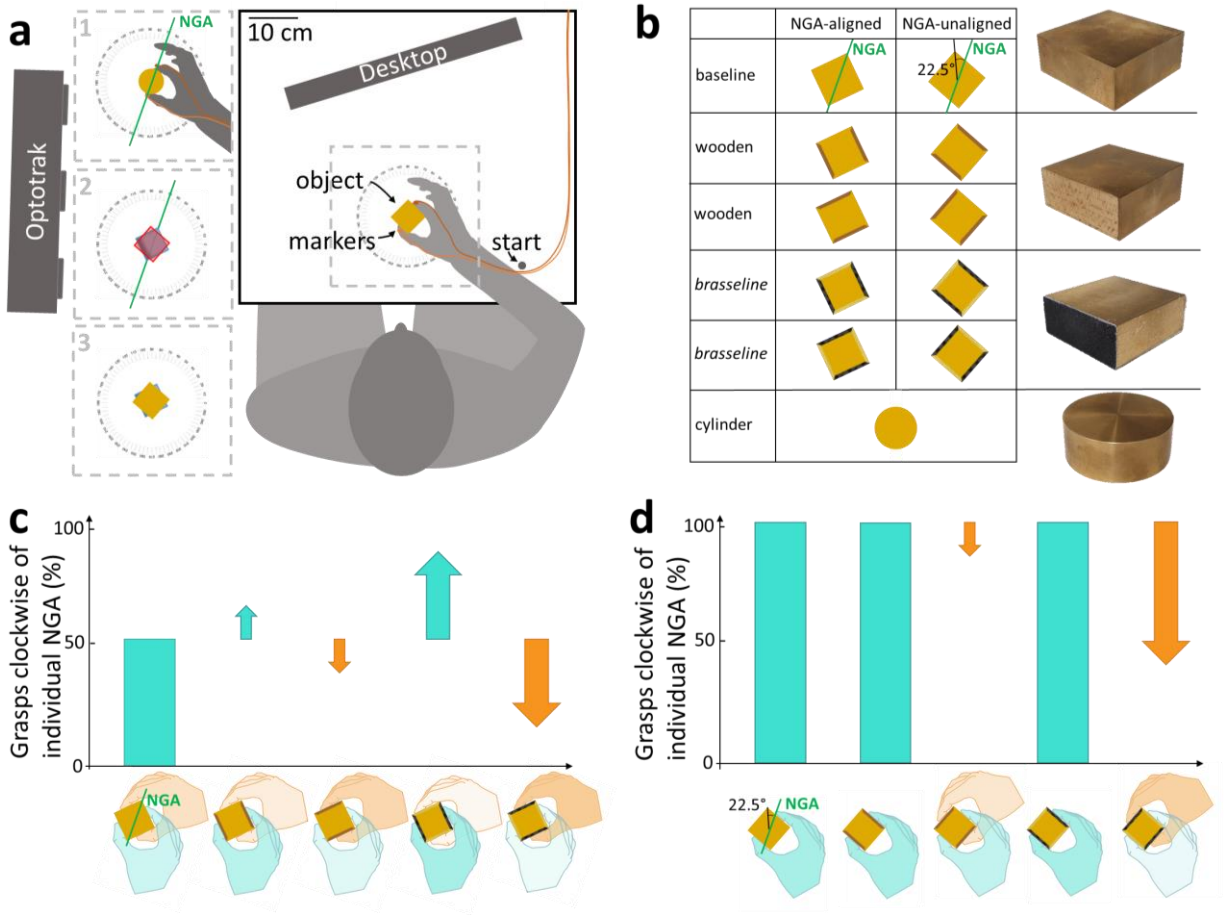

Figure 3.1: Experimental setup and predictions. a Participants reached to grasp and lift an object placed in front of them. After lifting it, they put the object back down, before returning to the start position. 1 They first grasped a cylinder 10 consecutive times to determine each individual's NGA. 2 The experimenter aligned the object outline template with the NGA. 3 The target cuboid object was aligned with a protractor template according to the condition angle and orientation. b Each cuboid was presented at two orientations: with its corners either aligned with the NGA or rotated 22.5° counterclockwise. The wooden and brasseline *objects were presented also in two configurations, so that their higher- and lower-friction sides were alternated clockwise and counterclockwise. The cylinder was only used to determine the NGA before the trials involving the cuboids. Object pictures are presented next to the corresponding conditions. c,d Predictions regarding the percentage of clockwise grasps for different surface material configurations, for c NGA-aligned and d NGA-unaligned conditions. Arrows visualize a change in behavior compared to the baseline prediction. A thin downwards pointing arrow predicts a small decrease in clockwise grasps, a large arrow a larger decrease. The hands' degree of translucency represents the amount of predicted clockwise (cyan hand) vs. counterclockwise (orange hand) grasps.*

Prior to the main experiment, to measure each individual's NGA, participants performed 10 grasps to a brass cylinder (diameter 5 cm, height 2 cm, weight 332 g). From these 10 trials, an individual's NGA was calculated as the median orientation of the grip at the moment of grasp. The experimenter then marked two orientations on the protractor template around the target position so that one corresponded to the calculated NGA (NGA-aligned) and another was rotated 22.5° counterclockwise (NGA-unaligned). Using these outlines, participants performed 6 practice trials drawn from a subset of the experimental conditions, during which they were familiarized with the task and cuboid objects.

The main experiment then started, in which participants grasped only the cuboids. Each of the 10 conditions (Figure 3.1b) was presented 10 times (100 trials per participant), across three object-specific sub-blocks to minimize trial-order effects (Maiello et al., 2018): presentation of baseline,

wooden, and the *brasseline* objects were shuffled across participants in a Latin square design. Within each sub-block, object orientation and configuration were presented in pseudorandomized order.

Immediately after the grasping experiment, we asked participants to judge the slipperiness and pleasantness to the touch of each of the four surfaces they could grasp during the experiment. On the monitor participants viewed pictures of the objects with one of the four possible materials facing the participants. Using the mouse in eight separate trials, they first set a slider on a scale from slippery to not slippery and afterwards rated the same four surfaces from pleasant to not pleasant.

3.2.4 Analyses

3.2.4.1 Endpoints

Endpoints of both fingers with the objects were determined as the coordinates of the markers on the fingernails at the time of contact, as this was determined using the method developed by Schot et al. 2010 and previously described in Paulun et al. (2016). In detail, the average position of the two markers on the fingernails, which represented the position of the hand, had to travel more than half the distance between the start and the target position, and the likelihood of a sample being the moment of contact increased with lower vertical positions and with lower speeds of the hand.

3.2.4.2 Grip Angle

We were interested in which pair of opposing sides was grasped at the moment of object contact in relation to the objects' surface material. Therefore, for each trial we first computed the final grip angle along the horizontal plane as: $\eta = atan2(y_{index} - y_{thumb}, x_{index} - x_{thumb})$. Then, we classified each grip as either clockwise, if the grip angle was $\eta < NGA$ (thumb to the left of finger in frontal plane), or counterclockwise, if $\eta \geq NGA$. Finally, we computed the percentage of clockwise grasps for each participant in each condition.

3.2.4.3 Predictions

Our a-priori, qualitative predictions are illustrated in Figure 3.1(c,d). For the NGA-aligned orientation there is no obvious preferred grasp configuration for the baseline object (Voudouris et al., 2012a), so participant grasps, at least in the group level, should be split equally between clockwise and counterclockwise. For wooden and *brasseline* objects, we predict more grasps on the wooden and sandpaper sides, respectively, as these surfaces have higher friction and facilitate more stable grasps. For the NGA-unaligned conditions, one pair of sides requires counterclockwise rotations away from the NGA that are twice as large as those required for the clockwise pair of sides (Voudouris et al., 2012a). Therefore, in these conditions we can directly contrast grasp configuration with grasp stability. If the former is more important, participant grasps should be predominantly clockwise, independently of the surface material. If, instead, grasp stability is prioritized, we predict lower proportions of clockwise grasps when the higher friction cube sides are oriented counterclockwise.

3.2.4.4 Statistical analyses: a priori, hypothesis-driven analyses

To assess whether our experimental manipulations shifted participants' grasps clockwise or counterclockwise, we analyzed the percentage of clockwise grasps using a repeated-measures generalized linear mixed effects model (GLMM) with fixed effects for object orientation, surface configuration, and the interaction between these, plus random subject-level effects. We defined a logit link function and the conditional distribution of the responses as a Binomial distribution. This is conceptually similar to repeated measures analysis of variance, but overcomes ANOVA shortcomings

with percentage data (Jaeger, 2008). Comparisons between condition pairs were performed via two-tailed, paired samples t-tests after variance-stabilizing the percentage data via arcsine square root transformation. We report effect size for differences between condition means on variance-stabilized data as $d = \mu_{C1-C2}/\sigma_{C1-C2}$. Statistical significance was set at $\alpha < 0.05$. All analyses were performed in Matlab version R2019b.

3.3 Results

We investigated grasp endpoint selection when trading-off between grasp configuration and grasp stability. Participants grasped and lifted a cuboid while we varied the surface material of each pair of its sides. This introduced conditions in which higher friction surfaces were orthogonal to the usual grasp configuration, and thereby we could quantify the contribution of each of these factors in endpoint selection.

Figure 3.2a displays each participant's ten grip orientations and the associated median (the NGA estimate) when grasping the brass cylinder. Across participants, the mean ± standard deviation NGA was 66° ± 9°. Figure 3.2b,c presents an overview of the distributions of the grip angles (relative to each individual's NGA) for each condition involving the cuboid. For objects aligned with the NGA (Figure 3.2b), baseline grips (top row) were bimodally distributed across participants. This bimodal distribution was somewhat skewed when grasping the low-constraint wooden object (rows 2,3), and became clearly unimodal when grasping the *brasseline* object (rows 4,5). For objects rotated 22.5° away from the NGA (Figure 3.2c), baseline grips were predominantly clockwise, and remained so when the higher friction surfaces were aligned with this natural grasp configuration (rows 2 and 4). Interestingly, when the higher friction surfaces were orthogonal to the baseline grip axis, participants switched their grasp configuration to choose more stable endpoints, subtly for the wooden object (row 3) but massively for the *brasseline* object (row 5).

These results were further confirmed by our statistical analyses. GLMM analysis on the percentage of clockwise grasps (Figure 3.2d,e) showed a significant main effect of object orientation ($p<.001$), as participants grasped the NGA-aligned objects with a bimodal distribution of grip angles, but the NGA-unaligned objects primarily with clockwise grips, in line with previous findings (Voudouris et al., 2012a). The percentage of clockwise grips was further affected by the surface material configuration ($p<.001$), and this effect was different depending on the object's orientation (interaction; $p<.001$). Specifically, for the *brasseline* object, grips were more often clockwise and counterclockwise following the higher friction material in both the NGA-aligned ($t(20)=17.9$, $p<.001$, $d=3.9$) and unaligned orientations ($t(20)=13$, $p<.001$, $d=2.8$). This pattern was observed also for the wooden object, but was weaker (NGA-aligned: $t(20)=3.4$, $p=.0031$, $d=0.73$; NGA-unaligned: $t(20)=2.8$, $p=.011$, $d=0.61$). Note that this interaction arose because in the NGA-aligned orientation, grips shifted both clockwise and counterclockwise from baseline, whereas in the NGA-unaligned orientation they only shifted counterclockwise.

Figure 3.2f further shows the effect of surface material assessed independently of object orientation. Specifically, for each object orientation we calculated the difference in clockwise grasps between the two configurations of each (wooden and *brasseline*) object, and then calculated the average difference across the two object orientations, with greater values indicating stronger preference for higher friction surfaces. We found that grasps were significantly attracted toward the higher friction sides both for the wooden ($t(20)=3.4$, $p=.003$, $d=0.74$) and the *brasseline* objects ($t(20)=16.5$, $p<.001$, $d=3.6$),

but that the strength of this attraction was greater in the *brasseline* than the wooden object (t(20)=10.4, p<.001, d=2.3). Participants performed repeated trials for each condition. We thus wondered whether the observed shifts in grasp orientation were based on visual estimation of object properties or on the memory from repeated experience with the object. To answer this question, we repeated our analyses using only the first trial from each participant in each condition, and found that our findings remained unvaried (correlation between full and reduced dataset: r = 0.99, p<.001).

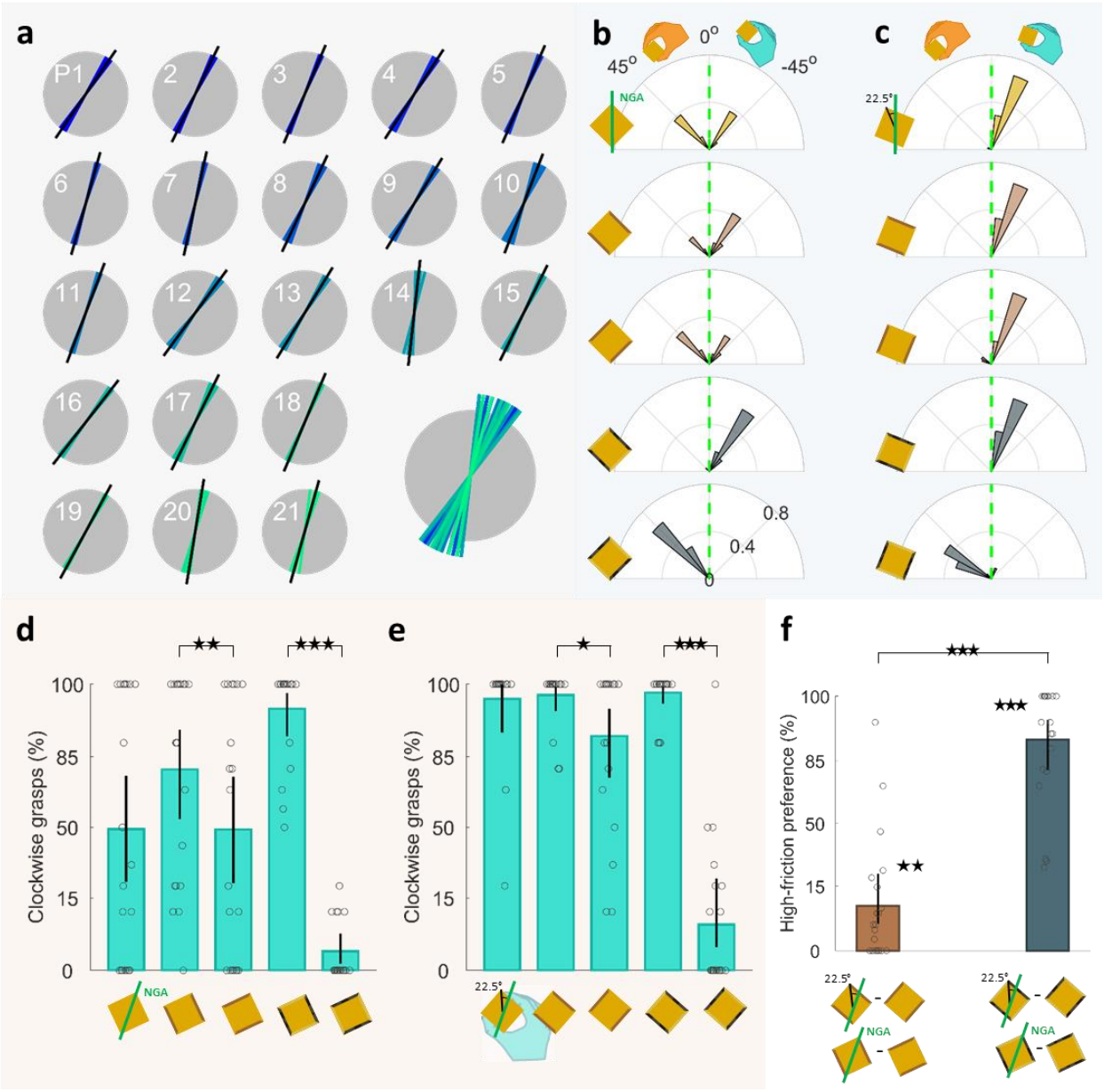

Figure 3.2: Shifts in grasp orientation following object orientation and surface material. a NGA estimation: grip orientation of all ten trials (colored lines) and median grip angles (black lines) for each participant (separate panels) when grasping the brass cylinder. All median NGA estimates are depicted in the lower right panel. b,c The proportion of grip angles, relative to each individual's NGA, for all material configurations. Grip angles to the left and right of the dotted green line (NGA) are counterclockwise (orange hand) and clockwise grasps (cyan hand), respectively. b Cube corners aligned with the NGA. c Cube corners rotated 22.5° away from the NGA. d,e The percentage of clockwise grip angles for each of the five conditions when cuboid corners were d aligned with the NGA and e when not. f Difference in %clockwise grips between surface configurations for the wooden and brasseline *objects, collapsed across object orientations. In panels d,e,f, circles denote individual participants, bars are means across participants, error bars are 95% bootstrapped confidence intervals. Y-axes are scaled following the arcsine square root transform. *p<.05; **p<.01;***p<.001.*

In short, participants grasped the higher friction surfaces more often than the lower friction surfaces. This was clearly evident when the higher friction surfaces were orthogonal to the baseline grip axis, and particularly apparent in the NGA-unaligned orientation conditions, when grasp stability and final grasp configuration were fully contrasted. Indeed, when grasping the NGA-unaligned *brasseline* object, participants used grasp configurations that were almost never used when grasping the NGA-unaligned baseline object (compare first and last rows of Figure 3.2c). It is possible that participants were content to select these unusual grasp configurations because they could readjust their grip and arm posture when lifting the object off the table. We thus compared grip angles at moment of first contact with grip angles 500 ms after contact, i.e., during object lift. Even when adopting the postures farthest from the NGA (last row of Figure 3.2c), participants readjusted their grip posture on average only by 1 ± 4°, suggesting they maintained postures away from the NGA throughout the grasping action. Therefore, humans prefer endpoints that facilitate stable grasps, even when this requires unusual grasp configurations.

3.3.1 A simple model: surface friction shifts participants' preferred grip angle

To gain further insights into the process by which grasp stability and grasp configuration interact when choosing endpoints, we devised a simple model to explain our pattern of results (Figure 3.3). First, we assumed that an individual participant will exhibit a preferred grip axis that follows a normal distribution $N(\mu, \sigma)$, with mean μ_{NGA} and standard deviation σ_{NGA}. In the equal material conditions (Figure 3.3a), a participant's grasps will be clockwise or counterclockwise depending on whether this participant's NGA is clockwise or counterclockwise of the cube's diagonal, here named ξ. Thus, in the NGA-aligned condition (Figure 3.3a, top), where we aligned the cube's diagonal with each participant's estimated NGA, approximately 50% of grasps should be oriented clockwise (green shaded region of the distribution) and 50% of grasps should be counterclockwise (orange region). In the NGA-unaligned condition (Figure 3.3a, middle), where the cube diagonal is rotated away from each participant's measured NGA, most of the NGA distribution should fall clockwise to this diagonal, thus most grasps should be clockwise. The proportion of clockwise grasps P_{cw} can thus be formalized as the value of the cumulative normal function $\Phi(x, \mu_{NGA}, \sigma_{NGA})$, evaluated at $x = \xi$:

$$P_{cw} = \Phi(\xi, \mu_{NGA}, \sigma_{NGA})$$

In conditions with different materials at the opposing pairs of surfaces (Figure 3.3a, bottom), we assumed that each individual's μ_{NGA} shifts clockwise and counterclockwise by amounts proportional to the perceived friction of the surfaces $\nu_{material}$ and to the clockwise or counterclockwise rotations required to grasp these surfaces, $\varphi_{\theta,cw}$ and $\varphi_{\theta,ccw}$, with:

$$\varphi_{0,cw} = -45;\ \varphi_{0,ccw} = +45;\ \varphi_{\pi/8,cw} = -22.5;\ \varphi_{\pi/8,ccw} = +67.5$$

Specifically:

$$\mu_{\theta,material-cw/material-ccw} = \mu_{NGA} + \nu_{material-cw} \times \varphi_{\theta,cw} + \nu_{material-ccw} \times \varphi_{\theta,ccw}$$

The unknown variables in this framework are thus the positive valued, perceived friction coefficients:

$$\nu_{wood}, \nu_{brass}, \nu_{sandpaper}, \nu_{brasseline}$$

Note that we measured each participant's NGA prior to our main experiment, and we could thus estimate μ_{NGA}, σ_{NGA} from these measurements. However, as validation of our model, we also seeded the model with the NGA measurements, but allowed μ_{NGA}, σ_{NGA} as free parameters. We fit this simple model to each individual participant's data, and found that the model is able to closely replicate the observed patterns of human data both at the group level (Figure 3.3b) and at the level of individual participants (Figure 3.3c), even after adjusting for the number of predictors in the model (r=0.98, p<.001, r^2=0.96, $r^2_{adjusted}$=0.90). Figures 3d and 3e show that the model's fitted μ_{NGA} and σ_{NGA} parameters both significantly correlate with the NGA measurements taken with the brass cylinder object prior to the main experiment (r=0.48, p=.027 and r=0.85, p<.001, respectively). Figure 3.3f further shows that the fitted friction coefficients also significantly correlate with human perceptual ratings of friction (r=0.75, p<.001; per participant average r=0.75, IQR = [1, 0.5]).

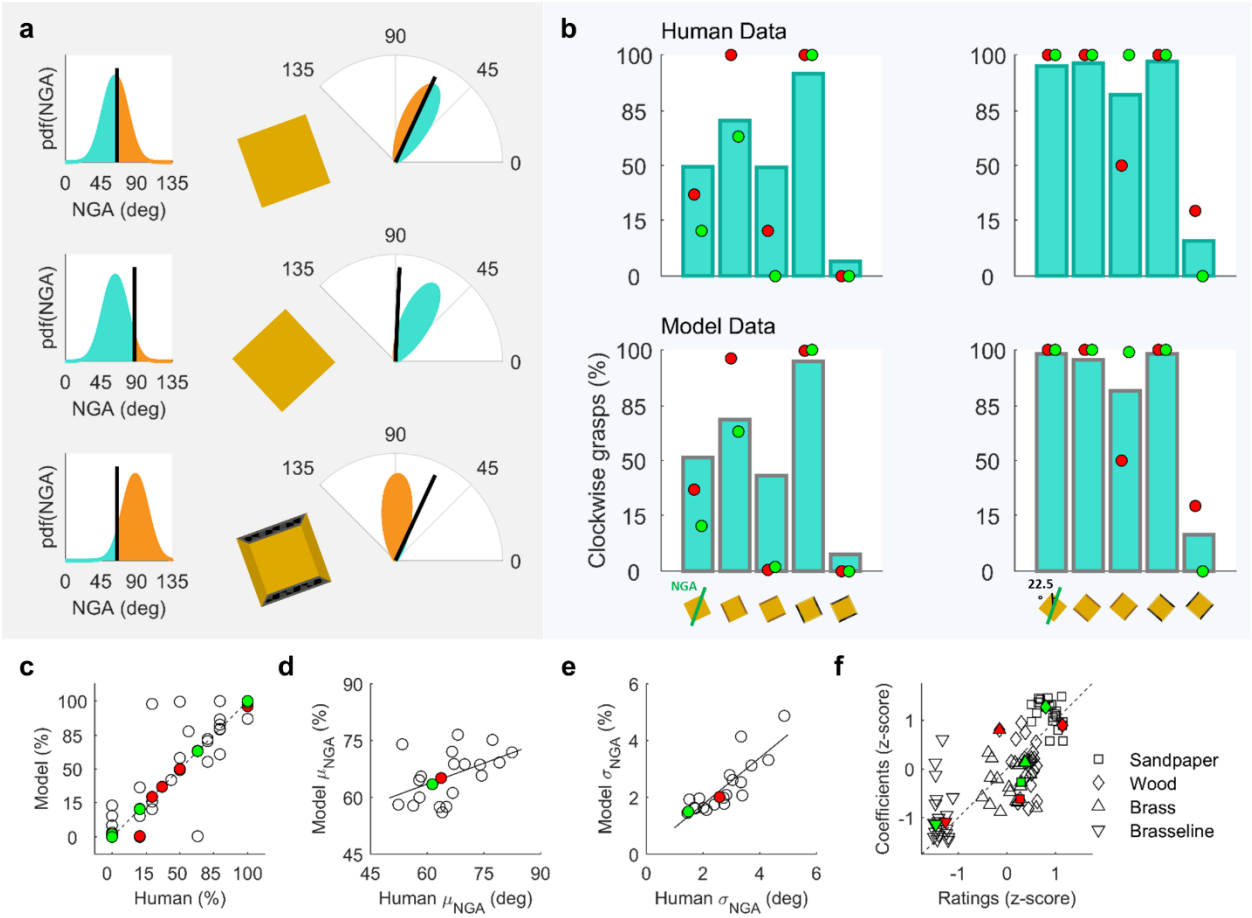

Figure 3.3. Model results. a Model behavior, exemplified at the group level. In the same material conditions (top and middle), the cube diagonals (black lines) in the aligned and unaligned conditions split the NGA distribution into clockwise (green) and counterclockwise (orange) grips by different amounts. In one example condition with different surface materials, the NGA distribution is shifted counterclockwise following the surface with higher friction (sandpaper/black). For clarity, here we show the NGA distribution in both Cartesian (left) and polar axes (right), but please note that these plots show absolute grip angles, not relative grip angles as in panels b and c of Figure 3.2. b These shifts very closely capture the patterns of human data, both at the group level, and at the level of individual participants (data for two example participants with corresponding fitted model outputs are shown as green and red dots). c Human vs Fitted model percent clockwise grasps. d,e Human vs Fitted model μ_{NGA} and σ_{NGA}. f Human ratings of perceived surface friction vs Fitted model friction coefficients.

Note that the human perceptual ratings of friction also correlated with the ratings of pleasantness (r=0.80, p<.001), and thus pleasantness ratings also correlated with model friction coefficients (r=0.58,

p<.001). However, human perceptual ratings of friction explain 20% more of the variance in the fitted model coefficients.

Given the correlations between model and human NGA parameters, it is also possible to construct a model with only the friction coefficients as free parameters, fixing μ_{NGA} and σ_{NGA} to the experimentally measured values for each participant. This reduced model is also able to replicate the observed patterns of human data (r=0.84, p<.001, r^2=0.71, $r^2_{adjusted}$=0.51), and the fitted friction coefficients again significantly correlate with human perceptual ratings of friction (r=0.65, p<.001) better than with pleasantness ratings (r=0.45, p<.001). This simple model is thus able to directly relate human perception of surface friction to the selected hand posture for grasping.

3.4 Discussion

We examined whether the selection of grasp endpoints depends primarily on the grasp stability or on the adoption of the usual grasp configuration at the moment of the grasp. To this end, we first measured individual NGAs and then oriented cuboid objects so that their corners were either aligned with the individual NGA or rotated 22.5° counterclockwise from the NGA. By having participants grasp cuboids, we implicitly asked them to grasp the cuboid object with one of two possible grasp configurations. By placing these cuboids at two different orientations, we created conditions in which grasps could be either bimodally distributed or systematically directed to one pair of the object's sides. By further manipulating the materials of the object's surfaces, we introduced conditions in which the axis connecting the higher friction surfaces was orthogonal to the grasp axis required for adopting the usual final grasp configuration, eventually allowing us to test which of the two factors is more important for contact point selection. Our results are clear: Humans choose endpoints that promote stable grasps, even if this requires adopting unusual grasp configurations.

The object's orientation influenced the selection of endpoints as expected (Voudouris et al., 2012a). When grasping the NGA-aligned all-brass object, grasp orientations at the population level were bimodally distributed, reflecting that objects could indeed be grasped from both pairs of sides without adopting awkward grasp configurations. Interestingly however, single participant grasps were less bimodally-distributed than at the group level, even when participants should not have had a clear preference in grip orientation, perhaps reflecting the fact that grasp planning is sensitive to sensorimotor memories obtained in previous trials (Dixon et al., 2012; Dixon & Glover, 2009; Jax & Rosenbaum, 2007; J. R. Lukos et al., 2013; Volcic & Domini, 2018; Witney et al., 2001). When grasping the NGA-unaligned all-brass object, the grasp distribution was clearly unimodal, suggesting that participants systematically chose grasp configurations within the midrange of their joints and avoided extreme joint angles at the moment of the grasp (Rosenbaum et al., 2001), likely to avoid pronounced endpoint errors (Rossetti et al., 1994).

Our main interest, though, was whether participants would sacrifice their usual grasp configuration to choose stable endpoints or whether they would tolerate endpoints on the lower friction surfaces to maintain their usual grasp configuration. We show that participants were content to adopt unusual grasp configurations that foster grasp stability. This is reflected in the systematic switches of grasps between the two different configurations of each (wooden and *brasseline*) object, and is highlighted in the clear change of behavior when grasping the different configurations of the *brasseline* object: Participants tailored their grasp configurations to ensure that their digits landed almost always on the

sandpaper rather than on the vaseline-covered surface (see Figure 3.2d,e). This behavior was also evident for the wooden object, but less pronounced. A possible reason for this difference might be that participants avoided the vaseline-covered surface for other reasons than slipperiness per se, for instance to avoid having vaseline stuck on their digits or due to the unpleasantness of that material. We believe that this is unlikely, as our modelling demonstrates that participant grasps are more directly related to perceived surface friction, rather than perceived pleasantness to the touch. Rather, the difference between the wooden and the *brasseline* objects should be attributed to the lower relative costs of grasping the two surfaces of the wooden object (brass over wooden) compared to the greater costs of grasping the two surfaces of the *brasseline* object (vaseline-covered brass over sandpaper). Of course, if grasping the higher friction surfaces required particularly extreme grasp configurations (e.g., at the very limits of what is biomechanically possible), participants may have favored the lower friction of the two alternative grasps, as long as they could produce sufficient forces to overcome the lack of friction. However, we find that within the range of conditions tested, participants spontaneously adopted grasp configurations that they otherwise would almost never produce to avoid the difficulties associated with grasping a slippery surface.

Our model linking perceptual ratings of friction to final grip orientation hints at how a simple neural circuit could implement these changes in grip selection in the brain, for example within the network formed between the Ventral Premotor Cortex (Area F5), Dorsal Premotor Cortex (Area F2), and the Anterior Intraparietal Sulcus (AIP). Areas F5 and F2 encode grip-wrist configuration and orientation (Raos et al., 2004, 2006). Both regions exhibit strong connections with AIP (Murata et al., 2000), which in turn plays a key role in linking the ventral visual stream (where visual material properties are encoded) to the hand motor system (Borra et al., 2008). Therefore, through area AIP, estimates of surface friction coming from ventral visual areas could bias our preferred grip orientation encoded in areas F5 and F2.

Choosing grasp endpoints requires the consideration of several factors. Two main factors are grasp stability and the final grasp configuration (Klein et al., 2020). Grasp stability is important when controlling grasping and choosing endpoints (Paulun et al., 2016; Smeets & Brenner, 1999). Interestingly, humans have been found to sacrifice grasp stability in order to adopt grasp configurations that minimize other energy-related costs, such as torques during object manipulation (Glowania et al., 2017). Yet the magnitude of grip force that is required to overcome surface friction also determines energy expenditure and thus places additional constraints on grasp point selection, suggesting a crucial role of surface material properties in grasping. By directly juxtaposing the contributions of grasp configuration and stability, we demonstrate that participants systematically chose endpoints that promote stable grasps, even when these endpoints required grasp configurations that would otherwise be avoided. We conclude that humans strive for stable grasp endpoints at the expense of their final grasping posture.

Chapter 4

STUDY III
Distinct neural components of visually guided grasping during planning and execution

A similar version of this manuscript is under preparation for submission to a peer-reviewed journal: Klein, L. K., Maiello, G., Stubbs, K., Proklova, D., Paulun, V. C., Culham. J. C., & Fleming, R. W. (in prep.) Distinct neural components of visually guided grasping during planning and execution.

Selecting suitable grasps on three-dimensional objects is a challenging visuomotor computation, which involves combining information about an object (e.g., its shape, size, and mass) with information about the actor's body (e.g., the optimal grip aperture and hand posture for comfortable manipulation). Here we used functional magnetic resonance imaging to investigate brain networks associated with these distinct aspects during grasp planning and execution. Human participants viewed and then executed preselected grasps on L-shaped objects made of wood and/or brass. By leveraging a computational approach that accurately predicts human grasp locations, we selected grasp points that disentangled the role of multiple grasp-relevant factors: grasp orientation, grasp size, and object mass. Representational Similarity Analysis revealed that grasp orientation was encoded along dorsal regions during grasp planning. Grasp size was first encoded in ventral areas during grasp planning, then in premotor regions during grasp execution. Object mass was encoded in ventral and (pre)motor regions only during grasp execution. Premotor regions further encoded visual predictions of grasp comfort, whereas the ventral stream encoded grasp comfort during execution, suggesting its involvement in haptic evaluation. These shifts in neural representations thus capture the sensorimotor transformations that allow humans to grasp objects.

4.1 Introduction

Grasping is one of the most frequent and essential everyday actions performed by humans and other primates (Betti et al., 2021), yet planning effective grasps is computationally challenging. Successful grasping requires identifying object properties including shape, orientation, and mass, and considering how these interact with the capabilities of our hands (Fabbri et al., 2016; Maiello et al., 2019, 2021; Klein, Maiello et al., 2020). Whether an object is large or small, heavy or light, determines how wide we open our hands to grasp it and how much force we apply at the fingertips to lift it (Cesari & Newell, 1999; Johansson & Westling, 1988). Such grasp-relevant object properties are often estimated visually. For example, by visually recognizing an object's material composition one can infer its weight, mass distribution, and surface friction (Fleming, 2017; Klein et al., 2021).

We recently developed a computational model that accurately predicts human precision-grip grasp locations on 3D objects of varying shape and non-uniform mass (Klein, Maiello et al., 2020). The model suggests that grasping may be solved by combining multiple constraints related to properties of the object and the effector, such as the torque associated with different grasps and the actor's natural grip axis. It remains unclear, however, which brain networks are involved in computing specific grasping constraints. Moreover, it is unknown whether all constraints are estimated during grasp planning (i.e., before initiation of the action; Gallivan et al., 2013, 2019) or whether some aspects are computed primarily during action execution, allowing the actor to refine grasp parameters on-line before or during contact with the object.

Previous studies show that grasp-relevant representations are distributed across ventral and dorsal visual processing streams. Representations of object shape are present throughout both streams (Konen & Kastner, 2008; Orban, 2011; Orban et al., 2006; Sereno et al., 2002), with dorsal representations emphasizing information required for grasp planning (Srivastava et al., 2009). For example, dorsomedial area V6A—which falls within the superior parieto-occipital cortex (SPOC) of humans—plays a role in selecting hand orientation given object shape (Fattori et al., 2004, 2009, 2010; Monaco et al., 2011). Visual representations of material properties—also crucial for grasping—have instead been identified predominantly in ventral regions such as lateral occipital cortex (LOC), the posterior fusiform sulcus (pFS), and parahippocampal place area (PPA; Cant and Goodale, 2011; Hiramatsu et al., 2011; Gallivan et al., 2014; Goda et al., 2014, 2016). Brain regions that transform these disparate visual representations into appropriate motor codes for grasping include Anterior Intraparietal Sulcus (aIPS), Ventral Premotor Cortex (PMv), Dorsal Premotor Cortex (PMd), and primary motor cortex (M1). Neurophysiological work in primates suggests that PMv (primate Area F5) encodes grip configuration (Murata et al., 1997; Raos et al., 2006; Theys et al., 2012), while PMd (primate Area F2) encodes grip/wrist orientation (Raos et al., 2004). Both regions exhibit strong connections with aIPS, which could play a key role in linking visual representations—including those in ventral stream regions (Borra et al., 2008)—to the motor commands generated and sent to the hand through M1 (Janssen & Scherberger, 2015; Murata et al., 2000).

How information flows and is combined across this complex network of brain regions is far from understood. We therefore sought to identify cortical regions associated with distinct components of grasping and test their relative importance during grasp planning and execution. To disentangle grasping constraints, we used our modelling approach (Maiello et al., 2021) to select grasps which placed different constraints in conflict with one another. For example, a selected grasp could be near optimal in terms of the required hand orientation, but sub-optimal in terms of grasp aperture. We

then measured functional magnetic resonance imaging (fMRI) blood-oxygen-level-dependent (BOLD) activity, during planning and execution of these preselected grasps. Combining this model-guided approach with representational similarity analysis (RSA; Kriegeskorte, 2008) let us tease apart the relative contributions of object mass, grip size, and orientation, at different stages of grasping.

4.2 Results

Participants in a 3-Tesla MRI scanner were presented with physical 3D objects on which predefined grasp locations were shown (Figure 4.1A). On each trial, participants first planned how to grasp the objects (planning phase, Figure 4.1B) and then executed the grasps (action phase). We designed objects and grasp locations to produce a set of nine distinct conditions (Figure 4.1C) that would differentiate three components of grasping: the grip orientation, the size of the grip aperture, and object mass. By computing pairwise distances between all conditions for each of these grasp-relevant dimensions, we constructed one representational dissimilarity matrix (RDM) for each component (Figure 4.1D-F). In each brain region of interest (ROI) tested in the study, brain-activity patterns elicited by each condition were compared to each other via Pearson correlation to construct brain RDMs. Figure 4.1G shows one such RDM computed from brain region PMv for one example participant during the planning phase. In this participant, this area appeared to strongly encode grasp axis.

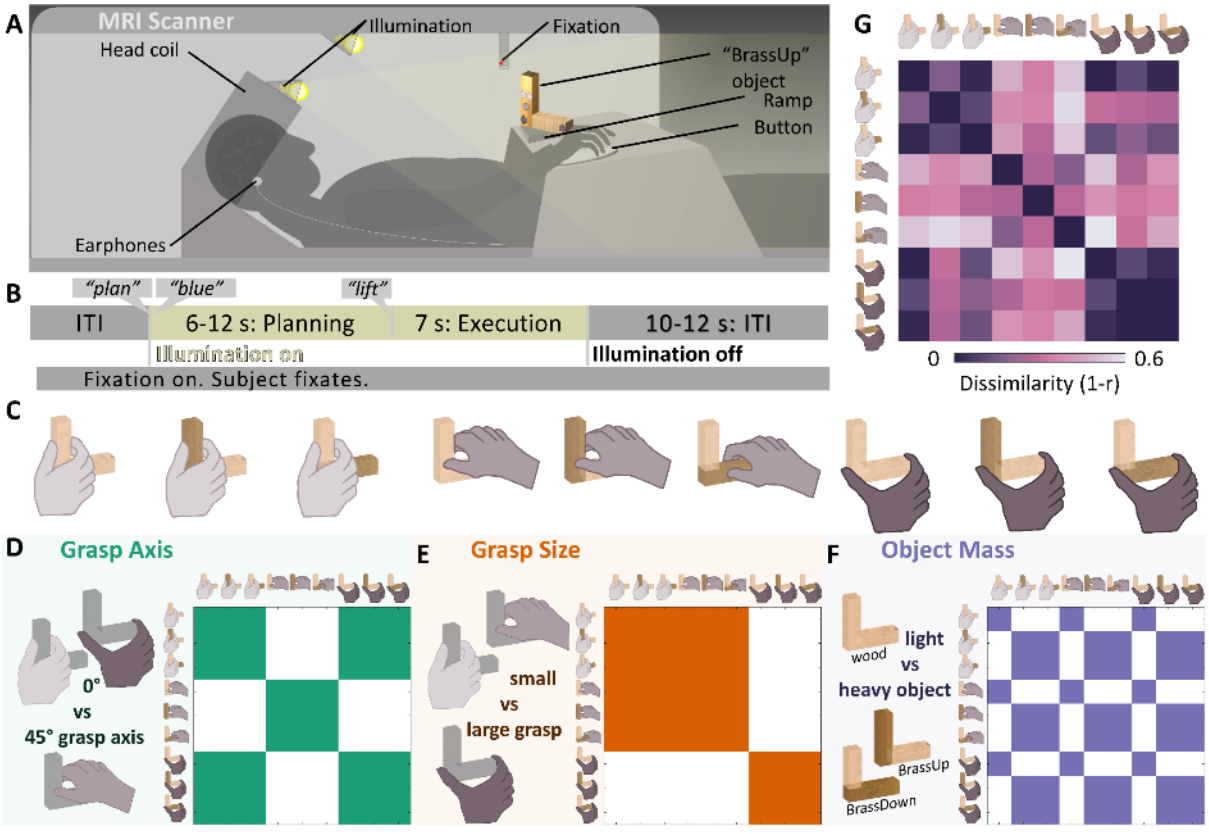

Figure 4.1. Study design. (A) Participants in the MRI scanner were cued to grasp 3D objects at specific locations. (B) Sequence of events for one example trial during which participants were instructed to grasp the object at the predefined location marked by different color dots or arrows. (C) Preselected grasps on stimulus objects of wood and brass produced nine distinct conditions designed to differentiate three components of grasping using RSA. (D-F) RDMs for grasp axis, grasp size, and object mass. Colored cells represent condition pairs with zero dissimilarity, white cells represent maximum dissimilarity. (G) An example RDM computed from fMRI BOLD activity patterns in region PMv of one participant during the planning phase. Note the strong similarity to the grasp axis RDM in panel D.

4.2.1 How grasp-relevant neural representations develop across the grasp network

Figure 4.2A shows average neural RDMs computed throughout the network of visuomotor brain regions we investigated. ROIs were selected from the literature as regions most likely specialized in the components of visually guided grasping investigated in our study. We included primary visual cortex, V1, as the first stage of cortical visual processing. Areas LOC, pFS, and PPA within the ventral visual stream (occipitotemporal cortex) were included as they are known to process visual shape and material appearance (Cant & Goodale, 2011; Gallivan et al., 2014; Goda et al., 2014, 2016; Hiramatsu et al., 2011), and could thus be involved in estimating object mass. Areas SPOC, aIPS, PMv, and PMd within the dorsal visual stream (occipitoparietal and premotor cortex) were included as they are thought to transform visual estimates of shape and orientation into motor representations (Janssen & Scherberger, 2015). Primary motor and somatosensory area (M1/S1, in the central sulcus) was included as the final stage of cortical sensorimotor processing. The patterns of correlations between model and neural RDMs across participants and ROIs (Figure 4.2B-G) reveal which information was encoded across these visuomotor regions during grasp planning and execution phases.

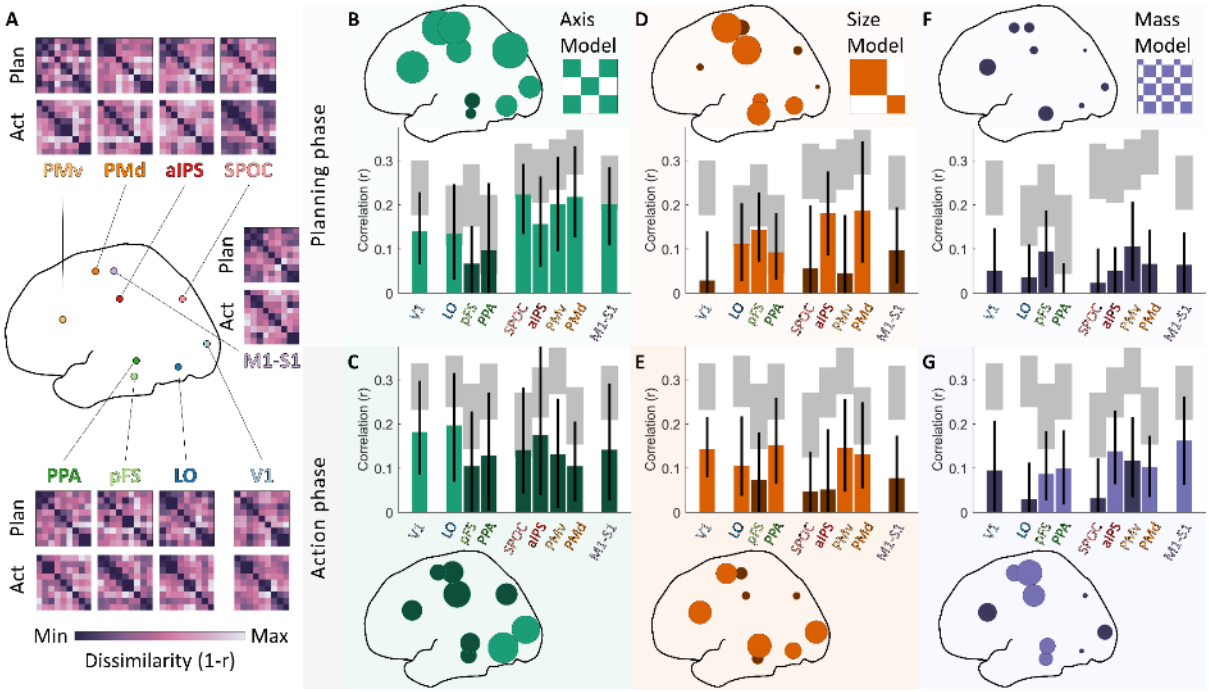

Figure 4.2. RSA results. (A) Mean neural RDMs computed in the nine ROIs included in the study. Only for visualization purposes, RDMs within each region are first averaged across participants and then rescaled. (B-G) Correlations between model and neural RDMs in each brain ROI during planning (top, B,D,F) and action phases (bottom, C,E,G). In bar graphs, grey shaded regions represent the noise ceiling for each ROI. Bars are means, error bars represent 95% bootstrapped confidence intervals. The same data are represented topographically as dots scaled proportionally to the mean correlation in each region. Bright colors represent significant positive correlations (p<.05 with FDR correction); correlations shown in dark colors are not statistically significant.

4.2.1.1 Grip orientation was encoded in visuomotor regions more robustly during grasp planning

Figure 4.2B,C shows that neural representations in V1 and ventral region LOC were significantly correlated with grip orientation during both grasp planning and action phases. In contrast, representations in ventral areas pFS and PPA were never significantly correlated with grip orientation.

Further, grip orientation was significantly correlated with neural representations across all dorsal areas (SPOC, aIPS, PMv, PMD), as well as M1/S1, but only during grasp planning. Dorsal and motor areas thus robustly encoded the orientation of the hand when preparing to grasp objects, suggesting that the hand-wrist orientation was among the first components of the action computed across these regions.

4.2.1.2 Grip aperture was encoded across both visual streams during grasp planning and execution

During the planning phase (Figure 4.2D), grip size significantly correlated with neural representations in all ventral areas (LOC, pFS, PPA), and with representations in dorsal regions aIPS and PMd. During the action phase (Figure 4.2E), grip size remained significantly correlated with neural representations in ventral areas LOC and PPA, but not pFS. In the dorsal stream during the action phase, grip size remained significantly correlated with neural representations in PMd but not aIPS, and became significantly correlated with representations in PMv. Neural representations in early visual area V1 were significantly correlated with grip size only in the action phase, but not during planning. Finally, neural representations in motor area M1/S1 were never significantly correlated with grip size. Thus, different ventral and dorsal areas encoded grip aperture at different time points. These data suggest that ventral regions may have been initially involved in computing grip size and might have relayed this information (e.g., through aIPS) to the premotor regions tasked with generating the motor codes to adjust the distance between fingertips during the action phase.

4.2.1.3 Object mass was encoded across dorsal and ventral streams and in motor areas, but only during grasp execution

During the planning phase (Figure 4.2F), none of the investigated ROIs exhibited any activity that was significantly correlated with object mass. Conversely, during the action phase (Figure 4.2G), object mass significantly correlated with representations in ventral areas pFS and PPA, dorsal areas aIPS and PMd, and sensorimotor area M1/S1. Object mass was thus encoded in the later stages of grasping, likely when the hand was approaching the object and preparing to apply appropriate forces at the fingertips.

4.2.2 Representational similarities within the grasp network

Figure 4.3 summarizes the structure of representational similarity across ROIs, both within and between planning and action phases. Specifically, we took the RDMs generated for each of the nine ROIs (Figure 4.2) and correlated them with one another to reveal inter-ROI similarity relationships. Neural representations were significantly correlated across many selected ROIs during both grasp planning (Figure 4.3A) and execution (Figure 4.3C).

4.2.2.1 The dorsal stream linked visual and motor regions during grasp planning

In the planning phase (Figure 4.3B), similarities among neural representations appeared to form one main cluster: dorsal stream areas aIPS and SPOC grouped together with premotor area PMd and sensorimotor area M1/S1, separately from remaining regions. To aid visualizing the similarities in representational content between ROIs, we also show these correlation patterns arranged topographically within a schematic brain, with the strength of connections between ROIs proportional to the correlations between their corresponding RDMs. This topographical plot highlights how the strongest correlations occurred along the dorsal stream between V1 and SPOC, SPOC and M1/S1, and

between M1/S1, PMd, and aIPS. The MDS plot also shows how dorsal regions SPOC and aIPS fell between V1 and motor regions. During grasp planning, we thus observed similar representational structure from early visual to dorsal regions, and from dorsal to motor regions.

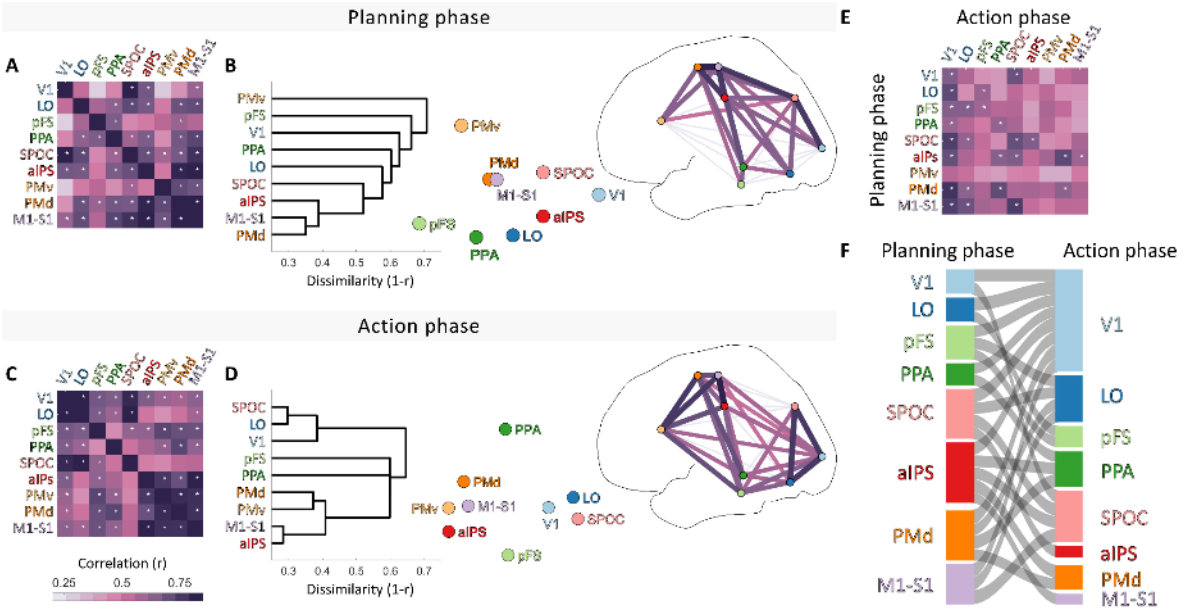

Figure 4.3. The representational structure of grasping. (A) Matrix showing correlations of data RDMs between regions during the planning phase. White asterisks represent significant correlations (p<.05 with Bonferroni correction). (B) The same data in A are shown through hierarchical clustering and 2D multidimensional scaling, and significant correlations are shown topographically. (C,D) As in A, except for the planning phase. (E) Correlations between ROIs across planning and action phases. (F) Sankey diagram depicting significant correlations from E.

4.2.2.2 The ventral stream linked visual and motor regions during action execution

In the action phase (Figure 4.3D) the similarities among brain regions formed two main clusters. One cluster of visual regions was formed by V1, SPOC, and LOC. The second cluster comprised aIPS, premotor areas PMv and PMd, and M1/S1. MDS and topographical plots highlight how these two clusters appeared to be share representational content predominantly through ventral stream regions pFS and PPA.

4.2.2.3 Shared representations across planning and action phases

Neural representation patterns were also partly correlated across grasp planning and execution phases (Figure 4.3E,F). Notably, aIPS representations during the planning phase were significantly correlated with representational patterns in ventral (PPA), dorsal (SPOC, PMd), and sensorimotor (M1/S1) regions during the action phase. This suggests that aIPS may play a key role in linking grasp planning to execution. Further, neural representation patterns in nearly all ROIs (except PMv) during the planning phase were robustly correlated with representations in V1 during the action phase, and representations in pFS, SPOC, PMd, and M1/S1 during action planning were correlated with LOC representations during action execution. In the discussion, we speculate how this might reflect mental simulation and prediction mechanisms at play.

4.2.3 Grasp comfort

We recently demonstrated that humans can visually assess which grasp is best among competing options and can refine these judgements by executing competing grasps (Maiello et al., 2021). These visual predictions and haptic evaluations of grasp comfort were well captured by our multi-factorial model (Klein, Maiello et al., 2020), suggesting they may play a role in grasp selection. We thus wondered whether we could identify, within the grasp network investigated here, brain regions that encoded visual predictions and haptic evaluations of grasp comfort. To this end, once an imaging session was completed, we asked participants (while still lying in the scanner) to execute once more each of the nine grasps and rate how comfortable each felt on a scale of 1 to 10. Comfort ratings were consistent across participants (Figure 4.4A). Comfort was slightly modulated by grip axis (Figure 4.4B, $t(20)=3.3$, $p=.0037$) and was not modulated by grip size (Figure 4.4C, $t(20)=0.89$, $p=.39$). The factor that most affected grasp comfort was object mass, with heavy objects being consistently rated as less comfortable than light objects (Figure 4.4D, $t(20)=8.1$, $p<.001$). This was also evident when we computed RDMs from comfort ratings (Figure 4.4E) and found that these were significantly correlated with the model RDM for object mass ($p<.001$) but not with RDMs for grasp axis ($p=.54$) or grasp size ($p=.83$) (Figure 4.4F).

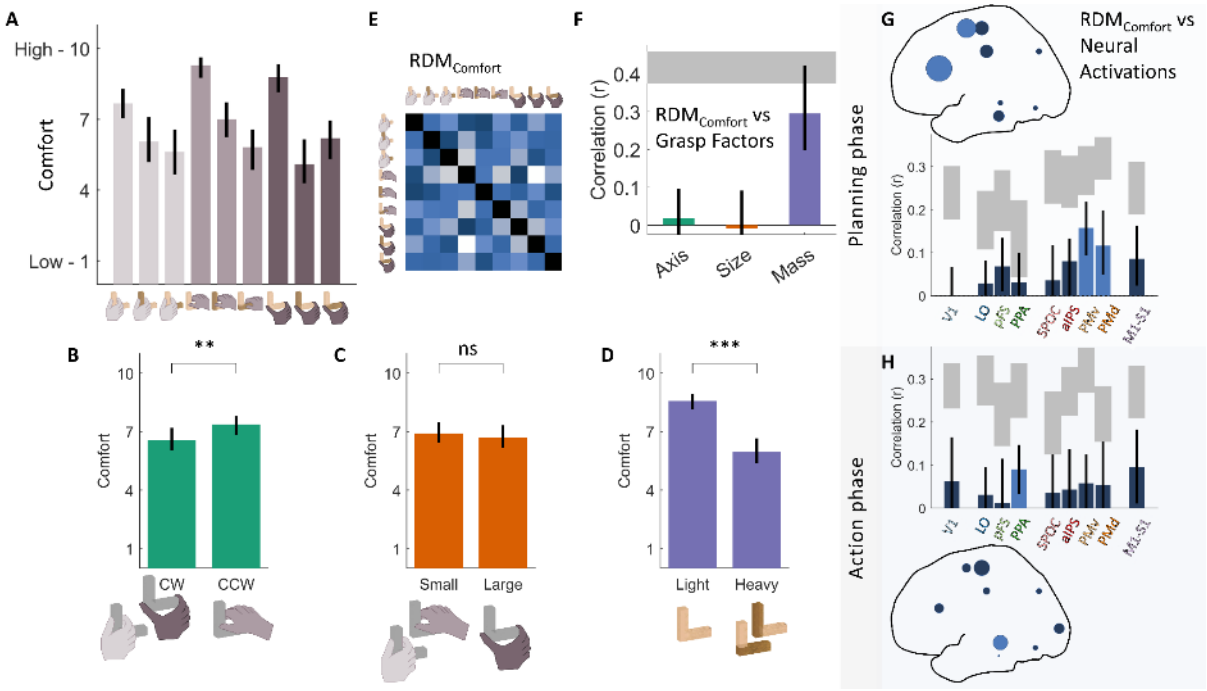

*Figure 4.4. Grasp comfort. (A) Average grasp comfort ratings for each grasp condition in the fMRI experiment. (B,C,D) Grasp comfort ratings averaged across (B) grasp axis, (C) grasp size, and (D) object mass. (E) Average RDM computed from participant comfort ratings. (F) Correlations between grasp comfort and model RDMs. (G,F) Correlations between grasp comfort and neural RDMs in each brain ROI during planning (top, G) and action phases (bottom, H). In bar graphs, grey shaded regions represent the noise ceiling for each ROI. Bright blue bars represent significant positive correlations ($p<.05$ with FDR correction); correlations shown in dark blue are not statistically significant. The same data are represented topographically as dots scaled proportionally to the mean correlation in each region. Across figure panels, bars are means, error bars represent 95% bootstrapped confidence intervals. **p<0.01, ***p<0.001*

4.2.3.1 Neural representations of grasp comfort were present during both grasp planning and execution phases

To identify brain regions that encoded grasp comfort, we next correlated neural RDMs with the average RDM derived from participant comfort ratings. Neural representations in premotor regions PMv and PMd were significantly correlated with grasp comfort during grasp planning (Figure 4.4G). During the action phase instead, grasp comfort correlated with neural representations in ventral stream region PPA (Figure 4.4H). This suggests that dorsal premotor regions encoded the visually predicted comfort of planned grasps (which in our conditions was primarily related to the object mass). Area PPA instead encoded comfort during the action phase, and might thus either be involved in the haptic evaluation of grasp comfort or it is involved in material properties, which are correlated with mass, which is correlated with comfort.

4.3 Discussion

We investigated how grasp-relevant information is represented across sensorimotor brain regions during visually guided grasping. We found that grip orientation, which is adjusted at the very beginning of reach-to-grasp movements (Cuijpers et al., 2004), was predominantly encoded across dorsal regions during grasp planning. Grip size, which is adjusted throughout reach-to-grasp movements (Cuijpers et al., 2004), was encoded in different sets of ventral and dorsal regions during grasp planning and execution. Object mass, which gains relevance when applying forces at the fingertips upon hand-object contact (Johansson & Flanagan, 2009; Johansson & Westling, 1988), was instead encoded across ventral, dorsal and motor regions during grasp execution. Broadly speaking, sensorimotor processing appeared to shift from the dorsal stream during grasp planning to the ventral stream during action execution. Our results also corroborate previously hypothesized mechanisms for sensorimotor prediction and evaluation that could enable the detection and correction of movement errors and help refine subsequent actions (Wolpert et al., 2011; Wolpert & Ghahramani, 2000). In the following, we first discuss our findings with respect to the individual ROIs investigated, and then we address network function as a whole.

4.3.1 Individual regions of interest

4.3.1.1 V1

Primary visual cortex represents the first stage of cortical visual processing upon which all subsequent visuomotor computations rely. In our data, V1 activity during grasp planning encoded grasp axis, whereas during grasp execution it encoded both grasp axis and size. The fact that V1 activity encoded grasp axis and size during action execution is perhaps unsurprising, since participants could view their own hands performing the distinct actions. The finding that the future grasp axis was encoded in V1 activity during action preparation instead is in line with previous work showing that future actions can be decoded from patterns of activity in early visual cortex during action preparation (Gallivan et al., 2019; Gutteling et al., 2015). This finding could be explained by top-down enhancement of grasp-relevant orientations from area aIPS (Gutteling et al., 2011, 2013). This would be coherent with our results, since during action preparation aIPS also encoded grasp axis, and neural representations in aIPS were significantly correlated with V1 representations.

4.3.1.2 LOC

Ventral visual area LOC encoded both grasp axis and grasp size during both planning and action phases. The area we selected resides within the lateral occipital complex, a large ventral stream region strongly implicated in visual object recognition (Grill-Spector et al., 2001), which was initially thought not to play a role in grasping (Cavina-Pratesi et al., 2007; Culham et al., 2003). More recent work however suggests that the lateral occipitotemporal cortex supports action perception and understanding, including the anticipated perceptual effects of planned movements (Lingnau & Downing, 2015). Gallivan et al. (2013) even demonstrated that action intentions can be decoded specifically from area LO within this broader region. Our data is therefore consistent with the notion that the selected region could be implicated in more abstract planning of the required movements. Such abstract action intentions could be communicated though the hypothesized ventro-dorsal stream (Rizzolatti & Matelli, 2003) for example to area aIPS, a possibility supported by the significant correlation we observed between neural representations in LOC and aIPS during grasp planning. Contrary to our expectations instead, and unlike previous work (Cant & Goodale, 2011; Gallivan et al., 2014; Goda et al., 2014, 2016; Hiramatsu et al., 2011; van Polanen, Rens, et al., 2020), we did not observe representations of object material and weight in LOC.

4.3.1.3 pFS and PPA

Perhaps due to their proximity to each other, patterns of results in ventral areas PPA and pFS were similar. Both regions encoded grasp size during grasp planning. During the execution phase, only PPA encoded grasp size, and both regions encoded object mass. Even though these regions are thought to be predominantly involved in object recognition (Grill-Spector et al., 2001) and scene perception (Epstein & Kanwisher, 1998), the fact that pFS and PPA representations correlated with grasp size during the planning phase is also consistent with (Gallivan et al., 2013) who found that action intentions could be decoded from these regions. Additionally, the finding that pFS representations correlated with object mass during grasp execution agreed with our expectations and with previous research (Gallivan et al., 2014; Goda et al., 2014; Hiramatsu et al., 2011). Further, during grasp execution representations in pFS and PPA correlated with representations in aIPS, PMv, PMd, and M1/S1. This result is consistent with the notion that ventral regions may communicate visual estimates of object weight to the dorsal and (pre)motor regions that use this information to plan and modulate the fingertip forces at object lift-off (Wolpert et al., 2011; Wolpert & Ghahramani, 2000). Finally, the fact that PPA encoded both object mass and grasp comfort during action execution could suggest a previously unexplored role of this region in the haptic evaluation of grasp quality.

4.3.1.4 SPOC

Dorsal visual region SPOC encoded grasp axis during the planning phase, and never encoded grasp size or object mass. Given that our stimulus objects were always presented in the same orientation, this result closely agrees with (Monaco et al., 2011). These authors found neural adaptation within this region when an object was repeatedly grasped with the same orientation, but not when participants simply reached towards or passively viewed an object in the same orientation, suggesting that SPOC encoded grasp orientation, not object orientation. In the macaque, activity in parieto-occipital area V6A is modulated by hand orientation during reach-to-grasp movements (Fattori et al., 2004, 2009, 2010). Our data are thus consistent with the notion that SPOC is the human homologue of macaque V6A (Monaco et al., 2011; Pitzalis et al., 2013). Additionally, during grasp planning, representations in SPOC correlated strongly with V1 representations, as well as with representations in aIPS, PMv, PMd,

and M1/S1. This suggests that SPOC may represent a key node in the dorso-dorsal visual stream involved in the early stages of reach to grasp movements (Rizzolatti & Matelli, 2003).

4.3.1.5 aIPS

In our results, aIPS encoded grip axis and size during the grasp planning phase, and object mass during the execution phase. This agrees with previous results showing that processing within aIPS is likely to be goal dependent and serial (Tunik et al., 2005), and that aIPS is specialized in integrating object properties in order to pre-shape the hand during grasping (Binkofski et al., 1999; Culham et al., 2003; Frey et al., 2005; Monaco et al., 2015; Rice et al., 2006). More specifically, (Taubert et al., 2010) showed that transcranial magnetic stimulation (TMS) disrupted grip rotations when applied to aIPS in earlier movement phases and when applied to PMd in later movement phases. Similarly, and in line with our results, (Glover et al., 2005) used TMS to show that aIPS was involved in planning but not execution of grasp size. Additionally, (Davare et al., 2007) found that TMS applied over aIPS in early movement phases disrupted hand shaping, whereas TMS applied during later movement phases disrupted grip force scaling. This agrees with Dafotakis et al. (2008) who suggest that this region is involved in the reactive online adjustment of grip force. Our results thus unify these previous findings—predominantly obtained using TMS—and suggest that aIPS likely first computes grasp axis (Taubert et al., 2010; Tunik et al., 2005), then grasp size (Davare et al., 2007; Tunik et al., 2005), then grip forces (Davare et al., 2007).

During grasp planning, aIPS representations correlated with representations in early ventral and dorsal regions LO, PPA, and SPOC, as well as (pre)motor regions PMd and M1/S1. During action execution, aIPS representations correlated with representations in ventral region pFS and (pre)motor regions PMv, PMd, and M1/S1. Further, aIPS representations during grasp planning correlated with representations in PPA, SPOC, PMd and M1/S1 during action execution. These patterns of representational similarity match the intricate patterns of structural connectivity exhibited by anterior intraparietal area with both ventral and dorsal regions in the macaque sensorimotor cortex (Borra et al., 2008). Taken together, these findings suggest that aIPS plays a key role in linking early visual representations in both ventral and dorsal regions to motor representations (Davare et al., 2010, 2011), even across movement planning and execution phases.

4.3.1.6 PMv

Premotor area PMv encoded grasp axis during the planning phase, and grasp size during the execution phase. These results confirm previous findings from macaque neurophysiology and extend these findings to humans. In macaque, Fogassi et al. (2001) showed that inactivation of area F5 (the homologue of human PMv) led to the loss of a monkey's ability to preshape the hand using visual object shape and size information. Raos et al. (2006) were perhaps the first to propose that area F5 encoded both grip configuration and the grip/wrist rotation required to match the axis orientation of the object. Fluet et al. (2010) further found that area F5 encoded grasp orientation more strongly during movement preparation, while during movement execution orientation representation dropped and grip type representation increased. This observation was confirmed by Townsend et al. (2011) who found that F5 exhibited orientation tuning during grasp planning, and strong grip type tuning during movement execution. Even though research in humans has shown that PMv is involved in controlling grip size during action execution Davare et al. (2006), to the best of our knowledge no previous research has shown that human PMv also separately encodes grasp orientation. Thus, our

results suggest that, similarly to what occurs in macaque F5, human PMv sequentially processes grip orientation during movement planning and grip size during action execution.

In the macaque, some authors have found cells in premotor ventral regions which were also modulated by grip force (Hepp-Reymond et al., 1994, 1999). In our data instead, even though representations in PMv did correlate with object mass to some extent, statistical significance for these patterns did not survive correction for multiple comparisons. This might agree with Davare et al. (2006), who did not observe changes in predictive grip force scaling when applying TMS over PMv. However, in our study PMv representations did significantly correlate with participant comfort ratings during grasp planning, i.e., before executing the grasps, and comfort ratings were predominantly related to object mass. Our results are thus more in line with Dafotakis et al. (2008), who found that applying TMS over PMv before hand-object contact disrupted the predictive scaling of grip force. Our findings thus suggest that PMv might process visual estimates of object mass to anticipate haptic and proprioceptive perceptual experience when applying forces at the fingertips (Johansson & Flanagan, 2009).

4.3.1.7 PMd

Premotor area PMd encoded grasp axis only during the planning phase, grasp size during both planning and execution phases, and object mass only during action execution. In macaque area F2, the putative homologue of human PMd, Raos et al. (2004) found neurons selective for grips of different sizes and for the grip/wrist orientation required for grasping an object, during both preparation and execution phases of grasp movements. Additionally, (Hendrix et al., 2009) identified F2 neurons which were modulated by grip aperture during reach-to-grasp movements, and by grip force predominantly during grasping, when forces were actively applied to an object. These findings have been largely confirmed in humans. For example, Taubert et al. (2010) found that TMS applied over PMd disrupted wrist rotations during goal directed grasps. Davare et al. (2006) further employed TMS to show that PMv and PMd sequentially process grip size after movement onset. Perhaps surprisingly however, these authors also found that premotor regions did not seem to be involved in the control of grip forces. Nevertheless, both Chouinard (2005) and Nowak et al. (2009) found that disrupting PMd activity interfered with the scaling of grip forces according to learned color to mass associations.

Our results thus confirm the role of PMd in encoding grip orientation. Additionally, the correlations we observed between representations in PMd, aIPS, and SPOC during grasp planning suggests that PMd could receive visual estimates of grasp-relevant object orientation from SPOC (Fattori et al., 2004, 2009, 2010, 2015) and aIPS (Taubert et al., 2010). This would corroborate neurophysiological data from the macaque monkey showing that area F2 receives visual input predominantly from area V6A and the intraparietal sulcus (Matelli et al., 1998).

The fact that in our data, grip size was encoded in PMd during both grasp planning and execution, but in PMv only during execution, might appear at odds with Davare et al., (2006) who found that PMd processed grip size after PMv during movement execution. This apparent incongruity is potentially resolved however by Vesia et al. (2018), who demonstrate that PMd encodes handgrip formation during action preparation. Our results thus suggest that PMd encodings of grip size serve different functions during planning and execution phases. During grasp planning, PMd could be involved in selecting the correct grip size and feedforward grasp plan from visual estimates of object dimensions (Monaco et al., 2015; Vesia et al., 2018). During the execution phase instead, PMd could be involved

in online monitoring and adjustment of grasp configuration to ensure a successful grip (Davare et al., 2006; Fattori et al., 2015).

Our data also corroborate the role of PMd in selecting appropriate grip forces based on visual estimates of object material and mass (Chouinard, 2005; Nowak et al., 2009). Further, we found that PMd representations were significantly correlated with participant comfort ratings during grasp planning, which in turn were related to object mass. Given that PPA representations during grasp execution were also correlated with grip comfort, it is suggestive to note that representations in areas PPA and PMd were significantly correlated during both grasp planning and execution phases, and that PMd representations during grasp planning were correlated to PPA representations during action execution. These patterns imply that PMd could play a previously unexplored role in mapping visual estimates of object material properties to haptic and proprioceptive evaluations of grasp quality.

4.3.1.8 M1/S1

The hand region of primary motor cortex is where motor commands are generated and sent to the arm and hand. In both humans and monkeys, this area is essential for grasping. Lesions to M1 lead to a near total loss of digit control and severe impairments in wrist rotations (e.g., Hoffman & Strick, 1995; Jeannerod, 1986; Lang & Schieber, 2003; Murata et al., 2008; Passingham et al., 1983), and neural activity recorded from M1 can be used to reconstruct finger joint angles and muscle kinematics during grasping (Michaels et al., 2020; Vargas-Irwin et al., 2010). Further, hand orientation can be decoded from M1 activity prior to movement initiation (Peng Zhang et al., 2014), whereas grip type can be decoded from M1 activity during movement execution (Schaffelhofer et al., 2015). M1 is also implicated in the fine adjustment of grip forces during grasping (Chouinard, 2005; Hendrix et al., 2009). It is unsurprising therefore that in our data, primary motor and somatosensory area M1/S1 encoded grasp axis during grasp planning, and object mass during action execution. We also found patterns of correlations between representations in M1/S1 and representations in aIPS, PMv, and PMd during both grasp planning and execution. These patterns reflect the crucial role played by aIPS, PMv, and PMd in transforming dorsal stream representations during action planning, and ventral stream representations during execution, into motor commands sent to the hand through M1 (Borra et al., 2008; Janssen & Scherberger, 2015; Murata et al., 2000).

4.3.2 Limitations and future directions

Our results provide compelling evidence of a distinct series of neural computations occurring across and even within different brain regions at different phases of grasping in humans. Nevertheless, the reader should be aware of the limitations of our study, and of how future research might attempt to address such limitations.

To begin with, while we should be reasonably confident in statistically significant findings—particularly those which survive corrections for multiple comparisons—lack of statistical significance should always be interpreted with caution. For this reason, we attempt to contextualize null results and interpret their plausibility through the lens of previous literature. One potential source for the absence of a significant effect is uncertainty in the localization of brain regions (Brett et al., 2002). Our standardized approach to defining ROIs across participants allowed us to investigate a relatively wide selection of ROIs, as it would have been impractical to employ functional localizers to study the same selection of ROIs. However, variability in brain anatomy between individuals could have led to mis-localization of ROIs in some participants. Cortical surface-based alignment methods might alleviate these issues (Fischl et al., 1999), yet such methods can also be sensitive to co-registration errors

(Jezzard & Clare, 1999). Thus, even though the alignment and ROI definition procedures we employed were appropriate for the goals of the current study, future work could employ more sophisticated techniques to further pinpoint specific processing steps across the visuomotor grasp network.

A related limitation of our study is that we tested a targeted selection of brain ROIs. We cannot therefore exclude that additional brain regions could be involved in the sensorimotor computations investigated here. One possibility to discover additional brain networks involved in grasp-related visuomotor processing would be to employ whole-brain RSA searchlight analysis (Kriegeskorte et al., 2006). As the exploratory nature of this technique limits its statistical power, our current dataset could be used to estimate appropriate sample sizes for future studies employing this method.

One notable finding of our study is that object mass is encoded in sensorimotor regions during action execution. This finding is sensible, as information about object mass is required to modulate grip and lift forces. However, we have previously demonstrated that mass and mass distribution also play an important role in selecting where to grasp an object (Klein, Maiello et al., 2020). It is thus reasonable to expect that visuomotor processing of object material and mass should occur also when planning how to grasp an object. However, in our study grasps were preselected, thus participants did not need to process an object's material properties to select appropriate grasp locations. In order to investigate the role of visual material representations in grasp selection, future research could use our computational framework (Klein, Maiello et al., 2020; Maiello et al., 2021) to identify objects that produce distinct grasp patterns, rather than constraining participants to predefined grasp locations. Conditions that require visual processing of object material properties to select appropriate grasp locations would then reveal whether the same or different sensorimotor regions process object mass during grasp planning and execution. However, such designs would require disentangling activity related to representing shape *per se* from activity related to grasp selection and execution.

One factor which is known to be important for grasp selection and execution is grip torque, i.e., the tendency of an object to rotate under gravity when grasped away from its center of mass (Eastough & Edwards, 2006; Goodale et al., 1994; Lederman & Wing, 2003; Lukos et al., 2007; Paulun et al., 2016). While torque is directly related to object mass, it is possible to select different grasps on the same object which produce substantially different torques (Maiello et al., 2021). Since grasps with high torque require greater forces at the fingertips to maintain an object level, humans tend to avoid such high-torque grasps (Klein, Maiello et al., 2020). We originally designed our stimuli in the hope of dissociating torque from object mass. Unfortunately, in pilot testing we observed that certain object and grip configurations in the magnetic field of the MRI scanner produced eddy currents in the brass portions of our stimuli. These currents caused unexpected magnetic forces to act on the stimuli, which in turn altered fingertip forces required to grasp and manipulate the objects. To avoid the occurrence of such eddy currents in our experiment, we decided to forgo conditions differentiating the effects of object mass from those of grip torques. By employing nonconductive materials, in future work our approach could be extended to test whether grasp-relevant torque computations occur in the same visuomotor regions responsible for estimating object material and shape.

An additional limitation related to fMRI is that the BOLD hemodynamic response signal is slow, it lags neural events by several seconds, and its time course varies across brain regions and individuals (Handwerker et al., 2004). For this reason, we only investigated a coarse binary distinction between grasp planning and execution. This level of analysis cannot closely track sensorimotor transformations across brain networks. Future work could combine fMRI with TMS and EEG, to establish temporally

precise and causal relationships in sensorimotor processing occurring across brain regions (Bergmann et al., 2021; Bestmann et al., 2008; Taylor et al., 2008).

A final yet important limitation to note is that RSA is a correlational analysis, from which causation or directionality cannot be directly inferred. In particular, if neural representations in two brain regions are correlated, this alone cannot tell us whether these regions are structurally and functionally connected, or whether information flows from region A to region B or from B to A, or from C to both A and B. We thus take care to only make such inferences where previous literature indicates that structural/functional connections and sequential processing are likely to exist. Cases where connections have not yet been proposed are nevertheless intriguing, and future research could test whether such connections exist.

4.3.3 Ideas and Speculation: Thoughts on mental simulation, sensory prediction, and motor evaluation

Our analyses regarding patterns of representational similarity across planning and action phases, and regarding grasp comfort, could reflect mental simulation, prediction, and evaluation mechanisms at play.

Neural representation patterns in many brain regions during grasp planning were significantly correlated with representations in V1 and LOC during the action phase. Could these patterns be due to sensorimotor simulation (Jeannerod, 2001)? While our study and analyses were not designed to answer this question, it is conceivable that activity across the grasp network during the planning phase could be due to participants mentally simulating the grasps they were preparing to execute (Jeannerod, 1995; Jeannerod & Decety, 1995). These simulations could be used to generate motor plans and sensory predictions. Sensory predictions could then be compared to visual, tactile, and proprioceptive inputs during the grasping phase, to facilitate online movement corrections and evaluate the success of the generated motor plan (Desmurget & Grafton, 2000; Wolpert et al., 2011; Wolpert & Ghahramani, 2000). The observed patterns of representational similarity across planning and execution phases could thus reflect the agreement of motor simulations and visual predictions computed during grasp planning with visual inputs during action execution. This possibility is supported by recent work showing that planned actions can be decoded from activity in V1 and LOC before movement onset (Gallivan et al., 2013, 2019; Gutteling et al., 2015; Monaco et al., 2020), and that V1 and LOC are re-recruited when performing delayed actions toward remembered objects (Singhal et al., 2013).

Relatedly, our analyses found that representations in areas PMv and PMd during grasp planning were correlated with grasp comfort, as were representations in area PPA during grasp execution. Further, representations in PMd during grasp planning were correlated with representations in PPA during action execution. Could these patterns be related to haptic prediction and evaluation processes? A recent study by Kilteni et al. (2018) has shown that motor imagery and action planning both entail sensorimotor simulations that predict the tactile consequences of movements. Previous research has also shown that PMd is involved in learning to associate appropriate grip forces based on visual (color) cues to object mass (Chouinard, 2005; Nowak et al., 2009), whereas Dafotakis et al. (2008) have shown that PMv is involved in the predictive scaling of grip forces according to the most recent lift. Additionally, scene-sensitive PPA and adjacent regions have been shown to process visual and tactile estimates of surface texture (Cant & Goodale, 2007, 2011; Hiramatsu et al., 2011; Podrebarac et al., 2014). Thus visual material information in our context might have been used not just to control the

fingertip forces, but also to anticipate haptic percepts by the fingertips at object lift-off (Johansson & Flanagan, 2009). We thus put forth a speculative interpretation of our results. We posit that during grasp planning, PMv and PMd could have been processing visual estimates of object mass to predict haptic and proprioceptive percepts. During grasp execution, these haptic expectations could have been communicated to PPA, which then monitored and evaluated the quality of the performed grasps. These three regions could thus be involved in learning to associate visual material cues to a particular object mass (Chouinard, 2005; Nowak et al., 2009), but also with the scaling grip forces based on previous lifts (Dafotakis et al., 2008). It would further be intriguing to examine whether PMv, PMd, and PPA are involved in the perceptual consequences of associative learning and sensorimotor adaptation, such as the material-weight (Paulun et al., 2019; Wolfe, 1898) and sequential-weight illusions (Maiello et al., 2018; van Polanen, Buckingham, et al., 2020; van Polanen & Davare, 2015).

4.3.4 The grasp circuit in action

Our results show that different ventral and dorsal regions encode different grasp components at different time points. Even though the design of our study and our analyses do not allow us to directly infer causality from these results, we believe it likely that the observed shifts in sensorimotor encodings reflect visuomotor transformations. Therefore, by combining the results of our study with previous literature, we can speculate how events unfolded throughout the sensorimotor grasp network investigated.

4.3.4.1 Planning phase: grasp axis

First, ventral regions LOC, pFS, and PPA jointly interpreted the cued grasp configuration (orientation and size) and communicated this abstract action representation (Gallivan et al., 2013) though the ventro-dorsal pathway to aIPS (Rizzolatti & Matelli, 2003). Through feedback connections (Gutteling et al., 2011, 2013), area aIPS enhanced V1 processing of orientations aligned with the required grasp axis (Gallivan et al., 2019; Gutteling et al., 2015). V1 signals were transformed into visual estimates of object shape and positioning by dorsal region SPOC (Monaco et al., 2011). This information was relayed, through aIPS along the dorso-dorsal visual stream (Rizzolatti & Matelli, 2003), to premotor regions PMv (Raos et al., 2006) and PMd (Raos et al., 2004), tasked with transforming the visually-derived orientation information into grip-wrist orientation codes. These motor commands were then ready to be sent to the arm and hand via primary motor region M1 (Peng Zhang et al., 2014). The orientation of the wrist and hand was thus quickly adjusted at the very beginning of reach-to-grasp movements (Cuijpers et al., 2004).

4.3.4.2 Planning phase: grasp size

In parallel to the visuomotor processing of grip axis, ventral regions LOC, pFS, and PPA also relayed the size of the cued grasp configuration to aIPS (Gallivan et al., 2013; Rizzolatti & Matelli, 2003). This information was sent to premotor region PMd, which selected an appropriate feedforward motor schema (Monaco et al., 2015; Vesia et al., 2018) and communicated it to PMv.

4.3.4.3 Action phase: grasp size

PMv implemented the motor plan (Davare et al., 2006), and the grip began to widen. As the reach-to-grasp movement progressed and the fingertips approached the surface of the object, PMd became involved in the online adjustment of grasp aperture (Davare et al., 2006; Fattori et al., 2015). PMv and PMd thus sequentially adjusted the grip size throughout the reaching movement (Cuijpers et al.,

2004), with PMv providing the triggering information to PMd about when the hand configuration was adequate to begin applying grip forces (Davare et al., 2006).

4.3.4.4 Action phase: object mass

Finally, as the fingertips approached the surface of the object, ventral areas pFS and PPA computed visual estimates of object material and mass (Hiramatsu et al., 2011; Gallivan et al., 2014; Goda et al., 2014). These estimates were sent through aIPS (Dafotakis et al., 2008; Davare et al., 2007; Rizzolatti & Matelli, 2003) to premotor region PMd (Davare et al., 2010, 2011). Here, mass estimates were transformed into fingertip forces sent to the hand through primary motor region M1 (Chouinard, 2005; Hendrix et al., 2009; Nowak et al., 2009), allowing participants to successfully grip and lift the object.

4.4 Materials and Methods

4.4.1 Participants

The study included 21 participants (13 female, mean [range] age: 25.5 [18-33]) recruited from the University of Western Ontario. Data from two additional participants were excluded due to excessive head motion. All participants had normal or corrected-to-normal vision and were fully right-handed as measured by the Edinburgh Handedness Inventory. Informed consent was given prior to the experiment. The study was approved by the Health Sciences Research Ethics Board at the University of Western Ontario and followed the principles in the Declaration of Helsinki. Participants were given instructions on how to perform the experimental task before entering the MRI room, yet remained naïve with respect to the study's hypotheses. All participants were financially compensated at a rate of 25 CA$/hour.

4.4.2 Setup

A schematic of our setup is shown in Figure 4.1A. Each participant lay supine inside the MRI scanner with their head placed in a head coil tilted by ~30° to allow direct viewing of real stimulus objects placed in front of them. Below the head we positioned the bottom 20 channels of a 32-channel head coil and we suspended a 4-channel flex coil via loc-line (Lockwood Products, Inc.) over the forehead. A black wooden platform, placed above a participant's hip, enabled the presentation of real objects that participants were required to grasp, lift, and set back down using their right hand. The platform's flat surface was tilted by ~15° towards a participant in order to maximize comfort and visibility. Objects were placed on a black cardboard target ramp (Figure 4.1A: "Ramp", dimensions: 15 x 5 x 13 cm) on top of the platform that created a level surface which prevented objects from tipping over. The objects' exact placement was adjusted such that all required movements were possible and comfortable. Between trials, a participant's right hand rested on a button at a start position on the table's lower right side. The button monitored movement start and end times. A participant's upper right arm was strapped to their upper body and the MRI table using a hemi-cylindrical brace (not displayed in Figure 4.1A). This prevented shoulder and head movements, thus minimizing movement artefacts while enabling reach-to-grasp movements through elbow and wrist rotations. A small red LED fixation target was placed above and at a slightly closer depth location than the object to control for eye movements. Subjects were required to maintain fixation on this target at all times during scanning. An MR-compatible camera was positioned on the left side of the head coil to record the participant's actions. Videos of the runs were screened offline and trials containing errors were

excluded from further analyses. A total of 22 error trials were excluded, 18 of which occurred in one run where the subject erroneously grasped the objects during planning phase.

Two bright LEDs illuminated the workplace for the duration of the planning and action phase of each trial, one was mounted on the head coil and the other was taped to the ceiling of the bore. Another LED was taped to the outside of the bore and was only visible to the experimenter to cue the extraction and placement of the objects. The objects were kept on a table next to the MRI-scanner, on which three LEDs cued the experimenter on which object to place inside the scanner. Participant's wore MR-safe headphones through which task instructions were relayed on every trial. The LEDs and headphones were controlled by a Matlab script on a PC that interfaced with the MRI scanner. Triggers were received from the scanner at the start of every volume acquisition. All other lights in the MRI room were turned off and any other potential light sources and windows were covered so that no other light could illuminate the participant's workspace.

4.4.3 Stimuli

Stimuli were three L-shaped objects of the same size, created from seven blocks (cubes of 2.5 cm side length). One object was constructed with seven cubes of beech wood (object weight: 67g), whereas the other two were both constructed of four brass and three wooden cubes (object weight: 557g). The two identical wood-brass objects were positioned in two different orientations, one with the brass "arm" pointing up (see Figure 4.1A: "BrassUp"), the other with the brass arm lying down ("BrassDown"). In a slow event-related fMRI design, on each trial participants directly viewed, grasped, and lifted an object placed on a platform.

4.4.4 Task

Participants performed three distinct grasps per object, each grasp marked on the objects with colored stickers during the experiment. The colors were clearly distinguishable inside the scanner and served to cue participants about which grasp to perform. Participants were instructed to perform three-digit grasps with their right hand, by placing the thumb in opposition to index and middle fingers. This grasp was similar to the precision grip grasps employed in our previous work (Maiello et al., 2019, 2021; Klein, Maiello et al., 2020; Klein et al., 2021), but ensured participants could apply sufficient grip force to lift all objects to a height of approximately 2 cm above the platform. Grasp contact locations for the index and thumb were selected in order to produce a set of uncorrelated—and thus independent—representational dissimilarity matrices (RDMs) for the three grasp factors investigated: grasp orientation, grasp size, and object mass. Specifically, grasps could be rotated 45° either clockwise or counter clockwise around the vertical axis, and could require small (2.5 cm) or large (7.5 cm) grip apertures. In pilot testing we further refined the positioning of the objects and grasps within the magnetic field of the MRI scanner to avoid the forming of eddy currents within the brass parts of the objects which could hinder participants from executing the grasps. The complete set of grasp conditions is shown in Figure 4.1C.

4.4.5 Procedure

4.4.5.1 fMRI Experiment

We employed a slow event-related fMRI design with trials spaced every 23-31 s. Participants underwent four experimental runs in which they performed each combination of 3 objects x 3 grasps twice per run in a pseudorandom order for each run (18 trials per run, 72 trials in total). The sequence of events occurring on each trial is schematized in Figure 4.1B. Prior to each trial, the experimenter

was first cued on which object to place inside the scanner. The experimenter placed the object on the ramp (6-12 s before trial onset). At trial onset, the illumination LEDs turned on and over the headphones the participant heard the instruction "plan", immediately followed by the auditory cue specifying which grasp to execute. The auditory cue was "blue", "green", or "red", which corresponded to colored stickers marking the grasp locations on the objects. The duration of the planning phase of the task was randomly selected to be 6, 8, 10, or 12 s. During this time, the participant was required to hold still and mentally prepare to grasp the object at the cued location. Once the planning phase ended, "lift" was played over headphones to cue the participant to execute the grasp. During the execution phase of the task, the participant had 7 s to reach, grasp, and lift the object straight up by approximately 2 cm, place it back down on the target ramp, and return their hand to the start position. The experimenter then removed the object and the next trial commenced. Participants were instructed about the task, familiarized themselves with the objects, and practiced the grasps outside of the MRI room for about 5 minutes prior to the experiment. Once participants were strapped into the setup, they practiced all grasps again, thus ensuring that they could comfortably grasp each object.

4.4.5.2 Grasp Comfort Ratings

At the end of the fMRI experiment, participants remained positioned in the scanner and performed a short rating task. Participants were asked to perform one more time each of the nine grasp conditions. For each grasp, participants verbally reported how comfortable the grasp was on a scale of 1-10 (1 being highly uncomfortable and 10 being highly comfortable). Verbal ratings were manually recorded by the experimenter.

4.4.6 Analyses

Data analyses were conducted using Brain Voyager 20.0 (BV20) and 21.4 (BV21.4) software packages (Brain Innovation, Maastricht, The Netherlands), as well as Matlab version R2019b.

4.4.6.1 fMRI data acquisition

Imaging was performed using a 3-Tesla Siemens Prisma Fit MRI scanner located at the Robarts Research Institute at the University of Western Ontario (London, Ontario, Canada). Functional MRI volumes were acquired using a T2*-weighted, single-shot, gradient-echo echo-planar imaging acquisition sequence. Functional scanning parameters were: time to repetition (TR) = 1000 ms; time to echo (TE) = 30 ms; field of view = 210 x 210 mm in-plane; 48 axial 3-mm slices; voxel resolution = 3-mm isotropic; flip angle = 40°; and multi-band factor = 4. Anatomical scans were acquired using a T1-weighted MPRAGE sequence with parameters: TR = 2300 ms; field of view = 248 x 256 mm in-plane, 176 sagittal 1-mm slices; flip angle = 8°; 1-mm isotropic voxels.

4.4.6.2 fMRI data preprocessing

Brain imaging data were preprocessed using the BV20 Preprocessing Workflow. First, we performed Inhomogeneity Correction and extracted the brain from the skull. We then coregistered the functional images to the anatomical images, and normalized anatomical and functional data to Montreal Neurological Institute (MNI) space. Functional scans underwent motion correction and high-pass temporal filtering (to remove frequencies below 3 cycles/run). No slice scan time correction and no spatial smoothing were applied.

4.4.6.3 General linear model

Data were further processed with a random-effects general linear model (GLM) that included one predictor for each of the 18 conditions (3 grasp locations x 3 objects x 2 phases [action vs. planning]) convolved with the default Brain Voyager "two-gamma" hemodynamic response function (Friston et al., 1998) and aligned to trial onset. As predictors of no interest, we included the six motion parameters (x, y, and z translations and rotations) resulting from the 3D motion correction.

4.4.6.4 Definition of Regions of Interest

We investigated a targeted range of regions of interest (ROIs). The locations of these ROIs are shown in Figure 4.5; the criteria used to define the regions and their MNI coordinates are given in Table 4.1. ROIs were selected from the literature as regions most likely specialized in the components of visually guided grasping investigated in our study. These included primary visual cortex V1, areas LO, pFS, and PPA within the ventral visual stream (occipitotemporal cortex), areas SPOC, aIPS, PMv, PMd within the dorsal visual stream (occipitoparietal and premotor cortex), and primary sensorimotor cortex M1/S1.

Primary visual cortex (V1) was included because it represents the first stage of cortical visual processing upon which all subsequent visuomotor computations rely. Primary motor area M1 was included instead as the final stage of processing, where motor commands are generated and sent to the arm and hand. In our study however we refer to this ROI as primary motor and somatosensory cortex M1/S1, because our volumetric data do not allow us to distinguish between the two banks of the central sulcus along which motor and somatosensory regions lie.

We next selected regions believed to perform the sensorimotor transformations that link the visual input to the motor output. The dorsal visual stream is thought to be predominantly specialized for visually guided actions, whereas the ventral stream mostly specializes in visual object recognition (Cavina-Pratesi et al., 2007; Culham et al., 2003; Goodale & Milner, 1992). Nevertheless, significant crosstalk occurs between these streams (Budisavljevic et al., 2018), and visual representations of object material properties have been found predominantly in ventral regions. We therefore selected areas across both dorsal and ventral visual streams that would encode grasp orientation, grasp size, and object mass.

Regions that we expected could encode grasp orientation were dorsal stream regions SPOC (Fattori et al., 2004, 2009, 2010; Monaco et al., 2011), aIPS (Taubert et al., 2010), PMv (Murata et al., 1997; Raos et al., 2006; Theys et al., 2012), and PMd (Raos et al., 2004). Regions that we expected could encode grasp size were dorsal stream regions SPOC, aIPS (Monaco et al., 2015), PMd (Monaco et al., 2015), and PMv (Murata et al., 1997; Raos et al., 2006; Theys et al., 2012), as well as ventral stream regions LO (Monaco et al., 2015). Finally, based on previous literature we expected visual estimates of object mass to be encoded in ventral stream regions LO, pFS, and PPA (Cant & Goodale, 2011; Gallivan et al., 2014; Goda et al., 2014, 2016; Hiramatsu et al., 2011). We further hypothesized that the network formed by aIPS, PMv, and PMd might play a role in linking ventral stream representations of object mass to the motor commands generated and sent to the hand through M1 (Borra et al., 2008; Janssen & Scherberger, 2015; Murata et al., 2000).

Figure 4.5 shows the locations of our selected ROIs as volumes within the Colin27 template brain (Figure 4.5A) and as cortical surface patches on an inflated brain (Figure 4.5B). To locate all other left hemisphere ROIs (except V1) in a standardized fashion we searched the automated meta-analysis website *neurosynth.org* (Yarkoni et al., 2011) for key words (See Table 4.1), which resulted in volumetric statistical maps in *nifti* files. Visual inspection of the maps allowed us to locate the ROIs we

had pre-selected based on a combination of activation peaks, anatomical criteria, and expected location from the relevant literature. For example, aIPS was selected based on the hotspot for "grasping" in Neurosynth nearest the intersection of the intraparietal and postcentral sulci (Culham et al., 2003). Spherical ROIs of 15-mm diameter, centered on the peak voxel, were selected for all regions except V1. Because Neurosynth is based on a meta-analysis of published studies, search terms like "V1" would be biased to the typical retinotopic locations employed in the literature and likely skewed towards the foveal representation (whereas the objects and hand would have been viewed across a larger expanse within the lower visual field). As such, we defined V1 in the left hemisphere's V1 using the atlas from Wang et al. (2015), which mapped retinotopic cortex +/- ~15° from the fovea.

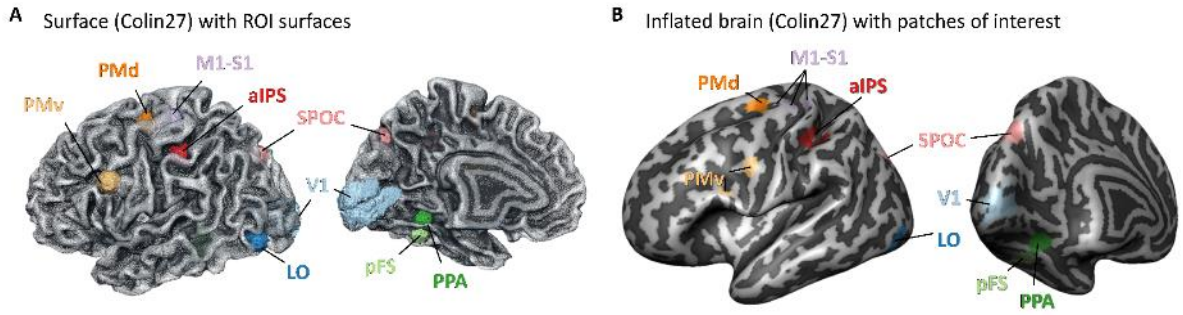

Figure 4.5. ROI locations. (A) Visualization of ROIs within the Colin27 template brain. All ROIs except V1 were built as spheres centered on coordinates recovered from neurosynth.org. V1 coordinates were taken from the (Wang et al., 2015) atlas. Note that surface-rendering is for presentation purposes only as data were analyzed in volumetric space and no cortex-based alignment was performed. (B) The same ROIs visualized as cortical surface patches on the Colin27 inflated brain.

Table 4.1 presents an overview of our ROI selection, where we list all our neurosynth-extracted ROIs with their peak coordinates, search terms and download dates.

Table 4.1. Regions of interest and their peak x-, y-, and z-coordinates in MNI space. Associated search term used on neurosynth.org with the number of studies the meta-analyses are based on and the extraction date (when the files were downloaded from the website). V1-coordinates were taken from (Wang et al., 2015).

ROIs in the left hemisphere	Center X	Center Y	Center Z	Search term (*neurosynth*)	Based on # of studies	Extraction date
V1 (primary visual)	see Wang et al. (2015)					
LO (lateral occipital)	-42	-78	-6	*lateral occipital*	226	July 17 2020
pFS (posterior fusiform sulcus)	-36	-45	-18	*objects*	692	May 14 2020
PPA (parahippocampal place area)	-30	-45	-9	*place*	189	Feb. 18 2021
SPOC (superior parietal occipital cortex)	-18	-78	39	*reaching*	99	June 25 2019
aIPS (anterior intraparietal area)	-42	-33	45	*grasping*	90	June 25 2019
PMv (ventral premotor)	-56	7	31	*grasping*	90	June 25 2019
PMd (dorsal premotor)	-24	-12	60	*grasping*	90	June 25 2019
M1/S1 (primary sensory/motor)	-33	-27	63	*grasping*	90	June 25 2019

4.4.6.5 Representational Similarity Analysis

The analysis of activation patterns within the selected ROIs was performed using multivoxel pattern analysis, specifically representational similarity analysis (RSA) (Kriegeskorte, 2008; Kriegeskorte et al., 2008). An activation pattern corresponded to the set of normalized β-weight estimates of the blood oxygenation level-dependent (BOLD) response of all voxels within a specific ROI for a specific condition. To construct representational dissimilarity matrices (RDMs) for each ROI, we computed the dissimilarity between activation patterns for each condition. Dissimilarity was defined as 1-r, where r was the Pearson correlation coefficient. RDMs were computed separately from both grasp planning and grasp execution phases. These neural RDMs computed were then correlated to model RDMs (Figure 4.1D,E,F) to test whether neural representations encoded grasp axis, grasp size, and object mass. To estimate maximum correlation values expected in each region given the between-participant variability, we computed the upper and lower bounds of the noise ceiling. The upper bound of the noise ceiling was computed as the average correlation of each participant's RDMs with the average RDM in each ROI. The lower bound of the noise ceiling was computed by correlating each participant's RDMs with the average of the other participants' RDMs. All correlations were performed between upper triangular portions of the RDMs excluding the diagonal. We then used one-tailed Wilcoxon signed rank tests to determine whether these correlations were significantly >0 within each ROI. We set statistical significance at $p<.05$ and applied false discovery rate (FDR) correction for multiple comparisons following (Benjamini & Hochberg, 1995).

To visualize the representational structure of the neural activity patterns within grasp planning and grasp execution phases, we first averaged RDMs across participants in each ROI and phase. We then correlated average RDMs across ROIs within each phase, and used hierarchical clustering and multidimensional scaling to visualize representational similarities across brain regions. We also correlated average RDMs across ROIs and across planning and action phases. Statistically significant correlations ($p<.05$ with Bonferroni correction) are shown also as topological connectivity plots (within-phase data) and as Sankey diagram (between-phase data).

4.4.6.6 Grasp Comfort Ratings

Grasp comfort ratings were analyzed using simple t-tests to assess whether ratings varied across different grasp orientations, grasp sizes, or object mass. The difference between ratings for each condition was then used to create grasp comfort RDMs for each participant. Grasp comfort RDMs were correlated to model RDMs to further test how strongly grasp comfort corresponded to grasp orientation, grasp size, and object mass. To search for brain regions that might encode grasp comfort, the average grasp comfort RDM was correlated to neural RDMs following RSA as described above.

Chapter 5

DISCUSSION

5.1 Main results

This thesis addressed the question of how the human brain determined effective and appropriate grasp locations on 3D objects, which factors affected grasp choice the most, and how different factors interacted.

In our first study, we focused on how object 3D shape, orientation, weight, and weight distribution, as well as properties of the hand jointly affect the location of grasp points. We found that grasping patterns are highly systematic, within and among participants, suggesting that humans chose grips for complex, novel 3D objects based on a common set of rules. Specifically, we found that it was both 3D shape and orientation that determined which portion of the object people grasped; humans exhibited spatial biases even when handling objects of different shapes and masses; the weight of the object influenced the degree to which humans took torque into consideration when selecting where to grasp objects. Fitting a normative model to human behavioral data revealed that force closure, hand posture, and grasp size were the major determinants of grasping behavior in humans, while torque and visibility played a less significant role. Our model accurately predicted human grasping patterns, even for novel 3D printed objects.

When trying to predict grasping behavior, it is essential to uncover the different factors at play, but it is also important to reveal how they interact and if there is a hierarchy. We first identified five constraints through behavioral analyses, then constructed penalty functions to reflect these constraints, and finally, by fitting our model, we assessed the costs associated with every possible combination of finger and thumb location on accessible object surfaces. The pattern of fitted weights revealed the relative importance of different constraints, the most important being force closure, followed by the natural grasp axis (NGA) and aperture. Torque and object visibility were taken into account far less when it came to choosing grasp locations. Still, there were factors that we did not consider in that first study. To study these, rather than just repeating our study with added factors, we chose to investigate, what happened when two factors were put in conflict with one another, to figure out which factor was the more important one when choosing grasp locations.

Many previous grasping studies have highlighted the importance of the human NGA, which we also observed in our first study. As one of the major factors in grasp choice, we chose this factor to pit against another potentially important determinant in grasping: surface friction. In our second study, we carefully analyzed sequences of human grasps directed at three different objects that varied in surface friction and orientation. Especially the condition where the object's extremely slippery pair of sides was aligned with the individual NGA, allowed us to investigate whether participants valued a stable grasp (contact points at the higher friction surface pair) over their NGA or vice versa. We clearly found that humans opted for the stable grasps and sacrificed their NGA-alignments.

The grasp-relevant object properties, which we investigated in the first two studies were often estimated visually. For example, by visually recognizing an object's material composition one could infer its mass and mass distribution. However, it remained unclear how the brain translated this piece of information into choosing appropriate grasp locations. In our third study, we thus examined the representation of grasp-relevant information across sensorimotor brain areas while participants planned and executed grasps to multi-material 3D-objects. We discovered that during grasp planning, dorsal areas were primarily used to encode grip orientation, which was adjusted in the very beginning of reach-to-grasp motions (Cuijpers et al., 2004). Different groups of ventral and dorsal areas were used to encode grip size during grasp planning and execution. Grip size was modified throughout reach-to-grasp motions (Cuijpers et al., 2004). Instead, during grasp execution, the object mass—which became important when applying forces at the fingertips—was encoded throughout ventral, dorsal, and motor areas. In general, we observed a switch in the encoding of sensorimotor information: from the dorsal stream during planning to the ventral stream during the execution of the grasp. Our findings also supported the idea, that mechanisms for sensorimotor prediction and evaluation could aid in the identification and correction of errors in movement as well as the improvement of subsequent movements (Wolpert et al., 2011; Wolpert & Ghahramani, 2000).

5.2 Individual factors influencing grasp selection

The past decades have seen an increase in research on motor coordination and object manipulation in a variety of fields, including robotics, artificial physical intelligence, sport psychology, cognitive and computational neuroscience, and engineering (Bach et al., 2014; W. Chen et al., 2018; Gibson, 1977; Grafton, 2010; Jeannerod, 2001; McDonough et al., 2020; Paulignan et al., 1997; Veiga et al., 2020; White, 2012; Wolpert & Ghahramani, 2000). However, there are still many open questions to be discussed. This is probably because the procedures involved in object handling are incredibly complex. In order to generate the proper afferent/efferent signals (e.g., relating to sensory and motor systems) for precise movement control, dexterous manipulation has to take into account information relating to an object's intrinsic properties (e.g., texture, hardness, curvature), biophysical-biomechanical characteristics (e.g., of the hand, fingertip and skin, and of joint kinematics), and interaction dynamics (e.g., forces, pressure, torsion) (O'Shea & Redmond, 2021). The development of an integrated account of skillful behavior is further complicated by the diverse theoretical viewpoints that exist regarding the respective contributions of the motor, sensory, and cognitive systems to dexterous object handling (Foglia & O'Regan, 2016; Friston, 2010; Jeannerod, 2006; Kawato, 1999; Wolpert & Ghahramani, 2000). In the following section, I will discuss this ongoing dialogue in the context of the work presented in Chapters 2-4.

5.2.1 Orientation and 3D shape

For an example grasp toward your coffee cup to be successful, many aspects must be taken into account, including the cup's location, weight, the surface structure, and shape and orientation of its handle (Schuetz & Fiehler, 2022). These visually perceived aspects influence where we choose to grasp objects, such as a cup. In the first experiment presented in Chapter 2, we manipulated 3D shape (by constructing 3D geometric shapes made of little cubes) and object orientation (by presenting the same objects in different orientations with respect to the participants). This allowed us to measure how allocentric 3D shape and egocentric perspective on those shapes interacted, as well as how consistent participants were in choosing grasp locations.

5.2.1.1 Orientation

For a particular object shape and orientation, previous studies have shown that the maximum grasp aperture depends on an object's size, whereas the transport component depends on the object's location in space (Jeannerod, 1981; Paulignan et al., 1991, 1997). A correlation also exists between object orientation and hand orientation (Cuijpers et al., 2004), e.g., as an object's orientation can change wrist pronation without altering its transport kinematics (Stelmach et al., 1994). In Chapter 2, object orientation was changed by rotating the objects on the table. We found grasp locations encoded in allocentric coordinates (tied to the object) increasingly varied with increasing object rotation. Specifically, for object rotations larger than 90 degrees, grasps were more similar when they were encoded in egocentric coordinates (tied to the observer).

It has been demonstrated that within the first half of the movement, the hand orientation is already adjusted to the object orientation (Glover & Dixon, 2001; Mamassian, 1997). This is consistent with our findings in Chapter 4, where grasp orientation was encoded already during the planning phase. An important aspect of the hand orientation is the preferred grasp orientation (called the natural grasp axis, or NGA) (Lederman & Wing, 2003; Roby-Brami et al., 2000; Schot et al., 2010; Voudouris et al., 2010). Where most previous research focused on hand kinematics (Cuijpers et al., 2006a; Goodale et al., 1994; Mamassian, 1997; Paulun et al., 2016), we used complex 3D shapes and a range of orientations to show that object shape and orientation together determine the final hand configuration.

5.2.1.2 Shape

Surprisingly little behavioral research has been done on how shape affects grasp choice; this previous research often used 2D or simple geometric 3D stimuli made of homogenous materials and hardly ever examined grasp selection (Z. Chen & Saunders, 2015; Cuijpers et al., 2004, 2006b; Eloka & Franz, 2011; Goodale et al., 1994; Lederman & Wing, 2003; Schettino et al., 2003a). It has also been shown, that it is usually preferable to choose grasp points on the cube's opposing faces rather than on its edges or vertices. This is because grasps on edges and vertices will be unstable due to the high curvatures at these edges and vertices (Montana, 1992). These findings were in line with our results for grasps on the cubic objects, presented in Chapters 2 and 3. Here, we demonstrated how complex 3D objects were grasped in systematically distinct object locations.

5.2.1.3 Curvature

Previous research in humans has demonstrated that grasping forces are modulated by surface characteristics such as friction (Burstedt et al., 1999; Cadoret & Smith, 1996), tilt (Jenmalm & Johansson, 1997), and curvature (Goodwin et al., 1998). However, the role of surface curvature is

somewhat unclear, since Jenmalm et al. (1998) found that as human participants grasped various convex and concave surfaces, when a grasp was subjected to linear load forces, surface curvature had little effect on fingertip forces or minimum grasp force required for grasp stability. The perception and impact of surface curvature of objects on grasping has also been particularly of interest in the robotics literature, where robotic grippers chose grasp locations and formed grasps based on different surface curvatures (Calli et al., 2011; Goodwin et al., 1998; Jenmalm et al., 2000; Sanz et al., 1999; Vahrenkamp et al., 2017). There, curvature has been shown to be an important factor for parallel gripper grasps, where curvature and symmetry could even be used to evaluate potential contact points on-line (Sanz et al., 1999). When investigating grasp stability instead, the majority of previous studies asked human participants to grasp flat surfaces. However, most objects that we encounter in our everyday life have curved surfaces (Jenmalm et al., 1998). Thus how surface curvature affects grasp choice is not yet well understood. In our studies we also did not explicitly manipulate surface curvature. We did however ask participants to grasp 3D printed objects with curved surfaces in the final experiment of Chapter 2. We found that our model was already able to predict grasp locations for those objects quite well. However, if we compare closely the model predictions to the human data, we notice subtle differences that could well be due to surface curvature. Specifically, when participants grasped the 3D printed cat in Chapter 2, our model predicted grasp locations positioned in a concave ridge, alongside the cat's front leg. Human grasps, however, did not fall along those predicted locations and instead fell on mostly convex surfaces. Further research on the effects of the extend of different surface curvature is needed to investigate, whether human grasps systematically avoid highly concave or convex local curvatures.

5.2.2 Material: Surface friction

The shape and curvature of an object are just some amongst many properties that make up an object's surface. When humans visually perceive an object, they can also quickly determine which material it is made of and draw appropriate conclusions about its specific physical properties. One factor of interest in material perception is surface friction. Our objects were composed of different materials in the experiments presented in Chapter 2. In the second experiment, participants could freely choose to grasp the objects at their brass or their wooden parts. In Chapter 3, we pitched surface friction against the relative importance of the natural grasp axis (NGA). The latter results will be discussed in section 5.3.4, where we focus on the relative importance of different factors.

How we perceive surface properties is not the focus of this thesis, but studies have shown that humans perceive friction through both vision and touch. Grasp and load forces are adjusted to variations in weight or friction (Johansson & Westling, 1984b; Westling & Johansson, 1984) in an anticipatory fashion (e.g. Flanagan & Beltzner, 2000; Forssberg et al., 1991). The higher friction object parts offered more desirable grasp locations (Wing & Lederman, 2009), whereas lower friction surfaces demanded greater precision and allowed for less grasp error tolerance, resulting in more grasp points close to the CoM (Fikes et al., 1994). The higher the weight and the lower the surface friction on the object, the slower the movements were both before and after making contact with it, and the more precisely the grasp points were chosen and approached (Paulun et al., 2016).

5.2.3 Material: Object weight, mass distribution, and torque

A person performing a grasp towards an object might need to consider that object's center of mass (CoM). The vector connecting the thumb and index finger contact points defines the grasp axis. When the object's CoM lies off the grasp axis, a torque will develop (Lederman & Wing, 2003). The torque is

approximately equal to the weight of the object multiplied by the distance between the CoM and the grasp axis (Lederman & Wing, 2003).

5.2.3.1 Torque

In our first study (Chapter 2), we observed frequent grasps far away from the object's CoM for lightweight objects, which suggested that torque was not taken into account when grasping. These findings were consistent with those from Kleinholdermann et al. (2013), but contrary to other studies (Eastough & Edwards, 2006; Goodale et al., 1994; Lederman & Wing, 2003; J. Lukos et al., 2007; Paulun et al., 2016). In many of these studies, the objects were relatively simple 2D shapes, which meant that torque was correlated with force closure. With our stimuli, instead, there were many possible force closure grasps that were far from the CoM. Thus, our initial results called into question the role of torque in determining grasp selection.

5.2.3.2 An object's center of mass (CoM)

Multiple studies have shown that humans can visually estimate the location of the CoM with varying accuracy for 2D objects (Samuel & Kerzel, 2011) and higher accuracy for 3D objects (Cholewiak et al., 2015) or stacks of objects (Battaglia et al., 2013). Even though the variability of the perceptual estimates of the location of an object's center have long been known to increase proportionally with size (Wolfe, 1923), humans can still use this information to inform their grasp choice. Lederman and Wing (2003) investigated whether participants use a visually derived estimate of the CoM when the positions of the digits are unconstrained to select a grasp axis that includes the CoM. They found that participants used visual cues of symmetry to determine the CoM and chose a grasp axis with a short perpendicular distance from the CoM. These findings are in line with our observations regarding grasp choice for heavier objects, where the average grasp distance from the CoM was much smaller than for our lightweight objects. As the lightweight objects were 10 times lighter than the heavy ones, torque was much smaller and probably below the threshold where it would have affected grasp location or grasp security or comfort. We thus reconciled our findings with the literature and concluded that object weight influences the degree to which humans take torque into consideration.

5.2.3.3 Processing of material and weight

Many fMRI studies investigating object recognition have focused on the role played by geometric features such as shape (Jenmalm et al., 1998; Kourtzi & Kanwisher, 2000; S. O. Murray et al., 2003), size (Cavina-Pratesi et al., 2007; G. L. Murray et al., 2006), and orientation (Rice et al., 2007; Valyear et al., 2006). Weight instead is an action-relevant, but predominantly non-visual material feature. However, by recognizing an object's material composition, humans can deduce its weight and mass distribution. For example, Sharan (2009) found that humans could visually identify and categorize materials even from images. Further, Buckingham et al (2009) have shown that humans could interact appropriately with objects using their empirical knowledge about material properties. Studying weight, Gallivan et al. (2014) further discovered that the human ventral visual stream represents object weight based on sensorimotor memory (i.e., prior grasps) or based on learned material-weight correlations. This theory is in line with our findings (Chapter 4) that representations in pFS and PPA during grasp execution were correlated with the representations in aIPS, PMv, PMd, and M1/S1. This suggests that ventral regions may transmit visual estimations of object weight to the dorsal and premotor regions, which then use this knowledge to anticipate and adjust the fingertip forces during object lift-off (Wolpert et al., 2011; Wolpert & Ghahramani, 2000).

5.2.3.4 The ventral visual stream's role in material and weight processing

Evidence that materials are processed in the ventral visual stream, was presented e.g., by Hiramatsu and colleagues (2011), who discovered that, without physically handling objects, image statistics were linked to activation in early visual areas, whereas perceptual variations between materials were linked to activation in higher ventral visual areas—and even some dorsal regions. In a related study, Gallivan et al. (2014) required participants to plan and execute lifting movements with equally sized cylinders of different weights. They discovered that the human ventral visual stream represents object weight based on sensorimotor memory (i.e., prior grasps) or based on learned material-weight correlations. In Chapter 4 participants grasped lightweight objects made of wood or heavier objects made of a combination of brass and wood. Participants could clearly visually distinguish the materials.

5.2.3.5 The LOC's role in material and weight processing

Given the previously discussed relationship between object material and weight, we studied the lateral occipital cortex (LOC), a region within the ventral stream, as this region encodes object shape (e.g., Cant & Goodale, 2007; Kanwisher et al., 1997; Kourtzi & Kanwisher, 2000; Malach et al., 1995; Romaiguère et al., 2014), object weight (Gallivan et al., 2014), and shows some activation in response to texture (Cant et al., 2009). Before or slightly after lifting an object, LOC also seems to be sensitive to differences in an object's CoM. This relates to LOC's involvement in hand shaping and to subtle grasp characteristics that must be integrated with lift forces in order to provide the required compensatory torque to offset the inherent object torque attribute (Marneweck & Grafton, 2020).

Contrary to these findings, as well as results from other previous work (Cant & Goodale, 2011; Gallivan et al., 2014; Goda et al., 2014, 2016; Hiramatsu et al., 2011; van Polanen, Rens, et al., 2020), we did not observe representations of object material and weight in LOC (Chapter 4). To discuss why that might be the case, we compared these findings with the results presented in lesion-studies. These have also shed light on the role of dorsal and ventral brain areas in perceiving material and weight. For example, different neurological patients (DF (Humphrey et al., 1994; Milner et al., 1991) and MS (Newcombe & Ratcliff, 1975)) exhibit dissociable patterns of deficits in perceiving object shape, material, texture, and color. These deficits depend on exactly where each patient's visual streams is damaged (Cavina-Pratesi et al., 2010a, 2010b; Heywood & Kentridge, 2003). According to structural MRI, patient DF suffered bilateral lateral occipital cortex (LOC) damage (James et al., 2003), which resulted in her significant visual form agnosia (Humphrey et al., 1994; Milner et al., 1991). Patient MS, instead, suffered extensive damage to his bilateral ventromedial occipitotemporal cortices, but can readily discriminate between different shapes. The study performed by Cavina-Pratesi et al. (2010a) found that patient DF performed well on a texture-discrimination task but at chance for shape discrimination, whereas MS showed the opposite pattern. The authors concluded that geometric shape, not the surface texture, was the causal role of LOC. That is consistent with the results presented by Gallivan et al. (2014), who could not reliably decode object texture from LOC. In our study, the objects all had the same shape and we did not explicitly task participants with object recognition, nor texture or material perception. In our case, participants performed preselected grasps towards objects. In most of the above mentioned imaging studies (excl. Gallivan et al., 2014) participants were not performing actions on objects with varying material properties. The specific role of LOC in material and weight perception for predefined grasping actions might therefore be a special case, for which more research could be beneficial.

5.2.3.6 Tactile suppression may affect haptic judgments of weight and friction

When a limb is actively moved while a stimulus is applied to that limb, the threshold for perceiving stimuli increases (Angel & Malenka, 1982; Broda et al., 2020; Buckingham et al., 2010; Dyhre-Poulsen, 1978; Garland & Angel, 1974; Gertz et al., 2017; Juravle et al., 2018; Voudouris & Fiehler, 2017). That effect is called tactile suppression and occurs when humans reach to grasp an object and during interaction with that object (Buckingham et al., 2010; Fraser & Fiehler, 2018; Voudouris & Fiehler, 2017). Even before a movement is initiated, the detection thresholds can be increased (Coquery, 1978; Voss et al., 2008) and can be increased correspondingly for both active and passive movements (Chapman et al., 1987).

During the second set of experiments presented in Chapter 2, we did observe slight slipping on some occasions when grasp locations were far from the CoM on our heavier objects. Nevertheless, participants reacted in time to adjust their grasps and keep the objects securely between their fingertips, i.e. no objects slipped out of the grasp completely or were dropped. Even though tactile suppression does occur during grasping movements, participants received sufficient online feedback while they executed the grasps and were able to adapt to those updated haptic signals. Studies performed by Broda et al. (2020) and Voudouris et al. (2019) found that tactile suppression is stronger for object interactions where mass distribution of the object was predictable compared to objects where mass distribution was not predictable. We can assume stronger tactile suppression when participants handled our objects, as participants could clearly view and distinguish the wooden from the brass cubes. That means, the movement-related object feature (mass distribution) was not concealed on our objects. Yet, participants were still able to feel the object slipping and could react fast enough to prevent the object from falling. These important and task-relevant information processes were not hampered to the extent where participants were not able to successfully perform a secure grasping movement throughout the complete duration of interaction.

5.2.4 Grasp aperture

Most research on the relationship between grip aperture and object size has focused on the maximum grip aperture (Cuijpers et al., 2004). In Chapters 2 and 4, our experiments considered grasp aperture as an important factor in grasp selection. Importantly, we investigated the final grasp aperture, the size of the grasp upon contact, once the object is securely in hand. The final grip aperture when grasping irregular objects is established by the grasping points on the surface of the object (Goodale et al., 1994). This is not to be confused with the maximum grasp aperture (MGA), which occurs as the hand opens up while travelling towards the object and has been subject to many previous studies (Castiello, 2005; Jeannerod, 1984, 1986; Mon-Williams & Tresilian, 2001; Smeets & Brenner, 1999). Yet, there are still connections to be drawn between the two measures of aperture.

According to Weber's law, the certainty of stimulus estimation decreases with stimulus magnitude (Fechner, 1860). This includes all aspects of a stimulus or what is perceived after a stimulus, with the exception of human grasping movements (Derzsi & Volcic, 2022). Accordingly, when an object is about to be grasped, the variability in the maximum grip aperture between fingers is independent of object size (Ganel et al., 2008). This violation of Weber's law present in grasping is thought to be related to the perception-action dissociation, stated in the two-streams hypothesis (visual size estimation is computed differently for perception and action)(Goodale, 2011, 2014; Goodale & Milner, 1992). According to this theory, vision for perception, which is carried out by the ventral visual stream, is based on relative metrics that take into account both the overall characteristics of the visual scene

and the size of the objects in the scene. The dorsal visual stream, which serves as the vision-for-action system, is instead thought to be based on absolute metrics that represent the object's true size, which results in a violation of Weber's law (Ganel et al., 2008, 2014).

A recent study (Derzsi & Volcic, 2022), however, found no signs of a perception-action dissociation. Participants were asked to either point to the center of elongated rectangular objects of different widths or grasp them with a precision grip and to keep them balanced during the lift. Grasping the center of the bar ensured a balanced lift. The authors thereby contrasted the degree of uncertainty in grasping contact points chosen for objects of various sizes with the degree of uncertainty in perceptual estimates of the same objects' centers. The results gave convincing proof that Weber's law influences both the variability of visually directed grasping as well as the variability of perceptual estimates. Additionally, their conditions were designed to test whether the two-streams hypothesis provides an explanation for the exception to Weber's law in grasping. If vision-for-action were based on absolute metrics, the variability of estimating the object center through grasping would have been expected to be constant over object sizes in this study. As this was not the case, the authors postulate that absolute metrics are used exclusively during grasping for shaping the grip aperture, but the selection of optimal grasp contact positions is based on relative metrics. In our study, however (fMRI study, Chapter 4), we found grip aperture encoding took place in both visual streams during planning and execution of the grasp. Our results showed that regions in the ventral stream linked visual and motor regions during action execution. Thus, our findings may help reconcile this previous literature by demonstrating interactions between dorsal and ventral visual stream estimates of objects size and grasp apertures.

5.3 The relative importance of different grasp factors

While many previous studies have discovered and investigated the various individual factors related to grasping, the question remains, how these different factors interact and what happens when multiple factors vary in competing directions.

5.3.1 The lack of visibility

Usually, an object is identified before humans move to grasp it. Using vision alone, surface clues can aid in object identification, even when parts of the object are occluded (Tanaka & Presnell, 1999). Occlusion can take place before the grasp, (i) when an object is (partly) hidden behind another, (ii) or when some object surfaces are not accessible to the viewer due to self-occlusion (i.e. the object's shape causes parts of the object to be in the line of view and thereby covers other parts of the object). It has been shown that without visibility, both the magnitude of the grasp aperture and the temporal characteristics of the transport component changed (Rand et al., 2007). In reach-to-grasp movements without vision, the transport duration increased, meaning participants moved their hand slower towards the object (Camponogara & Volcic, 2019a, 2019b; Connolly & Goodale, 1999; Gentilucci et al., 1994; Jakobson & Goodale, 1991; Schettino et al., 2003b; Watt & Bradshaw, 2000; Winges et al., 2003). Without vision, also the maximum grasp aperture (MGA) during the reach-to-grasp movement increased (Jackson et al., 1995; Jakobson & Goodale, 1991; Pettypiece et al., 2009, 2010; Wing et al., 1986; without vision of the hand: Berthier et al., 1996; Churchill et al., 2000; Gentilucci et al., 1994). This wider maximum grasp aperture was thought to result from participants increasing the safety margin for initial contact with the object.

Visibility of the object is therefore an important factor that can change various parameters of the grasping action. Object parts can also be occluded due to our own movements, e.g., due to how our hand and arm are positioned during both the approach and once in contact with the object. Although people tend to look at grasping points, they may not always and necessarily reach toward visible contact points (Voudouris et al., 2012b). The investigations of how grasp locations were affected by reach distance and occlusion are summarized in the following paragraph.

5.3.2 Object visibility versus the reach distance

Our investigations presented in Chapter 2 lead us to design an experiment to contrast effects of object visibility with the hand's trajectory against one another. Luckily, we realized that this experiment had already been conducted as one of the conditions in another study (Paulun et al., 2016). Together with Maiello and colleagues (Maiello et al., 2019), we reanalyzed some of the data presented in Paulun et al. (2016), as two conditions from that study serendipitously pitted reach distance against object visibility. We found that the aim to increase object visibility rather than reducing reach distance accounts for spatial biases observed in human grasping patterns and confirmed that visibility seemed to be the more important constraint when it came to predicting grasp locations in our study (Chapter 2), as well.

5.3.3 Object visibility versus the aim to reduce torque (depending on object weight):

Even though participants were attempting to increase object visibility (Maiello et al., 2019; Paulun et al., 2014) our data presented in Chapter 2 also replicated the findings that this bias was reduced when object weight increased. These findings are in line with the results from several studies (Maiello et al., 2019; Paulun et al., 2014, 2016). Paulun et al. (2014) found that a rougher (and heavier) object required more movement time than a smoother (and lighter) object. In the first case, grasp points remained closer to the object's center of mass and were less variable than in the latter case.

5.3.4 Influence of the previously handled object on weight perception – an illusion

In Chapter 3, we noted that group level grasps were more bimodally distributed than individual participant grasps and suggested that previously handled objects in the previous trials might have an effect on grasp choice. Additionally, the influence of previously handled objects has already been of special interest to us when we handled the objects used in Chapter 2. In fact, many studies have investigated the effect of previous sensory experience on grasping (Dixon et al., 2012; Dixon & Glover, 2009; Jax & Rosenbaum, 2007, 2007; Johansson & Westling, 1988; Kelso et al., 1994; J. R. Lukos et al., 2013; Rosenbaum & Jorgensen, 1992). We therefore reason that it is plausible for trial history to play a role here, as well. Due to these considerations, we discovered the strong illusion, where the perceived weight of an object changed, depending on the weight of the previously handled object (Maiello et al., 2018). This effect is likely related to sensorimotor memory (Maiello et al., 2018; van Polanen, Buckingham, et al., 2020; van Polanen & Davare, 2015). Interestingly, we observed that the effect was strong enough to cross hands but was not modulated by the material appearance of the objects, which instead occurs in the material-weight illusion (Paulun et al., 2019; Wolfe, 1898).

5.3.5 Natural grasp axis versus surface friction

In Chapter 3, we introduced conditions where the axis connecting the cube's higher friction surfaces was orthogonal to the grasp axis necessary for adopting the individual comfortable grasp axis (or NGA). Our primary focus was to answer the question of what happens when surface friction and natural grasp axis are competing factors. Would participants forego their typical grasp configuration in favor of stable endpoints or would they tolerate endpoints on the lower friction surfaces in order to keep their typical grip configuration?

We demonstrated that participants readily adopted grasp configurations that promoted grasp stability rather than adhering to their NGA. Our findings presented in Chapter 3 agree with the previous literature, that makes grasp stability out to be an important factor when choosing grasp locations (Paulun et al., 2016; Smeets & Brenner, 1999). Our findings were not in full agreement with those presented by Cuijpers et al. (2004), who found that their participants seem to value comfort of posture over grasp stability. Their findings lead them to suggest that subjects tolerated less stable grasps in order to increase the comfort of their grasp. They were investigating how grasp points were affected by the shape and size of different cylinders with elliptical bases. All objects were made of the same, uniform material and an unstable grasp in this case meant not aligning the grasp axis with one of the cylinder's principal axes. Even without aligning the grasp axis with one of those axes, however, one can still form a successful grasp, without dropping the object. Therefore, the danger of dropping the object due to unstable grasp locations in this case was probably much lower compared to grasping the Vaseline-covered cuboid objects employed in Chapter 3. In a related object manipulation study, participants sacrificed grasp stability in favor of minimizing energy-related costs, such as torques (Glowania et al., 2017). Our results extend this previous research by demonstrating that when it comes to a trade-off between NGA and stability, choosing the more stable grasp locations usually wins over adopting the usual grasp pose.

5.3.6 Natural grasp axis versus visibility

Work along the same lines as the study presented in Chapter 3 was published by Voudouris et al. (2012b). They investigated what happens when visibility and natural grasp axis conflict one another. Subjects saw cuboids resting on the table in front of them and grasped them in different orientations. Similar to our setup, these could be grasped with a clockwise or a counterclockwise grasp. In one condition, however, there was a screen, occluding one side of the cuboid, so in one condition only the counterclockwise grasp would allow participants to see their thumb while they grasped the object. They found that humans still prioritized their natural grasp configuration by tolerating these invisible grasp endpoints. The studies we mentioned in this section could be further expanded to pin the different factors against one another, in order to build a more complete understanding of the relative importance of the individual factors. This way, the ability to predict natural and unconstrained human grasping behavior can improve even more. Discussions along these lines are found in the next section of this thesis, giving an outlook onto potential future directions.

5.4 Limitations and future directions

5.4.1 Motion tracking using markers and cameras

One should always critically examine the methods used to acquire data, and grasping studies are no exception from this rule. In the case of the experiments presented in Chapter 2, we used an active motion tracking system with markers and cables. The advantages (high temporal and spatial accuracy) come at a cost: participants have markers attached to their fingers and cables running along their hands and arms, which can feel restrictive. Only a limited range of hand motions and therefore object orientations allowed for successful tracking, due to the system's requirements that all markers needed to be visible to the cameras at all times. As soon as any part of the object or other fingers were positioned in the line of sight between camera and marker, tracking data were unavailable. Even the orientation of the markers relative to the cameras posed an issue, as markers pointing away from the cameras were neither seen nor recorded.

In our studies, these issues meant that we had to design and pilot test our conditions such that objects were oriented specifically to allow for visible trackers during the performed grasps. That meant that we were limited in the preselection of object orientations, specifically by which grasps were used during piloting to determine marker visibility. Additionally, grasp poses, which differed largely from those employed by the pilot participants, were potentially lost to the tracking. The markers themselves were secured on participants' fingernails via adhesive reusable pads (UHU patafix) and the cables were taped to participants' fingers, the backs of their hands, and their arms. Despite those security measures, markers sometimes fell off during the experiments, or cables got hooked on something, restricting participants in their movements. Some of our findings may therefore not entirely generalize to unrestricted grasping. However, we think this is not the case, because we controlled for or manually recorded error trial data. When possible, error trials due to tracking or task execution issues were repeated. Where markers were not visible during grasping in the final experiment in Chapter 2, the experimenter manually recorded grasp positions. Analyses of the available error trial data revealed highly similar patterns to the grasp pose data from non-error trials, suggesting that our results were not affected by these tracking issues.

Nevertheless, future work could overcome the majority of these limitations by using marker-less tracking, such as DeepLabCut (Mathis et al., 2018; Nath et al., 2019), OpenMonkeyStudio (Bala et al., 2020), DANNCE (Dunn et al., 2021), DeepPoseKit (Graving et al., 2019), WormPose (Hebert et al., 2021), LEAP (Fernández-González et al., 2019), and TRex (Walter & Couzin, 2021). DeepLabCut (Mathis et al., 2018; Nath et al., 2019) is an open-source tool that can do high quality markerless pose estimation of bodies or body parts across frames in a method that is computationally affordable for the majority of labs. Pose estimation involves virtually marking animals so that they may be tracked throughout time using tracking software. In order to train the neural network that will handle the data, the experimenter first identified and marked the relevant body components in a series of video frames.

5.4.2 Contact points versus contact areas

In our studies, we focused on precision grips and contact points. When humans grasp in a natural context, however, the precision grip is only one of the many, many grips that are available. The human hand is extremely versatile and adapts very well to various objects and tasks. There is evidence that the effects of material properties are not limited to the precision grip. Therefore using marker-less

tracking of free grasps (where no instructions are given as to how many digits can be used) or whole-hand grasps specifically, would approximate natural grasping behavior better than restricted two-digit grasps with markers attached and could give new insights into unrestricted grasps.

When our fingers and hands come into contact with a grasped object, measuring contact points is merely an approximation of the grasp. In the methods employed in this thesis, contact points are only ever the best guess at where the contact locations are, because human fingertips (and the majority of robotic fingertips, as well) are continuous surfaces (that exhibit a range of curvature values (Montana, 1992)). Further, our skin deforms slightly or even heavily and contact areas can expand under the pressure created between skin and object. While we do primarily use our fingertips (i.e. the opposite side of the finger nail) in a precision grip to make contact with the object, the contact areas can be much more complex and differ greatly between different multi-digit and whole-hand grasps. An object can be encased by the entire hand, making contact with the complete inside of your fingers and palm, or we can even have an object rest between our fingers.

A major direction for future studies should move towards developing methods to study contact areas, instead of contact points of grasping (Hartmann et al., 2022; Moscatelli et al., 2016). Additional propositions for achieving this could be to use paint to leave behind finger- or handprints on the grasped objects, or objects made from a temperature-sensitive material that changes color when in contact with the warmth of a human hand. Potentially, a camera could even be encased in translucent objects to record contact areas from within the object.

5.4.3 Virtual reality follow-up study to Chapter 2

In Chapter 2, we demonstrated that human grasp behavior is close to optimal with respect to a weighted combination of different cost functions. In a peer-reviewed follow-up study, we asked whether the same behavior can be seen in virtual reality (VR) (Chessa et al., 2019).

In this study (Chessa et al., 2019) the same four wooden objects, used in our original study (Klein et al., 2020), were presented in a virtual environment. Participants viewed them in the same two orientations as our real-world wooden objects in the original experiment (Klein et al., 2020). In the VR setting, participants could see the virtual object, the table upon which it was resting, and a simplified model of their hand that moved synchronized with their own hand movements. Given a specific object and orientation, participants selected the same portions of the virtual objects as of the real-world objects in Chapter 2.

5.4.3.1 Advantages of virtual reality (VR)

The virtual reality (VR) approach in this follow-up-study (Chessa et al., 2019) offers major advantages in experimental control and reproducibility. Virtual environments are ideal for providing the user with rich, complex, multimodal sensory information and can significantly increase the impression of realness and agency in the person experiencing such an artificial world (Riva et al., 2006). Grasping studies, which combine visual and haptic inputs into one perceptual experience, are a particularly good candidate for being translated into VR. There, VR offers the advantage of interacting with many different objects with the appearance of different materials or surface properties, without having to build them or a setup that supports them. An experimenter can also convincingly offset the participant's hand or move the stimuli around and investigate participants' behavior in response to perturbations. Where grip force sensors may obscure your desired object shape or be blocking access to desired grasp locations or surface properties in a real-world experiment, there is no need for them

in a VR setting (e.g. when using a PHANToM device for force feedback based micromanipulation, for examples, see Seifi et al., 2022; Zoeller et al., 2019; Zoeller & Drewing, 2020). Specifically, a grasping experiment run with the appropriate VR-setup will offer the opportunity to measure grip forces without compromising object appearance and VR objects will not occlude grasp locations.

Particularly fMRI experiments could benefit from incorporating VR into the experimental design, as they come with their own set of specific challenges. During any fMRI experiment, participants sometimes struggle to focus on the task while the scanner is making loud noises and all they see is the tight bore. The goal, however, is for naturalistic, interactive behaviors to take place even while brain activity is being monitored. A grasping task virtually immersed in a natural environment might put participants at ease and allow them to perform more naturally while being more relaxed. Even joint actions could be simulated this way, without having multiple participants crammed in one scanner. Unfortunately, there is no standard option for combining the VR and fMRI (Beck et al., 2007), but there have been studies that did combine the two methods (Marsh et al., 2010).

5.4.3.2 Limitations of VR

Still, we need to be cautious about the fact that not all real-world experiences can be translated into the virtual environment. Depending on the setup, it might be difficult to have subjects experience e.g. different aspects of haptic feedback (such as object weight and surface properties). Even though VR software and hardware are evolving to be more reliable, cost effective, and pleasing in terms of size and appearance, the costs remain relatively high and equipment may still be too bulky to be used in some setups (Bohil et al., 2011). Hand tracking with a commercial setup, such as the Leap motion (*Leap Motion Controller*, 2022) or the integrated hand tracking in the Meta Quest 2 (formerly known as Oculus Quest (*Oculus Quest 2*, 2022)), now offers a cost effective option, however, those systems often struggle with occlusion. Some VR headsets even include fairly reliable eye tracking (Schuetz & Fiehler, 2022).

Cybersickness might also have a negative impact on certain studies depending on the methodology used as participants may drop out of the experiment (Dennison et al., 2016), or related to the topic of this thesis, cybersickness can lead to a change in sensory weighting (Weech et al., 2020). Errors in tracking or updating the headset or virtual scene might lead to displacements in the perception of where something is, such as a virtual hand. In a reaching and grasping task this could have serious consequences. However, misalignments between real and virtual body parts have been found to have less of an impact on our sense of ownership of that body part compared to the delays between our sensory experiences (Perez-Marcos et al., 2012). Temporal delays between head movements and updates to the visual scene can also lead to decreases in the sense of ownership and agency of a virtual body part (Ismail & Shimada, 2016), though this can improve over time (van Dam & Stephens, 2018). Stereo cues need to be implemented convincingly and studies have also shown that distances may be misjudged by participants in virtual reality (i.e. depth compression, see Armbrüster et al., 2008; Kim et al., 2022; Knapp & Loomis, 2004; Willemsen et al., 2008). However, since grasping studies generally have a relatively small range of action, because objects need to be close enough to be grasped, distance compression would likely not play a huge factor in these cases (Armbrüster et al., 2008). Additionally, there can be vergence and convergence issues as the VR display sits right in front of your eyes, yet you appear to be looking in the distance (for a review see Rushton & Riddell, 1999). Finally, the experimenter must be sure that the interpupillary distance (IPD) is appropriately set for each participant. Otherwise eye strain can occur (Kim et al., 2021) or double vision, if the offset was

extreme, leading to difficulties reaching to an object. Some VR headsets currently do not encompass a wide enough range of IPDs, particularly for women, as depending on the headset between 7 and 40% of women are not covered by the IPD range (Stanney et al., 2020). Given these challenges, it is already a substantial achievement, that we have been able to replicate our findings for the real-world setup with the four original shapes in a VR setting.

5.4.4 Chapter 2 - Follow-up study: Conscious access to grasp-relevant factors

In a second follow-up study (Maiello et al., 2021) we investigated, whether humans can consciously access four of the five grasp rules (excluding force closure) that help avoid large apertures and uncomfortable, unstable, impossible, and high torque grasps. We asked participants to explicitly report grasp optimality of specific grasps on a subset of our wood-brass objects, that either reflected near-optimal or sub-optimal grasp size, orientation, torque, or visibility according to our optimality functions. We tested whether participants could infer grasp quality from vision and haptics. In three separate experiments, participants were asked to identify the best between two competing grasps on an object through either vision alone, by watching videos of others executing grasps, or through executing the grasps themselves. Participants performed well for most objects using vision alone, already, but performance significantly improved in the video and grasping sessions. These findings suggest that we can already understand what makes up a good grasp, perhaps by using motor imagery, i.e. mentally simulating the motor task. Sensorimotor feedback or passively viewing others grasp the objects might lead to even further refinements of understanding all aspects of the grasp. Which aspects of a grasp specifically make individual participants consciously choose one grasp over another, has not been investigated yet. Whether individuals prioritize a more accessible grasp location, faster movements, an easier grip, or a more comfortable grasp configuration still needs to be addressed in order to fully understand how grasp quality is judged.

As we have seen a difference in grasp quality evaluation using vision alone, compared to watching videos of grasps and executing the grasp, a similar experiment using the VR-setup from Chessa et al. (2019) could investigate if that holds true in virtual reality as well. Specifically, this set of experiments could use the multi-material objects. If the same effects could be observed in VR, that could confirm the successful translation of real-world findings into the VR, meaning that participants find representations as convincing as in the real world.

5.4.5 How to investigate the factor torque

In our first study, we found the importance of torque was correlated with object weight. Participants seemed to consider torque significantly more in their grip choice when they picked up the brass-wood objects, compared to the wooden objects. The second set of experiments used two differently weighted object classes: wooden objects weighed 97g and wood-brass objects weighed 716g. It would be interesting to further investigate, how strongly humans considered torque in their grasp choice, using a greater variance of weights. Those experiments could examine, at what threshold torque would be taken into account above other factors.

5.4.5.1 Neural representations of torque

In our third study (Chapter 4), we found different activations for the factors of grasp size, grasp axis, and mass for planning and execution of the grasp, as well as for ventral, dorsal, and motor regions. Initially, we ran a pilot experiment, hoping to investigate grasps that also differ in their torques. Once participants tried to execute those grasps inside the fMRI scanner, however, the brass was reacting

inside the scanner's magnetic field. That meant that participants were neither able to lift the objects with ease, nor to keep their heads still, as they tried to perform the task. Especially in light of the recent study exploring the different kinds of forces needed to counteract the different possible torques (Hartmann, 2022; Maiello, 2022), future studies should investigate whether there are neural correlations for those different torques, as well. Appropriate grasp locations on differently shaped objects, made from materials that will not react with the MRI's magnetic field, could be chosen by using our model presented in Chapter 2.

5.4.5.2 Neural representations of estimates of the CoM

We used our computational modeling framework to design an fMRI experiment to test the processing of individual aspects of grasping. We focused on the natural grasp axis, the size of the grasp, and mass we experience when picking up an object. Naturally, there are multiple other factors that are of interest when we perform simple grasping tasks that we had not addressed here. Related to considerations of torque, future studies may explore brain activation patterns when human participants are performing visual estimations of an object's location of its center. Our fMRI study did investigate regions relevant for estimating object material and object shape, but we did not study how they are related to estimations of the object's centroid or its location of the CoM. We found that object mass was encoded in both streams and motor areas during grasping. In our study, participants were not free to choose their grasp points, as we did not investigate grasp choice. Therefore, participants had to adhere to pre-selected grasp locations, indicated on the objects. Another set of experiments, where participants are free to choose grasp locations on objects and their grasp locations can be tracked could be used to contrast the two conditions, if both low- and high-torque grasps were possible to perform.

Another way of investigating what goes on "behind the scenes" when humans visually estimate the center of mass of objects, could be through intuitive-physics experiments. For example, an experimenter could design and position a complexly shaped, multi-material object ("o") in a way that it would tip over. Preventing "o" from tipping over would be one of two guardian objects ("ag"= active guardian and "pg"= passive guardian), supporting the fall-prone "o". Only "ag", however, would be actively supporting "o" and preventing "o" from tipping over. The other guardian, "pg", could be cleverly positioned, so that it may superficially appear as if it was supporting "o", but no weight would be actually resting on "pg". Removing "pg" would thereby have no effect on "o's" position and it would not fall over. Removing the support-guardian "ag" would result in the definite fall of "o". By asking participants which object they could remove without causing the structure to tip over would reveal their estimates of an object's center of mass. Examining participants in the fMRI scanner while they choose, which of the two guardians is safe to remove, without "o" falling over, could give us insights into the neural mechanisms underlying the estimation of an object's CoM.

5.4.5.3 Measuring grasp force in response to high and low torque

Spatiotemporal data were an important source of information when we investigated grasp locations. On the path towards the full understanding of human grasp choice, a holistic approach might include measuring the kinetics, as well. Measuring and understanding the force profiles associated with different object shapes, orientations, materials, and tasks could give an even more in-depth perspective on which factors are at play in various grasping scenarios.

In the second and third experiments in Chapter 2, as well as the experiments presented in Chapters 3 and 4, participants were asked to keep the objects level while picking them up. It has even been shown that participants can anticipate torque loads for objects held with offset grip axes (Lederman & Wing, 2003), that occur due to inertial effects when they are accelerated and decelerated (Jenmalm & Johansson, 1997). Participants adjusted grasp force in parallel with rotations when an object held with an offset grasp axis was about to rotate about the grasp axis (Jenmalm & Johansson, 1997). This indicates that people can anticipate the consequences of off-axis loading (Lederman & Wing, 2003). It is conceivable that participants increased their grasp force to resist the object's rotational tendency under gravity in our studies, as well. In agreement with previous findings, that way they could have generated sufficient torsional friction to counteract the vertical load force.

The conventional approach when measuring grip force uses force plates attached to the object. This approach does not easily lend itself to researching the effects of surface properties, local shapes, and curvature effects, as the force plates alter exactly these variables of interest. It would, however be quite interesting to include these additional measurements into an experiment similar to the second study from Chapter 2. In at least one instance in that study, we have reports of a participant, who used a high-torque grasp, complaining about the task being very physically exhausting. That was the case, when the participant picked up the brass-wood objects, where the brass cubes were grouped, thereby shifting the CoM of the object further towards the brass side. Nevertheless, the participant did manage to keep the object level and did not change grasp positions to opt for a lower torque. We conclude that the only way he could have achieved keeping the object level, was by increasing his grasp force. Even though the participant felt uncomfortable enough to complain, apparently the grasp still was comfortable enough to be maintained and repeated. Therefore it would be interesting to measure grasp force on a spectrum of heavy objects and high-torque grasps, to investigate if participants switch to lower torque grasps upwards of certain grip force values.

5.4.6 Uncertainty in shape perception

An object's shape and orientation can be recognized with the use of prior knowledge or visual cues, but they are always accompanied by some uncertainty (Faisal et al., 2008; Faisal & Wolpert, 2009; Schultheis et al., 2021). One example of uncertainty derives from the way we perceive the world around us: the objects and scenes on our 3D world are reduced to a 2D projection onto our retina. Additionally, humans usually do not get to see an entire object in all its orientations and from all possible viewing angles before performing a grasp. Yet, many human grasping locations fall on the unseen side of objects, sometimes with the thumb location being the only one that allows visual access. That was also observed in the grasping experiments presented in Chapters 2 and 3, where participants were entirely free to choose their grasp locations on differently shaped objects. In the majority of experiments in Chapter 2, the objects were made of cubes, with flat surfaces and 90° corners. They were complex shapes, but since they followed a clear and simple geometric pattern, imagining what the unseen backside looked like was easily done, much more easily, compared to our unfamiliar 3D-printed shapes with surfaces of different curvatures.

It might therefore be an important direction for future research to investigate (i) how well participants can foresee what the backside is shaped like without visual access and, (ii) how they adjust their initial and final grip locations on the unseen backside accordingly. This could potentially be performed by presenting participants with an unfamiliar, irregular 3D shape positioned to be grasped. Ahead of the

grasp, they would have to pick from multiple differently rendered backside options, what they think the backside of the object in front of them looks like. Once, they made the choice, they have to perform the grasp, with their grasp locations being tracked. It could then be investigated, whether there is an interaction between how well their predictions line up with reality, and how much they adjust their initial contact locations and final grasp endpoints.

5.5 Conclusion

In our first set of experiments (Chapter 2), we investigated which factors were considered when choosing grasp locations and how these factors were ranked in terms of their relative importance. The most important rule, participants had to follow was obeying the restrictions force closure imposed on a grasp, followed by the natural grasp axis (NGA), and grasp aperture. Torque and object visibility were taken into account less. Our related work investigated a subset of these optimal grasp factors. Discussions around the factors torque and visibility inspired our discoveries of the Sequential-Weight Illusion (Maiello et al., 2018) and the greater importance of object visibility over the aim to reduce reach distance (Maiello et al., 2019). Two additional follow-up studies found that participants were able to consciously access the above mentioned grasp rules (where force closure was satisfied for all grasps (Maiello et al., 2021)) and that these rules were even used in a virtual reality setup (Chessa et al., 2019). In Chapter 3, we investigated whether participants valued a higher friction contact area over their natural grasp axis (NGA) or vice versa and found that humans sacrificed alignments with their NGA in order to achieve stable grasp configurations. Having investigated the different aspects of grasping, as well as their relative importance to some extent, we were curious to understand how the brain translated these pieces of information into choosing appropriate grasp locations. In Chapter 4 we used fMRI to investigate how considerations of grasp aperture, the NGA, as well as object mass are coded in the brain to inform grasping.

Taken together, these sets of experiments provide insights into how humans use a combination of factors to inform their choice of grasp locations. Yet, multiple considerations have not been discussed in this context: for example, how constraints on precision or timing, or the specifics of the task, comfort, and various material and surface properties might influence grasp selection. Even the factors already investigated in this thesis as well as previous research could be expanded upon. Expanding the research in order to map out the different factors important for grasp selection would certainly be an ambitious but important goal. In this context, for each specific factor, future research should aim to understand how, when, and where its relative importance trumps the other factor(s). These findings could then be incorporated into a unified model that could mimic natural, unconstrained human grasping.

Understanding how the combination of factors influences grasp choice is a fundamental endeavor in itself, but we can also use these basic-science findings to achieve additional, applied goals. In a (distant) future, we aim to have the action space fully mapped out, to know where the human hand is held comfortably and in what pose it can act upon which objects in the best way to achieve a given task. With this knowledge, we could then build a model to predict naturalistic grasping behavior. Such a model could be used with an intelligent prosthesis of the human hand (and arm). Having a prosthesis behave naturally could significantly cut down rejection rates and learning time. This might especially help amputees who need only one prosthesis (as the other hand and arm remain functional). Being

able to use two hands that behave similarly naturally would be a major advantage compared to having one naturalistic hand and one that requires an entirely different set of commands and exhibits a different set of behaviors. To date, our model still requires as input a 3D model of the object to be grasped. However, with the continuous advances in computer vision and with the help of artificial intelligence, soon a combination of sensors might be able to use a similar model to not only choose appropriate contact areas, but to also refine motor commands after the hand comes into contact with the object, to successfully grasp, lift, and interact with the object. On the journey towards a unified understanding of grasping, we are excited to report that this thesis has already taken steps to expand upon and combine different factors that influence **how humans choose where to grasp objects**.

References

Abbasi, B., Noohi, E., Parastegari, S., & Zefran, M. (2016). Grasp taxonomy based on force distribution. *2016 25th IEEE International Symposium on Robot and Human Interactive Communication (RO-MAN)*, 1098–1103. https://doi.org/10.1109/ROMAN.2016.7745245

Angel, R. W., & Malenka, R. C. (1982). Velocity-dependent suppression of cutaneous sensitivity during movement. *Experimental Neurology*, *77*(2), 266–274. https://doi.org/10.1016/0014-4886(82)90244-8

Armbrüster, C., Wolter, M., Kuhlen, T., Spijkers, W., & Fimm, B. (2008). Depth Perception in Virtual Reality: Distance Estimations in Peri- and Extrapersonal Space. *CyberPsychology & Behavior*, *11*(1), 9–15. https://doi.org/10.1089/cpb.2007.9935

Bach, P., Nicholson, T., & Hudson, M. (2014). The affordance-matching hypothesis: How objects guide action understanding and prediction. *Frontiers in Human Neuroscience*, *8*. https://www.frontiersin.org/articles/10.3389/fnhum.2014.00254

Bala, P. C., Eisenreich, B. R., Yoo, S. B. M., Hayden, B. Y., Park, H. S., & Zimmermann, J. (2020). Automated markerless pose estimation in freely moving macaques with OpenMonkeyStudio. *Nature Communications*, *11*(1), Article 1. https://doi.org/10.1038/s41467-020-18441-5

Battaglia, P. W., Hamrick, J. B., & Tenenbaum, J. B. (2013). Simulation as an engine of physical scene understanding. *Proceedings of the National Academy of Sciences*, *110*(45), 18327–18332. https://doi.org/10.1073/pnas.1306572110

Beck, L., Wolter, M., Mungard, N., Kuhlen, T., & Sturm, W. (2007). Combining Virtual Reality and Functional Magnetic Resonance Imaging (fMRI): Problems and Solutions. In A. Holzinger (Ed.), *HCI and Usability for Medicine and Health Care* (pp. 335–348). Springer. https://doi.org/10.1007/978-3-540-76805-0_28

Benjamini, Y., & Hochberg, Y. (1995). Controlling the False Discovery Rate: A Practical and Powerful Approach to Multiple Testing. *Journal of the Royal Statistical Society: Series B (Methodological)*, *57*(1), 289–300. https://doi.org/10.1111/j.2517-6161.1995.tb02031.x

Bergmann, T. O., Varatheeswaran, R., Hanlon, C. A., Madsen, K. H., Thielscher, A., & Siebner, H. R. (2021). Concurrent TMS-fMRI for causal network perturbation and proof of target engagement. *NeuroImage*, *237*, 118093. https://doi.org/10.1016/j.neuroimage.2021.118093

Bergmann Tiest, W. M., & Kappers, A. M. L. (2007). Haptic and visual perception of roughness. *Acta Psychologica*, *124*(2), 177–189. https://doi.org/10.1016/j.actpsy.2006.03.002

Berthier, N. E., Clifton, R. K., Gullapalli, V., McCall, D. D., & Robin, D. J. (1996). Visual Information and Object Size in the Control of Reaching. *Journal of Motor Behavior*, *28*(3), 187–197. https://doi.org/10.1080/00222895.1996.9941744

Bestmann, S., Ruff, C. C., Blankenburg, F., Weiskopf, N., Driver, J., & Rothwell, J. C. (2008). Mapping causal interregional influences with concurrent TMS–fMRI. *Experimental Brain Research*, *191*(4), 383–402. https://doi.org/10.1007/s00221-008-1601-8

Betti, S., Castiello, U., & Begliomini, C. (2021). Reach-to-Grasp: A Multisensory Experience. *Frontiers in Psychology*, *12*, 614471. https://doi.org/10.3389/fpsyg.2021.614471

Binkofski, F., Buccino, G., Stephan, K. M., Rizzolatti, G., Seitz, R. J., & Freund, H.-J. (1999). A parieto-premotor network for object manipulation: Evidence from neuroimaging. *Experimental Brain Research*, *128*(1–2), 210–213. https://doi.org/10.1007/s002210050838

Bohil, C. J., Alicea, B., & Biocca, F. A. (2011). Virtual reality in neuroscience research and therapy. *Nature Reviews Neuroscience*, *12*(12), 752–762. https://doi.org/10.1038/nrn3122

Borra, E., Belmalih, A., Calzavara, R., Gerbella, M., Murata, A., Rozzi, S., & Luppino, G. (2008). Cortical Connections of the Macaque Anterior Intraparietal (AIP) Area. *Cerebral Cortex*, *18*(5), 1094–1111. https://doi.org/10.1093/cercor/bhm146

Bozzacchi, C., Brenner, E., Smeets, J. B., Volcic, R., & Domini, F. (2018). How removing visual information affects grasping movements. *Experimental Brain Research*, *236*(4), 985–995. https://doi.org/10.1007/s00221-018-5186-6

Bozzacchi, C., Volcic, R., & Domini, F. (2016). Grasping in absence of feedback: Systematic biases endure extensive training. *Experimental Brain Research*, *234*(1), 255–265. https://doi.org/10.1007/s00221-015-4456-9

Brett, M., Johnsrude, I. S., & Owen, A. M. (2002). The problem of functional localization in the human brain. *Nature Reviews Neuroscience*, *3*(3), 243–249. https://doi.org/10.1038/nrn756

Brière, J., & Proteau, L. (2011). Automatic movement error detection and correction processes in reaching movements. *Experimental Brain Research*, *208*(1), 39–50.

Broda, M. D., Fiehler, K., & Voudouris, D. (2020). The influence of afferent input on somatosensory suppression during grasping. *Scientific Reports*, *10*(1), 18692. https://doi.org/10.1038/s41598-020-75610-8

Brodie, E. E., & Ross, H. E. (1985). Jiggling a Lifted Weight Does Aid Discrimination. *The American Journal of Psychology*, *98*(3), 469–471. JSTOR. https://doi.org/10.2307/1422630

Bruyninckx, H., Demey, S., & Kumar, V. (1998). Generalized stability of compliant grasps. *Proceedings. 1998 IEEE International Conference on Robotics and Automation (Cat. No.98CH36146)*, *3*, 2396–2402 vol.3. https://doi.org/10.1109/ROBOT.1998.680699

Buckingham, G., Cant, J. S., & Goodale, M. A. (2009). Living in A Material World: How Visual Cues to Material Properties Affect the Way That We Lift Objects and Perceive Their Weight. *Journal of Neurophysiology*, *102*(6), 3111–3118. https://doi.org/10.1152/jn.00515.2009

Buckingham, G., Carey, D. P., Colino, F. L., deGrosbois, J., & Binsted, G. (2010). Gating of vibrotactile detection during visually guided bimanual reaches. *Experimental Brain Research*, *201*(3), 411–419. https://doi.org/10.1007/s00221-009-2050-8

Budisavljevic, S., Dell'Acqua, F., & Castiello, U. (2018). Cross-talk connections underlying dorsal and ventral stream integration during hand actions. *Cortex*, *103*, 224–239. https://doi.org/10.1016/j.cortex.2018.02.016

Burstedt, M. K., Flanagan, J. R., & Johansson, R. S. (1999). Control of grasp stability in humans under different frictional conditions during multidigit manipulation. *Journal of Neurophysiology*, *82*(5), 2393–2405. https://doi.org/10.1152/jn.1999.82.5.2393

Cadoret, G., & Smith, A. M. (1996). Friction, not texture, dictates grip forces used during object manipulation. *Journal of Neurophysiology*, *75*(5), 1963–1969. https://doi.org/10.1152/jn.1996.75.5.1963

Calli, B., Wisse, M., & Jonker, P. (2011). *Grasping of Unknown Objects Via Curvature Maximization Using Active Vision*. 7.

Camponogara, I., & Volcic, R. (2019a). Grasping movements toward seen and handheld objects. *Scientific Reports*, *9*(1), Article 1. https://doi.org/10.1038/s41598-018-38277-w

Camponogara, I., & Volcic, R. (2019b). Grasping adjustments to haptic, visual, and visuo-haptic object perturbations are contingent on the sensory modality. *Journal of Neurophysiology*, *122*(6), 2614–2620. https://doi.org/10.1152/jn.00452.2019

Cant, J. S., Arnott, S. R., & Goodale, M. A. (2009). FMR-adaptation reveals separate processing regions for the perception of form and texture in the human ventral stream. *Experimental Brain Research*, *192*(3), 391–405. https://doi.org/10.1007/s00221-008-1573-8

Cant, J. S., & Goodale, M. A. (2007). Attention to Form or Surface Properties Modulates Different Regions of Human Occipitotemporal Cortex. *Cerebral Cortex*, *17*(3), 713–731. https://doi.org/10.1093/cercor/bhk022

Cant, J. S., & Goodale, M. A. (2011). Scratching Beneath the Surface: New Insights into the Functional Properties of the Lateral Occipital Area and Parahippocampal Place Area. *Journal of Neuroscience*, *31*(22), 8248–8258. https://doi.org/10.1523/JNEUROSCI.6113-10.2011

Carello, C. (1998). *Perception of Object Length by Sound*. https://journals.sagepub.com/doi/abs/10.1111/1467-9280.00040?casa_token=YS-bx6SkGfgAAAAA:3jx8ZQSQ_YGWVKwy3RmpFGugscCKXH9loooIpeKrjyHJYDFIWY-MjMCmysVl5rNwuqKqJ97tyRC-

Castiello, U. (2005). The neuroscience of grasping. *Nature Reviews Neuroscience*, *6*(9), 726–736. https://doi.org/10.1038/nrn1744

Castiello, U., & Begliomini, C. (2008). The Cortical Control of Visually Guided Grasping. *The Neuroscientist*, *14*(2), 157–170. https://doi.org/10.1177/1073858407312080

Cavina-Pratesi, C., Goodale, M. A., & Culham, J. C. (2007). FMRI Reveals a Dissociation between Grasping and Perceiving the Size of Real 3D Objects. *PLoS ONE*, *2*(5), e424. https://doi.org/10.1371/journal.pone.0000424

Cavina-Pratesi, C., Kentridge, R. W., Heywood, C. A., & Milner, A. D. (2010a). Separate Processing of Texture and Form in the Ventral Stream: Evidence from fMRI and Visual Agnosia. *Cerebral Cortex*, *20*(2), 433–446. https://doi.org/10.1093/cercor/bhp111

Cavina-Pratesi, C., Kentridge, R. W., Heywood, C. A., & Milner, A. D. (2010b). Separate Channels for Processing Form, Texture, and Color: Evidence from fMRI Adaptation and Visual Object Agnosia. *Cerebral Cortex*, *20*(10), 2319–2332. https://doi.org/10.1093/cercor/bhp298

Cesari, P., & Newell, K. M. (1999). The scaling of human grip configurations. *Journal of Experimental Psychology: Human Perception and Performance*, *25*(4), 927–935. https://doi.org/10.1037/0096-1523.25.4.927

Chan, T., Carello, C., & Turvey, M. T. (1990). Perceiving Object Width by Grasping. *Ecological Psychology*, *2*(1), 1–35. https://doi.org/10.1207/s15326969eco0201_1

Chao, E. Y., Opgrande, J. D., & Axmear, F. E. (1976). Three-dimensional force analysis of finger joints in selected isometric hand functions. *Journal of Biomechanics*, *9*(6), 387-IN2.

Chapman, C. E., Bushnell, M. C., Miron, D., Duncan, G. H., & Lund, J. P. (1987). Sensory perception during movement in man. *Experimental Brain Research*, *68*(3), 516–524. https://doi.org/10.1007/BF00249795

Chen, W., Khamis, H., Birznieks, I., Lepora, N. F., & Redmond, S. J. (2018). Tactile Sensors for Friction Estimation and Incipient Slip Detection—Toward Dexterous Robotic Manipulation: A Review. *IEEE Sensors Journal*, *18*(22), 9049–9064. https://doi.org/10.1109/JSEN.2018.2868340

Chen, Z., & Saunders, J. A. (2015). Online processing of shape information for control of grasping. *Experimental Brain Research*, *233*(11), 3109–3124. https://doi.org/10.1007/s00221-015-4380-z

Chessa, M., Maiello, G., Klein, L. K., Paulun, V. C., & Solari, F. (2019). Grasping objects in immersive Virtual Reality. *2019 IEEE Conference on Virtual Reality and 3D User Interfaces (VR)*, 1749–1754. https://doi.org/10.1109/VR.2019.8798155

Cholewiak, S. A., Fleming, R. W., & Singh, M. (2015). Perception of physical stability and center of mass of 3-D objects. *Journal of Vision*, *15*(2), 13. https://doi.org/10.1167/15.2.13

Chouinard, P. A. (2005). Role of the Primary Motor and Dorsal Premotor Cortices in the Anticipation of Forces during Object Lifting. *Journal of Neuroscience*, *25*(9), 2277–2284. https://doi.org/10.1523/JNEUROSCI.4649-04.2005

Christopoulos, V. N., & Schrater, P. R. (2009). Grasping Objects with Environmentally Induced Position Uncertainty. *PLOS Computational Biology*, *5*(10), e1000538. https://doi.org/10.1371/journal.pcbi.1000538

Churchill, A., Hopkins, B., Rönnqvist, L., & Vogt, S. (2000). Vision of the hand and environmental context in human prehension. *Experimental Brain Research*, *134*(1), 81–89. https://doi.org/10.1007/s002210000444

Colby, C. L. (1998). Action-Oriented Spatial Reference Frames in Cortex. *Neuron*, *20*(1), 15–24. https://doi.org/10.1016/S0896-6273(00)80429-8

Connolly, J. D., & Goodale, M. A. (1999). The role of visual feedback of hand position in the control of manual prehension. *Experimental Brain Research*, *125*(3), 281–286. https://doi.org/10.1007/s002210050684

Coquery, J. (1978). *Role of active movement in control of afferent input from skin in cat and man In: Gordon G, editor., editor. Active Touch*. Pergamon Press, Oxford.

Crajé, C., Lukos, J. R., Ansuini, C., Gordon, A. M., & Santello, M. (2011). The effects of task and content on digit placement on a bottle. *Experimental Brain Research*, *212*(1), 119–124. https://doi.org/10.1007/s00221-011-2704-1

Cuijpers, R. H., Brenner, E., & Smeets, J. B. J. (2006). Grasping reveals visual misjudgements of shape. *Experimental Brain Research*, *175*(1), 32–44. https://doi.org/10.1007/s00221-006-0531-6

Cuijpers, R. H., Smeets, J. B. J., & Brenner, E. (2004). On the Relation Between Object Shape and Grasping Kinematics. *Journal of Neurophysiology*, *91*(6), 2598–2606. https://doi.org/10.1152/jn.00644.2003

Culham, J. C., Danckert, S. L., De Souza, J. F., Gati, J. S., Menon, R. S., & Goodale, M. A. (2003). Visually guided grasping produces fMRI activation in dorsal but not ventral stream brain areas. *Experimental Brain Research*, *153*(2), 180–189. https://doi.org/10.1007/s00221-003-1591-5

Dafotakis, M., Sparing, R., Eickhoff, S. B., Fink, G. R., & Nowak, D. A. (2008). On the role of the ventral premotor cortex and anterior intraparietal area for predictive and reactive scaling of grip force. *Brain Research*, *1228*, 73–80. https://doi.org/10.1016/j.brainres.2008.06.027

Davare, M., Andres, M., Clerget, E., Thonnard, J.-L., & Olivier, E. (2007). Temporal Dissociation between Hand Shaping and Grip Force Scaling in the Anterior Intraparietal Area. *Journal of Neuroscience*, *27*(15), 3974–3980. https://doi.org/10.1523/JNEUROSCI.0426-07.2007

Davare, M., Andres, M., Cosnard, G., Thonnard, J.-L., & Olivier, E. (2006). Dissociating the role of ventral and dorsal premotor cortex in precision grasping. *Journal of Neuroscience*, *26*(8), 2260–2268. https://doi.org/10.1523/JNEUROSCI.3386-05.2006

Davare, M., Kraskov, A., Rothwell, J. C., & Lemon, R. N. (2011). Interactions between areas of the cortical grasping network. *Current Opinion in Neurobiology*, *21*(4), 565–570. https://doi.org/10.1016/j.conb.2011.05.021

Davare, M., Rothwell, J. C., & Lemon, R. N. (2010). Causal Connectivity between the Human Anterior Intraparietal Area and Premotor Cortex during Grasp. *Current Biology*, *20*(2), 176–181. https://doi.org/10.1016/j.cub.2009.11.063

de Haan, E. H. F., & Cowey, A. (2011). On the usefulness of 'what' and 'where' pathways in vision. *Trends in Cognitive Sciences*, *15*(10), 460–466. https://doi.org/10.1016/j.tics.2011.08.005

Dennison, M. S., Wisti, A. Z., & D'Zmura, M. (2016). Use of physiological signals to predict cybersickness. *Displays*, *44*, 42–52. https://doi.org/10.1016/j.displa.2016.07.002

Derzsi, Z., & Volcic, R. (2018). MOTOM toolbox: MOtion Tracking via Optotrak and Matlab. *Journal of Neuroscience Methods*, *308*, 129–134. https://doi.org/10.1016/j.jneumeth.2018.07.007

Derzsi, Z., & Volcic, R. (2022). Not only perception but also grasping actions can obey Weber's law. *bioRxiv,* 2022.06.15.496276. https://doi.org/10.1101/2022.06.15.496276

Desanghere, L., & Marotta, J. J. (2015). The influence of object shape and center of mass on grasp and gaze. *Frontiers in Psychology*, *6*. https://doi.org/10.3389/fpsyg.2015.01537

Desmurget, M., & Grafton, S. (2000). Forward modeling allows feedback control for fast reaching movements. *Trends in Cognitive Sciences*, *4*(11), 423–431. https://doi.org/10.1016/S1364-6613(00)01537-0

Desmurget, M., & Prablanc, C. (1997). Postural Control of Three-Dimensional Prehension Movements. *Journal of Neurophysiology*, *77*(1), 452–464. https://doi.org/10.1152/jn.1997.77.1.452

Dixon, P., & Glover, S. (2009). Perseveration and contrast effects in grasping. *Neuropsychologia*, *47*(6), 1578–1584. https://doi.org/10.1016/j.neuropsychologia.2008.12.032

Dixon, P., McAnsh, S., & Read, L. (2012). Repetition effects in grasping. *Canadian Journal of Experimental Psychology/Revue Canadienne de Psychologie Expérimentale*, *66*(1), 1–17. https://doi.org/10.1037/a0026192

Dötsch, D., Kurz, J., Helm, F., Hegele, M., Munzert, J., & Schubö, A. (2021). End in view: Joint end-state comfort depends on gaze and extraversion. *Human Movement Science*, *80*, 102867. https://doi.org/10.1016/j.humov.2021.102867

Dötsch, D., & Schubö, A. (2015). Social categorization and cooperation in motor joint action: Evidence for a joint end-state comfort. *Experimental Brain Research*, *233*(8), 2323–2334. https://doi.org/10.1007/s00221-015-4301-1

Dunn, T. W., Marshall, J. D., Severson, K. S., Aldarondo, D. E., Hildebrand, D. G. C., Chettih, S. N., Wang, W. L., Gellis, A. J., Carlson, D. E., Aronov, D., Freiwald, W. A., Wang, F., & Ölveczky, B. P. (2021). Geometric deep learning enables 3D kinematic profiling across species and environments. *Nature Methods*, *18*(5), Article 5. https://doi.org/10.1038/s41592-021-01106-6

Dyhre-Poulsen, P. (1978). Perception of tactile stimuli before ballistic and during tracking movements. *Active Touch. Pergamon Press, Oxford*, 171–176.

Eastough, D., & Edwards, M. G. (2006). Movement kinematics in prehension are affected by grasping objects of different mass. *Experimental Brain Research*, *176*(1), 193–198. https://doi.org/10.1007/s00221-006-0749-3

Edin, B. B., Westling, G., & Johansson, R. S. (1992). Independent control of human finger-tip forces at individual digits during precision lifting. *The Journal of Physiology*, *450*(1), 547–564. https://doi.org/10.1113/jphysiol.1992.sp019142

Eloka, O., & Franz, V. H. (2011). Effects of object shape on the visual guidance of action. *Vision Research*, *51*(8), 925–931. https://doi.org/10.1016/j.visres.2011.02.002

Endo, S., Wing, A. M., & Bracewell, R. M. (2011). Haptic and Visual Influences on Grasp Point Selection. *Journal of Motor Behavior*, *43*(6), 427–431. https://doi.org/10.1080/00222895.2011.621996

Epstein, R., & Kanwisher, N. (1998). A cortical representation of the local visual environment. *Nature*, *392*(6676), 598–601. https://doi.org/10.1038/33402

Fabbri, S., Stubbs, K. M., Cusack, R., & Culham, J. C. (2016). Disentangling Representations of Object and Grasp Properties in the Human Brain. *Journal of Neuroscience*, *36*(29), 7648–7662. https://doi.org/10.1523/JNEUROSCI.0313-16.2016

Faisal, A. A., Selen, L. P. J., & Wolpert, D. M. (2008). Noise in the nervous system. *Nature Reviews Neuroscience*, *9*(4), Article 4. https://doi.org/10.1038/nrn2258

Faisal, A. A., & Wolpert, D. M. (2009). Near Optimal Combination of Sensory and Motor Uncertainty in Time During a Naturalistic Perception-Action Task. *Journal of Neurophysiology*, *101*(4), 1901–1912. https://doi.org/10.1152/jn.90974.2008

Fan, J., He, J., & Tillery, S. I. H. (2006). Control of hand orientation and arm movement during reach and grasp. *Experimental Brain Research*, *171*(3), 283–296. https://doi.org/10.1007/s00221-005-0277-6

Fattori, P., Breveglieri, R., Amoroso, K., & Galletti, C. (2004). Evidence for both reaching and grasping activity in the medial parieto-occipital cortex of the macaque: Grasping activity in monkey area V6A. *European Journal of Neuroscience*, *20*(9), 2457–2466. https://doi.org/10.1111/j.1460-9568.2004.03697.x

Fattori, P., Breveglieri, R., Bosco, A., Gamberini, M., & Galletti, C. (2015). Vision for Prehension in the Medial Parietal Cortex. *Cerebral Cortex*, bhv302. https://doi.org/10.1093/cercor/bhv302

Fattori, P., Breveglieri, R., Marzocchi, N., Filippini, D., Bosco, A., & Galletti, C. (2009). Hand Orientation during Reach-to-Grasp Movements Modulates Neuronal Activity in the Medial Posterior Parietal Area V6A. *Journal of Neuroscience*, *29*(6), 1928–1936. https://doi.org/10.1523/JNEUROSCI.4998-08.2009

Fattori, P., Raos, V., Breveglieri, R., Bosco, A., Marzocchi, N., & Galletti, C. (2010). The Dorsomedial Pathway Is Not Just for Reaching: Grasping Neurons in the Medial Parieto-Occipital Cortex of the Macaque Monkey. *Journal of Neuroscience*, *30*(1), 342–349. https://doi.org/10.1523/JNEUROSCI.3800-09.2010

Fechner, G. T. (1860). *Elemente der Psychophysik (Vol. 2)*. Breitkopf u. Härtel.

Feix, T., Romero, J., Schmiedmayer, H.-B., Dollar, A. M., & Kragic, D. (2016). The GRASP Taxonomy of Human Grasp Types. *IEEE Transactions on Human-Machine Systems*, *46*(1), 66–77. https://doi.org/10.1109/THMS.2015.2470657

Fernández-González, P., Carratalá-Tejada, M., Monge-Pereira, E., Collado-Vázquez, S., Sánchez-Herrera Baeza, P., Cuesta-Gómez, A., Oña-Simbaña, E. D., Jardón-Huete, A., Molina-Rueda, F., Balaguer-Bernaldo de Quirós, C., Miangolarra-Page, J. C., & Cano-de la Cuerda, R. (2019). Leap motion controlled video game-based therapy for upper limb rehabilitation in patients with Parkinson's disease: A feasibility study. *Journal of NeuroEngineering and Rehabilitation*, *16*(1), 133. https://doi.org/10.1186/s12984-019-0593-x

Fikes, T. G., Klatzky, R. L., & Lederman, S. J. (1994). Effects of Object Texture on Precontact Movement Time in Human Prehension. *Journal of Motor Behavior*, *26*(4), 325–332. https://doi.org/10.1080/00222895.1994.9941688

Fischl, B., Sereno, M. I., & Dale, A. M. (1999). Cortical Surface-Based Analysis: II: Inflation, Flattening, and a Surface-Based Coordinate System. *NeuroImage*, *9*(2), 195–207. https://doi.org/10.1006/nimg.1998.0396

Flanagan, J. R., & Beltzner, M. A. (2000). Independence of perceptual and sensorimotor predictions in the size–weight illusion. *Nature Neuroscience*, *3*(7), Article 7. https://doi.org/10.1038/76701

Fleming, J., Klatzky, R. L., & Behrmann, M. (2002). Time course of planning for object and action parameters in visually guided manipulation. *Visual Cognition*, *9*(4–5), 502–527.

Fleming, R. W. (2017). Material Perception. *Annual Review of Vision Science*, *3*(1), 365–388. https://doi.org/10.1146/annurev-vision-102016-061429

Fluet, M. C., Baumann, M. A., & Scherberger, H. (2010). Context-Specific Grasp Movement Representation in Macaque Ventral Premotor Cortex. *Journal of Neuroscience*, *30*(45), 15175–15184. https://doi.org/10.1523/JNEUROSCI.3343-10.2010

Fogassi, L., Gallese, V., Buccino, G., Craighero, L., Fadiga, L., & Rizzolatti, G. (2001). Cortical mechanism for the visual guidance of hand grasping movements in the monkey: A reversible inactivation study. *Brain*, *124*(3), 571–586. https://doi.org/10.1093/brain/124.3.571

Foglia, L., & O'Regan, J. K. (2016). A New Imagery Debate: Enactive and Sensorimotor Accounts. *Review of Philosophy and Psychology*, *7*(1), 181–196. https://doi.org/10.1007/s13164-015-0269-9

Forssberg, H., Eliasson, A. C., Kinoshita, H., Johansson, R. S., & Westling, G. (1991). Development of human precision grip I: Basic coordination of force. *Experimental Brain Research*, *85*(2). https://doi.org/10.1007/BF00229422

Franz, V. H. (2004). *Optotrak Toolbox*. The Optotrak Toolbox: Control Your Optotrak from within Matlab. http://www.ecogsci.cs.uni-tuebingen.de/OptotrakToolbox/

Fraser, L. E., & Fiehler, K. (2018). Predicted reach consequences drive time course of tactile suppression. *Behavioural Brain Research*, *350*, 54–64. https://doi.org/10.1016/j.bbr.2018.05.010

Frey, S. H., Vinton, D., Norlund, R., & Grafton, S. T. (2005). Cortical topography of human anterior intraparietal cortex active during visually guided grasping. *Cognitive Brain Research*, *23*(2–3), 397–405. https://doi.org/10.1016/j.cogbrainres.2004.11.010

Friston, K. (2010). The free-energy principle: A unified brain theory? *Nature Reviews Neuroscience*, *11*(2), Article 2. https://doi.org/10.1038/nrn2787

Friston, K. J., Fletcher, P., Josephs, O., Holmes, A., Rugg, M. D., & Turner, R. (1998). Event-Related fMRI: Characterizing Differential Responses. *NeuroImage*, *7*(1), 30–40. https://doi.org/10.1006/nimg.1997.0306

Fukui, T., & Inui, T. (2013a). How vision affects kinematic properties of pantomimed prehension movements. *Frontiers in Psychology*, *4*, 44.

Fukui, T., & Inui, T. (2013b). Utilization of visual feedback of the hand according to target view availability in the online control of prehension movements. *Human Movement Science*, *32*(4), 580–595.

Gallivan, J. P., Cant, J. S., Goodale, M. A., & Flanagan, J. R. (2014). Representation of Object Weight in Human Ventral Visual Cortex. *Current Biology*, *24*(16), 1866–1873. https://doi.org/10.1016/j.cub.2014.06.046

Gallivan, J. P., Chapman, C. S., Gale, D. J., Flanagan, J. R., & Culham, J. C. (2019). Selective Modulation of Early Visual Cortical Activity by Movement Intention. *Cerebral Cortex*, *29*(11), 4662–4678. https://doi.org/10.1093/cercor/bhy345

Gallivan, J. P., Chapman, C. S., McLean, D. A., Flanagan, J. R., & Culham, J. C. (2013). Activity patterns in the category-selective occipitotemporal cortex predict upcoming motor actions. *European Journal of Neuroscience*, *38*(3), 2408–2424. https://doi.org/10.1111/ejn.12215

Ganel, T., Chajut, E., & Algom, D. (2008). Visual coding for action violates fundamental psychophysical principles. *Current Biology*, *18*(14), R599–R601. https://doi.org/10.1016/j.cub.2008.04.052

Ganel, T., Freud, E., & Meiran, N. (2014). Action is immune to the effects of Weber's law throughout the entire grasping trajectory. *Journal of Vision*, *14*(7), 11. https://doi.org/10.1167/14.7.11

Garland, H. T., & Angel, R. W. (1974). Modulation of tactile sensitivity during movement. *Neurology*, *24*(4), 361–361.

Garzorz, I. T., Knorr, A. G., Gilster, R., & Deubel, H. (2018). The influence of obstacles on grasp planning. *Experimental Brain Research*, *236*(10), 2639–2648. https://doi.org/10.1007/s00221-018-5321-4

Gentilucci, M., Daprati, E., Gangitano, M., Saetti, M. C., & Toni, I. (1996). On orienting the hand to reach and grasp an object. *Neuroreport*, *7*(2), 589–592. https://doi.org/10.1097/00001756-199601310-00051

Gentilucci, M., Toni, I., Chieffi, S., & Pavesi, G. (1994). The role of proprioception in the control of prehension movements: A kinematic study in a peripherally deafferented patient and in normal subjects. *Experimental Brain Research*, *99*(3), 483–500. https://doi.org/10.1007/BF00228985

Gertz, H., Voudouris, D., & Fiehler, K. (2017). Reach-relevant somatosensory signals modulate tactile suppression. *Journal of Neurophysiology*, *117*(6), 2262–2268. https://doi.org/10.1152/jn.00052.2017

Gibson, J. J. (1977). Gibson James J 1977 1979 The Theory of Affordances. *Theory of Affordances*. https://www.academia.edu/38620451/Gibson_James_J_1977_1979_The_Theory_of_Affordances

Gilster, R., Hesse, C., & Deubel, H. (2012). Contact points during multidigit grasping of geometric objects. *Experimental Brain Research*, *217*(1), 137–151. https://doi.org/10.1007/s00221-011-2980-9

Glover, S., Miall, R. C., & Rushworth, M. F. S. (2005). Parietal rTMS Disrupts the Initiation but not the Execution of On-line Adjustments to a Perturbation of Object Size. *Journal of Cognitive Neuroscience*, *17*(1), 124–136. https://doi.org/10.1162/0898929052880066

Glover, S. R., & Dixon, P. (2001). Dynamic illusion effects in a reaching task: Evidence for separate visual representations in the planning and control of reaching. *Journal of Experimental Psychology: Human Perception and Performance*, *27*, 560–572. https://doi.org/10.1037/0096-1523.27.3.560

Glowania, C., van Dam, L. C. J., Brenner, E., & Plaisier, M. A. (2017). Smooth at one end and rough at the other: Influence of object texture on grasping behaviour. *Experimental Brain Research*, *235*(9), 2821–2827. https://doi.org/10.1007/s00221-017-5016-2

Goda, N., Tachibana, A., Okazawa, G., & Komatsu, H. (2014). Representation of the Material Properties of Objects in the Visual Cortex of Nonhuman Primates. *Journal of Neuroscience*, *34*(7), 2660–2673. https://doi.org/10.1523/JNEUROSCI.2593-13.2014

Goda, N., Yokoi, I., Tachibana, A., Minamimoto, T., & Komatsu, H. (2016). Crossmodal Association of Visual and Haptic Material Properties of Objects in the Monkey Ventral Visual Cortex. *Current Biology*, *26*(7), 928–934. https://doi.org/10.1016/j.cub.2016.02.003

Goodale, M. A. (2011). Transforming vision into action. *Vision Research*, *51*(13), 1567–1587. https://doi.org/10.1016/j.visres.2010.07.027

Goodale, M. A. (2014). How (and why) the visual control of action differs from visual perception. *Proceedings of the Royal Society B: Biological Sciences*, *281*(1785), 20140337. https://doi.org/10.1098/rspb.2014.0337

Goodale, M. A., Meenan, J. P., Bülthoff, H. H., Nicolle, D. A., Murphy, K. J., & Racicot, C. I. (1994). Separate neural pathways for the visual analysis of object shape in perception and prehension. *Current Biology*, *4*(7), 604–610. https://doi.org/10.1016/S0960-9822(00)00132-9

Goodale, M. A., & Milner, A. D. (1992). Separate visual pathways for perception and action. *Trends in Neurosciences*, *15*(1), 20–25. https://doi.org/10.1016/0166-2236(92)90344-8

Goodwin, A. W., Jenmalm, P., & Johansson, R. S. (1998). Control of grip force when tilting objects: Effect of curvature of grasped surfaces and applied tangential torque. *Journal of Neuroscience*, *18*(24), 10724–10734.

Grafton, S. T. (2010). The cognitive neuroscience of prehension: Recent developments. *Experimental Brain Research*, *204*(4), 475–491. https://doi.org/10.1007/s00221-010-2315-2

Grassi, M. (2005). Do we hear size or sound? Balls dropped on plates. *Perception & Psychophysics*, *67*(2), 274–284. https://doi.org/10.3758/BF03206491

Grassi, M., Pastore, M., & Lemaitre, G. (2013). Looking at the world with your ears: How do we get the size of an object from its sound? *Acta Psychologica*, *143*(1), 96–104. https://doi.org/10.1016/j.actpsy.2013.02.005

Graving, J. M., Chae, D., Naik, H., Li, L., Koger, B., Costelloe, B. R., & Couzin, I. D. (2019). DeepPoseKit, a software toolkit for fast and robust animal pose estimation using deep learning. *ELife*, *8*, e47994. https://doi.org/10.7554/eLife.47994

Grea, H., Desmurget, M., & Prablanc, C. (2000). Postural invariance in three-dimensional reaching and grasping movements. *Experimental Brain Research*, *134*(2), 155–162.

Grill-Spector, K., Kourtzi, Z., & Kanwisher, N. (2001). The lateral occipital complex and its role in object recognition. *Vision Research*, *41*(10–11), 1409–1422. https://doi.org/10.1016/S0042-6989(01)00073-6

Gutteling, T. P., Kenemans, J. L., & Neggers, S. F. W. (2011). Grasping Preparation Enhances Orientation Change Detection. *PLoS ONE*, *6*(3), e17675. https://doi.org/10.1371/journal.pone.0017675

Gutteling, T. P., Park, S. Y., Kenemans, J. L., & Neggers, S. F. W. (2013). TMS of the anterior intraparietal area selectively modulates orientation change detection during action preparation. *Journal of Neurophysiology*, *110*(1), 33–41. https://doi.org/10.1152/jn.00622.2012

Gutteling, T. P., Petridou, N., Dumoulin, S. O., Harvey, B. M., Aarnoutse, E. J., Kenemans, J. L., & Neggers, S. F. W. (2015). Action Preparation Shapes Processing in Early Visual Cortex. *Journal of Neuroscience*, *35*(16), 6472–6480. https://doi.org/10.1523/JNEUROSCI.1358-14.2015

Handwerker, D. A., Ollinger, J. M., & D'Esposito, M. (2004). Variation of BOLD hemodynamic responses across subjects and brain regions and their effects on statistical analyses. *NeuroImage*, *21*(4), 1639–1651. https://doi.org/10.1016/j.neuroimage.2003.11.029

Hartmann, F. (2022). *Humans abandon the preferred grip axis in favor of low torques in precision grip grasping*. Vision Sciences Society, St. Pete Beach, Florida, USA.

Hartmann, F., Maiello, G., Rothkopf, C. A., & Fleming, R. W. (2022). A method to estimate contact regions between hands and objects during human multi-digit grasping. *bioRxiv,* 2022.09.30.510358. https://doi.org/10.1101/2022.09.30.510358

Hebert, L., Ahamed, T., Costa, A. C., O'Shaughnessy, L., & Stephens, G. J. (2021). WormPose: Image synthesis and convolutional networks for pose estimation in C. elegans. *PLOS Computational Biology*, *17*(4), e1008914. https://doi.org/10.1371/journal.pcbi.1008914

Hendrix, C. M., Mason, C. R., & Ebner, T. J. (2009). Signaling of Grasp Dimension and Grasp Force in Dorsal Premotor Cortex and Primary Motor Cortex Neurons During Reach to Grasp in the Monkey. *Journal of Neurophysiology*, *102*(1), 132–145. https://doi.org/10.1152/jn.00016.2009

Henry, F. M., & Rogers, D. E. (1960). Increased response latency for complicated movements and a "memory drum" theory of neuromotor reaction. *Research Quarterly. American Association for Health, Physical Education and Recreation*, *31*(3), 448–458. https://doi.org/10.1080/10671188.1960.10762052

Hepp-Reymond, M. C., Hüsler, E. J., Maier, M. A., & Qi, H.X. (1994). Force-related neuronal activity in two regions of the primate ventral premotor cortex. *Canadian Journal of Physiology and Pharmacology*, *72*(5), 571–579. https://doi.org/10.1139/y94-081

Hepp-Reymond, M. C., Kirkpatrick-Tanner, M., Gabernet, L., Qi, H. X., & Weber, B. (1999). Context-dependent force coding in motor and premotor cortical areas. *Experimental Brain Research*, *128*(1–2), 123–133. https://doi.org/10.1007/s002210050827

Hesse, C., & Franz, V. H. (2009). Corrective processes in grasping after perturbations of object size. *Journal of Motor Behavior*, *41*(3), 253–273. https://doi.org/10.3200/JMBR.41.3.253-273

Heywood, C. A., & Kentridge, R. W. (2003). Achromatopsia, color vision, and cortex. *Neurologic Clinics*, *21*(2), 483–500. https://doi.org/10.1016/S0733-8619(02)00102-0

Hiramatsu, C., Goda, N., & Komatsu, H. (2011a). Transformation from image-based to perceptual representation of materials along the human ventral visual pathway. *NeuroImage*, *57*(2), 482–494. https://doi.org/10.1016/j.neuroimage.2011.04.056

Hiramatsu, C., Goda, N., & Komatsu, H. (2011b). Transformation from image-based to perceptual representation of materials along the human ventral visual pathway. *NeuroImage*, *57*(2), 482–494. https://doi.org/10.1016/j.neuroimage.2011.04.056

Ho, Y. X., Landy, M. S., & Maloney, L. T. (2006). How direction of illumination affects visually perceived surface roughness. *Journal of Vision*, *6*(5), 8. https://doi.org/10.1167/6.5.8

Hoffman, D. S., & Strick, P. L. (1995). Effects of a primary motor cortex lesion on step-tracking movements of the wrist. *Journal of Neurophysiology*, *73*(2), 891–895. https://doi.org/10.1152/jn.1995.73.2.891

Hoisington, L. B. (1920). *On the non-visual perception of the length of lifted rods* (Vol. 472). Cornell university.

Houben, M. M. J., Kohlrausch, A., & Hermes, D. J. (2004). Perception of the size and speed of rolling balls by sound. *Speech Communication*, *43*(4), 331–345. https://doi.org/10.1016/j.specom.2004.03.004

Howard, W. S., & Kumar, V. (1996). On the stability of grasped objects. *IEEE Transactions on Robotics and Automation*, *12*(6), 904–917. https://doi.org/10.1109/70.544773

Huang, H. J., Kram, R., & Ahmed, A. A. (2012). Reduction of Metabolic Cost during Motor Learning of Arm Reaching Dynamics. *Journal of Neuroscience*, *32*(6), 2182–2190. https://doi.org/10.1523/JNEUROSCI.4003-11.2012

Humphrey, K., Goodale, M. A., Jakobson, L. S., & Servos, P. (1994). *The Role of Surface Information in Object Recognition: Studies of a Visual Form Agnosic and Normal Subjects*. https://journals.sagepub.com/doi/abs/10.1068/p231457

Iberall, T., Bingham, G., & Arbib, M. A. (1986). *Generation and modulation of action patterns. Vol. 15 of Experimental Brain Research Series. Opposition space as a structuring concept for the analysis of skilled hand movements*. Springer, Berlin.

Iberall, T., & Mackenzie, C. L. (1994). *The Grasping Hand* (1st ed., Vol. 104). North Holland.

Ismail, M. A. F., & Shimada, S. (2016). 'Robot' Hand Illusion under Delayed Visual Feedback: Relationship between the Senses of Ownership and Agency. *PLoS ONE*, *11*(7), e0159619. https://doi.org/10.1371/journal.pone.0159619

Jackson, S. R., Jackson, G. M., & Rosicky, J. (1995). Are non-relevant objects represented in working memory? The effect of non-target objects on reach and grasp kinematics. *Experimental Brain Research*, *102*(3), 519–530. https://doi.org/10.1007/BF00230656

Jackson, S. R., & Shaw, A. (2000). The Ponzo illusion affects grip-force but not grip-aperture scaling during prehension movements. *Journal of Experimental Psychology: Human Perception and Performance*, *26*(1), 418–423. https://doi.org/10.1037/0096-1523.26.1.418

Jaeger, T. F. (2008). Categorical data analysis: Away from ANOVAs (transformation or not) and towards logit mixed models. *Journal of Memory and Language*, *59*(4), 434–446. https://doi.org/10.1016/j.jml.2007.11.007

Jakobson, L. S., & Goodale, M. A. (1991). Factors affecting higher-order movement planning: A kinematic analysis of human prehension. *Experimental Brain Research*, *86*(1), 199–208. https://doi.org/10.1007/BF00231054

James, T. W., Culham, J., Humphrey, G. K., Milner, A. D., & Goodale, M. A. (2003). Ventral occipital lesions impair object recognition but not object-directed grasping: An fMRI study. *Brain*, *126*(11), 2463–2475. https://doi.org/10.1093/brain/awg248

Jameson, J. W., & Leifer, L. J. (1987). Automatic grasping: An optimization approach. *IEEE Transactions on Systems, Man, and Cybernetics*, *17*(5), 806–814. https://doi.org/10.1109/TSMC.1987.6499286

Janssen, P., & Scherberger, H. (2015). Visual Guidance in Control of Grasping. *Annual Review of Neuroscience*, *38*(1), 69–86. https://doi.org/10.1146/annurev-neuro-071714-034028

Jax, S. A., & Rosenbaum, D. A. (2007). Hand path priming in manual obstacle avoidance: Evidence that the dorsal stream does not only control visually guided actions in real time. *Journal of Experimental Psychology: Human Perception and Performance*, *33*, 425–441. https://doi.org/10.1037/0096-1523.33.2.425

Jeannerod, M. (1981). Specialized channels for cognitive responses. *Cognition*, *10*(1–3), 135–137. https://doi.org/10.1016/0010-0277(81)90036-6

Jeannerod, M. (1984). The Timing of Natural Prehension Movements. *Journal of Motor Behavior*, *16*(3), 235–254. https://doi.org/10.1080/00222895.1984.10735319

Jeannerod, M. (1986). The formation of finger grip during prehension. A cortically mediated visuomotor pattern. *Behavioural Brain Research*, *19*(2), 99–116. https://doi.org/10.1016/0166-4328(86)90008-2

Jeannerod, M. (1995). Mental imagery in the motor context. *Neuropsychologia*, *33*(11), 1419–1432. https://doi.org/10.1016/0028-3932(95)00073-C

Jeannerod, M. (2001). Neural Simulation of Action: A Unifying Mechanism for Motor Cognition. *NeuroImage*, *14*(1), S103–S109. https://doi.org/10.1006/nimg.2001.0832

Jeannerod, M. (2006). The simulation hypothesis of motor cognition. In M. Jeannerod (Ed.), *Motor Cognition: What actions tell the self* (p. 0). Oxford University Press. https://doi.org/10.1093/acprof:oso/9780198569657.003.0006

Jeannerod, M., Arbib, M. A., Rizzolatti, G., & Sakata, H. (1995). Grasping objects: The cortical mechanisms of visuomotor transformation. *Trends in Neurosciences*, *18*(7), 314–320. https://doi.org/10.1016/0166-2236(95)93921-J

Jeannerod, M., & Decety, J. (1990). The accuracy of visuomotor transformation: An investigation into the mechanisms of visual recognition of objects. In *Vision and action: The control of grasping* (pp. 33–48). Ablex Publishing.

Jeannerod, M., & Decety, J. (1995). Mental motor imagery: A window into the representational stages of action. *Current Opinion in Neurobiology*, *5*(6), 727–732. https://doi.org/10.1016/0959-4388(95)80099-9

Jeannerod, M., & Jacob, P. (2005). Visual cognition: A new look at the two-visual systems model. *Neuropsychologia*, *43*(2), 301–312. https://doi.org/10.1016/j.neuropsychologia.2004.11.016

Jenmalm, P., Dahlstedt, S., & Johansson, R. S. (2000). Visual and Tactile Information About Object-Curvature Control Fingertip Forces and Grasp Kinematics in Human Dexterous Manipulation. *Journal of Neurophysiology*, *84*(6), 2984–2997. https://doi.org/10.1152/jn.2000.84.6.2984

Jenmalm, P., Goodwin, A. W., & Johansson, R. S. (1998). Control of Grasp Stability When Humans Lift Objects With Different Surface Curvatures. *Journal of Neurophysiology*, *79*(4), 1643–1652. https://doi.org/10.1152/jn.1998.79.4.1643

Jenmalm, P., & Johansson, R. S. (1997). Visual and somatosensory information about object shape control manipulative fingertip forces. *Journal of Neuroscience*, *17*(11), 4486–4499.

Jezzard, P., & Clare, S. (1999). Sources of distortion in functional MRI data. *Human Brain Mapping*, *8*(2–3), 80–85. https://doi.org/10.1002/(SICI)1097-0193(1999)8:2/3<80::AID-HBM2>3.0.CO;2-C

Ji, Z. (1987). *Dexterous hands: Optimizing grasp by design and planning (Ph. D. Thesis)*.

Johansson, R. S. (1991). How is grasping modified by somatosensory input. *Motor control: concepts and issues*, *14*, 331-335.

Johansson, R. S., & Flanagan, J. R. (2009). Coding and use of tactile signals from the fingertips in object manipulation tasks. *Nature Reviews Neuroscience*, *10*(5), 345–359. https://doi.org/10.1038/nrn2621

Johansson, R. S., & Westling, G. (1984a). Influences of Cutaneous Sensory Input on the Motor Coordination During Precision Manipulation. In C. von Euler, O. Franzén, U. Lindblom, & D. Ottoson (Eds.), *Somatosensory Mechanisms* (pp. 249–260). Palgrave Macmillan UK. https://doi.org/10.1007/978-1-349-07292-7_17

Johansson, R. S., & Westling, G. (1984b). Roles of glabrous skin receptors and sensorimotor memory in automatic control of precision grip when lifting rougher or more slippery objects. *Experimental Brain Research*, *56*(3), 550–564. https://doi.org/10.1007/BF00237997

Johansson, R. S., & Westling, G. (1988). Coordinated isometric muscle commands adequately and erroneously programmed for the weight during lifting task with precision grip. *Experimental Brain Research*, *71*(1), 59–71. https://doi.org/10.1007/BF00247522

Johansson, R. S., & Westling, G. (1990). *Attention and performance XIII, chapter Tactile afferent signals in control of precision grip*. Lawrence Erlbaum Assoc., Hillsdale, NJ.

Julesz, B. (1981). Textons, the elements of texture perception, and their interactions. *Nature*, *290*(5802), 91–97. https://doi.org/10.1038/290091a0

Juravle, G., Colino, F. L., Meleqi, X., Binsted, G., & Farnè, A. (2018). Vision facilitates tactile perception when grasping an object. *Scientific Reports*, *8*(1), Article 1. https://doi.org/10.1038/s41598-018-33916-8

Kamp, C. van de, Bongers, R. M., & Zaal, F. T. (2009). Effects of changing object size during prehension. *Journal of Motor Behavior*, *41*(5), 427–435.

Kanwisher, N., McDermott, J., & Chun, M. M. (1997). The Fusiform Face Area: A Module in Human Extrastriate Cortex Specialized for Face Perception. *Journal of Neuroscience*, *17*(11), 4302–4311. https://doi.org/10.1523/JNEUROSCI.17-11-04302.1997

Karok, S., & Newport, R. (2010). The continuous updating of grasp in response to dynamic changes in object size, hand size and distractor proximity. *Neuropsychologia*, *48*(13), 3891–3900. https://doi.org/10.1016/j.neuropsychologia.2010.10.006

Kawato, M. (1999). Internal models for motor control and trajectory planning. *Current Opinion in Neurobiology*, *9*(6), 718–727. https://doi.org/10.1016/S0959-4388(99)00028-8

Kelso, J. A. S., Buchanan, J. J., & Murata, T. (1994). Multifunctionality and switching in the coordination dynamics of reaching and grasping. *Human Movement Science*, *13*(1), 63–94. https://doi.org/10.1016/0167-9457(94)90029-9

Kerr, J., & Roth, B. (1986). Analysis of multifingered hands. *The International Journal of Robotics Research*, *4*(4), 3–17. https://doi.org/10.1177/027836498600400401

Kilteni, K., Andersson, B. J., Houborg, C., & Ehrsson, H. H. (2018). Motor imagery involves predicting the sensory consequences of the imagined movement. *Nature Communications*, *9*(1), 1617. https://doi.org/10.1038/s41467-018-03989-0

Kim, J. J.-J., McManus, M. E., & Harris, L. R. (2022). Body Orientation Affects the Perceived Size of Objects. *Perception*, *51*(1), 25–36. https://doi.org/10.1177/03010066211065673

Kim, J. S., An, B. H., Jeong, W.-B., & Lee, S. W. (2021). Estimation of Interpupillary Distance Based on Eye Movements in Virtual Reality Devices. *IEEE Access*, *9*, 155576–155583. https://doi.org/10.1109/ACCESS.2021.3128991

Kinoshita, H., Bäckström, L., Flanagan, J. R., & Johansson, R. S. (1997). Tangential Torque Effects on the Control of Grip Forces When Holding Objects With a Precision Grip. *Journal of Neurophysiology*, *78*(3), 1619–1630. https://doi.org/10.1152/jn.1997.78.3.1619

Klatzky, R. L. (1990). Intelligent Exploration by the Human Hand. In *Dextrous Robot Hands* (pp. 66–81). Springer, New York, NY. https://doi.org/10.1007/978-1-4613-8974-3_4

Klatzky, R. L., & Lederman, S. (1988). *The intelligent Hand: Vol. Psychology of Learning and Motivation* (21st ed.). Academic Press. https://doi.org/10.1016/S0079-7421(08)60027-4

Klatzky, R. L., Lederman, S. J., & Reed, C. (1987). There's more to touch than meets the eye: The salience of object attributes for haptics with and without vision. *Journal of Experimental Psychology: General*, *116*, 356–369. https://doi.org/10.1037/0096-3445.116.4.356

Klein, L. K., Maiello, G., Fleming, R. W., & Voudouris, D. (2021). Friction is preferred over grasp configuration in precision grip grasping. *Journal of Neurophysiology*, *125*(4), 1330–1338. https://doi.org/10.1152/jn.00021.2021

Klein, L. K., Maiello, G., Paulun, V. C., & Fleming, R. W. (2020). Predicting precision grip grasp locations on three-dimensional objects. *PLOS Computational Biology*, *16*(8), e1008081. https://doi.org/10.1371/journal.pcbi.1008081

Kleinholdermann, U., Brenner, E., Franz, V. H., & Smeets, J. B. (2007). Grasping trapezoidal objects. *Experimental Brain Research*, *180*(3), 415–420. https://doi.org/10.1007/s00221-007-0867-6

Kleinholdermann, U., Franz, V. H., & Gegenfurtner, K. R. (2013). Human grasp point selection. *Journal of Vision*, *13*(8), 23–23. https://doi.org/10.1167/13.8.23

Knapp, J. M., & Loomis, J. M. (2004). Limited Field of View of Head-Mounted Displays Is Not the Cause of Distance Underestimation in Virtual Environments. *Presence: Teleoperators and Virtual Environments*, *13*(5), 572–577. https://doi.org/10.1162/1054746042545238

Konen, C. S., & Kastner, S. (2008). Two hierarchically organized neural systems for object information in human visual cortex. *Nature Neuroscience*, *11*(2), 224–231. https://doi.org/10.1038/nn2036

Kourtzi, Z., & Kanwisher, N. (2000). Cortical Regions Involved in Perceiving Object Shape. *Journal of Neuroscience*, *20*(9), 3310–3318. https://doi.org/10.1523/JNEUROSCI.20-09-03310.2000

Kriegeskorte, N. (2008). Representational similarity analysis – connecting the branches of systems neuroscience. *Frontiers in Systems Neuroscience*. https://doi.org/10.3389/neuro.06.004.2008

Kriegeskorte, N., Goebel, R., & Bandettini, P. (2006). Information-based functional brain mapping. *Proceedings of the National Academy of Sciences*, *103*(10), 3863–3868. https://doi.org/10.1073/pnas.0600244103

Kriegeskorte, N., Mur, M., Ruff, D. A., Kiani, R., Bodurka, J., Esteky, H., Tanaka, K., & Bandettini, P. A. (2008). Matching Categorical Object Representations in Inferior Temporal Cortex of Man and Monkey. *Neuron*, *60*(6), 1126–1141. https://doi.org/10.1016/j.neuron.2008.10.043

Kudoh, N., Hattori, M., Numata, N., & Maruyama, K. (1997). An analysis of spatiotemporal variability during prehension movements: Effects of object size and distance. *Experimental Brain Research*, *117*(3), 457–464. https://doi.org/10.1007/s002210050241

Kunkler-Peck, A. J., & Turvey, M. T. (2000). Hearing shape. *Journal of Experimental Psychology: Human Perception and Performance*, *26*, 279–294. https://doi.org/10.1037/0096-1523.26.1.279

Lakatos, S., McAdams, S., & Caussé, R. (1997). The representation of auditory source characteristics: Simple geometric form. *Perception & Psychophysics*, *59*(8), 1180–1190. https://doi.org/10.3758/BF03214206

Lang, C. E., & Schieber, M. H. (2003). Differential Impairment of Individuated Finger Movements in Humans After Damage to the Motor Cortex or the Corticospinal Tract. *Journal of Neurophysiology*, *90*(2), 1160–1170. https://doi.org/10.1152/jn.00130.2003

Lawrence, M. A., Kitada, R., Klatzky, R. L., & Lederman, S. J. (2007). Haptic Roughness Perception of Linear Gratings via Bare Finger or Rigid Probe. *Perception*, *36*(4), 547–557. https://doi.org/10.1068/p5746

Leap Motion Controller. (2022, October). https://www.ultraleap.com/product/leap-motion-controller/

Lederman, S. J., & Wing, A. M. (2003). Perceptual judgement, grasp point selection and object symmetry. *Experimental Brain Research*, *152*(2), 156–165. https://doi.org/10.1007/s00221-003-1522-5

Lee Hughes, C. M., Seegelke, C., & Schack, T. (2012). The Influence of Initial and Final Precision on Motor Planning: Individual Differences in End-State Comfort During Unimanual Grasping and Placing. *Journal of Motor Behavior*, *44*(3), 195–201. https://doi.org/10.1080/00222895.2012.672483

Levine, S., Pastor, P., Krizhevsky, A., Ibarz, J., & Quillen, D. (2018). Learning hand-eye coordination for robotic grasping with deep learning and large-scale data collection. *The International Journal of Robotics Research*, *37*(4–5), 421–436. https://doi.org/10.1177/0278364917710318

Lin, Q., Burdick, J., & Rimon, E. (1997). A quality measure for compliant grasps. *Proceedings of International Conference on Robotics and Automation*, *1*, 86–92 vol.1. https://doi.org/10.1109/ROBOT.1997.620020

Lingnau, A., & Downing, P. E. (2015). The lateral occipitotemporal cortex in action. *Trends in Cognitive Sciences*, *19*(5), 268–277. https://doi.org/10.1016/j.tics.2015.03.006

Lukos, J., Ansuini, C., & Santello, M. (2007). Choice of Contact Points during Multidigit Grasping: Effect of Predictability of Object Center of Mass Location. *Journal of Neuroscience*, *27*(14), 3894–3903. https://doi.org/10.1523/JNEUROSCI.4693-06.2007

Lukos, J. R., Choi, J. Y., & Santello, M. (2013). Grasping uncertainty: Effects of sensorimotor memories on high-level planning of dexterous manipulation. *Journal of Neurophysiology*, *109*(12), 2937–2946. https://doi.org/10.1152/jn.00060.2013

Macefield, V. G., Häger-Ross, C., & Johansson, R. S. (1996). Control of grip force during restraint of an object held between finger and thumb: responses of cutaneous afferents from the digits. *Experimental brain research*, *108*(1), 155-171. https://doi.org/10.1007/BF00242913

Maiello, G. (2022, September 28). *Not all torques are created equal: How vision and intuitive physics guide our grasping behaviour*. 44th European Conference on Visual Perception, Nijmegen, the Netherlands.

Maiello, G., Paulun, V. C., Klein, L. K., & Fleming, R. W. (2018). The Sequential-Weight Illusion. *I-Perception*, *9*(4), 204166951879027. https://doi.org/10.1177/2041669518790275

Maiello, G., Paulun, V. C., Klein, L. K., & Fleming, R. W. (2019). Object Visibility, Not Energy Expenditure, Accounts For Spatial Biases in Human Grasp Selection. *I-Perception*, *10*(1), 204166951982760. https://doi.org/10.1177/2041669519827608

Maiello, G., Schepko, M., Klein, L. K., Paulun, V. C., & Fleming, R. W. (2021). Humans Can Visually Judge Grasp Quality and Refine Their Judgments Through Visual and Haptic Feedback. *Frontiers in Neuroscience*, *14*, 591898. https://doi.org/10.3389/fnins.2020.591898

Malach, R., Reppas, J. B., Benson, R. R., Kwong, K. K., Jiang, H., Kennedy, W. A., Ledden, P. J., Brady, T. J., Rosen, B. R., & Tootell, R. B. (1995). Object-related activity revealed by functional magnetic resonance imaging in human occipital cortex. *Proceedings of the National Academy of Sciences*, *92*(18), 8135–8139. https://doi.org/10.1073/pnas.92.18.8135

Mamassian, P. (1997). Prehension of objects oriented in three-dimensional space: *Experimental Brain Research*, *114*(2), 235–245. https://doi.org/10.1007/PL00005632

Marneweck, M., & Grafton, S. T. (2020). Representational Neural Mapping of Dexterous Grasping Before Lifting in Humans. *Journal of Neuroscience*, *40*(13), 2708–2716. https://doi.org/10.1523/JNEUROSCI.2791-19.2020

Marsh, R., Hao, X., Xu, D., Wang, Z., Duan, Y., Liu, J., Kangarlu, A., Martinez, D., Garcia, F., Tau, G. Z., Yu, S., Packard, M. G., & Peterson, B. S. (2010). A virtual reality-based FMRI study of reward-based spatial learning. *Neuropsychologia*, *48*(10), 2912–2921. https://doi.org/10.1016/j.neuropsychologia.2010.05.033

Marteniuk, R. G., Leavitt, J. L., MacKenzie, C. L., & Athenes, S. (1990). Functional relationships between grasp and transport components in a prehension task. *Human Movement Science*, *9*(2), 149–176. https://doi.org/10.1016/0167-9457(90)90025-9

Marteniuk, R. G., Mackenzie, C. L., Jeannerod, M., Athenes, S., & Dugas, C. (1987). Constraints on human arm movement trajectories. *Canadian Journal of Psychology/Revue Canadienne de Psychologie*, *41*(3), 365–378. https://doi.org/10.1037/h0084157

Mason, M. T. (1986). *Mechanics and Planning of Manipulator Pushing Operations*. *5(3)*, 53–71. https://doi.org/10.1177/027836498600500303

Masquelier, T., & Thorpe, S. J. (2010). Learning to recognize objects using waves of spikes and Spike Timing-Dependent Plasticity. *The 2010 International Joint Conference on Neural Networks (IJCNN)*, 1–8. https://doi.org/10.1109/IJCNN.2010.5596934

Matelli, M., Govoni, P., Galletti, C., Kutz, D. F., & Luppino, G. (1998). Superior area 6 afferents from the superior parietal lobule in the macaque monkey. *The Journal of Comparative Neurology*, *402*(3), 327–352. https://doi.org/10.1002/(SICI)1096-9861(19981221)402:3<327::AID-CNE4>3.0.CO;2-Z

Mathis, A., Mamidanna, P., Cury, K. M., Abe, T., Murthy, V. N., Mathis, M. W., & Bethge, M. (2018). DeepLabCut: Markerless pose estimation of user-defined body parts with deep learning. *Nature Neuroscience*, *21*(9), Article 9. https://doi.org/10.1038/s41593-018-0209-y

McDonough, K. L., Costantini, M., Hudson, M., Ward, E., & Bach, P. (2020). Affordance matching predictively shapes the perceptual representation of others' ongoing actions. *Journal of Experimental Psychology: Human Perception and Performance*, *46*(8), 847. https://doi.org/10.1037/xhp0000745

Metelli, F. (1970). An Algebraic Development of the Theory of Perceptual Transparency. *Ergonomics*, *13*(1), 59–66. https://doi.org/10.1080/00140137008931118

Michaels, J. A., Schaffelhofer, S., Agudelo-Toro, A., & Scherberger, H. (2020). A goal-driven modular neural network predicts parietofrontal neural dynamics during grasping. *Proceedings of the National Academy of Sciences*, *117*(50), 32124–32135. https://doi.org/10.1073/pnas.2005087117

Milgram, P. (1987). A spectacle-mounted liquid-crystal tachistoscope. *Behavior Research Methods, Instruments, & Computers*, *19*(5), 449–456. https://doi.org/10.3758/BF03205613

Milner, A. D., Perrett, D. I., Johnston, R. S., Benson, P. J., Jordan, T. R., Heeley, D. W., Bettucci, D., Mortara, F., Mutani, R., Terazzi, E., & Davidson, D. L. W. (1991). Perception and action in 'visual form agnosia'. *Brain*, *114*(1), 405-428. https://doi.org/10.1093/brain/114.1.405

Mishkin, M., & Ungerleider, L. G. (1982). Contribution of striate inputs to the visuospatial functions of parieto-preoccipital cortex in monkeys. *Behavioural Brain Research*, *6*(1), 57–77. https://doi.org/10.1016/0166-4328(82)90081-X

Monaco, S., Cavina-Pratesi, C., Sedda, A., Fattori, P., Galletti, C., & Culham, J. C. (2011). Functional magnetic resonance adaptation reveals the involvement of the dorsomedial stream in hand orientation for grasping. *Journal of Neurophysiology*, *106*(5), 2248–2263. https://doi.org/10.1152/jn.01069.2010

Monaco, S., Malfatti, G., Culham, J. C., Cattaneo, L., & Turella, L. (2020). Decoding motor imagery and action planning in the early visual cortex: Overlapping but distinct neural mechanisms. *NeuroImage*, *218*, 116981. https://doi.org/10.1016/j.neuroimage.2020.116981

Monaco, S., Sedda, A., Cavina-Pratesi, C., & Culham, J. C. (2015). Neural correlates of object size and object location during grasping actions. *European Journal of Neuroscience*, *41*(4), 454–465. https://doi.org/10.1111/ejn.12786

Montagna, W., & Parakkal, P. F. (1974). *The Structure and Function of Skin—3rd Edition*. Academic Press. https://www.elsevier.com/books/the-structure-and-function-of-skin/montagna/978-0-12-505263-4

Montana, D. J. (1992). Contact stability for two-fingered grasps. *IEEE Transactions on Robotics and Automation*, *8*(4), 421–430. https://doi.org/10.1109/70.149939

Mon-Williams, M., & Tresilian, J. R. (2001). A simple rule of thumb for elegant prehension. *Current Biology*, *11*(13), 1058–1061. https://doi.org/10.1016/S0960-9822(01)00293-7

Moscatelli, A., Bianchi, M., Serio, A., Terekhov, A., Hayward, V., Ernst, M. O., & Bicchi, A. (2016). The Change in Fingertip Contact Area as a Novel Proprioceptive Cue. *Current Biology*, *26*(9), 1159–1163. https://doi.org/10.1016/j.cub.2016.02.052

Murata, A., Fadiga, L., Fogassi, L., Gallese, V., Raos, V., & Rizzolatti, G. (1997). Object Representation in the Ventral Premotor Cortex (Area F5) of the Monkey. *Journal of Neurophysiology*, *78*(4), 2226–2230. https://doi.org/10.1152/jn.1997.78.4.2226

Murata, A., Gallese, V., Luppino, G., Kaseda, M., & Sakata, H. (2000). Selectivity for the Shape, Size, and Orientation of Objects for Grasping in Neurons of Monkey Parietal Area AIP. *Journal of Neurophysiology*, *83*(5), 2580–2601. https://doi.org/10.1152/jn.2000.83.5.2580

Murata, Y., Higo, N., Oishi, T., Yamashita, A., Matsuda, K., Hayashi, M., & Yamane, S. (2008). Effects of Motor Training on the Recovery of Manual Dexterity After Primary Motor Cortex Lesion in Macaque Monkeys. *Journal of Neurophysiology*, *99*(2), 773–786. https://doi.org/10.1152/jn.01001.2007

Murray, G. L., Attridge, S. R., & Morona, R. (2006). Altering the Length of the Lipopolysaccharide O Antigen Has an Impact on the Interaction of Salmonella enterica Serovar Typhimurium with Macrophages and Complement. *Journal of Bacteriology*, *188*(7), 2735–2739. https://doi.org/10.1128/JB.188.7.2735-2739.2006

Murray, S. O., Olshausen, B. A., & Woods, D. L. (2003). Processing Shape, Motion and Three-dimensional Shape-from-motion in the Human Cortex. *Cerebral Cortex*, *13*(5), 508–516. https://doi.org/10.1093/cercor/13.5.508

Napier, J. R. (1956). The prehensile movements of the human hand. *The Journal of Bone and Joint Surgery. British Volume*, *38*(4), 902–913. https://doi.org/10.1302/0301-620X.38B4.902

Nath, T., Mathis, A., Chen, A. C., Patel, A., Bethge, M., & Mathis, M. W. (2019). Using DeepLabCut for 3D markerless pose estimation across species and behaviors. *Nature Protocols*, *14*(7), Article 7. https://doi.org/10.1038/s41596-019-0176-0

Newcombe, F., & Ratcliff, G. (1975). *Agnosia: A disorder of object recognition.* https://scholar.google.com/scholar_lookup?title=Agnosia%3A%20A%20disorder%20of%20object%20recognition&publication_year=1975&author=F.%20Newcombe&author=G.%20Ratcliff

Nguyen, V.-D. (1988). Constructing Force- Closure Grasps. *The International Journal of Robotics Research*, *7*(3), 3–16. https://doi.org/10.1177/027836498800700301

Nowak, D. A., Berner, J., Herrnberger, B., Kammer, T., Grön, G., & Schönfeldt-Lecuona, C. (2009). Continuous theta-burst stimulation over the dorsal premotor cortex interferes with associative learning during object lifting. *Cortex*, *45*(4), 473–482. https://doi.org/10.1016/j.cortex.2007.11.010

Oculus Quest 2. (2022, October). https://www.meta.com/de/quest/products/quest-2/

Orban, G. A. (2011). The Extraction of 3D Shape in the Visual System of Human and Nonhuman Primates. *Annual Review of Neuroscience*, *34*(1), 361–388. https://doi.org/10.1146/annurev-neuro-061010-113819

Orban, G. A., Janssen, P., & Vogels, R. (2006). Extracting 3D structure from disparity. *Trends in Neurosciences*, *29*(8), 466–473. https://doi.org/10.1016/j.tins.2006.06.012

O'Shea, H., & Redmond, S. J. (2021). A review of the neurobiomechanical processes underlying secure gripping in object manipulation. *Neuroscience & Biobehavioral Reviews*, *123*, 286–300. https://doi.org/10.1016/j.neubiorev.2021.01.007

Owens, A., Isola, P., McDermott, J., Torralba, A., Adelson, E. H., & Freeman, W. T. (2016). Visually Indicated Sounds. *2016 IEEE Conference on Computer Vision and Pattern Recognition (CVPR)*, 2405–2413. https://doi.org/10.1109/CVPR.2016.264

Passingham, R. E., Perry, V. H., & Wilkinson, F. (1983). The long-term effects of removal of sensorimotor cortex in infant and adult rhesus monkeys. *Brain*, *106*(3), 675–705. https://doi.org/10.1093/brain/106.3.675

Paulignan, Y., Frak, V. G., Toni, I., & Jeannerod, M. (1997). Influence of object position and size on human prehension movements. *Experimental Brain Research*, *114*(2), 226–234. https://doi.org/10.1007/PL00005631

Paulignan, Y., MacKenzie, C., Marteniuk, R., & Jeannerod, M. (1991). Selective perturbation of visual input during prehension movements. *Experimental Brain Research*, *83*(3), 502-512. https://doi.org/10.1007/BF00229827

Paulun, V. C., Buckingham, G., Goodale, M. A., & Fleming, R. W. (2019). The material-weight illusion disappears or inverts in objects made of two materials. *Journal of Neurophysiology*, *121*(3), 996–1010. https://doi.org/10.1152/jn.00199.2018

Paulun, V. C., Gegenfurtner, K. R., Goodale, M. A., & Fleming, R. W. (2016). Effects of material properties and object orientation on precision grip kinematics. *Experimental Brain Research*, *234*(8), 2253–2265. https://doi.org/10.1007/s00221-016-4631-7

Paulun, V. C., Kleinholdermann, U., Gegenfurtner, K. R., Smeets, J. B. J., & Brenner, E. (2014). Center or side: Biases in selecting grasp points on small bars. *Experimental Brain Research*, *232*(7), 2061–2072. https://doi.org/10.1007/s00221-014-3895-z

Paulun, V. C., Schmidt, F., van Assen, J. J. R., & Fleming, R. W. (2017). Shape, motion, and optical cues to stiffness of elastic objects. *Journal of Vision*, *17*(1), 20. https://doi.org/10.1167/17.1.20

Peng Zhang, Xuan Ma, Hailong Huang, & Jiping He. (2014). Predicting hand orientation in reach-to-grasp tasks using neural activities from primary motor cortex. *2014 36th Annual International Conference of the IEEE Engineering in Medicine and Biology Society*, 1306–1309. https://doi.org/10.1109/EMBC.2014.6943838

Perez-Marcos, D., Sanchez-Vives, M. V., & Slater, M. (2012). Is my hand connected to my body? The impact of body continuity and arm alignment on the virtual hand illusion. *Cognitive Neurodynamics*, *6*(4), 295–305. https://doi.org/10.1007/s11571-011-9178-5

Pettypiece, C. E., Culham, J. C., & Goodale, M. A. (2009). Differential effects of delay upon visually and haptically guided grasping and perceptual judgments. *Experimental Brain Research*, *195*(3), 473–479. https://doi.org/10.1007/s00221-009-1807-4

Pettypiece, C. E., Goodale, M. A., & Culham, J. C. (2010). Integration of haptic and visual size cues in perception and action revealed through cross-modal conflict. *Experimental Brain Research*, *201*(4), 863–873. https://doi.org/10.1007/s00221-009-2101-1

Peña-Pitarch, E., Yang, J., & Abdel-Malek, K. (2005, June). SANTOSTM Hand: A 25 degree-of-freedom model. In *SAE 2005 Digital Human Modeling for Design and Engineering Conference* (pp. 01-2727). https://doi.org/10.4271/2005-01-2727

Pitzalis, S., Sereno, M. I., Committeri, G., Fattori, P., Galati, G., Tosoni, A., & Galletti, C. (2013). The human homologue of macaque area V6A. *NeuroImage*, *82*, 517–530. https://doi.org/10.1016/j.neuroimage.2013.06.026

Podrebarac, S. K., Goodale, M. A., & Snow, J. C. (2014). Are visual texture-selective areas recruited during haptic texture discrimination? *NeuroImage*, *94*, 129–137. https://doi.org/10.1016/j.neuroimage.2014.03.013

Pont, S. C., & Koenderink, J. J. (2008). Shape, surface roughness and human perception. In *Handbook of texture analysis* (pp. 197-222). https://doi.org/10.1142/9781848161160_0007

Raj, D. V., Ingty, K., & Devanandan, M. S. (1985). Weight appreciation in the hand in normal subjects and in patients with leprous neuropathy. *Brain*, *108*(1), 95–102. https://doi.org/10.1093/brain/108.1.95

Rand, M. K., Lemay, M., Squire, L. M., Shimansky, Y. P., & Stelmach, G. E. (2007). Role of vision in aperture closure control during reach-to-grasp movements. *Experimental Brain Research*, *181*(3), 447–460. https://doi.org/10.1007/s00221-007-0945-9

Raos, V., Umiltá, M. A., Gallese, V., & Fogassi, L. (2004). Functional Properties of Grasping-Related Neurons in the Dorsal Premotor Area F2 of the Macaque Monkey. *Journal of Neurophysiology*, *92*(4), 1990–2002. https://doi.org/10.1152/jn.00154.2004

Raos, V., Umiltá, M. A., Murata, A., Fogassi, L., & Gallese, V. (2006). Functional Properties of Grasping-Related Neurons in the Ventral Premotor Area F5 of the Macaque Monkey. *Journal of Neurophysiology*, *95*(2), 709–729. https://doi.org/10.1152/jn.00463.2005

Rice, N. J., Tunik, E., & Grafton, S. T. (2006). The Anterior Intraparietal Sulcus Mediates Grasp Execution, Independent of Requirement to Update: New Insights from Transcranial Magnetic Stimulation. *Journal of Neuroscience*, *26*(31), 8176–8182. https://doi.org/10.1523/JNEUROSCI.1641-06.2006

Rice, N. J., Valyear, K. F., Goodale, M. A., Milner, A. D., & Culham, J. C. (2007). Orientation sensitivity to graspable objects: An fMRI adaptation study. *NeuroImage*, *36*, T87–T93. https://doi.org/10.1016/j.neuroimage.2007.03.032

Riva, G., Castelnuovo, G., & Mantovani, F. (2006). Transformation of flow in rehabilitation: The role of advanced communication technologies. *Behavior Research Methods*, *38*(2), 237–244. https://doi.org/10.3758/BF03192775

Rizzolatti, G., & Matelli, M. (2003). Two different streams form the dorsal visual system: Anatomy and functions. *Experimental Brain Research*, *153*(2), 146–157. https://doi.org/10.1007/s00221-003-1588-0

Roby-Brami, A., Bennis, N., Mokhtari, M., & Baraduc, P. (2000). Hand orientation for grasping depends on the direction of the reaching movement. *Brain Research*, *869*(1–2), 121–129. https://doi.org/10.1016/S0006-8993(00)02378-7

Romaiguère, P., Nazarian, B., Roth, M., Anton, J.-L., & Felician, O. (2014). Lateral occipitotemporal cortex and action representation. *Neuropsychologia*, *56*, 167–177. https://doi.org/10.1016/j.neuropsychologia.2014.01.006

Rosenbaum, D. A., & Jorgensen, M. J. (1992). Planning macroscopic aspects of manual control. *Human Movement Science*, *11*(1), 61–69. https://doi.org/10.1016/0167-9457(92)90050-L

Rosenbaum, D. A., Marchk, F., Barnes, H. J., Vaughan, J., Slotta, J. D., & Jorgensen, M. J. (2018). Constraints for action selection: Overhand versus underhand grips. In *Attention and performance XIII* (pp. 321-342). Psychology Press. https://doi.org/10.4324/9780203772010

Rosenbaum, D. A., Meulenbroek, R. G. J., Vaughan, J., & Jansen, C. (1999). Coordination of reaching and grasping by capitalizing on obstacle avoidance and other constraints. *Experimental Brain Research*, *128*(1–2), 92–100. https://doi.org/10.1007/s002210050823

Rosenbaum, D. A., Meulenbroek, R. J. G., Vaughan, J., & Elsinger, C. (1999). Approaching Grasping from Different Perspectives. *Motor Control*, *3*(3), 289–297. https://doi.org/10.1123/mcj.3.3.289

Rosenbaum, D. A., Meulenbroek, R. J., Vaughan, J., & Jansen, C. (2001). Posture-based motion planning: Applications to grasping. *Psychological Review*, *108*(4), 709. https://doi.org/10.1037/0033-295X.108.4.709

Rossetti, Y., Meckler, C., & Prablanc, C. (1994). Is there an optimal arm posture? Deterioration of finger localization precision and comfort sensation in extreme arm-joint postures. *Experimental Brain Research*, *99*(1), 131–136. https://doi.org/10.1007/BF00241417

Rossetti, Y., Pisella, L., & Vighetto, A. (2003). Optic ataxia revisited: *Experimental Brain Research*, *153*(2), 171–179. https://doi.org/10.1007/s00221-003-1590-6

Rousselet, G. A., Fabre-Thorpe, M., & Thorpe, S. J. (2002). Parallel processing in high-level categorization of natural images. *Nature Neuroscience*, *5*(7), 629–630. https://doi.org/10.1038/nn866

Rushton, S. K., & Riddell, P. M. (1999). Developing visual systems and exposure to virtual reality and stereo displays: Some concerns and speculations about the demands on accommodation and vergence. *Applied Ergonomics*, *30*(1), 69-78. https://doi.org/10.1016/S0003-6870(98)00044-1

Sacheli, L. M., Aglioti, S. M., & Candidi, M. (2015). Social cues to joint actions: The role of shared goals. *Frontiers in Psychology*, *6*. https://doi.org/10.3389/fpsyg.2015.01034

Sacheli, L. M., Candidi, M., Pavone, E. F., Tidoni, E., & Aglioti, S. M. (2012). And Yet They Act Together: Interpersonal Perception Modulates Visuo-Motor Interference and Mutual Adjustments during a Joint-Grasping Task. *PLoS ONE*, *7*(11), e50223. https://doi.org/10.1371/journal.pone.0050223

Sacheli, L. M., Tidoni, E., Pavone, E. F., Aglioti, S. M., & Candidi, M. (2013). Kinematics fingerprints of leader and follower role-taking during cooperative joint actions. *Experimental Brain Research*, *226*(4), 473–486. https://doi.org/10.1007/s00221-013-3459-7

Sakata, H., Taira, M., Murata, A., & Mine, S. (1995). Neural Mechanisms of Visual Guidance of Hand Action in the Parietal Cortex of the Monkey. *Cerebral Cortex*, *5*(5), 429–438. https://doi.org/10.1093/cercor/5.5.429

Samuel, F., & Kerzel, D. (2011). Is this object balanced or unbalanced? Judgments are on the safe side. *Journal of Experimental Psychology: Human Perception and Performance*, *37*, 529–538. https://doi.org/10.1037/a0018732

Sanz, P. J., In, J. M., & Pobil, A. P. D. (1999). *Planar Grasping Characterization Based on Curvature-Symmetry Fusion*. *10*, 25–36. https://doi.org/10.1023/A:1008381314159

Savelsbergh, G. J. P., Steenbergen, B., & van der Kamp, J. (1996). The role of fragility information in the guidance of the precision grip. *Human Movement Science*, *15*(1), 115–127. https://doi.org/10.1016/0167-9457(95)00039-9

Schaffelhofer, S., Agudelo-Toro, A., & Scherberger, H. (2015). Decoding a Wide Range of Hand Configurations from Macaque Motor, Premotor, and Parietal Cortices. *Journal of Neuroscience*, *35*(3), 1068–1081. https://doi.org/10.1523/JNEUROSCI.3594-14.2015

Schenk, T., & McIntosh, R. D. (2010). Do we have independent visual streams for perception and action? *Cognitive Neuroscience*, *1*(1), 52–62. https://doi.org/10.1080/17588920903388950

Schettino, L. F., Adamovich, S. V., & Poizner, H. (2003). Effects of object shape and visual feedback on hand configuration during grasping. *Experimental Brain Research*, *151*(2), 158–166. https://doi.org/10.1007/s00221-003-1435-3

Schot, W. D., Brenner, E., & Smeets, J. B. J. (2010a). Robust movement segmentation by combining multiple sources of information. *Journal of Neuroscience Methods*, *187*(2), 147–155. https://doi.org/10.1016/j.jneumeth.2010.01.004

Schot, W. D., Brenner, E., & Smeets, J. B. J. (2010b). Posture of the arm when grasping spheres to place them elsewhere. *Experimental Brain Research*, *204*(2), 163–171. https://doi.org/10.1007/s00221-010-2261-z

Schuetz, I., & Fiehler, K. (2022). Eye tracking in virtual reality: Vive pro eye spatial accuracy, precision, and calibration reliability. *Journal of Eye Movement Research*, *15*(3). https://doi.org/10.16910/jemr.15.3.3

Schultheis, M., Straub, D., & Rothkopf, C. A. (2021). Inverse Optimal Control Adapted to the Noise Characteristics of the Human Sensorimotor System. *Advances in Neural Information Processing Systems*, *34*, 9429–9442. https://proceedings.neurips.cc/paper/2021/hash/4e55139e019a58e0084f194f758ffdea-Abstract.html

Seifi, H., Kappers, A. M. L., Schneider, O., Drewing, K., Pacchierotti, C., Abbasimoshaei, A., Huisman, G., & Kern, T. A. (Eds.). (2022). *Haptics: Science, Technology, Applications: 13th International Conference on Human Haptic Sensing and Touch Enabled Computer Applications, EuroHaptics 2022, Hamburg, Germany, May 22–25, 2022, Proceedings* (Vol. 13235). Springer International Publishing. https://doi.org/10.1007/978-3-031-06249-0

Sereno, M. E., Trinath, T., Augath, M., & Logothetis, N. K. (2002). Three-Dimensional Shape Representation in Monkey Cortex. *Neuron*, *33*(4), 635–652. https://doi.org/10.1016/S0896-6273(02)00598-6

Sharan, L. (2009). *The perception of material qualities in real-world images.* Thesis, Massachusetts Institute of Technology. https://dspace.mit.edu/handle/1721.1/54644

Sharan, L., Rosenholtz, R., & Adelson, E. H. (2014). Accuracy and speed of material categorization in real-world images. *Journal of Vision*, *14*(9), 12. https://doi.org/10.1167/14.9.12

Short, M. W., & Cauraugh, J. H. (1999). Precision hypothesis and the end-state comfort effect. *Acta Psychologica*, *100*(3), 243–252. https://doi.org/10.1016/S0001-6918(98)00020-1

Singhal, A., Monaco, S., Kaufman, L. D., & Culham, J. C. (2013). Human fMRI Reveals That Delayed Action Re-Recruits Visual Perception. *PLoS ONE*, *8*(9), e73629. https://doi.org/10.1371/journal.pone.0073629

Singh-Curry, V., & Husain, M. (2009). The functional role of the inferior parietal lobe in the dorsal and ventral stream dichotomy. *Neuropsychologia*, *47*(6), 1434–1448. https://doi.org/10.1016/j.neuropsychologia.2008.11.033

Sivak, B., & Mackenzie, C. L. (1992). Chapter 10 - The Contributions of Peripheral Vision and Central Vision to Prehension. In L. Proteau & D. Elliott (Eds.), *Advances in Psychology* (Vol. 85, pp. 233–259). North-Holland. https://doi.org/10.1016/S0166-4115(08)62017-8

Smeets, J. B. J., & Brenner, E. (1999). A New View on Grasping. *Motor Control*, *3*(3), 237–271. https://doi.org/10.1123/mcj.3.3.237

Smeets, J., & Brenner, E. (2001). Independent movements of the digits in grasping. *Experimental Brain Research*, *139*(1), 92–100. https://doi.org/10.1007/s002210100748

Solomon, H. Y., Turvey, M. T., & Burton, G. (1989). Perceiving extents of rods by wielding: Haptic diagonalization and decomposition of the inertia tensor. *Journal of Experimental Psychology: Human Perception and Performance*, *15*, 58–68. https://doi.org/10.1037/0096-1523.15.1.58

Srivastava, S., Orban, G. A., De Maziere, P. A., & Janssen, P. (2009). A Distinct Representation of Three-Dimensional Shape in Macaque Anterior Intraparietal Area: Fast, Metric, and Coarse. *Journal of Neuroscience*, *29*(34), 10613–10626. https://doi.org/10.1523/JNEUROSCI.6016-08.2009

Stanney, K., Fidopiastis, C., & Foster, L. (2020). Virtual Reality Is Sexist: But It Does Not Have to Be. *Frontiers in Robotics and AI*, *7*, 4. https://doi.org/10.3389/frobt.2020.00004

Stelmach, G. E., Castiello, U., & Jeannerod, M. (1994). Orienting the Finger Opposition Space during Prehension Movements. *Journal of Motor Behavior*, *26*(2), 178–186. https://doi.org/10.1080/00222895.1994.9941672

Stival, F., Michieletto, S., Cognolato, M., Pagello, E., Müller, H., & Atzori, M. (2019). A quantitative taxonomy of human hand grasps. *Journal of NeuroEngineering and Rehabilitation*, *16*(1), 28. https://doi.org/10.1186/s12984-019-0488-x

Sundaram, S., Kellnhofer, P., Li, Y., Zhu, J. Y., Torralba, A., & Matusik, W. (2019). Learning the signatures of the human grasp using a scalable tactile glove. *Nature*, *569*(7758), 698–702. https://doi.org/10.1038/s41586-019-1234-z

Tanaka, J. W., & Presnell, L. M. (1999). Color diagnosticity in object recognition. *Perception & Psychophysics*, *61*(6), 1140–1153. https://doi.org/10.3758/BF03207619

Taubert, M., Dafotakis, M., Sparing, R., Eickhoff, S., Leuchte, S., Fink, G. R., & Nowak, D. A. (2010). Inhibition of the anterior intraparietal area and the dorsal premotor cortex interfere with arbitrary visuo-motor mapping. *Clinical Neurophysiology*, *121*(3), 408–413. https://doi.org/10.1016/j.clinph.2009.11.011

Taylor, P. C. J., Walsh, V., & Eimer, M. (2008). Combining TMS and EEG to study cognitive function and cortico–cortico interactions. *Behavioural Brain Research*, *191*(2), 141–147. https://doi.org/10.1016/j.bbr.2008.03.033

Theys, T., Pani, P., van Loon, J., Goffin, J., & Janssen, P. (2012). Selectivity for Three-Dimensional Shape and Grasping-Related Activity in the Macaque Ventral Premotor Cortex. *Journal of Neuroscience*, *32*(35), 12038–12050. https://doi.org/10.1523/JNEUROSCI.1790-12.2012

Theys, T., Romero, M. C., van Loon, J., & Janssen, P. (2015). Shape representations in the primate dorsal visual stream. *Frontiers in Computational Neuroscience*, *9*. https://doi.org/10.3389/fncom.2015.00043

Thorpe, S. J., Gegenfurtner, K. R., Fabre-Thorpe, M., & Bülthoff, H. H. (2001). Detection of animals in natural images using far peripheral vision: Detection of animals in natural images. *European Journal of Neuroscience*, *14*(5), 869–876. https://doi.org/10.1046/j.0953-816x.2001.01717.x

Touvet, F., Daoud, N., Gazeau, J.-P., Zeghloul, S., Maier, M. A., & Eskiizmirliler, S. (2012). A biomimetic reach and grasp approach for mechanical hands. *Robotics and Autonomous Systems*, *60*(3), 473–486. https://doi.org/10.1016/j.robot.2011.07.017

Townsend, B. R., Subasi, E., & Scherberger, H. (2011). Grasp Movement Decoding from Premotor and Parietal Cortex. *Journal of Neuroscience*, *31*(40), 14386–14398. https://doi.org/10.1523/JNEUROSCI.2451-11.2011

Tunik, E., Frey, S. H., & Grafton, S. T. (2005). Virtual lesions of the anterior intraparietal area disrupt goal-dependent on-line adjustments of grasp. *Nature Neuroscience*, *8*(4), 505–511. https://doi.org/10.1038/nn1430

Vahrenkamp, N., Koch, E., Waechter, M., & Asfour, T. (2017). Planning High-Quality Grasps using Mean Curvature Object Skeletons. *ArXiv:1710.02418 [Cs]*. http://arxiv.org/abs/1710.02418

Valyear, K. F., Culham, J. C., Sharif, N., Westwood, D., & Goodale, M. A. (2006). A double dissociation between sensitivity to changes in object identity and object orientation in the ventral and dorsal visual streams: A human fMRI study. *Neuropsychologia*, *44*(2), 218–228. https://doi.org/10.1016/j.neuropsychologia.2005.05.004

van Dam, L. C. J., & Stephens, J. R. (2018). Effects of prolonged exposure to feedback delay on the qualitative subjective experience of virtual reality. *PLOS ONE*, *13*(10), e0205145. https://doi.org/10.1371/journal.pone.0205145

van Polanen, V., Buckingham, G., & Davare, M. (2020). *Effects of TMS over the anterior intraparietal area on anticipatory fingertip force scaling and the size-weight illusion* [Preprint]. Neuroscience. https://doi.org/10.1101/2020.05.18.101675

van Polanen, V., & Davare, M. (2015). Sensorimotor Memory Biases Weight Perception During Object Lifting. *Frontiers in Human Neuroscience*, *9*. https://doi.org/10.3389/fnhum.2015.00700

van Polanen, V., Rens, G., & Davare, M. (2020). The role of the anterior intraparietal sulcus and the lateral occipital cortex in fingertip force scaling and weight perception during object lifting. *Journal of Neurophysiology*, *124*(2), 557–573. https://doi.org/10.1152/jn.00771.2019

Vargas-Irwin, C. E., Shakhnarovich, G., Yadollahpour, P., Mislow, J. M. K., Black, M. J., & Donoghue, J. P. (2010). Decoding Complete Reach and Grasp Actions from Local Primary Motor Cortex Populations. *Journal of Neuroscience*, *30*(29), 9659–9669. https://doi.org/10.1523/JNEUROSCI.5443-09.2010

Veiga, F., Akrour, R., & Peters, J. (2020). Hierarchical Tactile-Based Control Decomposition of Dexterous In-Hand Manipulation Tasks. *Frontiers in Robotics and AI*, *7*. https://www.frontiersin.org/articles/10.3389/frobt.2020.521448

Veijgen, N. K., van der Heide, E., & Masen, M. A. (2013). A multivariable model for predicting the frictional behaviour and hydration of the human skin. *Skin Research and Technology*, *19*(3), 330–338. https://doi.org/10.1111/srt.12053

Verheij, R., Brenner, E., & Smeets, J. B. (2014). The influence of target object shape on maximum grip aperture in human grasping movements. *Experimental Brain Research*, *232*(11), 3569–3578.

Vesia, M., Culham, J. C., Jegatheeswaran, G., Isayama, R., Le, A., Davare, M., & Chen, R. (2018). Functional interaction between human dorsal premotor cortex and the ipsilateral primary motor cortex for grasp plans: A dual-site TMS study. *NeuroReport*, *29*(16), 1355–1359. https://doi.org/10.1097/WNR.0000000000001117

Volcic, R., & Domini, F. (2014). The visibility of contact points influences grasping movements. *Experimental Brain Research*, *232*(9), 2997–3005. https://doi.org/10.1007/s00221-014-3978-x

Volcic, R., & Domini, F. (2016). On-line visual control of grasping movements. *Experimental Brain Research*, *234*(8), 2165–2177. https://doi.org/10.1007/s00221-016-4620-x

Volcic, R., & Domini, F. (2018). The endless visuomotor calibration of reach-to-grasp actions. *Scientific Reports*, *8*(1), 14803. https://doi.org/10.1038/s41598-018-33009-6

Volcic, R., & Kappers, A. M. L. (2008). Allocentric and egocentric reference frames in the processing of three-dimensional haptic space. *Experimental Brain Research*, *188*(2), 199–213. https://doi.org/10.1007/s00221-008-1353-5

von Helmholtz, H. (1867). LXIII. *On Integrals of the hydrodynamical equations, which express vortex-motion*. *The London, Edinburgh, and Dublin Philosophical Magazine and Journal of Science*, *33*(226), 485–512. https://doi.org/10.1080/14786446708639824

Voss, M., Ingram, J. N., Wolpert, D. M., & Haggard, P. (2008). Mere Expectation to Move Causes Attenuation of Sensory Signals. *PLoS ONE*, *3*(8), e2866. https://doi.org/10.1371/journal.pone.0002866

Voudouris, D., Brenner, E., Schot, W. D., & Smeets, J. B. J. (2010). Does planning a different trajectory influence the choice of grasping points? *Experimental Brain Research*, *206*(1), 15–24. https://doi.org/10.1007/s00221-010-2382-4

Voudouris, D., Broda, M. D., & Fiehler, K. (2019). Anticipatory grasping control modulates somatosensory perception. *Journal of Vision*, *19*(5), 4. https://doi.org/10.1167/19.5.4

Voudouris, D., & Fiehler, K. (2017). Enhancement and suppression of tactile signals during reaching. *Journal of Experimental Psychology: Human Perception and Performance*, *43*(6), 1238–1248. https://doi.org/10.1037/xhp0000373

Voudouris, D., Radhakrishnan, S., Hatzitaki, V., & Brenner, E. (2013). Does postural stability affect grasping? *Gait & Posture*, *38*(3), 477–482.

Voudouris, D., Smeets, J. B. J., & Brenner, E. (2012a). Do Humans Prefer to See Their Grasping Points? *Journal of Motor Behavior*, *44*(4), 295–304. https://doi.org/10.1080/00222895.2012.703975

Voudouris, D., Smeets, J. B. J., & Brenner, E. (2012b). Do obstacles affect the selection of grasping points? *Human Movement Science*, *31*(5), 1090–1102. https://doi.org/10.1016/j.humov.2012.01.005

Voudouris, D., Smeets, J. B. J., & Brenner, E. (2013). Ultra-fast selection of grasping points. *Journal of Neurophysiology*, *110*(7), 1484–1489. https://doi.org/10.1152/jn.00066.2013

Walter, T., & Couzin, I. D. (2021). TRex, a fast multi-animal tracking system with markerless identification, and 2D estimation of posture and visual fields. *ELife*, *10*, e64000. https://doi.org/10.7554/eLife.64000

Wang, L., Mruczek, R. E. B., Arcaro, M. J., & Kastner, S. (2015). Probabilistic Maps of Visual Topography in Human Cortex. *Cerebral Cortex*, *25*(10), 3911–3931. https://doi.org/10.1093/cercor/bhu277

Watt, S. J., & Bradshaw, M. F. (2000). Binocular cues are important in controlling the grasp but not the reach in natural prehension movements. *Neuropsychologia*, *38*(11), 1473–1481. https://doi.org/10.1016/S0028-3932(00)00065-8

Weech, S., Calderon, C. M., & Barnett-Cowan, M. (2020). Sensory Down-Weighting in Visual-Postural Coupling Is Linked With Lower Cybersickness. *Frontiers in Virtual Reality*, *1*, 10. https://doi.org/10.3389/frvir.2020.00010

Westling, G., & Johansson, R. S. (1984). Factors influencing the force control during precision grip. *Experimental Brain Research*, *53*(2). https://doi.org/10.1007/BF00238156

Westling, G., & Johansson, R. S. (1987). Responses in glabrous skin mechanoreceptors during precision grip in humans. *Experimental Brain Research*, *66*(1). https://doi.org/10.1007/BF00236209

White, P. A. (2012). The experience of force: The role of haptic experience of forces in visual perception of object motion and interactions, mental simulation, and motion-related judgments. *Psychological Bulletin*, *138*, 589–615. https://doi.org/10.1037/a0025587

Wiebel, C. B., Valsecchi, M., & Gegenfurtner, K. R. (2013). The speed and accuracy of material recognition in natural images. *Attention, Perception, & Psychophysics*, *75*(5), 954–966. https://doi.org/10.3758/s13414-013-0436-y

Willemsen, P., Gooch, A. A., Thompson, W. B., & Creem-Regehr, S. H. (2008). Effects of Stereo Viewing Conditions on Distance Perception in Virtual Environments. *Presence: Teleoperators and Virtual Environments*, *17*(1), 91–101. https://doi.org/10.1162/pres.17.1.91

Wing, A. M., & Lederman, S. J. (2009). In D. A. Nowak & J. Hermsdorfer (Eds.), *Points for precision grip. Sensorimotor control for grasping: Physiology and pathophysiology.* (pp. 193–203). Cambridge University Press.

Wing, A. M., Turton, A., & Fraser, C. (1986). Grasp Size and Accuracy of Approach in Reaching. *Journal of Motor Behavior*, *18*(3), 245–260. https://doi.org/10.1080/00222895.1986.10735380

Winges, S. A., Weber, D. J., & Santello, M. (2003). The role of vision on hand preshaping during reach to grasp. *Experimental Brain Research*, *152*(4), 489–498. https://doi.org/10.1007/s00221-003-1571-9

Witney, A. G., Vetter, P., & Wolpert, D. M. (2001). The influence of previous experience on predictive motor control. *Neuroreport*, *12*(4), 649–653.

Wolfe, H. K. (1898). Some effects of size on judgments of weight. *Psychological Review*, *5*(1), 25–54. https://doi.org/10.1037/h0073342

Wolfe, H. K. (1923). On the Estimation of the Middle of Lines. *The American Journal of Psychology*, *34*(3), 313–358. https://doi.org/10.2307/1413954

Wolpert, D. M., Diedrichsen, J., & Flanagan, J. R. (2011). Principles of sensorimotor learning. *Nature Reviews Neuroscience*, *12*(12), 739–751. https://doi.org/10.1038/nrn3112

Wolpert, D. M., & Ghahramani, Z. (2000). Computational principles of movement neuroscience. *Nature Neuroscience*, *3*(S11), 1212–1217. https://doi.org/10.1038/81497

Yarkoni, T., Poldrack, R. A., Nichols, T. E., Van Essen, D. C., & Wager, T. D. (2011). Large-scale automated synthesis of human functional neuroimaging data. *Nature Methods*, *8*(8), 665–670. https://doi.org/10.1038/nmeth.1635

Young, T. (1802). II. The Bakerian Lecture. On the theory of light and colours. *Philosophical Transactions of the Royal Society of London*, *92*, 12–48. https://doi.org/10.1098/rstl.1802.0004

Zoeller, A. C., & Drewing, K. (2020). A Systematic Comparison of Perceptual Performance in Softness Discrimination with Different Fingers. *Attention, Perception, & Psychophysics*, *82*(7), 3696–3709. https://doi.org/10.3758/s13414-020-02100-4

Zoeller, A. C., Lezkan, A., Paulun, V. C., Fleming, R. W., & Drewing, K. (2019). Integration of prior knowledge during haptic exploration depends on information type. *Journal of Vision*, *19*(4), 20. https://doi.org/10.1167/19.4.20

List of Publications

Klein, L. K., Maiello, G., Fleming, R. W., & Voudouris, D. (2021). Friction is preferred over grasp configuration in precision grip grasping. *Journal of Neurophysiology*, *125*(4), 1330–1338. https://doi.org/10.1152/jn.00021.2021

Maiello, G.*, Schepko, M.*, **Klein, L. K.**, Paulun, V. C., & Fleming, R. W. (2021). Humans Can Visually Judge Grasp Quality and Refine Their Judgments Through Visual and Haptic Feedback. *Frontiers in Neuroscience*, *14*, 591898. https://doi.org/10.3389/fnins.2020.591898

Klein, L. K.*, Maiello, G.*, Paulun, V. C., & Fleming, R. W. (2020). Predicting precision grip grasp locations on three-dimensional objects. *PLOS Computational Biology*, *16*(8), e1008081. https://doi.org/10.1371/journal.pcbi.1008081

Rohde, M., Narioka, K., Steil, J., **Klein, L. K.**, & Ernst, M. O. (2019) Goal-Related Feedback Guides Motor Exploration and Redundancy Resolution in Human Motor Skill Acquisition. *PLOS Computational Biology,* *15*(3): e1006676. https://journals.plos.org/ploscompbiol/article?id=10.1371/journal.pcbi.1006676

Maiello, G.*, Paulun, V. C.*, **Klein, L. K.**, & Fleming, R. W. (2019). Object Visibility, Not Energy Expenditure, Accounts For Spatial Biases in Human Grasp Selection. *I-Perception*, *10*(1), 204166951982760. https://doi.org/10.1177/2041669519827608

Chessa, M., Maiello, G., **Klein, L. K.**, Paulun, V. C., & Solari, F. (2019). Grasping objects in immersive Virtual Reality. *2019 IEEE Conference on Virtual Reality and 3D User Interfaces (VR)*, 1749–1754. https://doi.org/10.1109/VR.2019.8798155

Maiello, G., Paulun, V. C., **Klein, L. K.**, & Fleming, R. W. (2018). The Sequential-Weight Illusion. *I-Perception*, *9*(4), 204166951879027. https://doi.org/10.1177/2041669518790275

Klein, L. K.*, Maiello, G.*, Stubbs, K., Proklova, D., Paulun, V. C., Culham. J. C., & Fleming, R. W. (in preparation) Distinct neural components of visually guided grasping during planning and execution.

*These authors contributed equally and share first authorship on this work

Appendix

Supporting Information S1 Figure for Chapter 2

(a) Experiment 1

Human | Unfitted Model | Fitted Model

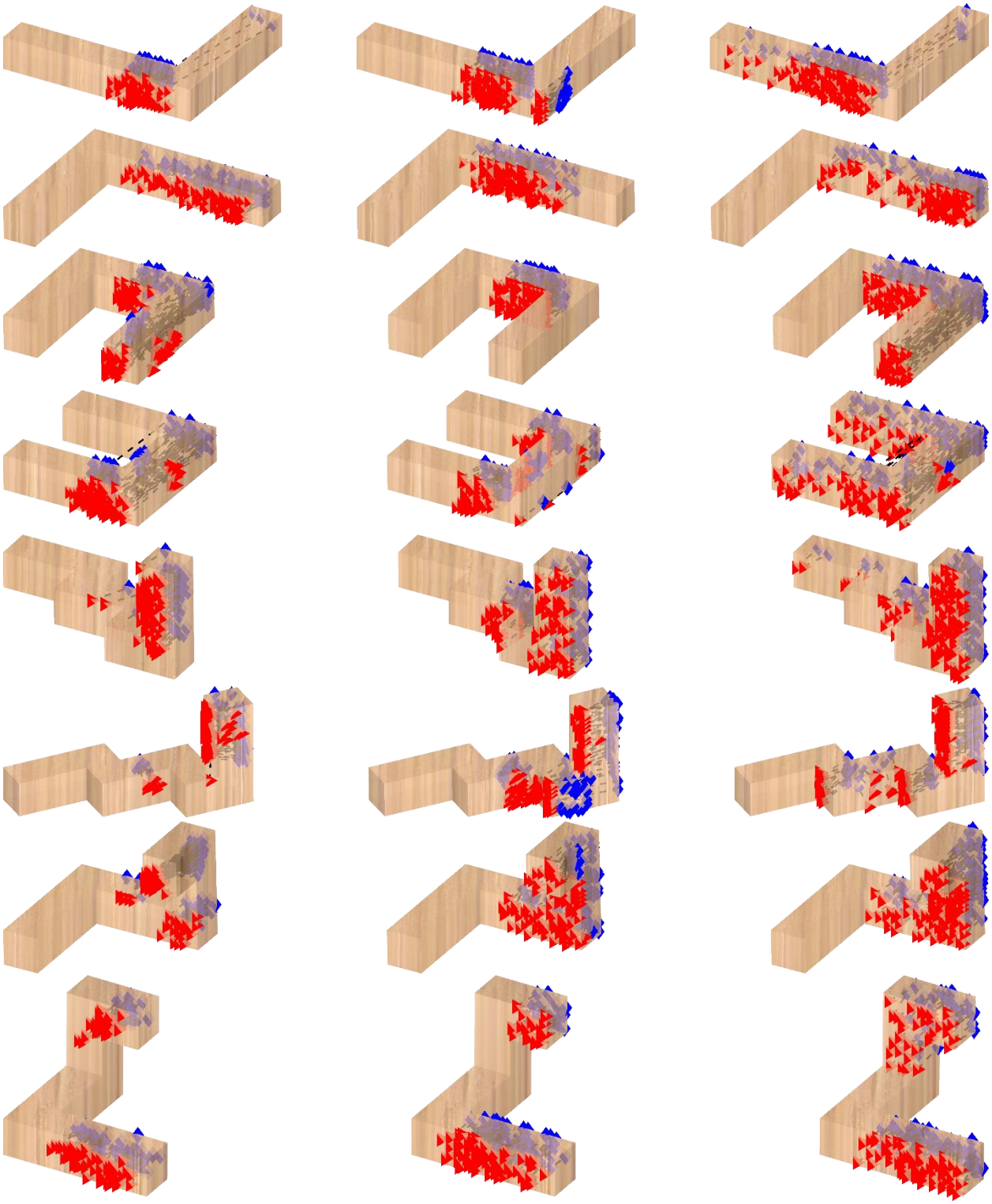

(b) Experiment 2

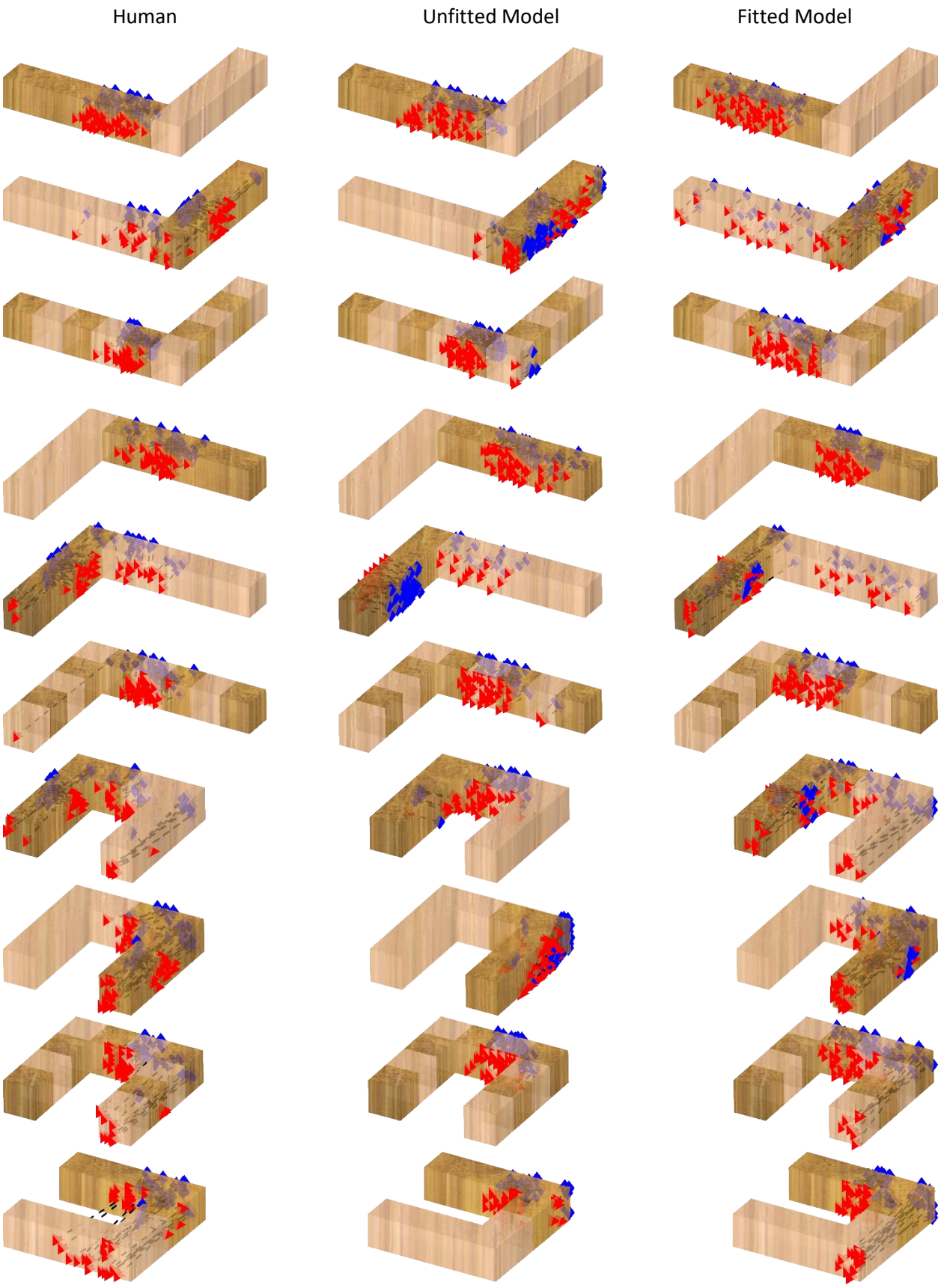

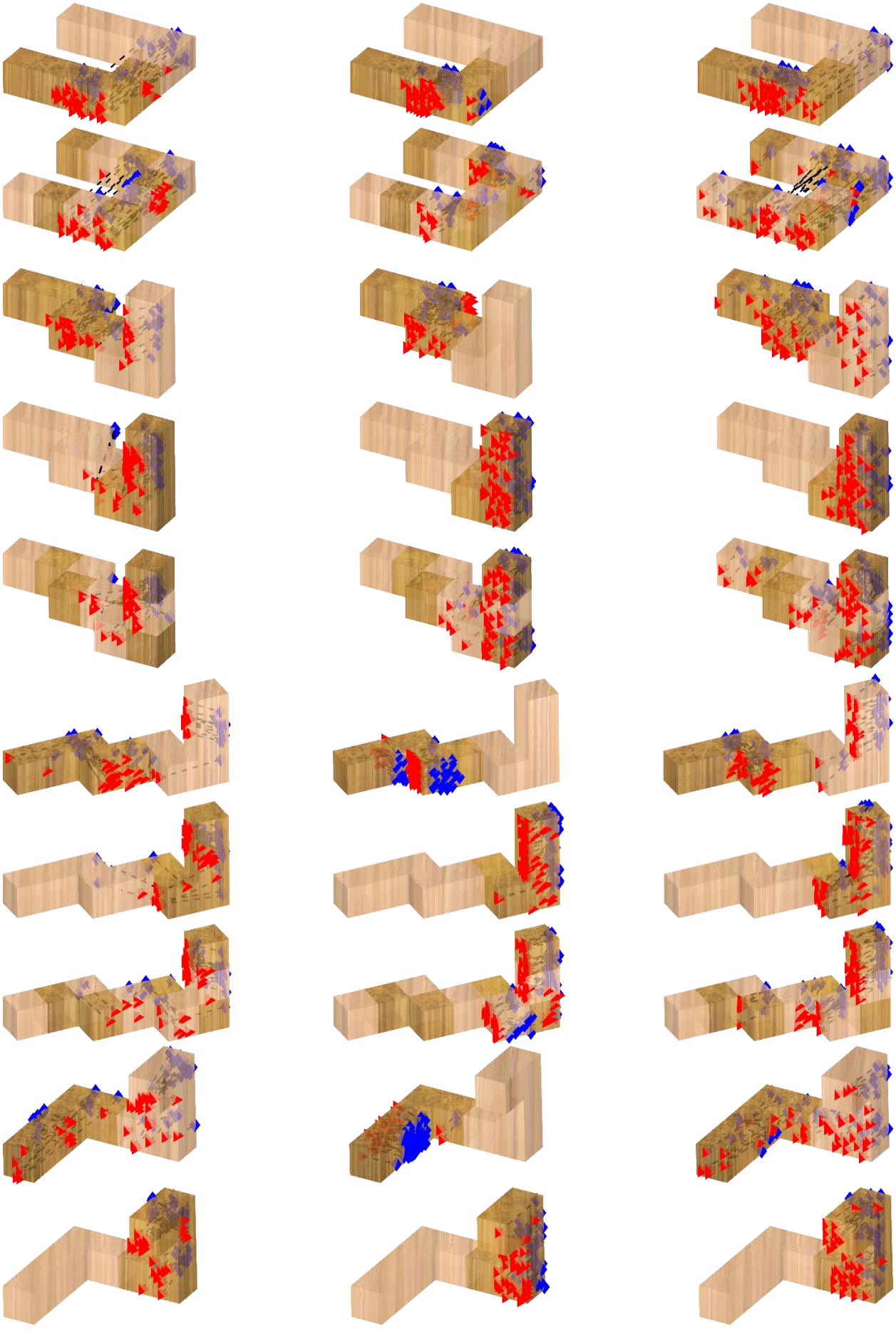

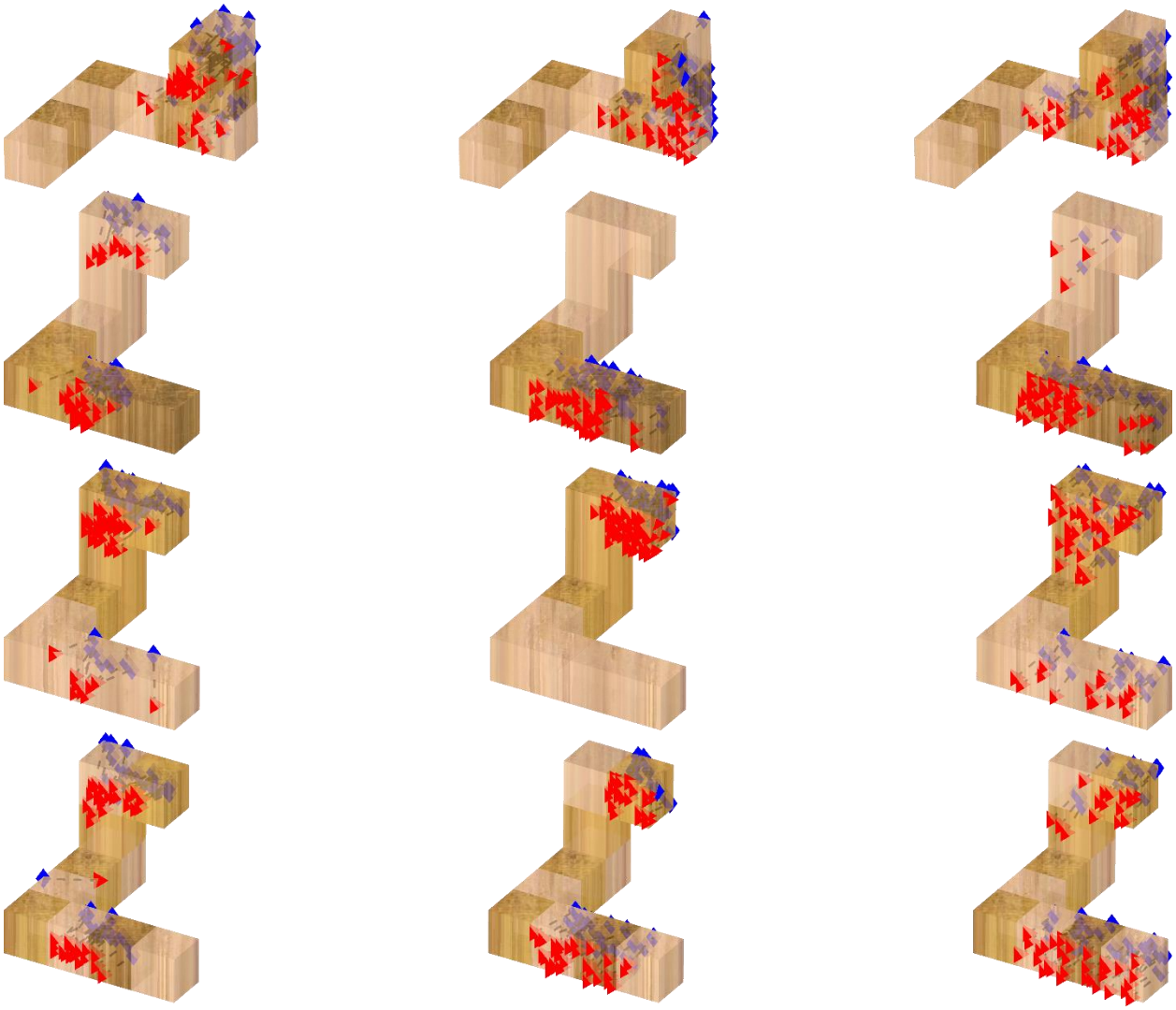

Figure S1. Grasping patterns from human participants (left), unfitted model (middle), and fitted model (right). *(a) Grasping patterns on wooden objects from Experiment 1 (Chapter 2). (b) Grasping patterns on mixed material objects from Experiment 2 (Chapter 2).*

Supporting Information S2 Figure for Chapter 2

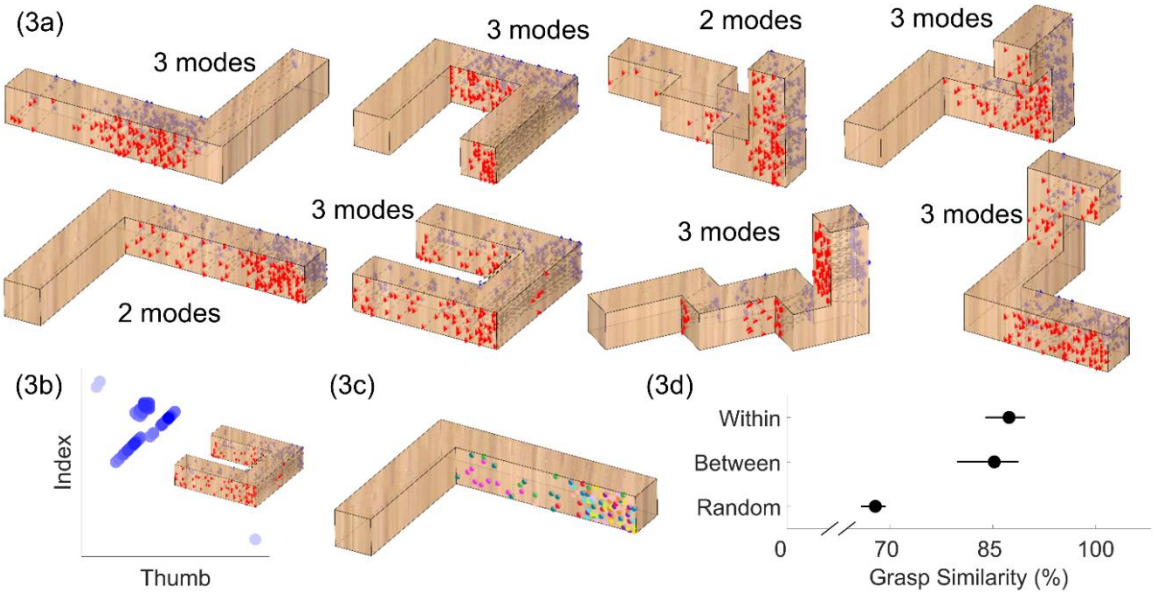

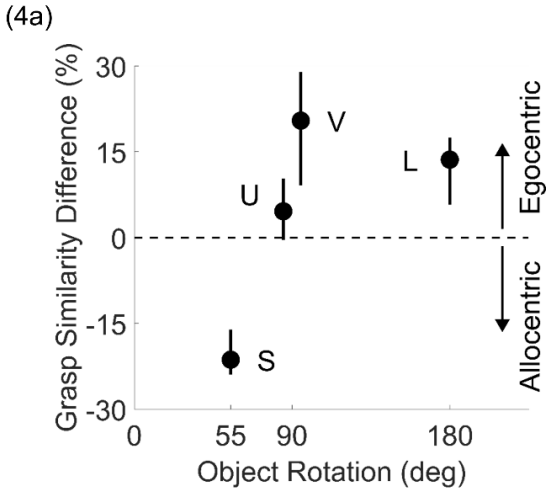

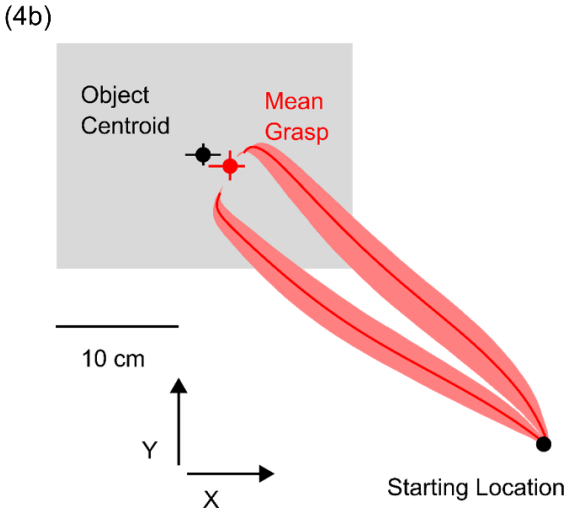

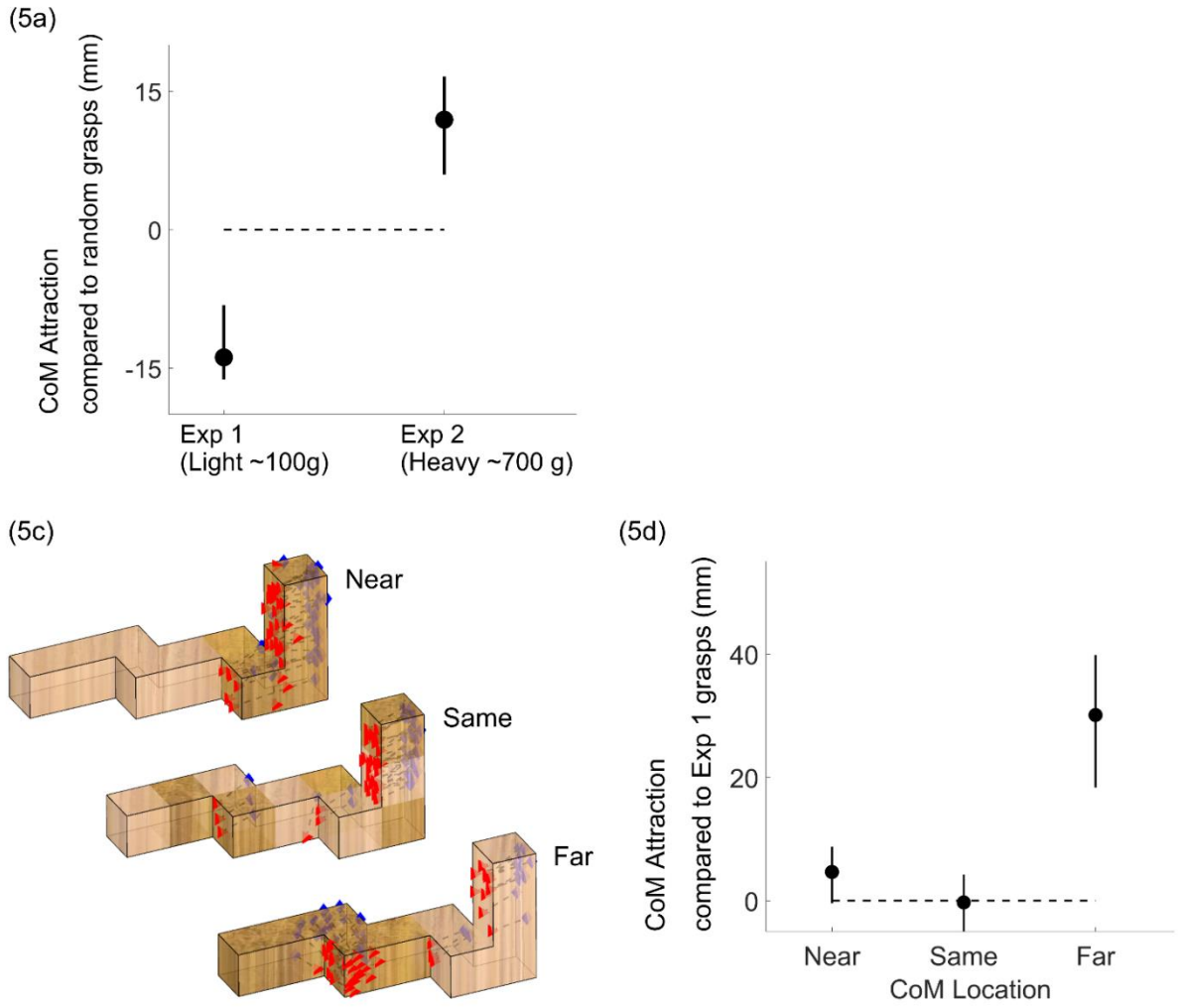

S2 Figure. Pattern of empirical results from Experiments 1 and 2 (Chapter 2) recreated from simulating grasps from the fitted model. Panels are the same as in Figures 2.3, 2.4 and 2.5 of this thesis, except that the data are simulated from the model. The grasp trajectories in panel (4b) are from the human data, to highlight how the model correctly reproduces the biases in human grasping patterns. Panel 5b is omitted since the model cannot learn to refine CoM estimates.

Supporting Information S3 Figure for Chapter 2

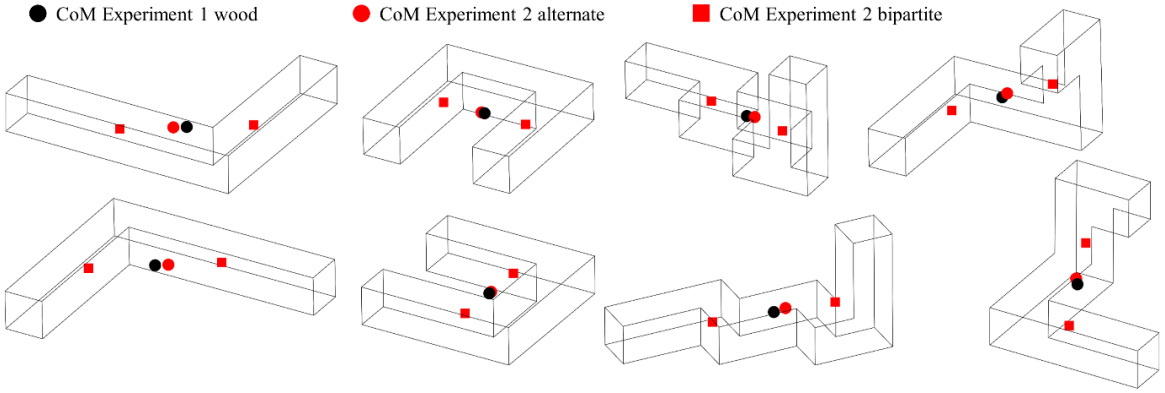

S3 Figure. Location of the center of mass for the stimuli employed in Experiments 1 and 2 (Chapter 2). *The center of mass of the light wooden objects from Experiment 1 is shown as a black dot. The centers of mass for the heavy alternate and bipartite wood/brass objects from Experiment 2 are shown as red dots and squares respectively.*

Written Statement

I hereby declare that I have prepared the thesis at hand independently and without undue aid or the use of any resources other than those indicated within the thesis. All parts of my thesis taken either verbatim or analogously from the published or unpublished works of or based on oral communications with others are indicated as such. Regarding all aspects of my scientific inquiries as they appear in my thesis, I have upheld the tenets of good scientific practice as laid out in the "Satzung der Justus-Liebig-Universität Giessen zur Sicherung guter wissenschaftlicher Praxis" and complied with the precept of ethics, data protection, and animal welfare. I declare that I have neither directly nor indirectly given monetary or any other valuable considerations to others in connection with the thesis at hand. I declare that I have not presented the thesis at hand, either in an identical or similar form, to an examination office or agency in Germany or any other country as part of any examination or degree. All materials from other sources as well as all works performed by others used or directly referenced within the thesis at hand have been indicated as such. In particular, all persons involved directly or indirectly in the development of the thesis at hand have been named. I agree with the screening of my thesis for plagiarism via offline or online detection software.

Gießen, 17.07.2023

_____

Lina Katharina Klein